Synthese, Struktur und Reaktivität von neuartigen Olefin- und Alkinplatin(II)-Komplexen

Dissertation

zur Erlangung des akademischen Grades

doctor rerum naturalium (Dr. rer. nat.)

vorgelegt der

Naturwissenschaftlichen Fakultät II - Chemie, Physik und Mathematik

der Martin-Luther-Universität Halle-Wittenberg

von Frau Dipl. Chem. Anja König

geb. am 24.09.1981 in Halle (Saale)

Gutachter:

1. Prof. Dr. D. Steinborn

2. Prof. Dr. W. Kläui

Datum der Verteidigung: 01.02.2013 Halle (Saale)

Inhaltsverzeichnis

Abkürzungsverzeichnis

Anhang

Publikationen zur Arbeit

A A. König, M. Bette, C. Wagner, R. Lindner, D. Steinborn, *Organometallics* **2011**, *30*, 5919–5927.

”On the Equilibrium between Alkyne and Olefin Platinum(II) Complexes of Zeise’s Salt Type: Syntheses and Characterization of [K(18C6)][$PtCl_3$-(RC≡CR′)]”.

http://dx.doi.org/10.1021/om200767q

B Anja König, Christoph Wagner, Martin Bette, Dirk Steinborn, *Dalton Trans.* **2012**, *41*, 7156–7162.

”On the Isomerization of Cyclooctyne into Cycloocta-1,3-diene: Synthesis, Characterization and Structure of a Dinuclear Platinum(II) Complex with a μ-η^2:η^2-1,3-COD Ligand”.

http://pubs.rsc.org/en/content/articlelanding/2012/dt/c2dt12405j

C Anja König, Martin Bette, Clemens Bruhn, Dirk Steinborn, *Eur. J. Inorg. Chem.* **2012**, 5881–5895.

”Dinuclear Olefin and Alkyne Complexes of Platinum(II)”.

http://onlinelibrary.wiley.com/doi/10.1002/ejic.201200744/abstract

D nicht publizierte Ergebnisse

Dinukleare Olefinkomplexe als Präkatalysatoren in Hydroaminierungsreaktionen

Abkürzungsverzeichnis

1,3-COD	Cycloocta-1,3-dien
1,5-COD	Cycloocta-1,5-dien
COC	Cyclooctin
COE	Cycloocten
c-Hex	Cyclohexen
t-Bu	*tert*-Butyl

Zur Nummerierung der Komplexe

Komplexe werden wie in den Publikationen **A**–**C** nummeriert, wobei der vorangestellte Buchstabe auf die entsprechende Publikation verweist. Bei Komplexen, die in mehr als einer Publikation vorkommen, wird die aus der zuerst genannten Publikation verwendet.

[K(18C6)][$PtCl_3$(*cis*-MeHC=CHMe)]	(**A2**)	[K(18C6)][$PtCl_3$(*t*-BuC≡C*t*-Bu)]	(**A6**)
[K(18C6)][$PtCl_3$(MeC≡CMe)]	(**A3**)	[K(18C6)][$PtCl_3$(MeC≡CPh)]	(**A7**)
[K(18C6)][$PtCl_3$(EtC≡CEt)]	(**A4**)	[K(18C6)][$PtCl_3$(MeC≡CCO_2Me)]	(**A8**)
[K(18C6)][$PtCl_3$(MeC≡C*t*-Bu)]	(**A5**)	[K(18C6)][$PtCl_3$(COC)]	(**A9/B1**)
[K(18C6)]$_2$[($PtCl_3$)$_2$(μ-η^2:η^2-1,3-COD)]	(**B2**)	[K(18C6)][$PtCl_3$(C_4H_8)]	(**A2/B4**)
[K(18C6)][$PtCl_3$(μ-η^2:η^2-1,3-COD)]	(**B3**)	[K(18C6)][$PtCl_3$(COE)]	(**B5**)
[{$PtCl_2$(H_2C=CH_2)}$_2$]	(**C1**)	[{$PtCl_2$((MeC≡C*t*-Bu)}$_2$]	(**C11**)
[{$PtCl_2$(MeHC=CHMe)}$_2$]	(**C2**)	[{$PtCl_2$(*t*-BuC≡C*t*-Bu)}$_2$]	(**C12**)
[{$PtCl_2$(*c*-Hex)}$_2$]	(**C3**)	[$PtCl_2$(H_2C=CH_2)$_2$]	(**C13**)
[$PtCl_2$(C_4Me_4)]	(**C4**)	[$PtCl_2$(H_2C=CH_2)(MeC≡C*t*-Bu)]	(**C14**)
[$PtCl_2$(C_4Et_4)]	(**C5**)	[$PtCl_2$(H_2C=CH_2)(*t*-BuC≡C*t*-Bu)]	(**C15**)
[$PtCl_2$($C_4Me_2Pr_2$)]	(**C6**)	[$PtCl_2$(C_4Me_2*t*-Bu_2)]	(**C16**)
[{$PtCl_2$($C_4Me_2Ph_2$)}$_2$]	(**C7**)	[$PtCl_2$(C_4*t*-Bu_4)]	(**C17**)
[$PtCl_2$(H_2C=CH_2)(MeC≡C*t*-Bu)]	(**C8**)	[{$PtCl_2$($OCMe_2$)(H_2C=CH_2)]	(**C18**)
[$PtCl_2$(H_2C=CH_2)(*t*-BuC≡C*t*-Bu)]	(**C9**)	[$PtCl_2$(*t*-BuC≡C*t*-Bu)$_2$]	(**C19**)
[$PtCl_2$(H_2C=CH_2)$_2$]	(**C10**)	[$PtCl_2$(MeC≡C*t*-Bu)$_2$]	(**C20**)

1. Einleitung

Aus historischer Sicht stellt das Jahr 1825 mit der Synthese des ersten Organoübergangsmetallkomplexes, des Zeise-Salzes $K[PtCl_3(C_2H_4)]\cdot H_2O$, einen Meilenstein in der Geschichte der metallorganischen Chemie dar. [1] Die exakte Natur der Bindung von Ethen an Platin war jedoch lange unbekannt und Gegenstand zahlreicher Diskussionen. Sie wurde erst durch das Bindungsmodell von Dewar, Chatt und Duncanson im Jahre 1951/1953 und die Strukturanalyse durch Röntgen- und Neutronenbeugung (1954/1974) geklärt. [2,3,4] Danach sind zwei Bindungskomponenten maßgebend, eine Wechselwirkung des besetzten, bindenden π-Orbitals des Olefins als Donorkomponenente mit einem unbesetzten Metallorbital (donation) und die Wechselwirkung eines besetzen Orbitals des Metalls mit dem unbesetzten, antibindenden π*-Orbitals des Olefins (π-back-donation), vgl. Abbildung 1.

Nach heutigem Wissensstand ist diese Beschreibung für η^2-Olefinmetallkomplexe mit nicht zu großer back-donation zutreffend. Liegt diese jedoch vor, wird die elektronische Situation besser durch eine oxidative Addition des Olefins an das Metall unter Ausbildung eines Metallacyclopropankomplexes beschrieben. Im Bild der VB-Theorie sind beide Formen als Grenzstrukturen zu formulieren (Schema 1), wobei die Frage, ob ein η^2-Olefinmetallkomplex besser als π-Komplex oder als Metallacyclopropankomplex zu beschreiben ist, aus spektroskopischen und/oder strukturellen Untersuchungen abgeleitet werden muss.

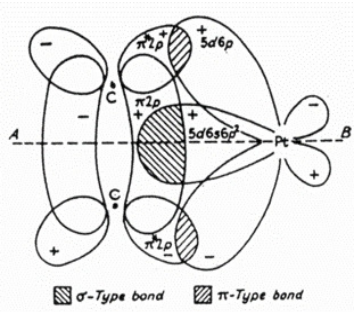

Abbildung 1. Dewar-Chatt-Duncanson-Modell für die Bindung von Ethen an Platin, entnommen der klassischen Publikation [2].

Darüber hinaus erlauben Modellierungen auf Grundlage quantenchemischer Rechnungen besonders mittels der Dichtefunktionaltheorie (DFT) einen genaueren Einblick in die elektronische Struktur. In diesem Zusammenhang besonders zu erwähnen, sind Modelle zur Ladungspartitionierung von Gleichgewichtstrukturen wie NBO (natural bond orbital) und AIM (atoms in molecules) sowie zur Charakterisierung von Energie- und Ladungsänderungen bei Bindungsknüpfungen und -spaltungen wie CDA (charge decomposition analysis) und EDA (energy decomposition analysis). [5,25,26,37]

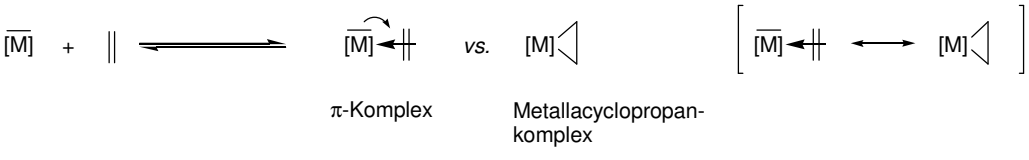

Schema 1.

Nachdem die Natur der Bindung von Ethen im Zeise-Salz geklärt war, stellte sich die Frage nach der Existenz von Alkinkomplexen vom Zeise-Salz-Typ. 1961 gelang es Chatt *et al.* [6], entsprechende Komplexe $K[PtCl_3(RC{\equiv}CR')]$ (R, R' = *t*-Bu, C(OH)RR') zu synthetisieren, aber nur mit sperrigen *tert*-Butylsubstituenten oder solchen, die sauerstofffunktionalisiert sind (für R, R' = Ph vgl. [7]). Die im Vergleich zu Olefinen höhere Reaktivität von Alkinen kann die Synthese von Alkinkomplexen erschweren, wie in Schema 2 an einer Reihe von möglichen Reaktionen gezeigt ist. So können terminale Alkine zu Hydrido–Alkinyl-Komplexen oder zu Vinylidenkomplexen reagieren (Schema 2, Pfad **a/b**). Isomerisierungen zu Allen- oder 1,3-Dienkomplexen (Pfad **c/d**) sowie oxidative Kupplungen zu Metallacyclopentadienen (Pfad **e**) sind weitere Beispiele. Die Bildung von Cyclobutadienkomplexen (Pfad **f**) durch eine (formale) [2+2]-Cycloaddition ist ein instruktives Beispiel dafür, dass Metalle reaktive organische Spezies durch Komplexbildung stabilisieren können.

Olefin- und Alkinmetallkomplexe nehmen in der Komplexkatalyse eine herausragende Rolle ein, da sie in vielen Prozessen wie Hydrierungen, Oligomerisierungsen, Polymerisationen, Cyclisierungen, Hydroformylierungen, Oxidationen und Hydrosilylierungen als Intermediate auftreten. [8,9] Dabei spielen insbesondere Palladiumkomplexe eine herausragende Rolle, während an Platinkomplexen, die vielfach kinetisch stabiler sind, zahlreiche metallorganische Elementarreaktionen detailliert untersucht und katalytisch relevante Intermediate isoliert und charakterisiert werden konnten.

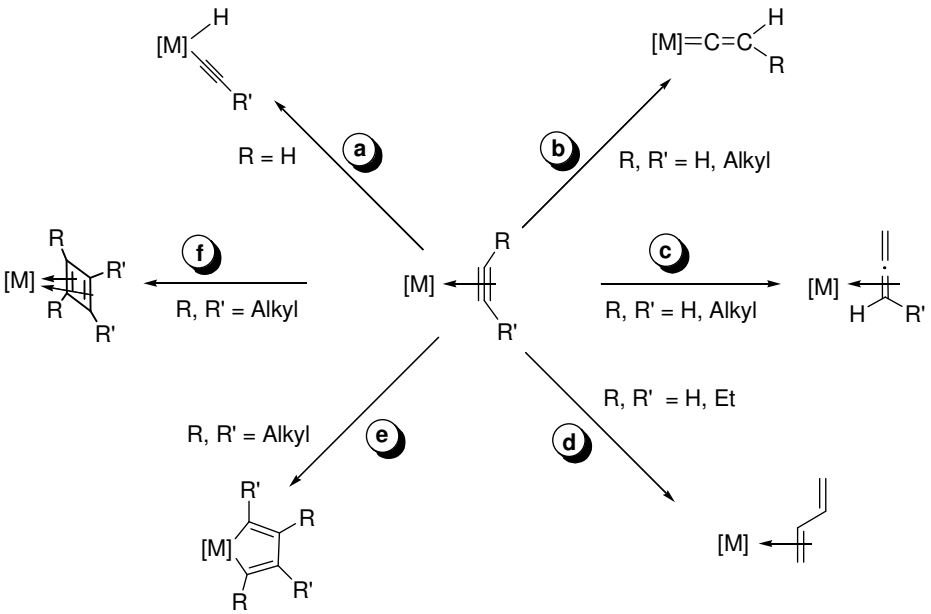

Schema 2.

Zum detaillierten Verständnis von Katalysezyklen sind Kenntnisse zur thermodynamischen Stabilität von Metall–Ligand-Bindungen erforderlich, das heißt zum Beispiel darüber, wie die Stärke einer Metall–Olefin- oder Metall–Alkin-Bindung vom Substitutionsmuster des Olefins bzw. Alkins abhängt oder ob ein Olefin stärker oder schwächer als ein Alkin an ein bestimmtes Komplexfragment gebunden wird. So sind z. B. für Olefinplatin(0)-Komplexe des Typs $[Pt(RHC{=}CHR')(PPh_3)_2]$ (R, R' = H, Ph, CN) Dissoziationenergien für der Olefinliganden von 36.4–66.3 kcal/mol gefunden worden. [10] Beeinflußt durch die Art und den sterischen Anspruch der Substituenten am Olefin RHC=CHR' wirken elektronenziehende Substituenten (Ph, CN) stabilisierend auf die Olefin–Platin-Bindung während für den Ethenliganden die geringste Dissoziationsenergie gefunden wurde (36.4 kcal/mol). [11] Im Gegensatz hierzu zeigen Untersuchungen zur relativen Bindungsstärke von Olefinliganden an Platin(II)-Komplexen des Typs $[PtCl_2(py)(RHC{=}CHR')]$ (R, R' = H, Me, *p*-NO_2Ph) ein anderes Bild. Hier ist Ethen am stärksten gebunden, während Olefine mit elektronenziehenden als auch -donierenden Substituenten schwächer gebunden werden. [12]

Zielstellung dieser Arbeit

Obwohl seit den klassischen Versuchen von Chatt *et al*. Anfang der 60er Jahre des vorigen Jahrhunderts eine Reihe von weiteren Alkinkomplexen vom Zeise-Salz-Typ wie $[K(18C6)][PtCl_3(RC{\equiv}CR)]$ (R, R' = H, Alkyl) synthetisiert und charakterisiert werden konnten, [15] bleibt die Frage nach der relativen Stabilität von Olefin- und Alkinkomplexen diesen Typs weitgehend ungeklärt. Ausgangspunkt der vorliegenden Arbeit ist es deshalb, energetische Parameter für die Bindung von Alkinen an Platin zu untersuchen, insbesondere im Hinblick auf sterische und elektronische Einflüsse der Substituenten am Alkinliganden. Hierzu soll vor allem die Substitution von Olefinliganden in Zeise-Salz-Typ Komplexen $[K(18C6)][PtCl_3(RHC{=}CHR)]$ gegen Alkinliganden herangezogen werden, welche sich durch NMR spektroskopische Charakterisierung des Gleichgewichtszustandes quantifizieren lässt.

Ein weiterer zentraler Aspekt der vorliegenden Arbeit war die Frage zum Einfluss der Komplexladung bei derartigen Reaktionen. So sollten ausgehend vom neutralen Zeise-Dimer $[\{PtCl_2(H_2C{=}CH_2)\}_2]$ Ligandsubstitutionen (Olefin *vs.* Alkine) und die Reaktivität hinsichtlich der Brückenspaltung gegenüber Alkinen untersucht werden.

2. Ergebnisse und Diskussion

2.1 Reaktionen an Zeise-Salz analogen Olefinplatin(II)-Komplexen

2.1.1 Einführung

Trotz der Vielzahl an Olefinkomplexen des Zeise-Salz-Typs $M^I[PtCl_3(R_2C{=}CR_2)]$ (M^I = Alkalimetall; R = H, Alkyl, Aryl), sind nur verhältnismäßig wenige analoge Alkinkomplexe bekannt. Die klassische Methode zur Herstellung von Alkinkomplexen von Chatt *et al*. beinhaltet die Reaktion von $M^I_2[PtX_4]$ (X = Cl, Br) mit wasserlöslichen Alkinen RR‘(OH)C–C≡C–C(OH)RR‘ (R, R‘ = Alkyl, Aryl) in Wasser als Lösungsmittel (Schema 3, Pfad **a**) oder von $K[PtCl_3(C_2H_4)]$ mit sterisch anspruchsvollen Alkinen in Aceton bei 60 °C (Schema 3, Pfad **b**). [6] Im eigenen Arbeitskreis wurde ein Zugang zur Darstellung von Alkin- und Olefinkomplexen des Zeise-Salz-Typs [K(18C6)][$PtCl_3$(RHC=CHR’)] (R, R‘ = H, *n*-Alkyl, Aryl) bzw. [K(18C6)][$PtCl_3$(RC≡CR’)] (R, R‘ = Me, Et, *n*-Pr, Ph) ausgehend von dem dinuklearen Platin(II)-Komplex $[K(18C6)]_2[Pt_2Cl_6]$ (18C6 = 18-crown-6) gefunden (Schema 3, Pfad **c/d**). [13,14,15] Diese Darstellungsmethode ist jedoch auf innere Alkine beschränkt. Komplexe dieses Typs mit terminalen Alkinliganden [K(18C6][$PtCl_3$(RC≡CH)] (R = *n*-Pr, *n*-Bu, *t*-Bu, Ph) konnten hingegen durch Umsetzung des But-2-in-Komplexes mit dem entsprechenden terminalen Alkin synthetisiert werden (Schema 3, Pfad **e**). [15]

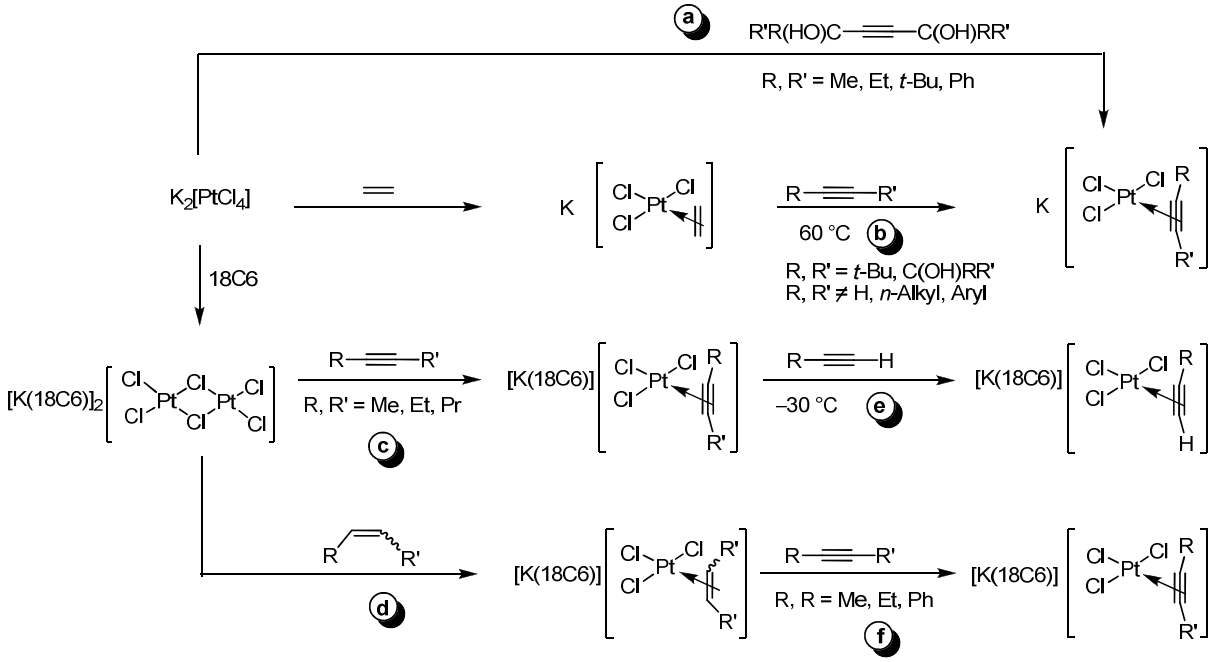

Schema 3.

In den beschriebenen Untersuchungen der eigenen Diplomarbeit (Schema 3, Pfad **f**, [16]), in denen die Substitution von *cis*-But-2-en in [K(18C6)][$PtCl_3$(*cis*-MeHC=CHMe)] (**A2**) mit Alkinen RC≡CR'(R, R' = Me, Et, Ph) unter Bildung der entsprechenden Alkinkomplexe [K(18C6)][$PtCl_3$(RC≡CR')] (**A3/A4/A7**) untersucht wurde, sind Gleichgewichtszustände zwischen dem *cis*-But-2-en und den korrespondierenden Alkinkomplexen beobachtet wurden.

2.1.2 Synthese und Charakterisierung

In Weiterführung der in [16] beschriebenen Untersuchungen, wurden nun sterisch anpruchsvoller substituierte und elektronenarme Alkine RC≡CR' (R, R' = *t*-Bu, CO_2Me) sowie Cyclooctin (COC) als ein cyclisches Alkin in die Untersuchungen einbezogen. Dabei wurden Gleichgewichtszustände zwischen dem Olefin- und den korrespondierenden Alkinkomplexen im abgeschmolzenen NMR-Röhrchen beobachtet (Schema 4), wobei nur im Fall des cyclischen Alkins die Reaktion quantitativ abläuft.

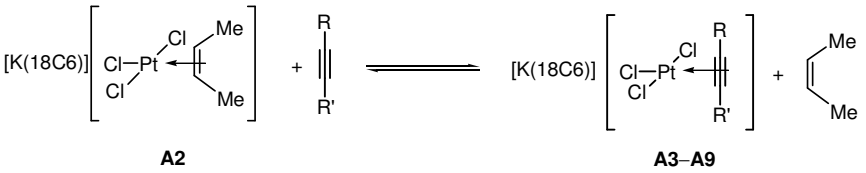

A2 **A3–A9**

	A3	A4	A5	A6	A7	A8	A9
R/R'	Me/Me	Et/Et	Me/*t*-Bu	*t*-Bu/*t*-Bu	Me/Ph	Me/CO_2Me	COC

Schema 4.

Durch Arbeiten mit einem Überschuss des Alkins sowie durch Verflüchtigung des freigesetzten *cis*-But-2-ens konnten diese Reaktionen jedoch zu vollständigen Umsätzen gebracht werden, was die Synthese und Isolation der entsprechenden Alkinkomplexe [K(18C6)][$PtCl_3$(RC≡CR')] (**A3**–**A9**) als gelbliche, leicht luftempfindliche kristalline Substanzen in moderaten bis guten Umsätzen erlaubte. Die Komplexe wurden zweifelsfrei mittels Elementaranalyse und ^{1}H-/^{13}C-NMR-Spektroskopie sowie im Fall der Komplexe **A5**, **A6**, **A7** und **A9** zusätzlich durch Röntgeneinkristallstrukturanalysen charakterisiert.

2.1.3 Thermodynamik der Substitutionsreaktion

Mittels der NMR-Spektroskopie konnten die Gleichgewichtskonstanten der Substitutionsreaktionen (Schema 5) des *cis*-But-2-en-Komplexanions $[PtCl_3(cis\text{-}MeHC{=}CHMe)]^-$ (**A2a**; ohne Berücksichtigung des Einflusses des $[K(18C6)]^+$-Kations) zu den verschiedenen Alkinkomplexanionen $[PtCl_3(RC{\equiv}CR')]^-$ (**A3a**–**A8a**) im abgeschmolzenen NMR-Röhrchen bei 27 °C bestimmt werden.

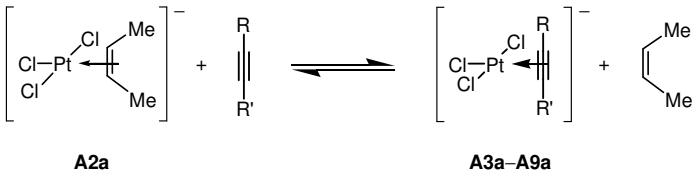

	A3a	A4a	A5a	A6a	A7a	A8a	A9a
R/R'	Me/Me	Et/Et	Me/*t*-Bu	*t*-Bu/*t*-Bu	Me/Ph	Me/CO_2Me	COC

Schema 5.

Hierbei wurden für die untersuchten Alkine Gleichgewichtskonstanten K_{NMR} zwischen 0.0055 (**A8a**) und 0.47 (**A4a**) beobachtet. Im Unterschied dazu zeigte die Umsetzung von **A2a** mit dem Cyclooctin einen vollständigen Umsatz ($K_{NMR} > 500$) (Tabelle 1). Die freie Standardbildungsenthalpie der Substitutionsreaktionen ist damit für die untersuchten Alkine leicht positiv, wohingegen der Wert für den Cyclooctinkomplex stark negativ ist. Die ermittelten Gleichgewichtskonstanten spiegeln dabei die relative Bindungsstärke der Platin–Alkin-Bindung wider.

Tabelle 1. Freie Standardreaktionsenthalpien $\Delta_rG°$ (in kcal/mol) sowie NMR-spektroskopisch ermittelte Gleichgewichtskonstanten K_{NMR} der Substitutionsreaktionen nach Schema 5.

	R/R'	K_{NMR}	$\Delta_rG°_{NMR}$	$\Delta_rG°_{gp}$ [a]	$\Delta_rG°_{CHCl_3}$ [b]
A3a	Me/Me	0.25	0.8	1.5	1.1
A4a	Et/Et	0.47	0.5	0.8	0.6
A5a	Me/*t*-Bu	0.26	0.8	1.8	1.9
A6a	*t*-Bu/*t*-Bu	0.020	2.3	2.3	3.0
A7a	Me/Ph	0.061	1.7	2.0	4.1
A8a	Me/CO_2Me	0.0055	3.1	–0.3	3.4
A9a	COC	> 500[c]	< –3.7[c]	–10.9	–9.8

a) Berechnete freie Standardbildungsenthalpie unter Gasphasenbedingungen. b) Berechnete freie Standardbildungsenthalpie unter Berücksichtigung des Lösungsmitteleffektes ($CHCl_3$). c) Die Abwesenheit eines Signals für nichtumgesetztes COC im ^{1}H-NMR-Spektrum belegt einen Umsatz zu **A9a** von > 0.96.

2.1.4 Strukturelle Aspekte der Zeise-Salz analogen Alkinplatin(II)-Komplexe

In den Zeise-Salz analogen Alkinkomplexen [K(18C6)][$PtCl_3$(RC≡CR')] (**A3**–**A9**) zeigen die Anionen die typische Struktur mit einem nahezu senkrecht zur Koordinationsebene (Pt,Cl1,Cl2,Cl3) stehenden Alkinliganden (Φ(Pt,Cl1,Cl2,Cl3/Pt,C1,C2): 84.1(6)–89.6(4)°, Abbildung 2). Alle Pt–C- sowie C–C-Bindungslängen sind nach dem 3σ-Kriterium identisch (Pt–Cl 2.286(4)–2.316(5) Å in **A5**–**A7**). Im Gegensatz dazu zeigt der Cyclooctin-Komplex **A9** eine deutliche verlängerte Pt–Cl-Bindung in *trans*-Position zum Alkinliganden auf (Pt–Cl1 2.329(2) Å *vs*. Pt–Cl2/Cl3 2.292(2)/2.296(2) Å), was auf einen deutlich stärkeren *trans*-Einfluss des COC-Liganden deutet.

Die koordinationschemisch bedingte Abwinkelung der Substituenten R/R' am Alkinliganden, welche durch den Winkel α (α = 180 − γ(C≡C−C); vgl. Formelskizze **I**) definiert wird, beträgt in den Komplexen **A5**–**A7** 16(1)–21(1)°, wohingegen signifikant größere Werte für den Cyclooctinkomplex **A9** beobachtet werden können (26.8(7)/26.0(7)°). Als Ursache kann hierfür die durch die Ringbildung bedingte Abwinkelung des nicht-koordinierten Moleküls (α = 26(2)°) genannt werden. [17]

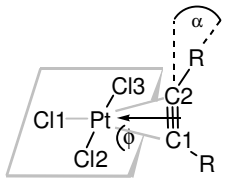

I

Diese strukturellen Parameter der Komplexe **A5**–**A7** sind damit mit anderen Alkinplatin(II)-Komplexen (M^I[$PtCl_3$(RC≡CR)] [18,14] (M^I = K, [K(18C6)]), [$PtCl_2$(RC≡CR')(Amin)] [19] (R, R' = H, Me, Et, *t*-Bu, Ph, CMe_2OH, CEt_2OH; Amin = NH_2Me, NH_2Et, $NH_2C_4H_7$, $NH_2C_5H_9$, *p*-NH_2PhMe) und [PtI_2(Me_2phen)(PhC≡CPh)] [15,18,19,20,49] vergleichbar, welche Abwinkelungen zwischen 15(1) und 27(2)° aufweisen.

Tabelle 2. Ausgewählte Bindungsparameter (Längen in Å, Winkel in °) der Komplexe [K(18C6)][$PtCl_3$(RC≡CR')] (R/R' = Me/*t*-Bu, **A5**; *t*-Bu/*t*-Bu, **A6**; Me/Ph, **A7**; RC≡CR' = COC, **A9**). Vergleichend sind die analogen Werte aus den DFT-Rechnungen der Komplexanionen aufgeführt.

R/R'	Me/*t*-Bu (**A5**)		*t*-Bu/*t*-Bu (**A6**)		Me/Ph (**A7**)		COC (**A9**)	
	X-ray	DFT	X-ray	DFT	X-ray	DFT	X-ray	DFT
Pt–C1	2.10(1)	2.136	2.141(9)	2.147	2.12(1)	2.119	2.132(6)	2.118
Pt–C2	2.13(1)	2.150	2.130(9)	2.147	2.125(8)	2.136	2.125(7)	2.118
C2≡C1	1.24(1)	1.245	1.24(1)	1.248	1.23(1)	1.251	1.27(1)	1.246
α	16(1)	18.2	21(1)	21.5	16(1)	18.9	26.8(7)	27.5
α	18(1)	21.9	20(1)	21.5	20(1)	22.2	26.0(7)	27.5

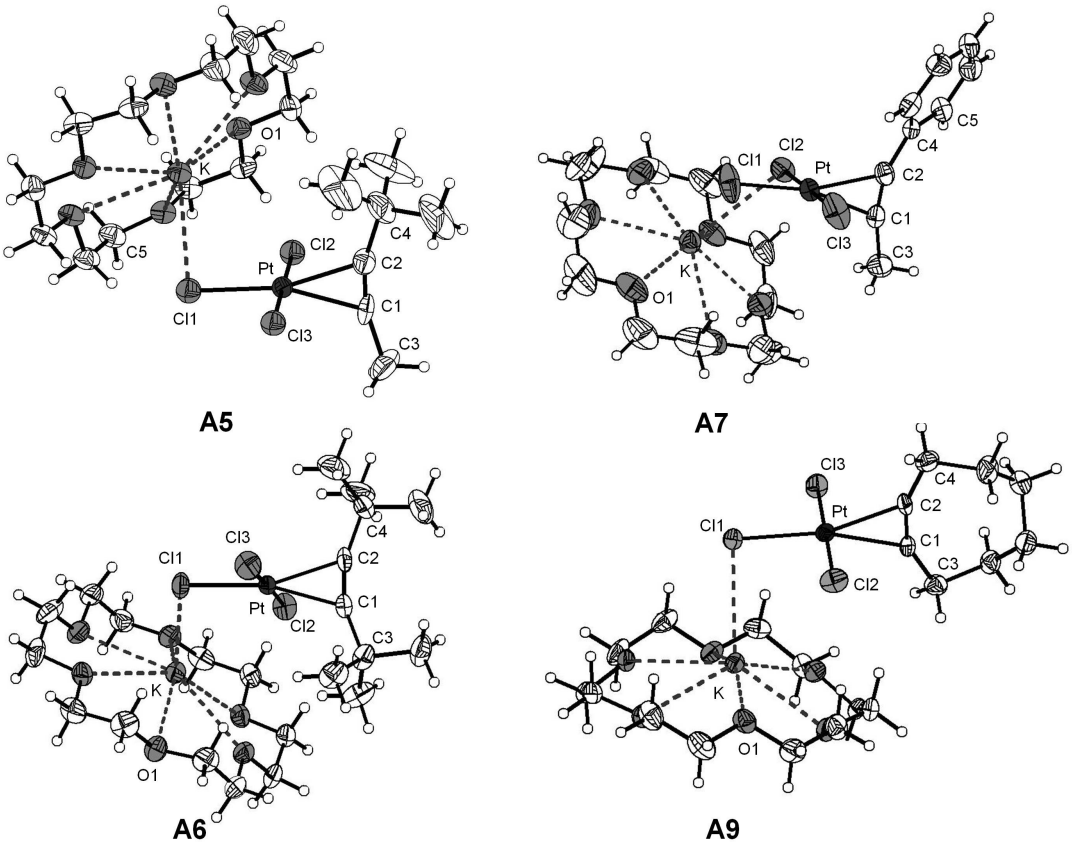

Abbildung 2. Molekülstruktur von [K(18C6)][$PtCl_3$(RC≡CR')] (R/R' = Me/*t*-Bu, **A5**; *t*-Bu/*t*-Bu, **A6**; Me/Ph, **A7**; RC≡CR' = COC, **A9**). Die Ellipsoide sind mit einer Wahrscheinlichkeit von 30% dargestellt.

2.1.5 DFT-Rechnungen

Einen weiteren Einblick in die Bindungssituation der verschiedenen Alkinliganden erlauben quantenchemische Rechnungen. Aus diesem Grund wurden die Strukturen der komplexen Anionen [$PtCl_3$(RC≡CR')]$^-$ (**A3a'**–**A9a'**)[1] mittels der Dichte-Funktional-Theorie (DFT) berechnet. Um zuverlässige Werte zu erhalten, wurden neben der Verwendung geeigneter Funktionale (B3LYP) und Basissätze (triple-ζ-Qualität) der Lösungsmitteleinfluß mittels des „polarizable continuum model" (PCM) simuliert. [21,22,23,24] Die berechneten freien Standardbildungsenthalpien der Substitutionsreaktionen stimmen mit den NMR-spektroskopisch ermittelten Werten gut überein (Tabelle 1), was die Anwendbarkeit des gewählten quantenchemischen Modells auf diese Systeme demonstriert. Die berechneten Strukturen dieser Anionen und ausgewählte strukturelle Parameter sind in Abbildung 3 bzw. Tabelle 2 wiedergegeben.

[1] Anionen werden mit dem Buchstaben "**a**" und berechnete Strukturen mit einem " **'** " gekennzeichnet.

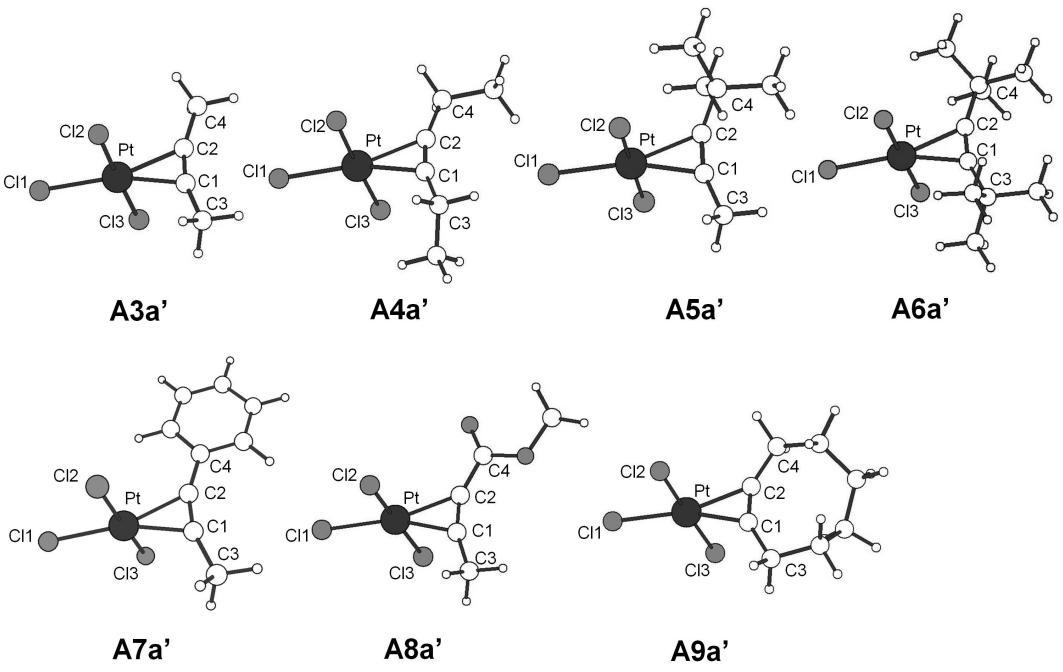

Abbildung 3. Berechnete Strukturen der Komplexanionen $[PtCl_3(RC{\equiv}CR')]^-$ (R/R' = Me/Me, **A3a'**; Et/Et, **A4a'**; Me/*t*-Bu, **A5a'**; *t*-Bu/*t*-Bu, **A6a'**; Me/COOMe, **A8a'** and RC≡CR' = COC, **A9a'**).

Die berechneten strukturellen Parameter stimmen ebenfalls gut mit den experimentell ermittelten Werten überein. Hierbei werden dieselben Trends wie in den diffraktometrisch bestimmten Einkristallstrukturanalysen beobachtet. Darüber hinaus ist zu erkennen, dass für die Alkinkomplexe mit elektronenziehenden Substituenten (Ph, CO_2Me) und COC deutlich kürzere Pt–C-Bindungen beobachtet werden (Pt–C 2.136–2.150 Å, **A3a'**–**A6a'** *vs.* 2.119/ 2.136 Å, **A7a'**; 2.103/2.110 Å, **A8a'**; 2.118/2.118 Å, **A9a'**).

Des Weiteren können zusätzliche Informationen über die „energy decomposition analysis" (EDA) [25] sowie über eine NBO-Analyse [26] gewonnen werden (Tabelle 3 und 4). Nach der „energy decomposition analysis" kann die Dissoziationsenergie ΔE_{diss} einer Metall–Ligand-Bindung eines Komplexes durch die Summe zweier Beiträge ausgedrückt werden. Zum einen die Wechselwirkungsenergie $\Delta E_{int.}$ Dieser Betrag beschreibt die Wechselwirkung zwischen den isolierten, „präparierten" Fragmenten (Fragmente in derselben Geometrie wie im Komplex). Zum anderen die Präparationsenergie ΔE_{prep} (preparation energy). Diese gibt an welche Energie zur Verformung der Fragmente aus ihrer Gleichgewichtsstruktur in jene, welche sie im Komplex einnehmen, aufgewendet werden muss. Der Zusammenhang zwischen beiden Größen ist hierbei durch die Gleichung $-\Delta E_{diss} = \Delta E_{int} + \Delta E_{prep}$ definiert. Für eine nähere Erläuterung der entsprechenden Beträge siehe Referenz [25].

Tabelle 3. Bindungsparameter der verschiedenen Alkinliganden in Komplexen $[PtCl_3(RC{\equiv}CR')]^-$ (**A3a'**–**A9a'**) abgeleitet aus der „energy decomposition analysis" EDA (ΔE_{diss} = Bindungsdissoziationsenergie, ΔE_{int} = Wechselwirkungsenergie, ΔE_{prep} = Präparationsenergie; alle Energien in kcal/mol.

	A3a'	**A4a'**	**A5a'**	**A6a'**	**A7a'**	**A8a'**	**A9a'**
R/R'	Me/Me	Et/Et	Me/*t*-Bu	*t*-Bu/*t*-Bu	Me/Ph	Me/CO_2Me	COC
EDA							
ΔE_{diss} [a]	26.5	26.6	26.0	25.0	26.0	28.3	38.0
ΔE_{int} [a]	–37.9	–37.7	–39.2	–39.4	–39.8	–42.6	–44.8
ΔE_{prep} [b]	11.4	11.1	13.2	14.5	13.8	14.3	6.9
$\Delta E_{prep(Alkin)}$	8.1	7.8	9.5	10.8	10.3	11.0	3.3
$\Delta E_{prep(PtCl_3^-)}$	3.3	3.3	3.7	3.7	3.5	3.3	3.6

a) Unter Berücksichtigung der über „counterpoise"-Berechnungen ermittelten BSSE Fehler (BSSE = 1.71–2.56 kcal/mol). b) $\Delta E_{prep} = \Delta E_{prep(Alkin)} + \Delta E_{prep(PtCl_3^-)}$.

Ein Vergleich der Bindungsparameter zeigt die besondere Stellung des Komplexes mit dem elektronenarmen Alkinliganden MeC≡CCO_2Me in **A8a'** sowie mit dem Cyclooctinliganden in **A9a'**. So wird im Vergleich zu den anderen untersuchten Alkinkomplexen (ΔE_{diss} = 25.0–26.6 kcal/mol, **A3a'**–**A7a'**), eine geringfügig höhere Bindungsdissoziationsenergie E_{diss} (28.3 kcal/mol) für den Alkinkomplex **A8a'** und noch einmal deutlich höhere Werte für den Cyclooctinkomplex **A9a'** beobachtet (38.0 kcal/mol). Dieser Trend ist auch in den Wechselwirkungsenergien zu beobachten (ΔE_{int} = –37.7... –39.8 kcal/mol, **A3a'**–**A7a'**; –42.6 kcal/mol, **A8a'**; –44.8 kcal/mol, **A9a'**). Darüber hinaus weist der gespannte Cyclooctinligand auch mit Abstand die niedrigste Präparationsenergie auf, was maßgeblich zur ungewöhnlich großen Stärke der Pt–C-Bindung in **A9a'** führt.

Denselben Trend ergibt die NBO-Analyse (Tabelle 4): So zeigen die Alkinkomplexe **A7a'-A9a'** mit elektronenziehenden Substituenten (Ph, CO_2Me) und mit dem COC-Liganden eine signifikant höhere Besetzung des antibindenden π*-Orbitals (P_{π^*}: 0.297–0.307, **A3a'**–**A6a'** *vs.* 0.322–0.377, **A7a'**–**A9a'**), was auf einen deutlich höheren Beitrag der back-donation in diesen Komplexen hindeutet. Dieser Unterschied in der back-donation drückt sich dabei auch in einer unterschiedlichen Ladung des Ligandenfragmentes aus, welche für die alkylsubstituierten Komplexe **A3a'**–**A6a'** leicht positiv (0.001 … 0.024 e), hingegen für **A7a'**–**A9a'** signifikant negativ (–0.021 … –0.071 e) ist.

Tabelle 4. Bindungsparameter der verschiedenen Alkinliganden in Komplexen $[PtCl_3(RC{\equiv}CR')]^-$ (**A3a'**–**A9a'**) abgeleitet aus der NBO-Analyse (P_π/P_{π^*} = Population der π/π^*-Orbitale der Alkinkomplexe sowie der nicht-koordinierten Alkine; q_{Alkin} = Ladung des Liganden in Elektronen).

	A3a'	**A4a'**	**A5a'**	**A6a'**	**A7a'**	**A8a'**	**A9a'**
R/R'	Me/Me	Et/Et	Me/*t*-Bu	*t*-Bu/*t*-Bu	Me/Ph	Me/CO_2Me	COC
Alkinkomplexe							
p_π	1.642	1.648	1.642	1.645	1.642	1.631	1.625
p_{π^*}	0.301	0.297	0.301	0.307	0.322	0.377	0.365
q_{Alkin}	0.024	0.012	0.011	0.001	–0.021	–0.071	–0.036
nicht-koordiniertes Alkin							
p_π	1.962	1.962	1.963	1.963	1.917	1.905	1.955
p_{π^*}	0.063	0.055	0.054	0.046	0.092	0.061	0.060

2.1.6 Diskussion der Ergebnisse

Der im Rahmen dieser Arbeit entwickelte Zugang zu Zeise-Salz analogen Alkinplatin(II)-Komplexen durch Substitution von *cis*-But-2-en in $[K(18C6)][PtCl_3(cis\text{-}MeHC{=}CHMe)]$ (**A2**) erlaubt im Vergleich zu alternativen Prozeduren, wie der Umsetzung von $M^I_2[PtCl_4]$ (M^I = Na, K), $M^I[PtCl_3(H_2C{=}CH_2)]$ oder $[K(18C6)]_2[Pt_2Cl_6]$ mit Alkinen, eine höhere strukturelle Vielfalt sowie deutlich mildere Reaktionsbedingungen. [6,14,15]

Als Precursorligand ist *cis*-But-2-en hierbei vorteilhaft, da er zum einen ausreichend flüchtig ist, um die Substitutionsreaktion schwächer gebundener Alkine voranzutreiben und zum anderen weniger stark gebunden ist als Ethen. So erfordert die Synthese von Alkinkomplexen $K[PtCl_3(R'R(OH)CC{\equiv}CC(OH)RR')]$ (R, R' = Me, Et, *t*-Bu, Ph) aus dem korrespondierenden Ethenkomplex $K[PtCl_3(H_2C{=}CH_2)]$ nach Chatt *et al*. [6] Temperaturen von ca. 60 °C, während eine vergleichbare Reaktion zur Bildung von $[K(18C6)][PtCl_3(t\text{-}BuC{\equiv}Ct\text{-}Bu)]$ aus $[K(18C6)][PtCl_3(cis\text{-}MeHC{=}CHMe)]$ im Zuge dieser Arbeit bei Raumtemperatur gelang.

Die in dieser Arbeit durchgeführten quantenchemischen Untersuchungen, speziell die „energy decomposition analysis" (EDA) sowie die NBO Analyse, zeigen bei den Alkinplatin(II)-Komplexen – analog zu den entsprechenden Olefinplatin(II)-Komplexen –einen großen Einfluss der back-donation auf die Stabilität der Pt–C-Bindung. Im allgemeinen ist aber der Alkinligand schwächer gebunden, wie ein Vergleich der Energien[1] ΔE_{diss} und ΔE_{int} erkennen lässt: In den Alkinkomplexen **A3a'**–**A7a'** wurden im Vergleich zu den Olefinkomplexen $[PtCl_3L]^-$ (L = *cis*-But-2-en, **A2a'**; COE, **B5a'**) kleinere Werte für ΔE_{diss} (27.1–28.4 kcal/mol *vs*. 30.4/31.7 kcal/mol) und weniger stark negative Werte für ΔE_{int} (–39.5…–41.6 kcal/mol *vs.* –44.9/–46.0 kcal/mol) berechnet. Interessanterweise nehmen die Komplexe mit dem

[1] Um eine Vergleichbarkeit zu gewährleisten, beziehen sich hier alle Werte auf die Gasphase ohne Berücksichtigung von BSSE-Effekten.

Cyclooctin-(**A9a'**) sowie dem Methoxycarbonyl-substituierten Alkinliganden (**A8a'**) hier eine Sonderrolle ein, da hier eine deutlich stärkere Pt–C-Bindung vorliegt (ΔE_{diss} = 30.8/39.8 kcal/mol, ΔE_{int} = –45.2/–46.6 kcal/mol; **A8a'/A9a'**), welche im Falle des Cyclooctinliganden sogar noch erheblich stärker als Platin–Olefin-Bindung ist. Grund hierfür ist zum einen die geringere Ligandenpräperationsenergie aufgrund der bereits vorliegenden Abwinkelung (C–C≡C 153°) im nicht-koordinierten COC. Zum anderen bewirkt die durch die Ringbildung bedingte Abwinkelung der Substituenten am Alkinliganden eine deutliche Variation der elektronischen Eigenschaften der Dreifachbindung was sich in einer deutlich stärkeren Wechselwirkung zum Platinatom, sowie eines größeren Anteils der back-donation (siehe NBO) niederschlägt.

Durch die im Rahmen dieser Arbeit durchgeführten Analysen der Olefin–Alkin-Liganden-substitution konnte ein Einblick in energetische Parameter von Alkin–Platin(II)-Bindungen sowie in den Substituenteneinfluss auf diese Bindungen gegeben werden. Die back-donation übt einen erheblichen Einfluss auf die Bindungssituation aus, was sich insbesondere in der Sonderstellung des Methoxycarbonyl-substituierten Alkinliganden sowie des gespannten Cyclooctinliganden (COC) widerspiegelt.

2.2 Isomerisierungsreaktionen an Zeise-Salz analogen Alkinplatin(II)-Komplexen

2.2.1 Einführung

Isomerisierungsreaktionen von Alkinen unter Bindungsmigration (Schema 6, **II** → **III**), Bildung von Allenen (**III** → **IV**) [27] sowie von 1,3-Dienen (**II** → **I**) sind von besonderem Interesse in der organischen Chemie und homogenen Katalyse. Obwohl 1,3-Diene thermodynamisch am stabilsten sind, werden Isomerisierungen von Alkinen zu 1,3-Dienen (**II** → **I**) nur vergleichsweise selten beobachtet. [31] Die Bildung von 1,3-Dienen ist sowohl unter stark basischen oder sauren Bedingungen als auch heterogen katalysiert beschrieben, wobei relativ drastische Bedingungen mit Temperaturen von 100–400 °C und eine geringe Selektivität vorherrschen. [28]

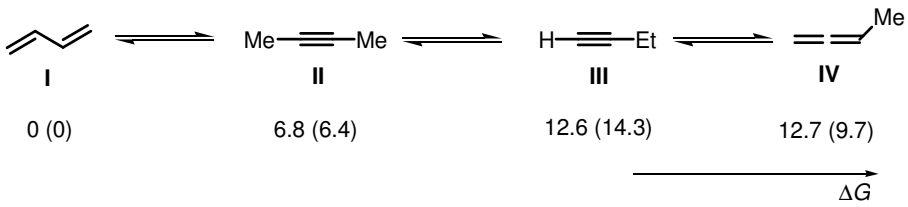

Schema 6. Freie Standardreaktionsenthalpie $\Delta_r G°$ (in kcal/mol) von verschiedenen But-2-in-isomeren basierend auf kalorimetrischen Untersuchungen [29] und DFT-Rechnungen (in Klammern; eigene Berechnungen).

Das erste Beispiel (1980) für eine Isomerisierung eines Alkins in ein 1,3-Dien durch ein Übergangsmetall ist an Propargylsilylethern als Substrat durch einen Hydridoruthenium-Komplex beschrieben. [30] Im Folgenden wurden zahlreiche Isomerisierungsreaktionen von inneren Alkinen durch Co-, Rh-, Ir-, Ru-, Re-, Pd-Metallkomplexe [31,32] und (metallfrei) durch Phosphinkatalysatoren [33] beobachtet. Der Substratumfang ist hierbei jedoch auf aktivierte Alkine mit elektronenziehenden Substituenten in α-Position beschränkt (Schema 7).

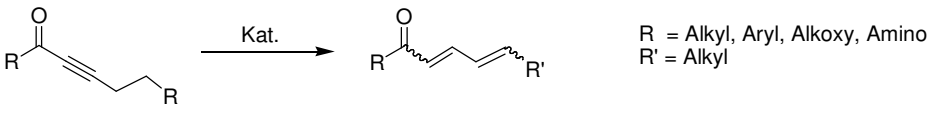

Schema 7.

Im Gegensatz dazu sind Reaktionen von nicht-aktivierten Alkinen zu 1,3-Dienen bedeutend weniger bekannt. Abgesehen von Alkinen mit perfluorierten Alkylsubstituenten ist nur die Isomerisierung des Cyclododecins zu (*E*,*Z*)-Cyclododeca-1,3-dien unter Verwendung eines Rhodiumkomplexes als Katalysator formuliert. [34]

2.2.2 Synthese und Charakterisierung

Unerwarteterweise zeigte eine Lösung des Zeise-Salz analogen Cyclooctinkomplexes [K(18C6)][$PtCl_3$(COC)] (**A9**) innerhalb einiger Wochen eine Isomerisierung zu einem Cycloocta-1,3-dien (1,3-COD) Komplex [K(18C6)]$_2$[($PtCl_3$)$_2$(μ-η^2:η^2-1,3-COD)]·Me_2CO (**B2**·Me_2CO) (Schema 8b). Diese Isomerisierung verlief sehr selektiv, wobei nach 8 Wochen > 90% der Ausgangsverbindung umgesetzt wurde. Als einziges weiteres Produkt wurde Cycloocta-1,3-dien gefunden. Der dinukleare Komplex **B2**·Me_2CO konnte mit einer Ausbeute von 60 % als gelbe kristalline Substanz isoliert werden und wurde mittels Elementaranalyse, ESI-MS und NMR-Spektroskopie sowie Röntgeneinkristallstrukturanalyse charakterisiert.

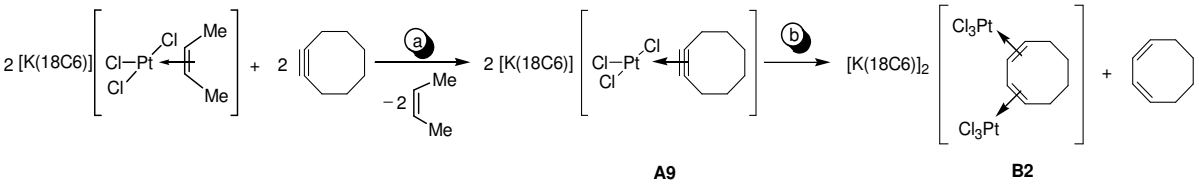

Schema 8.

Die ^{13}C-NMR-spektroskopischen Verschiebungen Δδ des Olefinfragmentes in **B2** (–41.9/ –47.7 ppm) stimmen mit den typischen Werten (CIS(=*C*H) = −40 … −55 ppm) für Olefinplatin(II)-Komplexe des Typs M^I[$PtCl_3$(R_2C=CR_2')] (M^I = [K(18C6)], [N(*n*-Bu)$_4$], [PPh_4]; R, R' = H, Alkyl, Aryl) überein. [13,14] Für die $^1J_{Pt,C}$-Kopplungskonstanten (204/259 Hz) werden hingegen größere Werte als in den aufgeführten Olefinkomplexen beobachtet (180–193 Hz).

2.2.3 Molekülstruktur von [K(18C6)]$_2$[($PtCl_3$)$_2$(μ-η^2:η^2-1,3-COD)] (B2)

Die Molekülstruktur von **B2** in **B2**·Me_2CO sowie ausgewählte strukturelle Parameter sind in Abbildung 4 dargestellt. Hierbei wird ersichtlich, dass beide Platinatome durch einen verbrückenden μ-η^2:η^2-Cycloocta-1,3-dien Liganden verknüpft sind. Im Unterschied zu der überwiegenden Anzahl von 1,3-Butadien-Komplexen (vgl. als Beispiel [{$PtCl_2$(PMe_2Ph)$_2$}$_2$(μ-η^2:η^2-C_4H_6)] [35]) sind die Doppelbindungen in **B2** nicht konjugiert, wie der Diederwinkel C1=C2–C3=C4 von 59.7(9)° belegt. Im Komplex ist der 1,3-COD-Ligand um mehr als 20° stärker verdrillt als im nicht-koordinierten 1,3-COD (37.8(1)°). [36]

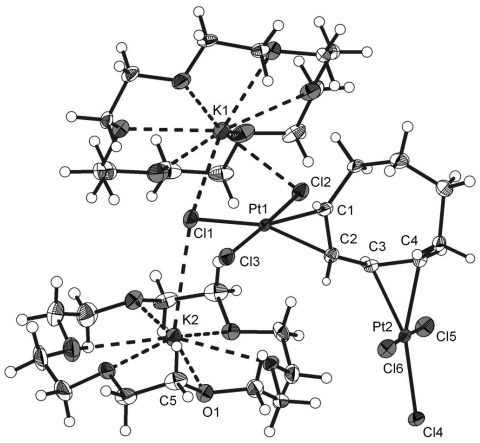

Abbildung 4. Molekülstruktur von $[K(18C6)]_2[(PtCl_3)_2(\mu\text{-}\eta^2\text{:}\eta^2\text{-}1,3\text{-COD})]$ (**B2**) in Kristallen von **B2**·Me_2CO. Die Ellipsoide sind mit einer Wahrscheinlichkeit von 30% dargestellt. Pt1–C1 2.149(6), Pt1–C2 2.152(6), Pt2–C3 2.153(7), Pt2–C4 2.174(7), C1–C2^{a}1.412(9) (1.347(5)), C2–C3^{a}1.513(9) (1.47(1)), C3–C4^a 1.394(9) (1.347(5)), Cl–C2–C3–C4^a 59.7(9). a) Werte des nicht-koordinierten 1,3-COD sind in Klammern angegeben.

2.2.4 DFT-Rechnungen

Um weitere Einblicke in die Thermodynamik der Isomerisierung des Cyclooctinliganden zu erhalten, wurde der betreffende Komplex mittels quantenchemischer Methoden simuliert. Einen genaueren Einblick erlaubt hierbei die „energy decomposition analysis“ (EDA). Die freie Standardreaktionsenthalpie der Reaktion nach Schema 9 wird durch ein Lösungsmittel stark beeinflusst. Während unter Gasphasenbedingungen die Reaktion stark endergonisch ist ($\Delta_r G°_{GP}$ = 16.5 kcal/mol), ist unter Berücksichtigung von Lösungsmitteleffekten ($CHCl_3$) die Reaktion stark exergonisch ($\Delta_r G°_{CHCl_3}$ = −15.9 kcal/mol). Das ist auf die starke Solvatisierung der doppelt negativ geladenen Spezies **B2a'** zurückzuführen.

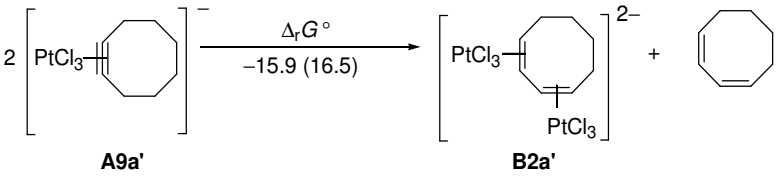

Schema 9. Berechnete Standardreaktionsenthalpien (in kcal/mol) unter Berücksichtigung von $CHCl_3$ als Lösungsmittel (ΔG_{CHCl_3}) und unter Gaspasenbedingungen in Klammern.

Um weitere Einblicke in die elektronische Struktur des dinuklearen Komplexes zu erhalten, wurde die Dissoziation des Komplexes in nicht-koordiniertes 1,3-COD und zwei $PtCl_3^-$-Fragmente in zwei Teilschritte unterteilt (Schema 10). Zum Vergleich sind in analoger Weise die Zeise-Salz Olefinkomplexe $[PtCl_3L]^-$ (L = COE, *cis*-But-2-en) berechnet worden. Im Folgen-

den wird nur auf die um den Lösungsmitteleffekt ($CHCl_3$) korrigierten Werte eingegangen (für die Werte in der Gasphase vgl. Supplemental Material Anhang **B**).

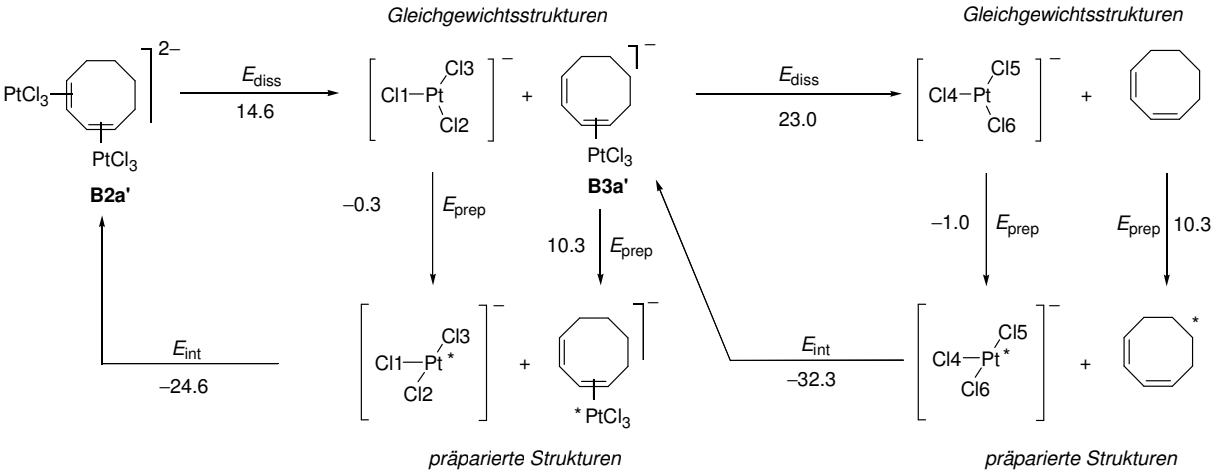

Schema 10. Energien in kcal/mol unter Berücksichtigung von $CHCl_3$ als Solvens.

Die Dissoziation des ersten $PtCl_3^-$-Fragmentes erfordert signifikant weniger Energie (14.6 kcal/mol) als der zweite Dissoziationsschritt (23.0 kcal/mol). Der zweite Wert liegt in einer ähnlichen Größenordnung wie die Werte in den Zeise-Salz analogen Olefinkomplexen des Typs $[PtCl_3L]^-$ (26.7 kcal/mol, Tabelle 5). Die Auswertung der Präperationsenergien ΔE_{prep} der Olefinliganden ergibt für 1,3-COD (10.3 kcal/mol) vergleichbare Werte wie für COE und *cis*-But-2-en (9.2 kcal/mol). Der Unterschied der Dissoziationsenergien der beiden Stufen ($\Delta\Delta E_{diss}$ = 8.4 kcal/mol) ist damit auf den Unterschied der Wechselwirkungsenergien ΔE_{int} (7.7 kcal/mol) zurückzuführen, welche ihrerseits wahrscheinlich in den unterschiedlichen Coulombwechselwirkungen der beiden Teilreaktionen (anionisch/anionisch *vs.* anionisch/ neutral) begründet sind. Diese Ergebnisse zeigen, dass die Triebkraft der Reaktion nach Schema 9 nicht auf unterschiedliche Pt–C-Bindungsstärken im Edukt oder Produkt zurückzuführen ist, sondern im Abbau der Ringspannung des Cyclooctinliganden begründet liegt ($\Delta_r G°$ = – 27.0 kcal/mol Schema 11).

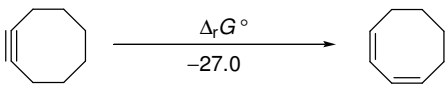

Schema 11. Energien in kcal/mol.

Die elektronische Bindungssituation der 1,3-COD-Liganden in $[(PtCl_3)_2(\mu\text{-}\eta^2\text{:}\eta^2\text{-1,3-COD})]^{2-}$ (**B2a'**) und $[PtCl_3(\eta^2\text{-1,3-COD})]^-$ (**B3a'**) sowie des *cis*-But-2-en- und COE-Liganden in

$[PtCl_3L]^-$ (L = *cis*-But-2-en, **A2a'**; COE, **B5a'**) kann mittels CDA [37] sowie NBO-Analyse [26] genauer untersucht werden. Ausgewählte Ergebnisse sind in Tabelle 5 aufgeführt. Die CDA-Analyse ergibt für den dinuklearen Komplex **B2a'** deutlich höhere Werte *d*/*b* (*d* = donation, *b* = back-donation) als für die analogen mononuklearen Komplexe **B3a'**, **B5a'**, **A2a'** (1.205 *vs.* 0.864 … 1.011), was auf eine höhere Olefin→Pt donation (0.300 *vs.* 0.228 … 0.278) sowie eine geringere back-donation (0.249 *vs.* 0.264 … 0.289) im Komplex **B2a'** hinweist. Die NBO Analyse liefert ein ähnliches Bild: Hier beobachtet man etwas geringere Besetzungszahlen der π-Bindung (P_π = 1.621, **B2a'** *vs.* 1.626 … 1.636, **B3a'**, **B5a'**, **A2a'**) sowie geringere Besetzung des antibindenden π*-Orbitals (P_{π^*} = 0.327, **B2a'** *vs.* 0.348 … 0.351, **B3a'**, **B5a'**, **A2a'**).

Tabelle 5. Charakteristische Bindungsparameter der Komplexanionen $[(PtCl_3)_2(\mu\text{-}\eta^2\text{:}\eta^2\text{-}1,3\text{-COD})]^{2-}$ (**B2a'**), $[PtCl_3(\eta^2\text{-}1,3\text{-COD})]^-$ (**B3a'**), und $[PtCl_3L]^-$ (L = *cis*-But-2-en, **A2a'**; COE, **B5a'**). Die Ergebnisse der „energy decomposition analysis" (EDA) (ΔE_{diss} = Bindungsdissoziationsenergie, ΔE_{int} = Wechselwirkungsenergie, ΔE_{prep} = Präperationsenergie sowie der „charge decomposition analysis" (CDA) (*d* = donation, *b* = back-donation und der NBO-Analyse (P_π/P_{π^*} = Besetzungszahl der π/π*-Orbitale der Olefine, q_{PtCl3}- = Ladung des $PtCl_3^-$-Fragmentes; Werte in Elektronen; alle Energien in kcal/mol).

	B2a'	**B3a'**	**A2a'**	**B5a'**
L	η^2,η^2-1,3-COD	η^2-1,3 COD	*cis*-But-2-en	COE
EDA				
ΔE_{diss} [a]	14.6	23.0	26.4	26.7
$\Delta E_{prep}(PtCl_3^-)$ [a]	–0.3	–1.0	–0.8	–0.8
$\Delta E_{prep}(L)$ [a]	10.3	10.3	9.5	9.2
ΔE_{int} [a]	–24.6	–32.3	–35.2	–35.1
CDA				
donation (*d*)	0.300	0.278	0.228	0.278
back-donation (*b*)	0.249	0.275	0.264	0.289
repulsive polarization	–0.667	–0.689	–0.702	–0.705
residual term	–0.020	–0.017	–0.018	–0.019
d/*b*	1.205	1.011	0.864	0.962
NBO				
Olefinkomplex				
P_π	1.621/1.621	1.636/1.950	1.626	1.628
P_{π^*}	0.327/0.327	0.351/0.056	0.348	0.349
q_{PtCl3}-	–1.011	–0.965	–0.999	–0.981
nicht-koordiniertes Olefin				
P_π	1.950	1.931/1.931	1.961	1.964
P_{π^*}	0.056	0.075/0.075	0.066	0.052

a) Werte sind um den Lösungsmitteleffekt von $CHCl_3$ korrigiert (PCM).

2.2.5 Diskussion der Ergebnisse

Die platinassistierte Isomerisierungsreaktion COC → 1,3-COD ([K(18C6)][$PtCl_3$(COC)], **A9** → [K(18C6)]$_2$[($PtCl_3$)$_2$(1,3-COD)], **B2**) stellt die erste Beschreibung einer Isomerisierung von Cyclooctin in 1,3-Cyclooctadien dar. Die quantenchemischen Rechnungen legen hierbei nahe, dass die Triebkraft der Isomerisierung wesentlich auf eine Verringerung der Ringspannung im Cyclooctin (COC) zurückzuführen ist. Die Struktur des μ-1,3-COD-Liganden im Komplex **B2** zeigt klar, dass das Doppelbindungssystem nicht konjugiert ist, was Komplex **B2** von den meisten anderen 1,3-Dien-Komplexen charakteristisch unterscheidet. Somit handelt es sich bei **B2** um einen Bis(olefin)-Platinkomplex und die Olefin–Platin-Bindungen in diesem Komplex lassen sich mit denen in klassischen Zeise-Salz analogen Olefinkomplexen vergleichen.

Die Abdissoziation von 1,3-COD in **B2** ist ein konsekutiver Prozess:

$$[(PtCl_3)_2(1,3\text{-COD})]^{2-} \xrightarrow[-\,[PtCl_3]^-]{\text{a}} [PtCl_3(1,3\text{-COD})]^- \xrightarrow{\text{b}} [PtCl_3(1,3\text{-COD})]^- + 1,3\text{-COD}$$

Die Abspaltung von 1,3-COD im zweiten Schritt (**b**) geht wie die Abspaltung von Olefinen aus Zeise-Salz-Komplexen $[PtCl_3L]^-$ (L = *cis*-But-2-en, COE) von einem einfach negativ geladenen Komplexanion aus. In beiden Komplextypen ergibt die EDA und CDA sehr ähnliche energetische Parameter (ΔE_{int}, ΔE_{prep}; *d*/*b*-Verhältnis). Im ersten Schritt (**a**) handelt es sich allerdings um die Abspaltung eines Olefins (1,3-COD) aus einem zweifach negativ geladenen Komplexanion. Das spiegelt sich bei der EDA in einer signifikant geringeren Dissoziationsenergie ΔE_{diss} wider, was eine zwanglose Erklärung in der elektrostatischen Abstoßung der beiden einfach negativ geladenen Fragmente findet. Des Weiteren zeigt die CDA auch eine geringere back-donation.

Somit lässt sich zusammenfassend feststellen, dass neben der erstmalig nachgewiesenen metallassistierten Isomerisierung von Cyclooctin in 1,3-Cyclooctadien eine quantenchemische Analyse dieses Prozessen einen detaillierten Einblick in Struktur, Bindung und Reaktivität von Olefin/Alkin–Platinkomplexen ermöglicht.

2.3 Synthese, Charakterisierung und Reaktivität von dinuklearen Olefin- und Alkinplatin(II)-Komplexen

2.3.1 Einführung

Während die Synthese des klassischen Zeise-Dimers $[\{PtCl_2(C_2H_4)\}_2]$ (**C1**), [40] durch direkte Umsetzung von $K_2[PtCl_4]$ mit Ethen in salzsaurer wässriger Lösung beschrieben wird (Schema 12, Pfad **c**), sind analoge Reaktionen mit höheren Olefinen aufgrund der geringen Löslichkeit der Olefine kaum möglich. Die Darstellung analoger dinuklearer Komplexe mit höheren Olefinen erfolgte deshalb durch Substitution des Ethens im Zeise-Dimer **C1** durch ein höheres Olefin, das in stöchiometrischer Menge eingesetzt werden muss (Schema 12, Pfad **d**). [38,39]

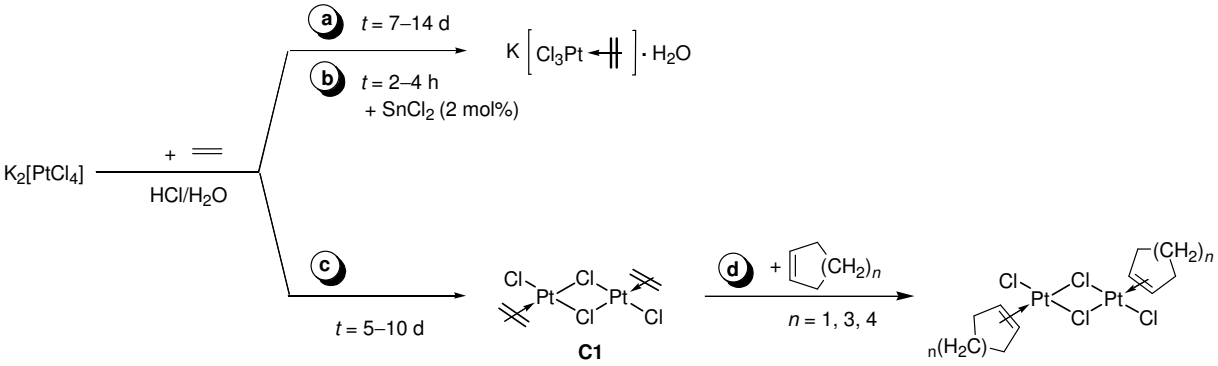

Schema 12.

Zeise's Dimer $[\{PtCl_2(C_2H_4)\}_2]$ (**C1**) reagiert mit einer Vielzahl von Nucleophilen unter Spaltung der Pt–μ-Cl-Brücke. [38,42,47] So führt z.B. die Reaktion von **C1** mit einem Überschuss an Ethen zur Bildung von *trans*-$[PtCl_2(C_2H_4)_2]$ (**C13**), [40] welches auch als kurzlebiges Intermediat beim Selbstaustausch von Ethen in $[PtCl_3(C_2H_4)]^-$ postuliert wurde. [41,42]

Brückenspaltungen in Zeise-Dimer-Komplexen $[\{PtCl_2L\}_2]$ (L = Ethen, Styren, COE) mit Olefinen L (L = Ethen, Styren, COE) sind in der Regel reversibel. [38,47] Es wurden Gleichgewichtskonstanten von K = 0.0235 ± 0.003 (Styren), 2.05 ± 0.06 (COE) und 6.8 ± 0.6 (Ethen) M^{-1} bestimmt, woraus Aussagen über die relative Stabilität der Olefinkomplexe abgeleitet werden können. [47] Die gebildeten mononuklearen Komplexe unterliegen darüber hinaus *cis-trans*-Isomerisierungsreaktionen. Neben sterischen Faktoren ist für die Stabilität der Isomere vor allem der *trans*-Einfluss entscheidend, wobei zwei Liganden mit starkem *trans*-Einfluss eine gegenseitige *trans*-Position meiden. [43] Die nach abnehmmenden *trans*-

Einfluss geordnete Ligandenreihe, [44] $CH_3^-, H^- > C_2H_4$, CN^-, CO > H_2O, zeigt, dass π-Akzeptoren einen sehr starken *trans*-Einfluss ausüben.

So reagiert Zeise's Dimer **C1** mit Ethen nach Schema 13 zunächst unter Bildung des mononuklearen *trans*-konfigurierten Platin(II)-Komplexes *trans*-$[PtCl_2(C_2H_4)_2]$ (**C13**) aufgrund des größeren *trans*-Effektes des Ethens im Vergleich zum Chlorido-Liganden. **C13** isomerisiert jedoch anschließend unter Bildung des Komplexes *cis*-$[PtCl_2(C_2H_4)_2]$ (**C10**), welcher von Elding *et al.* unter Ethen-Atmosphäre isoliert werden konnte. [47]

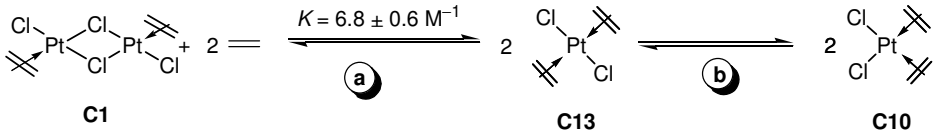

C1 **C13** **C10**

Schema 13.

Die Darstellung dinuklearer Zeise-Dimer analoger Bisalkinkomplexe $[\{PtCl_2(RC{\equiv}Ct\text{-}Bu)\}_2]$ (R = Et, *t*-Bu) gelang Chatt ausgehend von $K_2[PtCl_4]$ mit sterisch anspruchsvoll *tert*-butylsubstiuierten Alkinen *t*-BuC≡CR (R = Et, *t*-Bu) in Aceton, [6] während die analoge Umsetzung mit sterisch weniger anspruchsvoll substiuierten Alkinen RC≡CR' (R, R' = H, Me, Et, *n*-Pr, *i*-Pr, *n*-Bu, *t*-Bu, Ph) zu Zersetzungsreaktionen unter Bildung von metallischem Platin führte. [6]

Im Rahmen dieser Arbeit sollte deshalb die Reaktion ausgehend von Zeise's Dimer mit sterisch wenig anspruchsvollen Substituenten in nicht koordinierenden Lösungsmitteln (wie $CH_2Cl_2/CHCl_3$) untersucht werden.

2.3.2 Synthese und Charakterisierung von dinuklearen Olefinplatin(II)-Komplexen

Erste orientierende Untersuchungen zeigten, dass die Umsetzung von $K_2[PtCl_4]$ mit *cis*-But-2-en aufgrund der geringen Löslichkeit des Olefins eine erhebliche Reaktionszeit von mehreren Wochen erfordert (Schema 14). In der Literatur ist bereits bekannt, dass die Reaktionszeit für die analoge Synthese des Zeise-Salzes $K[PtCl_3(C_2H_4)]\cdot H_2O$ ausgehend von $K_2[PtCl_4]$ und Ethen durch Einsatz von $SnCl_2$ in katalytischen Mengen erheblich verkürzt werden kann (Schema 12, Pfad **b**). [45,46] Aus diesem Grunde wurde im Rahmen dieser Untersuchungen der Zeise-Dimer analoge *cis*-But-2-en-Komplex $[\{PtCl_2(MeHC{=}CHMe)\}_2]$ (**C2**) unter Verwendung von $SnCl_2/HCl_{aq}$ als Katalysator dargestellt, wodurch eine erhebliche Verkürzung der Reaktionszeit erreicht werden konnte (Schema 14, Pfad **b/c**).

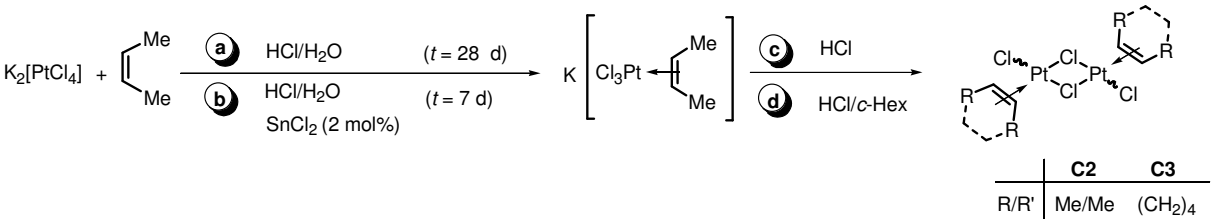

Schema 14.

Durch Umsetzung des Zwischenproduktes K[$PtCl_3$(MeHC=CHMe)] aus der Synthese von **C2** mit Cyclohexen konnte darüber hinaus der analoge dinukleare Cyclohexenkomplex [{$PtCl_2$(*c*-Hex)}$_2$] (**C3**) erhalten werden (Schema 14, **b/d**). Die Komplexe **C2** und **C3** konnten als orangefarbene, kristalline, mäßig luftempfindliche Substanzen in guten bzw. moderaten Ausbeuten (75/60%) isoliert werden. Sie wurden mittels Elementaranalyse, NMR-Spektroskopie sowie Röntgeneinkristallstrukturanalyse (**C2**) charakterisiert. Die in Tabelle 6 gegebenen ^{1}H- und ^{13}C-NMR-spektroskopischen Verschiebungen Δδ der Olefinliganden in **C1–C3** (–35.8 ... –51.2 ppm) entsprechen etwa den typischen Werten (–40 … –55 ppm) für Zeise-Salz analoge Olefinplatin(II)-Komplexe M^I[$PtCl_3$(R_2C=CR_2')] (M^I = [K(18C6)], [N(*n*-Bu)$_4$], [PPh_4]; R, R' = H, Alkyl, Aryl). [13,14] Während für die $^1J_{Pt,C}$-Kopplungskonstanten (182−199 Hz) Werte in der gleichen Größenordnung (180–193 Hz) [13,14] wie in den Zeise-Salz analogen Olefinplatin(II)-Komplexen M^I[$PtCl_3$(R_2C=CR_2')] (M^I = [K(18C6)], [N(*n*-Bu)$_4$], [PPh_4]; R, R' = H, Alkyl, Aryl) erhalten werden, findet man für mononukleare neutrale Platin(II)-Komplexe vom Typ *cis*-[$PtCl_2L_2$] (L = Ethen, 1,5-COD) signifikant kleinere $^1J_{Pt,C}$-Kopplungskonstanten (131/152 Hz). [47,48]

Tabelle 6. Ausgewählte ^{1}H- und ^{13}C-NMR-spektroskopische Daten (δ in ppm, *J* in Hz) von [{$PtCl_2L$}$_2$] (L = Ethen, **C1**; *cis*-But-2-en, **C2**; *c*-Hex, **C3**) und Zeise-Salz analoger Platin(II)-Komplexe K[$PtCl_3$(RHC=CHR)] (R = H, Me).

	δ(=*C*H)	Δδ[a]	$^1J_{Pt,C}$	δ(=C*H*)	$^2J_{Pt,H}$	Δδ[a]
C1	72.1	–51.2	199	4.82	74	–0.46
C2	86.9/87.4	–37.3/–36.8	190/182	5.55	71	0.10
C3	91.5/90.9	–35.8/–36.4	196/[c]	5.96	81	0.30
K[$PtCl_3$(C_2H_4)]·H_2O[b]	68.0	–55.3	192	4.46	64	–0.82
K[$PtCl_3$(C_4H_8)]	84.2	–40.0	183	5.13	76	–0.32

a) $\Delta\delta = \delta_{Komplex} - \delta_{nichtkoord.\ Olefin}$. b) Werte entnommen aus Ref. [14]. c) Aufgrund der Intensitätsverhältnisse nicht gefunden.

2.3.3 Reaktivität der dinuklearen Olefinplatin(II)-Komplexe gegenüber Alkinen

Im Zuge dieser Arbeit sollte die Reaktivität von Olefinkomplexen vom Zeise-Dimer-Typ gegenüber Alkinen RC≡CR‘ untersucht werden. Hierbei war eine starke Abhängigkeit von der Art der Substituenten R/R’ am Alkin zu beobachten. Im Falle sterisch wenig anspruchsvoll substituierter Alkine RC≡CR‘(R/R‘ = Me/Me; Et/Et, Me/*n*-Pr) erfolgte eine schnelle [2+2]-Cycloadditionsreaktion unter Bildung von mononuklearen Cyclobutadienkomplexen [$PtCl_2(C_4R_2R'_2)$] (**C4–C6**) in Ausbeuten von 73–81% (Schema 15, Pfad **a**). Die Cycloaddition des phenylsubstituierten Alkins verlief hierbei regioselektiv, wobei aus den NMR-Daten auf eine dinukleare Struktur des Komplexes ([{$PtCl_2(C_4Me_2Ph_2)$}$_2$], **C7**) geschlossen wurde. Im Gegensatz hierzu verläuft die analoge [2+2]-Cycloaddition des Me/*n*-Pr-substituierten Alkins nicht regioselektiv, sodass beide Isomere des Komplexes **C6** im Verhältnis 1:1 erhalten wurden (Schema 15).

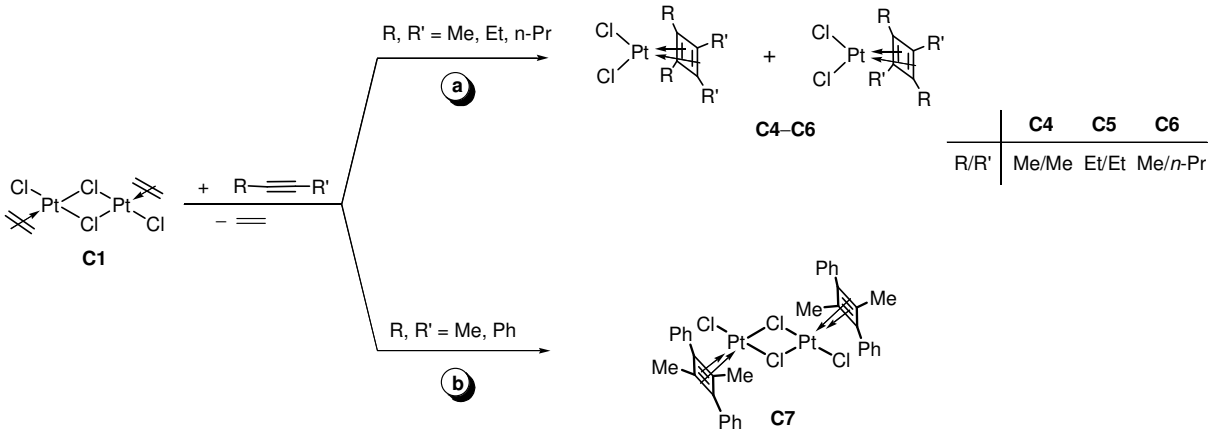

Schema 15.

Im Unterschied zu den sterisch wenig anspruchsvollen *n*-alkyl- bzw. phenylsubstituierten Alkinen führen analoge Reaktionen mit *tert*-butylsubstituierten Alkinen RC≡C*t*-Bu (R = Me, *t*-Bu) zur sofortigen Bildung dinuklearer Alkinkomplexe [{($PtCl_2$(RC≡C*t*-Bu)}$_2$] (R = Me, **C11**; *t*-Bu, **C12**), die in sehr guten Ausbeuten (90/95%) isoliert wurden (Schema 16, Pfad **a**).
Des Weiteren hängt die Reaktivität maßgeblich davon ab, ob das freigesetzte Ethen aus dem System entfernt wird (wie bei den voranstehenden Versuchen) oder nicht. Führt man analoge Reaktionen in einem abgeschmolzenen NMR-Röhrchen durch, sodass das freigesetzte Ethen nicht entweichen kann, so lassen sich NMR-spektroskopisch die gemischten Ethen–Alkin-Komplexe [$PtCl_2(H_2C{=}CH_2)$(RC≡C*t*-Bu)] (R = Me, **C8**; *t*-Bu, **C9**) nachweisen (Schema 16, **b/c**). Im Falle von *t*-BuC≡C*t*-Bu wird darüber hinaus die Bildung des dinuklearen Komplexes **C12** sowie von *cis*-[$PtCl_2(H_2C{=}CH_2)_2$] (**C10**), welcher bereits in der Literatur beschrieben ist,

[47] nachgewiesen. Abgesehen von **C8** bilden sich bei der Umsetzung von MeC≡C*t*-Bu geringe Mengen des Cyclobutadienkomplexes [$PtCl_2(C_4Me_2t\text{-}Bu_2)$] (**C16**) sowie von **C10**.

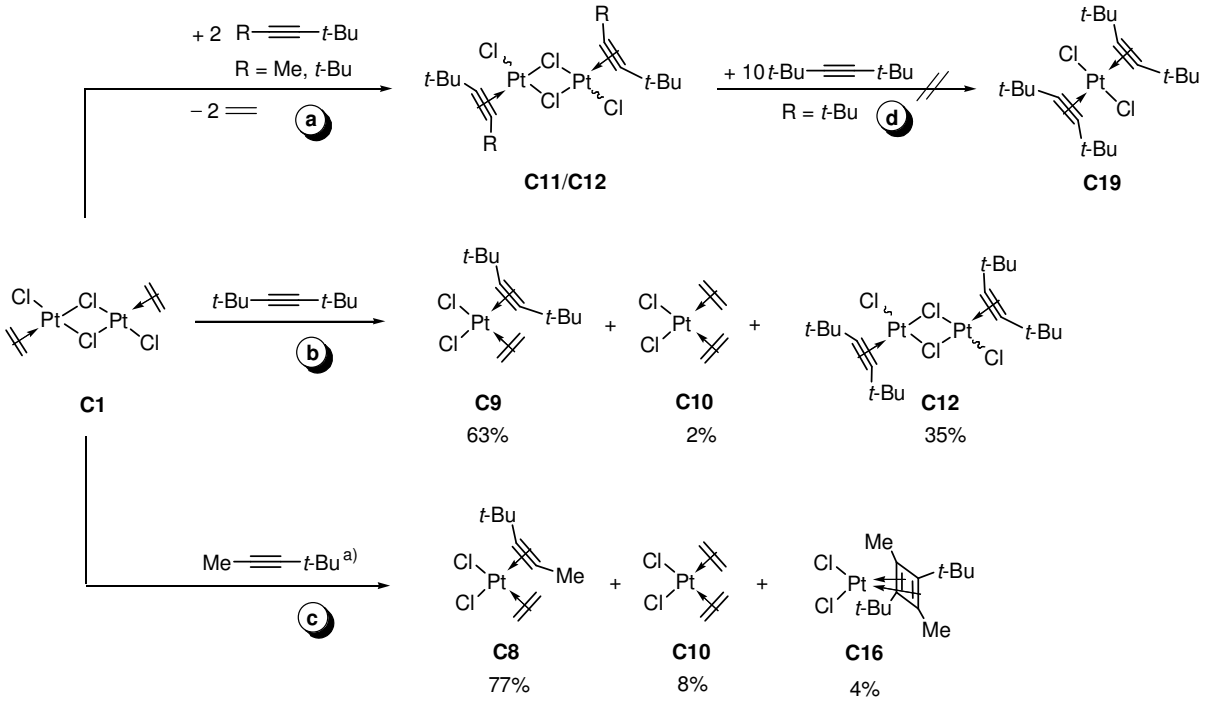

Schema 16. a) Zusätzlich enthielt die Reaktionslösung noch 11% von **C1**.

Die in Tabelle 7 gegebenen ^{13}C- und ^{195}Pt-NMR-spektroskopischen Verschiebungen der Olefin- bzw. Alkinliganden sowohl der mononuklearen gemischten Ethen–Alkin-Komplexe [{$PtCl_2(CH_2{=}CH_2)(RC{\equiv}Ct\text{-}Bu)$}$_2$] (R = Me, **C8**; *t*-Bu, **C9**); [{$PtCl_2(CH_2{=}CH_2)_2$] (**C10**) als auch der dinuklearen Komplexe [{$PtCl_2(RC{\equiv}Ct\text{-}Bu)$}$_2$] (R = Me, **C11**; *t*-Bu, **C12**) stimmen mit den typischen Werten für Zeise-Salz analoge Olefin- und Alkinkomplexe gut überein. [13,14,15,49] Charakteristische Unterschiede zwischen den einzelnen Komplextypen sind nicht zu beobachten. Für die $^1J_{Pt,C}$-Kopplungskonstanten werden jedoch charakteristische Unterschiede sowohl für die Olefin- als auch für die Alkinliganden zwischen den einzelnen Komplextypen (mononukleare neutrale Ethen–Alkin-Komplexe **C8/C9**; [{$PtCl_2(CH_2{=}CH_2)_2$], **C10**; dinukleare neutrale Alkinkomplexe **C11/C12**; mononukleare anionische Olefin- und Alkinkomplexe vom Zeise-Salz-Typ) beobachtet, sodass aus der Größe dieser Kopplungskonstanten auf den Komplextyp geschlossen werden kann (Tabelle 7).

Signalaufspaltungen in den NMR-Spektren der dinuklearen Komplexe **C1–C3**, **C11** und **C12** infolge des Vorliegens von Konfigurations- und Konformationsisomeren in Lösung werden in Kapitel 2.3.5 diskutiert.

Tabelle 7. Ausgewählte ^{13}C- und ^{195}Pt-NMR spektroskopische Daten (δ in ppm, *J* in Hz) von $[PtCl_2(CH_2{=}CH_2)(RC{\equiv}Ct\text{-}Bu)]$ (R = Me, **C8**; *t*-Bu, **C9**); $[\{PtCl_2(CH_2{=}CH_2)_2]$ (**C10**), $[\{PtCl_2(RC{\equiv}Ct\text{-}Bu)\}_2]$ (R = Me, **C11**; *t*-Bu, **C12**) und $M^I[PtCl_3(R_2C{=}CR_2')]$ ($Z_=$); $M^I[PtCl_3(RC{\equiv}CR')]$ ($Z_\equiv$), M^I = [K(18C6)], [N(*n*-Bu)$_4$], [PPh$_4$]; R, R' = H, Alkyl, Aryl) [13,15,38,49].

	δ(=*C*H)	Δδ[a]	$^1J_{Pt,C}$	δ(≡*C*R)	Δδ[a]	$^1J_{Pt,C}$	δ(^{195}Pt)
C8	80.2	–43.1	141	74.9/84.8	1.2/–3.2	115/156	–3145
C9	80.4	–42.9	138	85.9	–1.6	151	–3143
C10	84.3	–39.0	131				–3642
C11				70.0/80.0[b]	–3.7/–8.0	190/224	–1960[b]
				69.7/79.5[c]	–4.0/–8.5	[d]/228	–1955[c]
				69.4/79.4[c]	–4.3/–8.6	[d]/[d]	–1971[c]
C12				80.7	–6.4	221	–1968[b]
				80.6	–6.5	231	–2005[c]
$Z_=$		–40… –55	180–193				
$Z_\equiv$					–5.6… –17.8	173–236	

a) $\Delta\delta = \delta_{komplex} - \delta_{nichtkoord.Ligand}$. b) Hauptisomer. c) Nebenisomer. d) Aufgrund der Intensitätsverhältnisse nicht gefunden.

Aus chemiehistorischer Sicht ist es von Interesse zu klären, warum Chatt *et al*. in seinen klassischen Arbeiten zur Synthese von Alkinkomplexen vom Zeise-Salz-Typ $K[PtCl_3(RC{\equiv}CR')]$ durch Umsetzung von $K_2[PtCl_4]$ oder Zeise's Dimer mit Alkinen konstatiert, dass nur *tert*-butylsubstituierte Alkine oder solche mit C(OH)RR`-Substituenten eingesetzt werden können. [6] In der vorliegenden Arbeit konnten dagegen auf analogem Wege eine breite Palette von Alkinkomplexen $K[PtCl_3(RC{\equiv}CR')]$ (R, R' = *n*-Alkyl, *tert*-Alkyl, Ph) und $[\{PtCl_2(RC{=}Ct\text{-}Bu)\}_2]$ (R, R' = Me, *t*-Bu) synthetisiert werden. Wesentlicher Grund dafür ist das verwendete Lösungsmittel: Die eigenen Arbeiten wurden in Dichlormethan durchgeführt, während Chatt in Aceton gearbeitet hat. Dichlormethan hat den Vorteil, dass es nicht als Konkurrenzdonor für das Alkin wirkt, wie ein Vergleich der Donorzahlen nach Gutmann zeigt (*DN*(Aceton) = 17.0 *vs*. *DN*(CH_2Cl_2) = 1). [50] Des Weiteren – und das ist wahrscheinlich der entscheidende Grund – weist Aceton durch die Carbonylgruppe eine höhere Reaktivität auf, sodass unter den Reaktionsbedingungen bedingt durch die Lewis-Acidität des Platins Aldoladditions- und Aldolkondensationsreaktionen stattfinden, die neben 4–Hydroxy-4-Methyl-2-pentanon und 4-Methyl-pent-3-en-2-on zu oligomeren Verbindungen mit der Struktureinheit Me–$(MeC{=}CH)_n$–C(O)Me (*n* = 5–7) führen.

2.3.4 Strukturelle Aspekte von dinuklearen Olefin- und Alkinplatin(II)-Komplexen

Die Komplexe [{($PtCl_2$(MeC≡C*t*-Bu)}$_2$] (**C11**) und [{($PtCl_2$(*t*-BuC≡C*t*-Bu)}$_2$] (**C12**) stellen die ersten Vertreter von strukturell charakterisierten Zeise-Dimer analogen Alkinkomplexen dar. Darüberhinaus konnten von dem dinuklearen Komplex [{$PtCl_2$(MeHC=CHMe)}$_2$] (**C2**) Kristalle erhalten werden, welche für eine Einkristallstrukturanalyse geeignet sind. Die entsprechenden Molekülstrukturen sind in Abbildung 5 dargestellt. Sowohl der Olefinkomplex **C2** als auch der Alkinkomplex **C11** liegen im Kristall in der *transoiden*-Konfiguration vor. Der analoge *t*-BuC≡C*t*-Bu Komplex **C12** kristallisierte hingegen in zwei Konfigurationsisomeren, in denen die Alkinliganden einerseits in der *transoiden*- (**C12a**) und andererseits in der *cisoiden*-Konfiguration (**C12b**·$CHCl_3$) vorliegen.

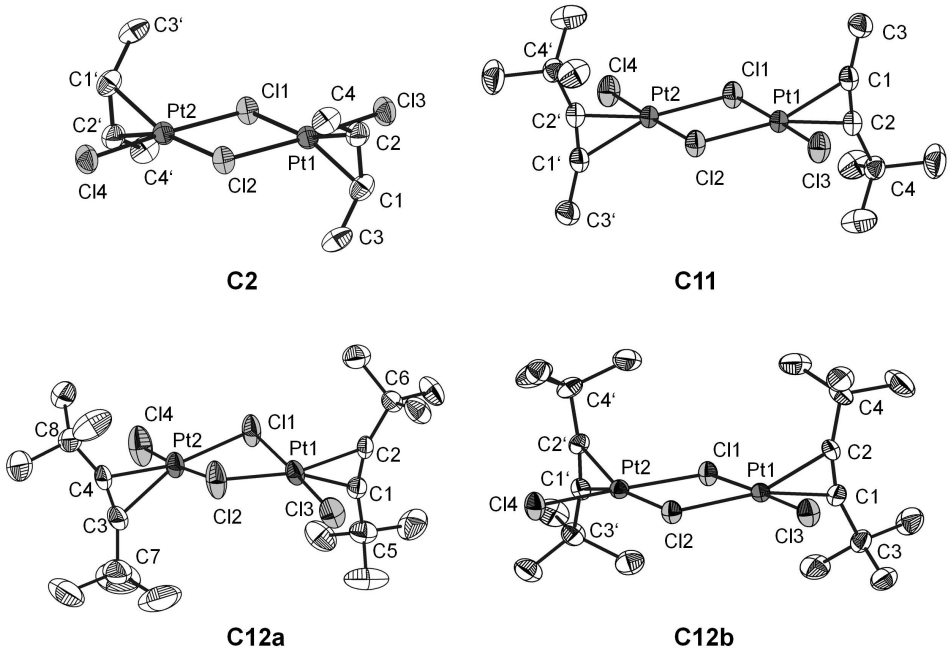

Abbildung 5. Molekülstrukturen von [{$PtCl_2$(*cis*-MeHC=CHMe)}$_2$] (**C2**), [{($PtCl_2$(MeC≡C*t*-Bu)}$_2$] (**C11**), *trans*-[{($PtCl_2$(*t*-BuC≡C*t*-Bu)}$_2$] (**C12a**) und *cis*-[{($PtCl_2$(*t*-BuC≡C*t*-Bu)}$_2$] (**C12b**) in Kristallen von **C12b**·$CHCl_3$. Die Ellipsoide sind mit einer Wahrscheinlichkeit von 50% dargestellt. H-Atome sind der Übersichtlichkeit halber nicht dargestellt.

Alle dinuklearen Komplexen (**C2**, **C11**, **C12a**, **C12b)** zeigen die typische Struktur mit einem nahezu senkrecht zur Koordinationsebene (Pt1,Cl1,Cl2,Cl3/Pt2,Cl1,Cl2,Cl4) stehenden π-Liganden (Φ($PtCl_3$/PtC_2): 87.5(2)–89.8(2)°, Tabelle 8). Während die Pt–C- sowie C≡C/C=C-Bindungslängen nach dem 3σ-Kriterium gleich sind, werden für die Pt–Cl-Bindungen Unterschiede beobachtet; die Pt–μ-Cl-Bindungen sind charakteristisch länger als die terminalen Pt–Cl-Bindungen (2.330(1)–2.378(3) Å *vs.* 2.262(1)–2.278(3) Å). Des Weiteren spiegelt sich in **C2** für den μ-verbrückenden Choridoliganden in *trans*-Position zum *cis*-But-2-en-Liganden

eine längere Pt–Cl-Bindung (2.378(3) *vs.* 2.338(3) Å) wider, was auf einen stärkeren *trans*-Einfluss des Olefin-im Vergleich zum Chloridoliganden zurückzuführen ist. In den analogen *transoid*-konfigurierten Alkinkomplexen **C11** und **C12a** hingegen wird kein signifikanter Unterschied zwischen den μ-verbrückenden Choridoliganden in *trans*-Position zum Alkin- bzw. zum Chloridoliganden (2.346(1)–2.354(1) Å *vs.* 2.330(1)–2.349(1) Å) beobachtet. Während in dem *cisoid*-konfigurierten Alkinkomplex **C12b** für die Pt–Cl-Bindung des μ-verbrückenden Choridoliganden, welcher zwei Alkinliganden in *trans*-Position aufweist, eine ähnliche Bindungslänge (2.3779(9) Å) wie die des Olefinkomplexes **C2** (2.378(3) Å) gefunden wird. Damit ergibt sich eine folgende Abstufung des *trans*-Einflusses in der Reihenfolge Olefin > Alkin > Cl. Die koordinationschemisch bedingte Abwinkelung der Substituenten R/R' am Alkinliganden (definiert durch den Winkel α) in den Komplexen **C11**, **C12a** und **C12b** beträgt 17.0(5)–20.8(4)° und entspricht damit den Werten (16(1)–21(1)°) in mononuklearen neutralen Alkinkomplexen $[PtCl_2(RC{\equiv}CR)L]$ (R = CMe_2OH, *t*-Bu; L = $NMeH_2$, Toluidin) und in Zeise-Salz analogen Alkinkomplexen $[K(18C6)][PtCl_3(RC{\equiv}CR')]$ (R/R' = Me, *t*-Bu). [15,19,49]

Tabelle 8. Ausgewählte Bindungslängen (in Å) und Winkel (in °) von $[\{PtCl_2(cis\text{-}MeHC{=}CHMe)\}_2]$ (**C2**) und $[\{PtCl_2(RC{\equiv}Ct\text{-}Bu)\}_2]$ (R = Me, **C11**; *t*-Bu, **C12a/C12b**).

	C2	**C11**	**C12a**	**C12b**
Pt–C	2.18(2)/2.16(2)	2.143(5)/2.147(5)	2.126(4)–2.142(4)	2.135(4)/2.144(4)
C≡C		1.254(7)	1.226(6)–1.244(6)	1.258(5)
C=C	1.40(2)			
Pt1–Cl1	2.378(3)	2.341(1)	2.347(1)/2.349(1)	2.3394(9)
Pt1–Cl2	2.338(3)	2.354(1)	2.351(1)/2.346(1)	2.3779(8)
Pt1–Cl3	2.278(3)	2.267(1)	2.262(1)/2.263(1)	2.272(1)
Pt2–Cl4	2.278(3)	2.267(1)	2.263(1)/2.267(1)	
α^a		17.0(5)/20.2(5)	18.6(4)/20.8(4)	19.2(3)/20.2(4)
Φ^b	87.5(2).	87.5(2)	89.0(2)–89.8(2)	89.7(2)

a) α (α = 180 − γ (C≡C–C). b) Winkel zwischen den Ebenen Pt1,Cl1,Cl2,Cl3/Pt,C1,C2 bzw. Pt2,Cl1,Cl2,Cl3/Pt,C3,C4).

2.3.5 Zur Isomerie von Olefin- und Alkinplatin(II)-Komplexen

Zur Konfigurationsisomerie

Signalaufspaltungen in den ^{1}H-, ^{13}C- und ^{195}Pt-NMR-Spektren der dinuklearen Komplexe **C1**–**C3**, **C11** und **C12** belegen das Vorliegen verschiedener Konfigurations- und Konformationsisomere in Lösung. So finden sich in den ^{1}H-,^{13}C- und ^{195}Pt-NMR-Spektren dieser Komplexe (mit Ausnahme von **C1**) im Bereich der Platin-, Olefin- und Alkinresonanzen mehrere Signale sehr ähnlicher Verschiebung. Um einen Einblick in die

relative Stabilität der verschiedenen Konfigurationsisomere (*cisoid vs. transoid*) zu bekommen, wurden DFT-Rechnungen zur Lage des entsprechenden Gleichgewichtes durchgeführt (Schema 17, Tabelle 9). In allen untersuchten Fällen erwies sich die *transoide*-Konfiguration als geringfügig stabiler als die *cisoide*. In Abhängigkeit vom Lösungsmittel sind Werte für die freie Standardenthalpie ΔG_{DFT} von −0.2 bis −1.5 kcal/mol gefunden worden. Somit liegt in Lösung ein Gleichgewicht zwischen den beiden Isomeren vor. Ein Vergleich dieser Werte mit den aus NMR-spektroskopischen Untersuchungen ermittelten Werten (K_{NMR}, ΔG_{NMR}) zeigt eine sehr gute Übereinstimmng.

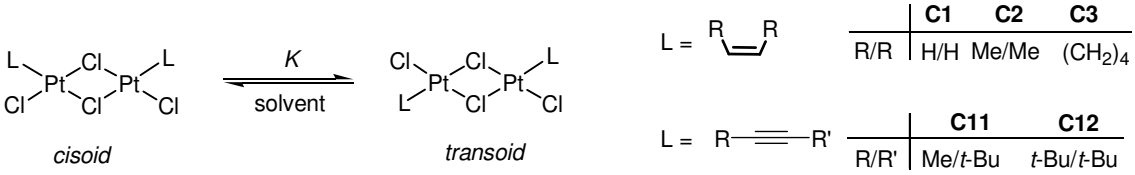

Schema 17.

Der Vergleich der berechneten aus den Einkristallstrukturanalysen erhaltenen XRD-Diagramme von [{$PtCl_2$(*cis*-MeHC=CHMe)}$_2$] (**C2**) und [{$PtCl_2$(RC≡C*t*-Bu)}$_2$] (R = Me, **C11**; *t*-Bu, **C12**) und den gemessenen Pulverdiffraktogrammen von **C2**, **C11** und **C12** zeigt sehr gute Übereinstimmung und bestätigen, das Vorhandensein verschiedener Konformere im Festkörper.

Tabelle 9. Lösungsmittelabhängigkeit der nach Schema 17 aus ^{13}C- und ^{195}Pt-NMR-Spektren erhaltenen Gleichgewichtskonstanten (K_{NMR}) der *cisoid*/*transoid*-Isomerisierung. Korrespondierende Freie Standardenthalpie (in kcal/mol) aus K_{NMR} (ΔG_{NMR}) und den Freien Standardenthalpien aus DFT-Rechnungen (ΔG_{DFT}).

Solvent	CH_3NO_2	CH_2Cl_2	$CHCl_3$	CCl_4	Et_2O	C_6H_6	Gasphase
[{$PtCl_2$(H_2C=CH_2)}$_2$] (**1**)							
K_{NMR}		2.2	1.7			6.8	
ΔG_{NMR}		−0.5	−0.3			−1.1	
ΔG_{DFT}	−0.5	−0.7	−0.8	−1.0		−1.0	−1.1
[{$PtCl_2$(*cis*-MeHC=CHMe)}$_2$] (**2**)							
K_{NMR}	1.5	3.0	4.7	7.5			
ΔG_{NMR}	−0.2	−0.7	−0.9	−1.2			
ΔG_{DFT}	−0.8	−0.9	−1.5	−1.4		−1.5	−1.4
[{$PtCl_2$(*t*-BuC≡C*t*-Bu)}$_2$] (**12**)							
K_{NMR}		2.7	2.5		2.2	5.1	
ΔG_{NMR}		−0.6	−0.5		−0.4	−1.0	
ΔG_{DFT}		−0.2	−1.1		−0.4	−0.6	−1.6

a) Bezogen auf das jeweils stabilste Konformere, vgl. Supplemental Material Anhang **C**.

Zur Rotation von Olefin und Alkinliganden in Platin(II)-Komplexen

Der NMR-spektroskopisch nachgewiesene (vgl. Anhang **C**) Olefin–Alkin-Komplex [$PtCl_2$-(H_2C=CH_2)(RC≡C*t*-Bu)] (**C8**) zeigt ein komplexes ^{1}H-NMR-Spektrum, das zudem noch ausgeprägt temperaturabhängig ist. Eine Spektrensimulation (vgl. Supplemenatal Material zu Anhang **C**) für die Signale der Olefinprotonen bei Raumtemperatur zeigt ein AA'BB'-Spinsystem, wobei jeweils *trans*-ständige Protonen chemisch äquivalent sind. Dies spricht für eine schnelle Rotation des Ethenliganden bei 298 K. Bei 193 K wird dagegen ein Spinsystem mit vier inäquivalenten Protonen (ABCD) beobachtet, womit belegt ist, dass die Rotation bei dieser Temperatur langsam auf der NMR-Zeitskala, also „eingefroren" ist. Eine Rotation des Alkinliganden wurde nicht einmal bei Raumtemperatur beobachtet. Um einen weiteren Einblick in diese Moleküldynamik zu erhalten, sind entsprechende quantenchemische Rechnungen auf DFT-Niveau durchgeführt worden. Zunächst wurden für die dinuklearen Komplexe [{$PtCl_2$(MeHC=CHMe)}$_2$] (**C2'**, *transoid*) und [{$PtCl_2$(MeC≡C*t*-Bu)}$_2$] (**C11'**, *transoid*) sowie für den mononuklearen Ethen–Alkin-Komplex [$PtCl_2$(H_2C=CH_2) (MeC≡C*t*-Bu)] (**C8'**) alle denkbaren Konformationsisomere (insgeamt 5) berechnet (vgl. Supplemenatal Material - Anhang **C**). Des Weiteren sind – bezogen auf das jeweils stabilste Isomer – die freien Standardaktivierungsenthalpien ($\Delta G^{\ddagger}$) für die Rotation der π-Olefin/Alkin-Liganden berechnet worden (Tabelle 10). In allen Komplexen weist die Rotation des Olefinliganden eine geringere Barriere (12.1–13.4 kcal/mol) auf. Im Falle der Alkinliganden ergeben sich für **C11a'/C8'** höhere Werte der Rotationsbarrieren (20.6–23.9 kcal/mol) was bestätigt, dass unterschiedliche Konformere NMR-spektroskopisch beobachtet werden können. Das erhaltene Bild ist somit in sich konsistent und stimmt mit den experimentellen Befunden sehr gut überein.

Tabelle 10. Berechnete freie Standardaktivierungsenthalpien ($\Delta G^{\ddagger}$, in kcal/mol) sowie daraus ermittelte Geschwindigkeitskonstanten erster Ordnung (k, in s^{-1}) für die Rotation von π-Liganden in den dinuklearen Komplexen [{$PtCl_2$(MeHC=CHMe)}$_2$] (**C2'**) und [{$PtCl_2$(MeC≡C*t*-Bu)}$_2$] (**C11'**) sowie in dem mononuklearen Ethen–Alkin-Komplex [$PtCl_2$(H_2C=CH_2)(MeC≡C*t*-Bu)] (**C8'**).

	Olefin	$\Delta G^{\ddagger}$	k		Alkin	$\Delta G^{\ddagger}$	k
C2'	*cis*-But-2-en	13.4	$9.1\cdot10^{2}$	**C11a'**	MeC≡C*t*-Bu	20.6	$4.7\cdot10^{-3}$
C8'	Ethen	12.1	$8.2\cdot10^{3}$	**C8'**	MeC≡C*t*-Bu	23.9	$1.8\cdot10^{-5}$
C8'[a]	Ethen	11.8	$1.7\cdot10^{-1}$	**C8'**[a]	MeC≡C*t*-Bu[a]	22.9	$4.5\cdot10^{-14}$

a) T = 193 K.

2.3.6 Zur Thermodynamik der Substitution von Olefin- und Alkinliganden

Die Unterschiede in der Reaktivität der dinuklearen Olefinplatin(II)-Komplexe gegenüber verschieden substituierten Alkinen sollten durch quantenchemische Rechnungen vertieft analysiert werden. Die Thermodynamik der Brückenspaltungs- und Ligandensubstitutionsreaktionen ausgehend vom Zeise-Dimer **C1'** gegenüber den *tert*-butylsubstitutierten Alkinen RC≡C*t*-Bu (R = Me, *t*-Bu) ist in Schema 18 wiedergegeben.

Ausgehend von **C1'** ist die Substitution des Ethenliganden durch Alkine (Schema 18, Pfad **a/d**) endergonisch, aber Gleichgewichtsreaktionen sind zwischen den dinuklearen und mononu-klearen Platin(II)-Komplexen zu erwarten. Daraus folgt, dass der Ethenligand stärker gebunden ist als die Alkinliganden. Die Brückenspaltung im Zeise-Dimer durch Ethen (Pfad **b**) ist schwach exergonisch (ΔG = −0.7 kcal/mol), was sehr gut mit experimentell ermittelten Werten (ΔG = −1.1 kcal/mol; Elding *et al.* [47]) im Einklang steht. Des Weiteren wird in Übereinstimmung mit den experimentellen Beobachtungen ersichtlich, dass die Bildung des Cyclobutadienkomplexes **C16'** nur im Falle des MeC≡C*t*-Bu Liganden thermodynamisch erlaubt ist, während die [2+2]-Cyloaddition mit *t*-BuC≡C*t*-Bu als Edukt stark endergonisch ist.

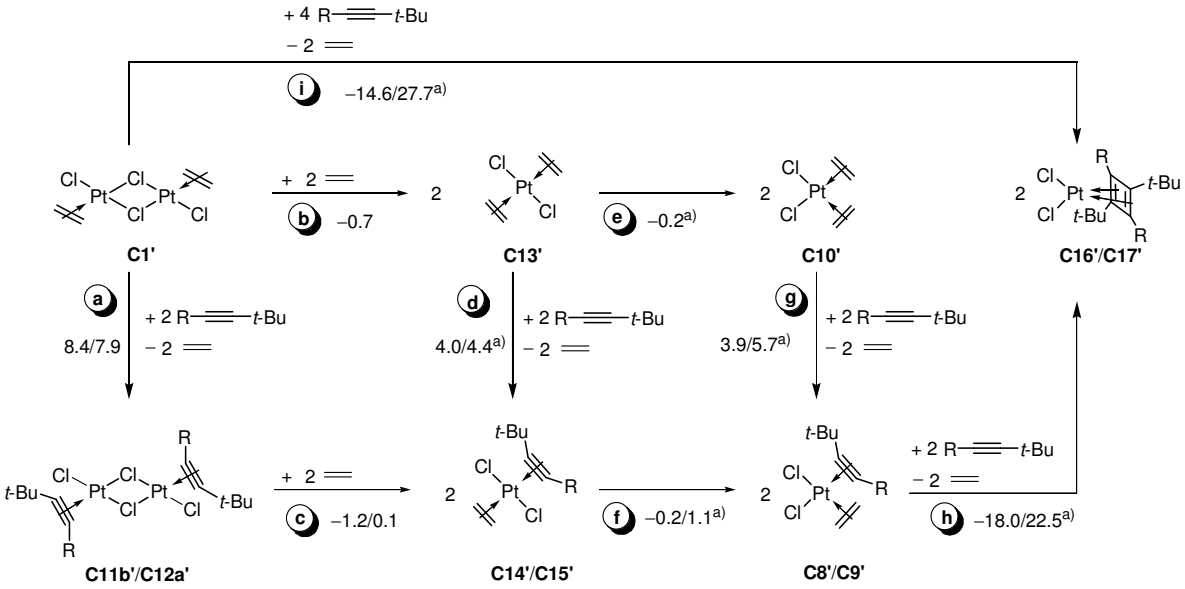

Schema 18. Berechnete Standardreaktionsenthalpien (in kcal/mol) unter Berücksichtigung von $CHCl_3$ als Lösungsmittel (ΔG_{solv}). Die Werte für R = Me und R = *t*-Bu sind durch einen Schrägstrich getrennt angegeben. a) ΔG_{solv} bezogen auf die Bildung von 1 mol Komplex.

2.3.7 Dinukleare Olefinkomplexe als Präkatalysatoren in der Hydroaminierung

Die Addition von N–H-Bindungen an Kohlenstoff–Kohlenstoff-Doppelbindungen (Schema 19) bietet einen einfachen und effizienten Weg zu höher substituierten Aminen ausgehend von Olefinen, welche petrochemische Grundstoffe sind. [51]

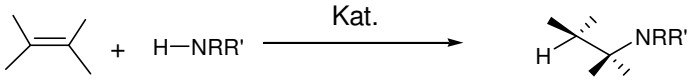

Schema 19.

Derartige Hydroaminierungsreaktionen bedürfen der Aktivierung durch katalystische Systeme. Neben Alkalimetallen und Komplexen der frühen Übergangsmetalle (einschließlich der Seltenerdmetalle) werden auch Komplexe der späten Übergangsmetalle als Katalysatoren eingesetzt, [51] darunter Platin. [52] So ist von Brunet und Poli [53] durch Hydroaminierung von Ethen mit Anilin mit Platin(II)-halogeniden als Katalysator in Tetraalkylphosphoniumhalogeniden als ionische Flüssigkeiten *N*-Ethylanilin als Hauptprodukt erhalten worden (Schema 20, Pfad **a**). In Gegenwart von Phosphinen ist Zeise's Dimer als Präkatalysator von Widenhoefer *et al.* [54] bei der Hydroaminierung von Styrol mit Benzamidderivaten eingesetzt worden, wobei bevorzugt Markovnikov-Produkte erhalten werden (Schema 20, Pfad **b**).

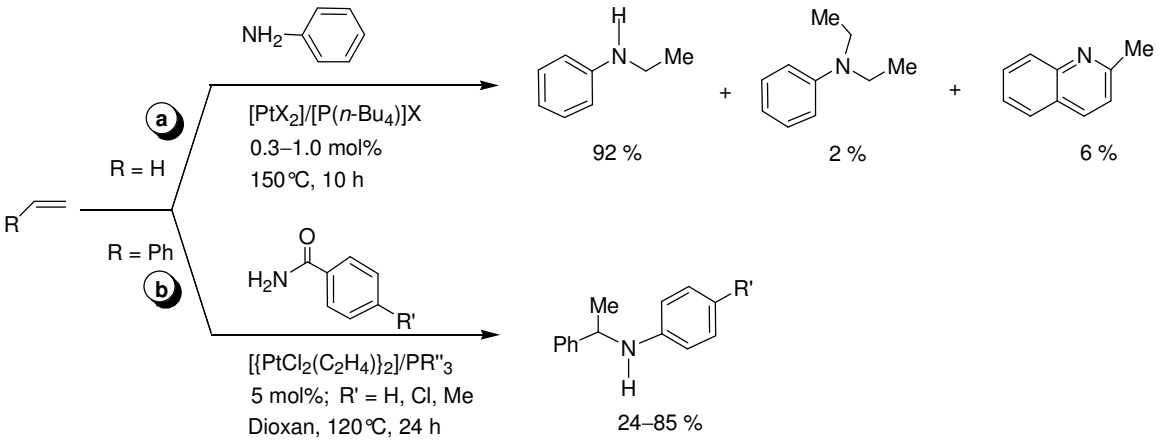

Schema 20.

Insbesondere die Arbeiten von Widenhöfer [54] veranlassten uns, orientierende Untersuchungen zur Hydroaminierung von Styrol mit dem *cis*-Buten-Dimer [{$PtCl_2$(MeHC=CHMe)}$_2$] (**C2**) als Präkatalysator durchzuführen, aber ohne die Verwendung von Phosphinen als Cokatalysator. Als Aminkomponente fanden aromatische Amine (Anilin, pK_a = 30.6 [55]; Pentafluoranilin, pK_a = 23.1 [56]) sowie Benzamid (pK_a = 23.3 [55]) Verwendung. Die Reak-

tionen wurden in Toluol als unpolares Lösungsmittel bei 110 °C mit einer Katalysatorkonzentration von 1 mol% durchgeführt. Anilin reagierte unter den angegebenen Reaktionsbedingungen überhaupt nicht, während das stärker saure Pentafluoranilin bevorzugt (27%) unter Markovnikov-Addition reagiert (Schema 21, Pfad **a**). Als Nebenprodukte wurden das *anti*-Markovnikov-Produkt (3%) sowie ein tertiäres Amin (4%) durch Weiterreaktion des Hauptproduktes erhalten. Benzamid setzt sich unter gleichen Reaktionsbedingungen quantitativ um, wobei Markovnikov- und *anti*-Markovnikov-Produkt im Verhältnis 4 : 1 gebildet wurden (Pfad **b**).

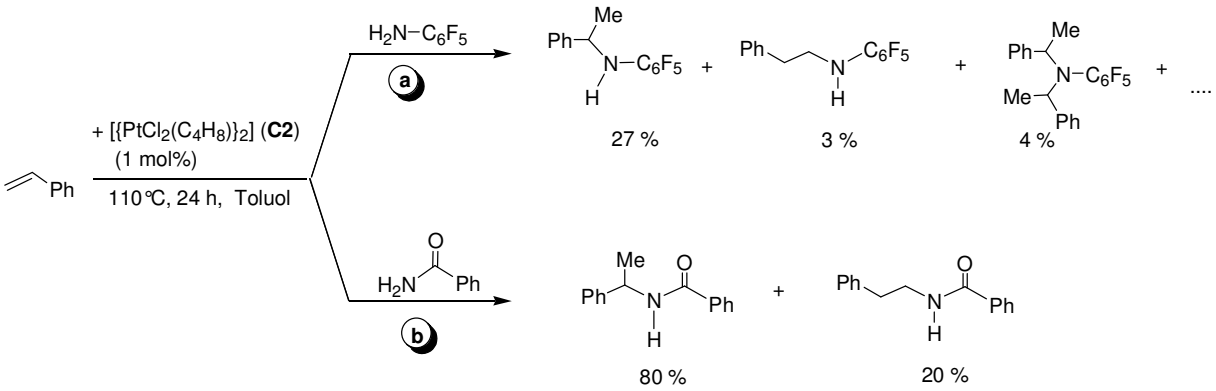

Schema 21.

Im Vergleich zu Arbeiten von Widenhoefer [54] zeigt sich im vorliegenden System für das Benzamid, bei milderen Reaktionsbedingungen und einer deutlich geringeren Katalysatorkonzentration sowie gleicher Reaktionszeit, vergleichbare Umsätze jedoch in geringerer Regioselektivität. Im Gegensatz dazu werden für das Pentafluoranilin bei analogen Reaktionsbedingungen sowohl ein geringerer Umsatz als auch eine geringere Regioselektivität beobachtet.

2.3.8 Diskussion der Ergebnisse

Obwohl Zeise's Dimer und entsprechende Alkinkomplexe seit mehr als 150 bzw. 50 Jahren bekannt sind, wurde im Rahmen der vorliegenden Arbeit nicht nur eine neuartige Synthesemethode für die Alkinkomplexe gefunden, die eine breite Variation des Alkinliganden ermöglicht, sondern auch erstmals ein *cisoid*/*transoid*-Gleichgewicht sowohl bei den dinuklearen Olefin- als auch Alkinkomplexen nachgewiesen.

Aus historischer Sicht stellte sich die Frage warum Chatt *et al*. dinukleare Zeise-Dimer analoge Alkinkomplexe des Typs $[\{PtCl_2(RC{\equiv}Ct\text{-}Bu)\}_2]$ (R = Et, *t*-Bu) darstellen konnte, jedoch

die analoge Umsetzung von Zeise's Dimer [{$PtCl_2(C_2H_4)$}$_2$] mit weniger anspruchsvoll substituierten Alkinen RC≡CR' (R = H, *n*-Alkyl) zu Zersetzungsreaktionen unter Bildung von metallischem Platin führte. Als wesentliche Gründe können eine verminderte Stabilität des Zeise-Dimers in Aceton unter Spaltung der Pt–μ-Cl Brücke genannt werden. Desweiteren ist Aceton das von Chatt verwendete Lösungsmittel nicht inert, sodass Aldoladditionen und Aldolkondensationsreaktionen stattfinden. Der im Zuge dieser Arbeit erfolgte Wechsel des Lösungsmittels von Aceton zu Dichlormethan erlaubte die Darstellung von Alkinkomplexen K[$PtCl_3$(RC≡CR'] (R, R' = *n*-Alkyl, *tert*-Alkyl, Ph) des Zeise-Salz-Typs sowie von Zeise-Dimer analogen Komplexen des Typs [{$PtCl_2$(RC=C*t*-Bu)}$_2$] (R, R' = Me, *t*-Bu).

Die Substitution der Olefinliganden in Zeise's Dimer und analogem Olefinkomplex [{$PtCl_2$(MeHC=CHMe)}$_2$] durch Alkine hängt ausgeprägt vom sterischen Anspruch der Substituenten am Alkin ab. Zeise-Dimer analoge Alkinkomplexe werden mit Alkinen RC≡C*t*-Bu gebildet, die mindestens einen sterisch raumgreifenden *tert*-Butylsubstituenten aufweisen. Mit Alkinen RC≡CR' (R, R' = *n*-Alkyl, Ph) werden dagegen in einer [2+2]-Cycloaddition Cyclobutadienkomplexe gebildet. Quantenchemische Rechnungen zeigen die wesentliche Ursache für die unterschiedliche Reaktivität auf: Für *tert*-butylsubstituierte Alkine RC≡C*t*-Bu ist die Bildung von Cyclobutadienkomplexen thermodynamisch ungünstig (R = *t*-Bu) bzw. kinetisch gehemmt (R = Me).

Die höhere Reaktivität von Alkinen bedingt, dass Zeise-Salz und Zeise-Dimer analoge Alkinkomplexe deutlich reaktiver als die analogen Olefinkomplexe sind. Das führt dazu, dass die im Rahmen der vorliegenden Arbeit beschriebenen Umsetzungen nicht nur Ligandsubstitutionsreaktionen (Olefine *vs.* Alkine), sondern auch [2+2]-Cycloadditionsreaktionen und auch andere C–C-Knüpfungsreaktionen beinhalten. Des Weiteren liefern die Untersuchungen einen weiteren Beleg, wie das Substitutionsmuster der Alkine die Reaktionen beeinflussen und wie quantenchemische Rechnungen detaillierte Einblicke in den Reaktionsablauf gestatten.

3. Zusammenfassung

Während Olefin- und Alkinpalladium-Komplexe als Intermediate in zahlreichen homogen katalysierten Reaktionen auftreten, sind entsprechende Platinkomplexe in vielen Fällen kinetisch und auch thermodynamisch stabiler, was sie als Modellkomplexe für Untersuchungen von katalytisch relevanten metallorganischen Elementarreaktionen prädestiniert. Mit Bezug auf die älteste übergangsmetallorganische Verbindung, dem Zeise-Salz $K[PtCl_3(C_2H_4)]\cdot H_2O$ (Zeise, 1825), sowie Zeise's Dimer $[\{PtCl_2(H_2C{=}CH_2)\}_2]$ (Zeise/Anderson, 1831/1934) sind im Rahmen dieser Arbeit analoge Alkinkomplexe synthetisiert wurden.

Zur Gleichgewichtsreaktion zwischen Alkin- und Olefinplatin(II)-Komplexen vom Zeise-Salz-Typ

1. Reaktionen von [K(18C6)][$PtCl_3$(*cis*-MeHC=CHMe)] (**A2**), einem Komplex vom ZeiseSalz-Typ, mit Alkinen RC≡CR' (R, R' = Me, Et, *t*-Bu, Ph, CO_2Me) sowie mit Cyclooctin (COC) führt zur Bildung der entsprechenden Alkinkomplexe [K(18C6)][$PtCl_3$(RC≡CR')] (**A3**–**A9**). Alle Komplexe wurden isoliert und NMR-spektroskopisch sowie elementaranalytisch vollständig charakterisiert. Darüber hinaus konnten von vier Komplexen (**A5**–**A7**, **A9**) Röntgeneinkristallstrukturanalysen erhalten werden. Während in den alkyl-/arylsubstituierten Alkinkomplexen **A5**–**A7** Abwinkelungen der Substituenten R, R' = Me, *t*-Bu, Ph von α = 16(1)–21(1)° beobachtet wurden, sind für den Cyclooctinkomplex **A9** deutlich größere Abwinkelungen (26.8(7)/26.0(7)°) beobachtet wurden, was dessen Sonderstellung verdeutlicht.

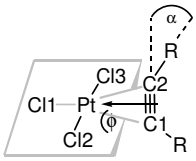

2. Werden die unter 1. beschriebenen Reaktionen im abgeschmolzenen NMR-Röhrchen durchgeführt, so werden Gleichgewichtsreaktionen zwischen dem Olefin- und den korrespondierenden Alkinkomplexen beobachtet:

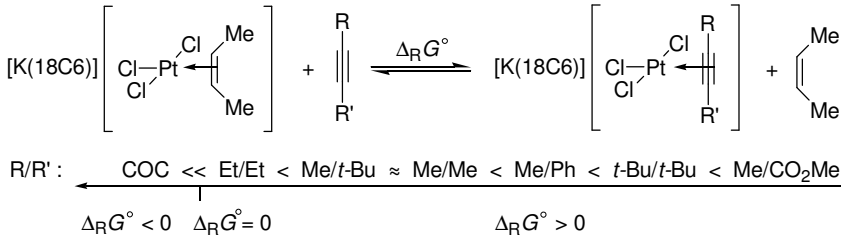

Die Lage des Gleichgewichtes kann hierbei zur Bestimmung der relativen Bindungsstärke des Alkinliganden herangezogen werden. Auch hierbei zeigt sich die Sonderstellung des Cyclooctinliganden in **A9**, welcher eine deutlich höhere Bindungsstärke (> 10 kcal/mol) aufweist.

3. Die unter 2. beschriebenen Ligandensubstitutionsreaktionen wurden auch mittels quantenchemischen Rechnungen auf DFT-Niveau modelliert, wobei eine gute Übereinstimmung mit den spektroskopisch bestimmten Werten der freien Standardreaktionsenthalpie $\Delta_r G°$ erhalten wurde. Des Weiteren konnte mittels der „energy decomposition analysis" (EDA) gezeigt werden, dass die ungewöhnlich hohe Stärke der Pt–COC-Bindung zu annähernd gleichen Teilen auf eine Verringerung der Präparationsenergie des Alkinliganden ΔE_{prep} (COC) als auch auf eine stärkere Wechselwirkung ΔE_{int} der beteiligten Fragmente zurückzuführen ist. Die NBO-Analyse zeigt hierbei sowohl im methoxycarbonylsubstituierten Alkinkomplex **A8** als auch im COC-Komplex **A9** ein erheblich größeres Maß an back-donation.

Zur Isomerisierung von Cyclooctin zu Cycloocta-1,3-dien

4. Der Zeise-Salz analoge Cyclooctinkomplex [K(18C6)][$PtCl_3$(COC)] (**A9/B1**) reagierte bei Raumtemperatur in Lösung ($CHCl_3$, Aceton, …) innerhalb einiger Wochen zu dem dinuklearen Cycloocta-1,3-dienkomplex **B2**:

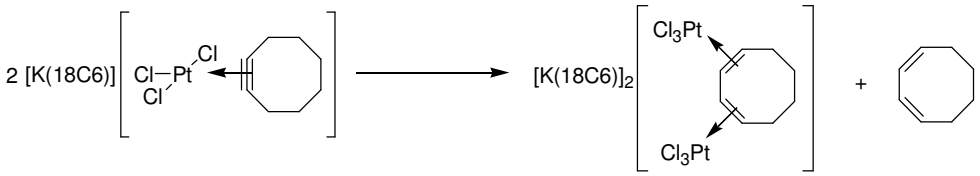

B1 **B2**

Die Konstitution von **B2** wurde zweifelsfrei mittels NMR-Spektroskopie, Elementaranalyse, ESI-MS sowie Röntgeneinkristallstrukturanalyse sichergestellt. Mit dieser Reaktion konnte erstmalig eine Isomerisierung eines Cyclooctinliganden in Cycloocta-1,3-dien nachgewiesen werden.

5. Quantenchemische Rechnungen auf DFT-Niveau zeigen, dass die Triebkraft der Reaktion ein Abbau der Ringspannung vom Cyclooctin ist. Der entstehende dinukleare Cycloocta-1,3-dienkomplex **B2** lässt sich nach den Ergebnissen der EDA- sowie der NBO-Analyse im Sinne des Dewar-Chatt-Duncanson-Modells – analog dem Zeise-Salz – als Olefin–Platin-Komplex beschreiben. Eine Konjugation der beiden Doppelbindungen im Cycloocta-1,3-dienliganden

liegt nicht vor, wie durch die große Abwinkelung der beiden π-Ebenen (59.7(9)) belegt wird. Eine derartige Bindung ist für 1,3-Dien-Komplexe untypisch.

Zur Synthese und Reaktivität von dinuklearen Zeise-Dimer analogen Olefin- und Alkinplatin(II)-Komplexen

6. Die Synthese von Zeise's Dimer und von analogen Komplexen diesen Typs, [{$PtCl_2$(RHC=CHR)}$_2$] (R = H, Me, $(CH_2)_4$; **C1**–**C3**), aus $K_2[PtCl_4]$ und dem entsprechenden Olefin konnte durch Verwendung von $SnCl_2$ als Katalysator erheblich vereinfacht werden.
[{$PtCl_2(H_2C=CH_2)$}$_2$] (**C1**) reagiert mit *n*-alkylsubstituierten Alkinen RC≡CR' (R, R' = Me, Et, *n*-Pr) unter [2+2]-Cycloaddition zu den entsprechenden Cyclobutadienkomplexen [$PtCl_2$-($C_4R_2R'_2$)] (**C4**–**C6**). Im Falle des unsymmetrisch substituierten Alkins MeC≡C*n*-Pr erfolgt die Addition nicht regioselektiv, während im Falle von MeC≡CPh die Cycloaddition regioselektiv ist.

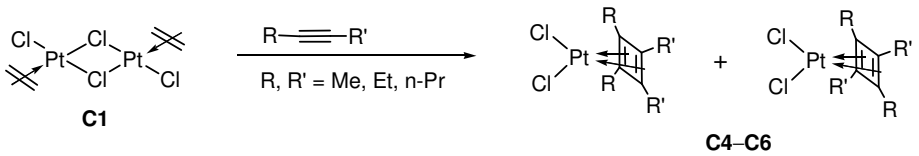

C1 **C4**–**C6**

7. Die Reaktion von Zeise's Dimer **C1** mit *tert*-alkylsubstituierten Alkinen RC≡C*t*-Bu, (R = Me, *t*-Bu) führt zur Bildung von dinuklearen Bis(alkin)-Komplexen **C11/C12**. Wird das freigesetzte Ethen nicht aus dem Reaktionsgemisch entfernt, so bilden sich mononukleare Olefin–Alkin-Komplexe **C8/C9**:

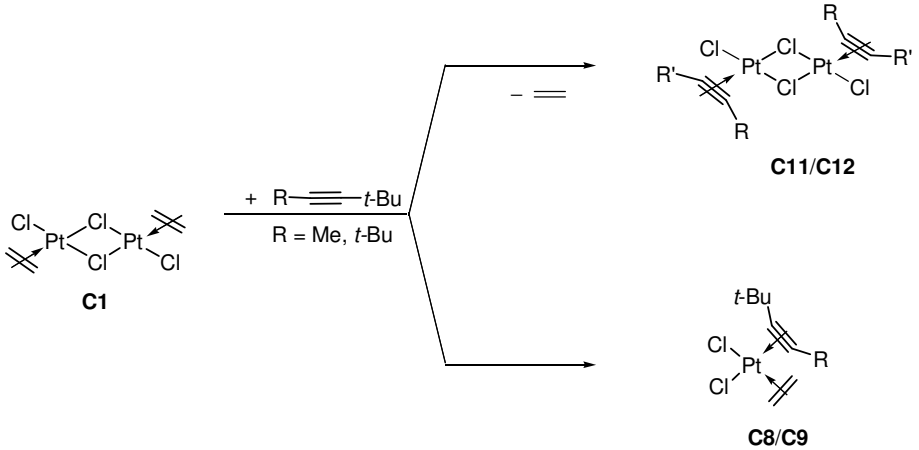

C1 **C11/C12** **C8/C9**

Während die Bis(alkin)-Komplexe **C11/C12** in Substanz isoliert und analytisch sowie NMR-spektroskopisch vollständig charakterisiert wurden, konnten die Komplexe **C8/C9** aufgrund ihrer fehlenden Stabilität in Abwesenheit von Ethen nicht isoliert, jedoch zweifelsfrei mittels NMR-Spektroskopie charakterisiert werden.

8. NMR-spektroskopische Untersuchungen sowie Röntgeneinkristallstrukturanalysen belegen erstmalig sowohl für die Olefin- (**C1**–**C3**) als auch die analogen Alkinkomplexe (**C11/C12**) vom Zeise-Dimer-Typ die Existenz von zwei Konstitutionsisomeren (*transoid* und *cisoid)*:

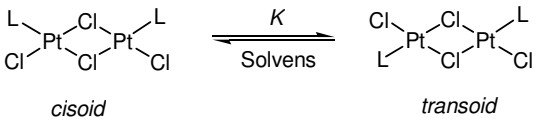

Sowohl die NMR-spektroskopischen Analysen als auch quantenchemische Rechnungen zeigen hierbei lösungsmittelabhängige Gleichgewichte zwischen den beiden Isomeren.
Darüber hinaus zeigen Tieftemperatur-NMR-spektroskopische Untersuchungen, in Übereinstimmung mit DFT-Rechnungen, eine schnelle Rotation der Olefinliganden um die Ethen–Platin-Bindung, während im Gegensatz dazu die analoge Rotation der *tert*-butylsubstituierten Alkinliganden langsam auf der NMR-Zeitskala ist.

9. In orientierenden Untersuchungen wurde die Eignung des dinuklearen Olefinkomplexes [{$PtCl_2$(MeHC=CHMe)}$_2$] (**C2**) als Präkatalysator für die Hydroaminierung von Styrol mit aromatischen Aminen ($PhNH_2$, $C_6F_5NH_2$) und Benzamid in Toluol als Lösungsmittel untersucht (Kat.: 1 mol%, 110 °C, 24 h). Mit Anilin (pK_a = 30.6) wurde überhaupt keine Umsetzung beobachtet, während das stärker saure Pentafluoranilin (pKa = 23.1) unter Bildung des Markovnikov-Produktes C_6F_5NH–CH(Me)–Ph als Hauptprodukt (27%) reagiert und das Benzamid (pK_a = 23.3) sich vollständig umsetzt, wobei das Markovnikov- und *anti*-Markovnikov-Produkt (AcNH–CH(Me)–Ph/AcNH–CH_2–CH_2Ph) im Verhältnis 4:1 gebildet werden.

Die vorliegende Arbeit erlaubt aus Olefinkomplexen vom Zeise-Salz- und Zeise-Dimer-Typ via Ligandsubstitution einen leichten Zugang zu den entsprechenden Alkinkomplexen, erstmals bei breiter Variation des Alkins. Spektroskopische und strukturelle Untersuchungen sowie quantenchemische Rechnungen geben detaillierte Einblicke in Konfigurations- und Konformationsisomere in Komplexen dieser Typen sowie in die relative Stärke der Bindung von Olefinen und Alkinen an Platin(II) und in den elektronischen und sterischen Substitutenten-einfluss auf die Stärke dieser Bindungen. Die Arbeit zeigt auf, wie subtil Ligandadditions- und abspaltungsreaktionen bei katalytisch relevanten Substraten vom Substitutionsmuster des Olefins bzw. Alkins und des Komplexfragments abhängen und trägt damit zum vertieften Verständnis von Struktur–Eigenschaftsbeziehungen bei metallorganischen Elementarreaktionen bei.

4. Literaturverzeichnis

[1] (a) W. C. Zeise, *Overs K. Dan. Vidensk. Selsk. Forh.* **1825–1826**, 13. (b) W. C. Zeise, *Pogg. Ann. Phys.* **1827**, *9*, 632.

[2] (a) M. J. S. Dewar, *Bull. Soc. Chim. Fr.* **1951**, *18*, C71–C79. (b) J. Chatt, L. A. Duncanson, *J. Chem. Soc.***1953**, 2939.

[3] D. Seyferth, *Organometallics,* **2001***, 20,* 2.

[4] (a) J. A. Wunderlich, D. P. Mellor, *Acta Crystallogr.* **1954**, *7*, 130. (b) R. A. Love, T. F. Koetzle, G. J. B. Williams, L. C. Andrews, R. Bau, *Inorg. Chem.* **1975**, *14*, 2653.

[5] R. F. W. Bader, *Atoms in Molecules, A Quantum Theory*, Oxford University Press, Oxford (U.K.) 1990.

[6] (a) J. Chatt, R. G. Guy, L. A. Duncanson, *J. Chem. Soc.* **1961**, 827. (b) J. Chatt, R. G. Guy, L. A. Duncanson, D. T. Thompson, *J. Chem. Soc.* **1963**, 5170.

[7] S. V. Bukhovets, N. K. Pukhov, *Zh. Neogr. Khim*, **1958**, *3*, 1714.

[8] (a) D. Steinborn, *Grundlagen der metallorganischen Komplexkatalyse,* 2. Aufl., Viewieg + Teubner, Wiesbaden 2010.

[9] C. Elschenbroich, *Organometallchemie*, 6. Aufl., Viewieg + Teubner, Wiesbaden 2008.

[10] C. A. Tolman, *J. A. Chem. Soc.* **1974**, 96, 2780.

[11] C. T. Mortimer, *Rev. Inorg. Chem.* **1984**, *6*, 233.

[12] W. Partenheimer, *J. Am. Chem. Soc.* **1976**, *98*, 2779.

[13] D. Steinborn, V. V. Potechin, M. Gerisch, C. Bruhn, H. Schmidt, *Trans. Met. Chem.* **1999**, *24*, 67.

[14] S. Schwieger, C. Wagner, C. Bruhn, H. Schmidt, D. Steinborn, *Z. Anorg. Allg. Chem.* **2005**, *631*, 2696.

[15] (a) D. Steinborn, M. Tschoerner, A. v. Zweidorf, J. Sieler, H. Bögel, *Inorg. Chim. Acta* **1995**, *234*, 47. (b) M. Gerisch, F. W. Heinemann, H. Bögel, D. Steinborn, *J. Organomet. Chem.* **1997**, *548*, 247.

[16] A. König, Diplomarbeit, Martin-Luther-Universität Halle-Wittenberg, 2007.

[17] Landolt-Börnstein, *Zahlenwerte und Funktionen aus Naturwissenschaft und Technik, Vol. 7/15/23*, Springer, Berlin 1976/1983/1988.

[18] (a) A. L. Beauchamp, F. D. Rochon, T. Theophanides, *Can. J. Chem.* **1973**, *51*, 126. (b) R. J. Dubey, *Acta Cryst.* **1976**, *32*, 199.

[19] (a) F. D. Rochon, R. Melanson, M. Doyon, *Can. J. Chem.* **1989**, *67*, 2209. (b) G. R. Davies, W. Hewertson, R. H. B. Mais, P. G. Owston, C. G. Patel, *J. Chem. Soc. A* **1970**, 1873.

[20] F. P. Fanizzi, G. Natile, M. Lanfranchi, A. Tiripicchio, G. Pacchioni, *Inorg. Chim. Acta* **1998**, *275–276*, 500.

[21] M. J. Frisch, G. W. Trucks, H. B. Schlegel, G. E. Scuseria, M. A. Robb, J. R. Cheeseman, V. G. Zakrzewski, J. A. Montgomery, Jr., R. E. Stratmann, J. C. Burant, S. Dapprich, J. M. Millam, A. D. Daniels, K. N. Kudin, M. C. Strain, O. Farkas, J. Tomasi, V. Barone, M. Cossi, R. Cammi, B. Mennucci, C. Pomelli, C. Adamo, S. Clifford, J. Ochterski, G. A. Petersson, P. Y. Ayala, Q. Cui, K. Morokuma, D. K. Malick, A. D. Rabuck, K. Raghavachari, J. B. Foresman, J. Cioslowski, J. V. Ortiz, B. B. Stefanov, G. Liu, A. Liashenko, P. Piskorz, I. Komaromi, R. Gomperts, R. L. Martin, D. J. Fox, T. Keith, M. A. Al-Laham, C. Y. Peng, A. Nanayakkara, C. Gonzalez, M. Challacombe, P. M. W. Gill, B. Johnson, W. Chen, M. W. Wong, J. L. Andres, C. Gonzalez, M. Head-Gordon, E. S. Replogle, J. A. Pople, *Gaussian 03*, Revision B.04; Gaussian, Inc.: Wallingford, CT, **2004**.

[22] (a) M. J. S. Dewar, C. H. Reynolds, *J. Comput. Chem.* **1986**, *7*, 140. (b) K. Raghavachari, J. A. Pople, E. S. Replogle, M. Head-Gordon, *J. Phys. Chem.* **1990**, *94*, 5579.

[23] (a) F. Weigend, M. Häser, H. Patzelt, R. Ahlrichs, *Chem. Phys. Lett.* **1998**, *294*, 143. (b) T. Leininger, A. Nicklass, W. Küchle, H. Stoll, M. Dolg, A. Bergner, *Chem. Phys. Lett.* **1996**, *255*, 274. (c) D. Andrae, U. Häussermann, M. Dolg, H. Stoll, H. Preuss, *Theor. Chem. Acc.* **1990**, *77*, 123.

[24] (a) B. Mennucci, J. Tomasi, *J. Chem. Phys.* **1997**, *106*, 5151. (b) E. Cancès, B. Mennucci, J. Tomasi, *J. Chem. Phys.* **1997**, *107*, 3032. (c) M. Cossi, V. Barone, B. Mennucci, J. Tomasi, *Chem. Phys. Lett.* **1998**, *286*, 253.

[25] (a) G. Frenking, N. Fröhlich, *Chem. Rev.* **2000**, *100*, 717. (b) G. Frenking, K. Wichmann, N. Fröhlich, C. Loschen, M. Lein, J. Frunzke, V. M. Rayón, *Coord. Chem. Rev.* **2003**, *238–239*, 55.

[26] (a) E. D. Glendening, J. K. Badenhoop, A. E. Reed, J. E. Carpenter, J. A. Bohmann, C. M. Morales, F. Weinhold, *NBO 5.0*, Theoretical Chemistry Institute, University of Wisconsin: Madison, WI, 2001. (b) F. Weinhold, C. R. Landis, *Chemistry Education Research and Practice.* **2001**, *2*, 91. (c) J. P. Foster, F. Weinhold, *J. Am. Chem. Soc.*

1980, *102*, 7211. (d) A. E. Reed, F. Weinhold, *J. Chem. Phys.* **1983**, *78*, 4066. (e) A. E. Reed, R. B. Weinstock, F. Weinhold, *J. Chem. Phys.* **1985**, 83, 735.

[27] (a) A. J. L. Pombeiro, *J. Organomet. Chem.* **1984**, *358*, 273. (b) S. Patai, *Supplement C2: The Chemistry of Triple Bonded Functional Groups,* Vol. 2, Thieme Verlag, Stuttgart 1994. (c) Houben-Weyl, *Methoden der Organischen Chemie*, Vol. 15/3, Thieme Verlag, Stuttgart 1993.

[28] Houben-Weyl, *Methoden der Organischen Chemie*, Vol. 5/1c, Thieme Verlag, Stuttgart 1970.

[29] a) H. Zeise, *Thermodynamik*, Vol. 3/1, Hirzel Verlag, Leipzig 1954. b) Houben-Weyl, *Methoden der Organischen Chemie*, Vol. 5/2a, Thieme Verlag, Stuttgart 1977. c) B. J. Barry, W. J. Beale, M. D. Carr, S.-K. Hei, I. Reid, *J. Chem. Soc., Chem. Commun.* **1973**, 177.

[30] K. Hirai, H. Suzuki, Y. Moro-Oka, T. Ikawa, *Tetrahedron Lett.* **1980**, *21*, 3413.

[31] C. K.-W. Kwong, M. Y. Fu, C. S.-L. Lam, P. H. Toy, *Synthesis* **2008**, *15*, 2307.

[32] (a) B. Trost, T. Schmidt *J. Am. Chem. Soc.* **1988**, *110*, 2301. (b) D. Ma, Y. Lin, X. Lu, *Tetrahedron Lett.* **1988**, *29*, 1045. (c) Y. Inoue, S. Imaizumi, *J. Mol. Catal.* **1988**, *49*, L19. (d) D. Ma, Y. Yu, X. Lu, *J. Org. Chem.* **1989**, *54*, 1105. (e) C. Guo, X. Lu, *Synlett* **1992**, 405. (f) D. Ma, X. Lu, *Tetrahedron Lett.* **1989**, *30*, 843. (g) D. Ma, X. Lu, *Tetrahedron* **1990**, *46*, 3189. (h) C. Guo, X. Lu, *Tetrahedron Lett.* **1991**, *32*, 7549. (i) X. Lu, D. Ma, *Pure Appl. Chem.* **1990**, *62*, 723.

[33] (a) B. Trost, U. Kazmaier, *J. Am. Chem. Soc.*, **1992**, *114*, 7933. (b) B. Trost, C.-J. Li, *J. Am. Chem. Soc.*, **1994**, *116*, 10819. (c) C. Guo, X. Lu, *J. Chem. Soc., Perkin Trans*, **1993**, 1921.

[34] H. Yasui, H. Yorimitsu, K. Oshima, *Synlett*, **2006**, *11*, 1783.

[35] (a) V. G. Albano, F. Demartin, V. De Felice, G. Morelli, A. Vitagliano, *Gazz. Chim. Ital.* **1987**, *437*, 117. (b) J. R. Briggs, C. Crocker, W. S. McDonald, B. L. Shaw, *J. Chem. Soc., Dalton Trans.* **1982**, 457.

[36] M. Trætteberg, *Acta Chem. Scand.* **1970**, *24*, 2285.

[37] S. Dapprich, G. Frenking, *J. Phys. Chem.* **1995**, *99*, 9352.

[38] S. Otto, A. Roodt, L. I. Elding, *Dalton Trans.* **2003**, 2519.

[39] J. Bordner, D. W. Wertz, *Inorg. Chem.* **1974**, *13*, 1639.

[40] J. Chatt, M. L. Searle, *Inorg. Synth.* **1957**, *5*, 210.

[41] R. Cramer, *Inorg. Chem.* **1965**, *4*, 445.

[42] M. R. Plutino, S. Otto, A. Roodt, L. I. Elding, *Inorg Chem.* **1999**, *38*, 1233.

[43] M. P. Mitoraj, H. Zhu, A. Michalak, T. Ziegler, *Int. J. Quantum Chem.* **2009**, *109*, 3379.

[44] A. F. Hollemann, E. Wiberg *Lehrbuch der Anorganischen Chemie*, 102. Auflage, Gruyter Verlag, Berlin, 2007.

[45] W. P. Fehlhammer, W. A. Herrmann, K. Öfele, *Handbuch der Präparativen Anorgani schen Chemie*, 3. Auflage, Bd. 3, Ferdinand Enke Verlag, Stuttgart 1981.

[46] P. B. Chock, , J. Halpern, F. E. Paulik, *Inorg. Synth*., **1973**, *14*, 90.

[47] S. Otto, A. Roodt, L. I. Elding, *Inorg. Chem. Commun.* **2006**, *9*, 764.

[48] A. Singh, P. R. Sharp, *Organometallics* **2006**, *25*, 678.

[49] A. König, M. Bette, C. Wagner, R. Lindner, D. Steinborn, *Organometallics* **2011**, *30*, 5919.

[50] a) Y. Marcus, *J. Solution Chem.* **1984**, *13*, 599. b) G. Capozzi, G. Romeo, F. Marcuzzi, *J. Chem. Soc, Chem. Commun.* **1982**, 959.

[51] T. E. Müller, K. C. Hultzsch, M. Yus, F. Foubelo, M. Tada, *Chemical Reviews* **2008**, *108*, 3795.

[52] J. L. McBee, A. T. Bell, T. D. Tilley, *J. Am. Chem. Soc*. **2008**, *130*, 16562.

[53] a) J. J. Brunet, N. C. Chu, M. Rodriguez-Zubiri, *Eur. J. Inorg. Chem*. **2007**, 4711 b) A. A. Koridze, S. A. Kuklin, A. M. Scheloumov, F. M. Dolgushin, V. Y. Lagunova, I. I. Petukhova, M. G. Ezernitskaya, A. S. Peregudov, P. V. Petrovskii, E. V. Vorontsov, M. Baya, R. Poli, *Organometallics* **2004**, *23*, 4585.

[54] H. Qian, R. A. Widenhoefer*, Org. Lett.* **2005**, *7*, 2635.

[55] F. G. Bordwell, D. J. Algrim *J. Am. Chem. Soc*. **1988**, *110*, 2964.

[56] V. M. Vlasov, M. I. Terekhova, E. S. Petrov, A. I. Shatenshtein, G. G. Yakobson, Zh. *Org. Khim*, **1982**, *18*, 1672.

Danksagung

An meinem Lehrer, Herrn Prof. Dr. D. Steinborn, möchte ich an dieser Stelle ein besonderes Wort des Dankes richten, da er durch seinen Enthusiasmus meine Leidenschaft für die Metallorganische Chemie und Homogene Katalyse geweckt hat. Desweiteren danke ich ihm für die Überlassung des interessanten Themas, für die Möglichkeit der freien Gestaltung sowie für seine zahlreichen Anregungen, Hinweise und Diskussionen, die wesentlich zum Gelingen dieser Arbeit beigetragen haben.

Für die Aufnahme der zahlreichen NMR-Spektren bedanke ich mich bei Herrn Dr. D. Ströhl, Frau R. Flächsenhaar sowie Frau Y. Schiller.

Herrn Dr. C. Bruhn, Herrn Dr. C. Wagner sowie Herrn Dipl. Chem. M. Bette danke ich für die Anfertigung der Röntgeneinkristallstrukturanalysen und der immer gewährten Hilfe bei deren Auswertung.

Herrn Dr. T. Müller und Frau Dr. M. Zenkner danke ich für die Anfertigung der Röntgen-Pulverdiffraktogramme und der immer gewährten Hilfe bei deren Auswertung.

Herrn Dr. R. Kluge und Herrn Dr. J. Schmidt für die Aufnahme der ESI-Massenspektren sowie Frau R. Ziehn für die Anfertigung der Elementaranalysen.

Für das sehr angenehme Arbeitsklima und die interessanten Diskussionen und Gespräche, möchte ich an dieser Stelle bei allen Mitgliedern und ehemaligen Mitgliedern der Arbeitsgruppe um Prof. Steinborn bedanken. Außerdem danke ich allen Mitarbeitern und Angehörigen des Institues, die zum Gelingen dieser Arbeit beigetragen haben.

Ein besonderer Dank gilt meinem Freund Ronald, der mir durch sein Verständnis und Unterstützung während der letzten Jahre stets ein Rückhalt bot, ohne ihn wäre diese Arbeit niemals zustande gekommen. Nicht zuletzt gilt mein Dank meiner Familie für ihre gewährte Unterstützung.

Lebenslauf

Name	Anja König
Geburtsdatum	24.09.1981
Geburtsort	Halle (Saale)
Familienstand	ledig
Staatsangehörigkeit	deutsch
Wohnanschrift	Berliner Straße 11, 06886 Lutherstadt-Wittenberg

10/2007 – 02/2013	Promotion an der Martin-Luther-Universität Halle-Wittenberg Halle (Saale), Deutschland Dissertation: *„Synthese, Struktur und Reaktivität von neuartigen Olefin- und Alkinplatin(II)-Komplexen*“ Betreuer: Prof. Dr. D. Steinborn
10/2002 – 09/2007	Studium der Chemie (Diplom) an der Martin-Luther-Universität Halle-Wittenberg, Halle (Saale), Deutschland Diplomarbeit: *„Untersuchungen zur Synthese und Charakterisierung neuartiger Platin(II)-Komplexe*“ Betreuer: Prof. Dr. D. Steinborn, Abschluss: Diplom-Chemiker
04/2002 – 09/2002	Kassierer im *HIT* Verbrauchermarkt München-Fasangarten, Deutschland
11/2001 – 03/2002	Skilehrer in Saalbach Salzburger Land, Österreich
10/2000 – 10/2001	AuPair Aufenthalt in Woodstock Maryland, USA
09/1992 – 07/2000	Gymnasium, Burg-Gymnasium, Wettin Abschluss: Abitur
09/1988 – 08/1992	Grundschule

Lutherstadt-Wittenberg, den 06.05.2013

Eidesstattliche Erklärung

Hiermit erkläre ich an Eides statt, dass ich die vorliegende Arbeit selbstständig und nur unter Verwendung der angegebenen Quellen und Hilfsmittel angefertigt habe.
Diese Arbeit wurde bisher an keiner anderen Universität oder Hochschule vorgelegt.

Lutherstadt-Wittenberg, den 06.05.2013

ORGANOMETALLICS Article
pubs.acs.org/Organometallics

On the Equilibrium between Alkyne and Olefin Platinum(II) Complexes of Zeise's Salt Type: Syntheses and Characterization of [K(18C6)][PtCl$_3$(RC≡CR′)]

Anja König, Martin Bette, Christoph Wagner, Ronald Lindner, and Dirk Steinborn*

Institut für Chemie −Anorganische Chemie, Martin-Luther-Universität, Kurt-Mothes-Strasse 2, D-06120 Halle, Germany

Supporting Information

ABSTRACT: Zeise's type alkyne complexes [K(18C6)]-[PtCl$_3$(RC≡CR′)] (R/R′ = Me/Me, **3**; Et/Et, **4**; Me/*t*-Bu, **5**; *t*-Bu/*t*-Bu, **6**; Me/Ph, **7**; Me/CO$_2$Me, **8**; RC≡CR′ = COC, **9**; COC = cyclooctyne; 18C6 = 18-crown-6) were obtained from the *cis*-but-2-ene complex [K(18C6)][PtCl$_3$(*cis*-but-2-ene)] (**2**) and the requisite alkyne via a ligand substitution reaction. ^{1}H NMR spectroscopically determined equilibrium constants showed that the formation of all these alkyne complexes is endergonic, except that of the cyclooctyne complex **9**, which is strongly exergonic. The identities of the complexes were proved by microanalysis and NMR spectroscopy (^{1}H, ^{13}C). X-ray diffraction analyses of complexes **5**−**7** exhibited slightly elongated C≡C triple bonds (1.23(1)−1.24(1) Å) and a back bending of the substituents on the alkyne between 16(1)° and 21(1)°. In contrast, a longer C≡C bond (1.27(1) Å) was found for the cyclooctyne complex **9**, whereas the C−C≡C angles in this complex (26.8(7)°/26.0(7)°) are the same as in the noncoordinated cyclooctyne (26(2)°). Quantum chemical calculations on the DFT level of theory of the complex anions [PtCl$_3$(RC≡CR′)]$^-$ (**3a**′−**9a**′) showed analogous structural features for the coordinated alkynes. Furthermore, energy decomposition analysis exhibited that the extraordinarily high stability of the cyclooctyne complex **9a**′ can be understood in terms of a very low preparation energy of the cyclooctyne (due to the "prebended" structure of the noncoordinated COC) and a relatively high (instantaneous) interaction energy. NBO analyses made clear that the π back-donation in complexes bearing alkynes with electron-withdrawing substituents (Ph, CO$_2$Me) and in the COC complex is significantly greater than that in complexes bearing alkynes with alkyl substituents (Me, Et, *t*-Bu).

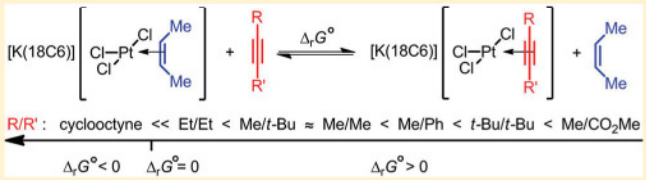

1. INTRODUCTION

Zeise's salt, K[PtCl$_3$(C$_2$H$_4$)]·H$_2$O, the first organo transition metallic compound, was synthesized in 1825 by W. C. Zeise.[1] However, the exact nature of this compound was the subject of long discussions,[2] which finally ended with the development of the corresponding bonding model by M. J. S. Dewar, J. Chatt, and L. A. Duncanson in 1951/1953[3] and the determination of the molecular structure by X-ray and neutron diffraction analysis in 1954 and 1975, respectively.[4] Although numerous olefin complexes of Zeise's salt type M^I[PtCl$_3$(R$_2$C═CR$_2$)] (M^I = alkaline metal; R = H, alkyl, aryl) have been synthesized, alkyne complexes of Zeise's salt type, M^I[PtCl$_3$(RC≡CR′)],[5,6] could be obtained only to a limited extent. These complexes were mainly obtained for alkyne ligands with sterically demanding *tert*-butyl substituents or oxygen-functionalized substituents such as −C(OH)R$_2$ (R = alkyl, aryl) as well as phenyl substituents. Typically, they were synthesized by (i) halide displacement reactions starting from M$^I_2$[PtX$_4$] (X = Cl, Br) or (ii) ethylene displacement reactions starting from M^I[PtCl$_3$(C$_2$H$_4$)].

In our group it was found that the chloro-bridged dinuclear platinum(II) complex [K(18C6)]$_2$[Pt$_2$Cl$_6$] (18C6 = crown ether 18-crown-6) reacts readily not only with olefins but also with alkynes in methylene chloride at room temperature to yield complexes [K(18C6)][PtCl$_3$(RHC═CHR′)][7] (Scheme 1a) and [K(18C6)][PtCl$_3$(RC≡CR′)][8] (Scheme 1b), respectively. The synthesis of the alkyne complexes was found to be restricted to internal alkynes, whereas analogous reactions with terminal alkynes failed due to fast oligo- and polymerization reactions. However, the synthesis of such complexes with terminal alkyne ligands, [K(18C6][PtCl$_3$(RC≡CH)],[8] succeeded via ligand substitution of a volatile alkyne (MeC≡CMe) by a terminal alkyne (Scheme 1c).

Here, we present a straightforward method for the preparation of alkyne platinum(II) complexes of the type [K(18C6)][PtCl$_3$(RC≡CR′)] via ligand substitution (olefin/alkyne) starting from the easily accessible *cis*-but-2-ene complex [K(18C6)][PtCl$_3$(*cis*-MeHC═CHMe)] (**2**). The influence of the alkyne substituents R/R′ on the equilibria of the ligand substitution reactions and, thus, on the course of these reactions is the subject of this study, which permits, with the use of DFT calculations, statements about the relative stability of olefin and alkyne complexes.

2. RESULTS AND DISCUSSION

2.1. Synthesis and Spectroscopic Characterization of [K(18C6)][PtCl$_3$(RC≡CR′)] (3−9).

[K(18C6)][PtCl$_3$(*cis*-MeHC═CHMe)] (**2**), a Zeise's salt type complex, was

Received: August 17, 2011
Published: October 24, 2011

   dx.doi.org/10.1021/om200767q | Organometallics 2011, 30, 5919−5927

Scheme 1

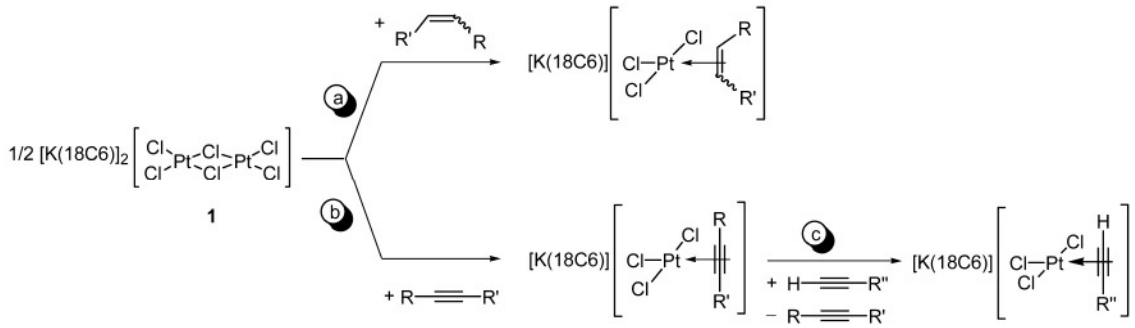

found to react with different internal alkynes in methylene chloride or chloroform as solvent within several minutes, yielding the corresponding alkyne complexes [K(18C6)]-[$PtCl_3$(RC≡CR′)] (**3**–**9**) with liberation of *cis*-but-2-ene (Scheme 2). As revealed by NMR experiments in sealed NMR tubes, alkyne complexes **3**–**8** are in equilibrium with the starting olefin complex **2** (see Section 2.4, Table 5). Thus, a complete degree of conversion toward the alkyne complexes could be achieved only by the addition of an excess of the alkynes supported by evaporation of the volatile olefin in vacuo. Complexes **3**–**9** were isolated as yellow or orange-yellow, slightly air-sensitive microcrystalline substances in 54–96% yields. NMR spectra of complexes **3** and **4** proved to be identical with those prepared according to route b in Scheme 1.[8] The identities of the new complexes **5**–**9** were confirmed by microanalysis, ^{1}H and ^{13}C NMR spectroscopic measurements, and single-crystal X-ray diffraction analyses (**5**–**7**, **9**).

Selected ^{1}H and ^{13}C NMR spectroscopic parameters of the alkyne complexes **3**–**9** are presented in Table 1. The coordination induced shifts (CIS; $\Delta\delta = \delta_{complex} - \delta_{noncoord.ligand}$)[9] of the acetylenic carbon atoms (≡CR/≡CR′) are between −5.6 and −17.8 ppm. The $^1J_{Pt,C}$ coupling constants in complexes with η^2-RC≡CR′ ligands (R, R′ = primary alkyl, aryl) were found to be in the range between 173 and 188 Hz, whereas in complexes with *tert*-butyl-substituted alkyne ligands and in the cyclooctyne (COC) complex values between 216 and 236 Hz were observed. These values differ from those found in Pt(0) complexes of the type [$Pt(RC{\equiv}CR')_2$] (R/R′ = Me, *t*-Bu, Ph; CIS: 35.2–41.6 ppm; $^1J_{Pt,C}$ = 266–311 Hz).[10] In complexes of the type [Pt(Cl)Me(Me_2phen)(RC≡CR)][11] (R = CF_3, CO_2Me) coupling constants of $^1J_{Pt,C}$ = 476–497 Hz are observed. Within the framework of the valence bond theory the magnitude of these coupling constants points to a substantial contribution of a platina(IV)-cyclopropene resonance (canonical) structure.

Due to $^nJ_{H,H}$ couplings and signal overlapping, in the ^{1}H NMR spectra only spectral parameters of methyl-substituted alkynes are indicative. The coordination-induced shifts of the methyl protons were found to be between 0.35 and 0.43 ppm, and the $^3J_{Pt,H}$ coupling constants are in a narrow range of 31–33 Hz. Both parameters are comparable to analogous data of alkyne platinum complexes of the type [PtX_2(Me_2phen)-(MeC≡CR)] (R = H, Me, Ph; X = Br, I; CIS: 0.37–0.45 ppm; $^3J_{Pt,H}$ = 30–39 Hz) described in the literature.[12]

2.2. Molecular Structures of Alkyne Platinum(II) Complexes. Crystals suitable for X-ray diffraction analyses were obtained from the alkyne complexes **5**–**7** and **9**. In all crystals contact ion pairs were found without unusual intermolecular interactions between them. The molecular structures of these complexes are depicted in Figure 1, and selected structural parameters are given in Table 2. The geometry around the Pt(II) center is square planar, in very good approximation (Cl2–Pt–Cl3, Cl1–Pt–Cg(C1/C2)[13] 178.07(5)–179.2(1)°). The alkyne ligands are orientated almost perpendicularly to the coordination plane (Pt,Cl1,Cl2,Cl3) as measured by the interplanar angle Φ (Pt,Cl1,Cl2,Cl3/Pt,C1,C2: 84.1(6)–89.6(4)°, Scheme 3). Within the 3σ criterion the two Pt–C distances in the alkyne complexes are of the same length (Pt–C 2.10(1)–2.141(9) Å). Furthermore, the C1≡C2 triple bonds in the alkyne complexes **5**–**7** (1.23(1)–1.24(1) Å) are only slightly elongated, compared to those in noncoordinated alkynes RC≡CR′ (R, R′ = alkyl, aryl; median: 1.191 Å, lower/upper quartile: 1.185/1.199 Å, number of observations n = 85).[14,15] A similar situation was found in the cyclooctyne complex **9**, where the C≡C bond of both the noncoordinated and coordinated COC are slightly longer (1.23 Å versus 1.27(1) Å) than the respective values in acyclic alkynes. The coordination-induced back bending of the alkyne substituents R/R′ (measured by the angle α, Scheme 3) was found to be between 16(1)° and 21(1)° for complexes **5**–**7**, whereas significantly higher angles (26.8(7)°/26.0(7)°) were observed for the COC complex **9**, although it has to be taken into consideration that, as a consequence of ring formation, the C–C≡C angles in the

Scheme 2

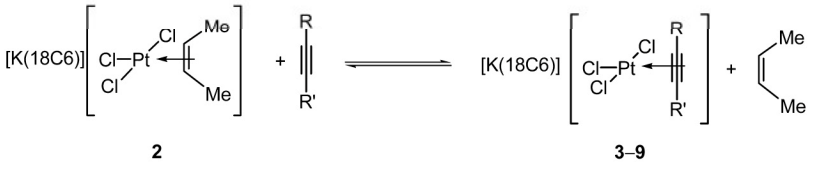

	3	4	5	6	7	8	9
R/R′	Me/Me	Et/Et	Me/*t*-Bu	*t*-Bu/*t*-Bu	Me/Ph	Me/CO_2Me	COC

dx.doi.org/10.1021/om200767q | *Organometallics* 2011, 30, 5919–5927

Organometallics Article

Table 1. Selected ^{1}H and ^{13}C NMR Spectroscopic Data of $[K(18C6)][PtCl_3(RC{\equiv}CR')]$ (3–9) (δ in ppm, J in Hz)[a]

	3	4	5	6	7	8	9
R/R′	Me/Me	Et/Et	Me/*t*-Bu	*t*-Bu/*t*-Bu	Me/Ph	Me/CO_2Me	COC
$\delta(\equiv CCH_3)$	2.11		2.15		2.44	2.35	
$\Delta\delta$	0.39		0.41		0.43	0.35	
$^{3}J_{Pt,H}$	33		32		31	33	
$\delta(\equiv C)$	67.3	72.6	68.1/77.7	78.8	68.2/76.6	–[b]	76.6
$\Delta\delta$	−7.3	−8.4	−5.6/−10.3	−8.3	−11.5/−9.6		−17.8
$^{1}J_{Pt,C}$	173	188	176/223	216	172/180		236
$^{2}J_{Pt,C}$	27	20	27/17	14	27/28		11
$^{3}J_{Pt,C}$		27	19	20	20		42

[a]Values for complexes **3** and **4**, taken from ref 8, are given for comparison. [b]In concentrated solutions of **8** a decomposition within 12 h was observed at rt.

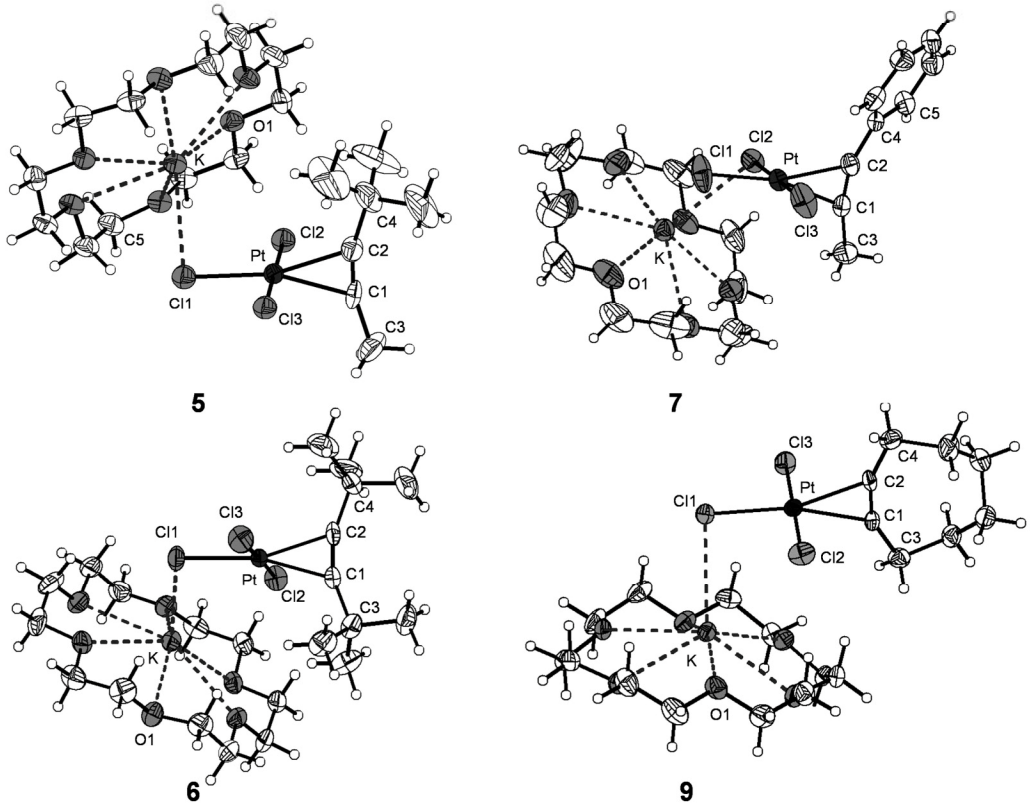

Figure 1. Structures of $[K(18C6)][PtCl_3(RC{\equiv}CR')]$ (R/R′ = Me/*t*-Bu, **5**; *t*-Bu/*t*-Bu, **6**; Me/Ph, **7**; RC≡CR′ = COC, **9**). Displacement ellipsoids are drawn at 30% probability.

noncoordinated cyclooctyne are already severely bent (α = 26(2)°).[14] The structural parameters of complexes **5**–**7** were found to be similar to other alkyne platinum(II) complexes $M^{I}[PtCl_3(RC{\equiv}CR)]$[5,8] ($M^{I}$ = K, [K(18C6)]), $[PtCl_2(RC{\equiv}CR')(amin)]$[16] (R/R′ = H, Me, Et, *t*-Bu, Ph, CMe_2OH, CEt_2OH), and $[PtI_2(Me_2phen)(PhC{\equiv}CPh)]$[12] described in the literature (C≡C 1.18(3)–1.27(4) Å, Pt–C 2.01(2)–2.18(1) Å, α = 15(1)–27(2)°). Furthermore, the significantly higher back bending found in complex **9** (α = 26.8(7)°/26.0(7)°) is comparable to that in other COC complexes $[\{Cu(X)(COC)\}_2]$ and $[Cu(X)(COC)_2]$[17] (X = Cl, Br, I; median: 25.4°, lower/upper quartile: 24.8/26.4°, number of observations n = 9), but significantly lower than in the alkyne platinum(0) complex $[Pt(COC)(PPh_3)_2]$ (α = 35(1)°/34.5(9)°).[18]

In complexes **5**–**7** all Pt–Cl bond lengths are between 2.286(4) and 2.316(5) Å; significant differences in the length between the Pt–Cl bond *trans* to the alkyne and *trans* to Cl were not found. In contrast, the Pt–Cl1 bond in **9** *trans* to the cyclooctyne ligand proved to be significantly longer than those *trans* to the chloro ligand (Pt–Cl1 2.329(2) Å vs Pt–Cl2/Cl3 2.292(2)/2.296(2) Å), thus indicating a relatively high *trans* influence of the COC ligand.

In all structures relatively short distances between the cation $[K(18C6)]^+$ and one of the chloro ligands of the anion indicate cation–anion interactions. The shortest K···Cl contacts (Cl1: **5**, **6**, **9**; Cl2: **7**) were determined to be 3.071(3)–3.191(5) Å (Table 2). These values are in the range of the K···Cl distance in solid $\{KCl\}_s$ (CN(K) = 6; 3.146 Å) but slightly longer than that in gaseous mono- and dinuclear $\{(KCl)_n\}_g$ (CN(K) = 1, n = 1, 2.667 Å; CN(K) = 2, n = 2, 2.950 Å).[19] For a discussion of the conformation of the crown ethers see the Supporting Information (S2).

dx.doi.org/10.1021/om200767q | *Organometallics* 2011, 30, 5919–5927

Table 2. Selected Interatomic Distances (in Å) and Angles (in deg) in Complexes [K(18C6)][$PtCl_3$(RC≡CR′)] (5–7, 9)

	5	6	7	9
R/R′	Me/*t*-Bu	*t*-Bu/*t*-Bu	Me/Ph	COC
Pt–C1	2.10(1)	2.141(9)	2.12(1)	2.132(6)
Pt–C2	2.13(1)	2.130(9)	2.125(8)	2.125(7)
Pt–Cl1	2.316(5)	2.310(3)	2.296(3)	2.329(2)
Pt–Cl2	2.301(3)	2.309(3)	2.286(4)	2.292(2)
Pt–Cl3	2.314(3)	2.299(3)	2.286(3)	2.296(2)
C1–C2	1.24(1)	1.24(1)	1.23(1)	1.27(1)
K···Cl1	3.191(5)	3.071(3)	3.265(4)	3.114(3)
K···Cl2	3.410(6)	3.345(4)	3.176(4)	3.541(3)
K···O	2.796(8)–2.98(1)	2.791(7)–2.967(8)	2.813(8)–2.933(8)	2.781(5)–2.971(6)
K···(O1,... ,O6)[a]	0.780(3)	0.709(2)	0.743(2)	0.774(1)
Cl1–Pt–Cl3	90.9(1)	89.1(1)	89.5(1)	90.67(8)
Cl2–Pt–Cl3	179.2(1)	178.2(1)	179.0(1)	178.87(8)
Cl1–Pt–Cl2	89.7(1)	89.7(1)	90.7(1)	89.53(8)
Cl1–Pt–Cg[b]	178.7(1)	178.62(8)	178.64(8)	178.07(5)
α(C2–C1–C3)[c]	16(1)	21(1)	16(1)	26.8(7)
α(C1–C2–C4)[c]	18(1)	20(1)	20(1)	26.0(7)
Φ[d]	88.3(6)	89.6(4)	84.1(6)	86.7(3)

[a]Distance between the K atom and the mean plane of the crown ether defined by its six O atoms. [b]Cg: Center of gravity between the two acetylenic C atoms (C1/C2). [c]Measure of the back bending α; see Scheme 3. [d]Φ: Angle between the Pt,Cl1,Cl2,Cl3 and the Pt,C1,C2 planes.

2.3. Quantum Chemical Calculations of Alkyne Platinum(II) Complexes. In order to gain deeper insight into the nature of the bond of the alkynes RC≡CR′ to platinum and the influence of the substituents R/R′ in complexes **3**–**9**, DFT calculations of the corresponding anions [$PtCl_3$(RC≡CR′)]$^-$ (**3a′**–**9a′**)[20] have been performed, using high-quality functional and basis sets. The structures of these complex anions as well as selected structural parameters are given in Figure 2 and Table 3. In general, a good agreement between the calculated values (representing structures of anions in the gas phase) and the corresponding values in crystals of [K(18C6)][$PtCl_3$(RC≡CR′)] complexes was found.

The Pt–C bond lengths of all complexes [$PtCl_3$(RC≡CR′)]$^-$ (**3a′**–**9a′**) were found in a narrow range (2.136–2.150 Å) except for the complexes with alkyne ligands MeC≡CPh and MeC≡CCO_2Me bearing electron-withdrawing substituents (**7a′**, 2.119/2.136 Å; **8a′**, 2.103/2.110 Å) as well as with the cyclooctyne ligand (**9a′**; 2.118/2.118 Å). The coordination-induced bond lengthening of the C≡C bonds amounts to 0.039–0.050 Å, and the back bending (measured by the angle α) of alkyl/phenyl substituents R/R′ in the alkyne complexes **5a′**–**7a′** to 18.0–22.2°, whereas the back bending of the strongly electron-withdrawing CO_2Me substituent in **8a′** was found to be 27.9°. In the cyclooctyne complex **9a′** α values of 27.5°/27.5° were found, which proved to be similar to those in noncoordinated cyclooctyne (27.0°/25.3°).

Energy decomposition analysis (EDA) allows to investigate the metal–ligand bond strength. According to the EDA, the energy for the [M]–L bond formation ([M] + L → [M]–L, $-E_{diss}$) can formally be split up into the contribution of two processes: (i) The preparation energy, which is required to promote the two isolated fragments [M] and L from their equilibrium structures to the structures that they acquire in the complex ([M] + L → [M]* + L*, E_{prep}); and (ii) the interaction energy, which is the instantaneous interaction energy of the two "prepared" fragments ([M]* + L* → [M]–L, E_{int}). Thus, the equation $-E_{diss} = E_{int} + E_{prep}$ holds. For a brief explanation of these fundamental steps, see ref 21. The results of the energy decomposition analysis of the platinum–alkyne bonds on the complexes **3a′**–**9a′** are shown in Scheme 4 and Table 4.

A comparison of the values of the dissociation energy E_{diss} of complexes **3a′**–**9a′** demonstrates the order R/R′ = *t*-Bu/*t*-Bu, **6a′** < Me/*t*-Bu, **5a′** ≈ Me/Ph, **7a′** < Me/Me, **3a′** ≈ Et/Et, **4a′** < Me/CO_2Me, **8a′** ≪ COC, **9a′**. Thus, similar values (25.0–26.6 kcal/mol) were found for complexes **3a′**–**7a′**, bearing acyclic alkyl- and aryl-substituted alkyne ligands, whereas a slightly larger value was calculated for **8a′** (28.3 kcal/mol) and an exceptionally high value for the COC complex **9a′** (38.0 kcal/mol). Evaluation of the different energetic contributions shows that the preparation energies of the $PtCl_3^-$ fragment from the equilibrium structure (Cl2–Pt–Cl3 166.3°, Scheme 4) into the "prepared" T-shaped structure (Cl2–Pt–Cl3 177.4–179.7°, Scheme 4) requires less energy (ΔE_{prep} = 3.3–3.7 kcal/mol) than the promotion of the alkyne fragments (ΔE_{prep} = 7.8–11.0 kcal/mol). An exception was found in the case of the cyclooctyne ligand, where a significantly lower preparation energy (ΔE_{prep}(COC) = 3.3 kcal/mol) is required. Interestingly, *t*-Bu substituents as well as electron-withdrawing CO_2Me and Ph substituents in **5a′**–**8a′** give rise to both an increase of the preparation energy of the alkyne fragment by about 1.7–3.2 kcal/mol and an increase in the interaction energy by about 1.5–4.9 kcal/mol, compared to **3a′** and **4a′**, having coordinated alkynes with sterically less bulky methyl and ethyl substituents. By far the highest dissociation energy was found in the cyclooctyne complex **9a′**. It exhibits the highest interaction energy of all investigated complexes as well as a significantly lower preparation energy of the alkyne fragment, which can be attributed to the already bent structure of cyclooctyne in the noncoordinated state.

Scheme 3

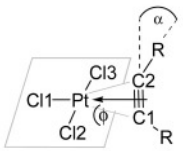

Organometallics Article

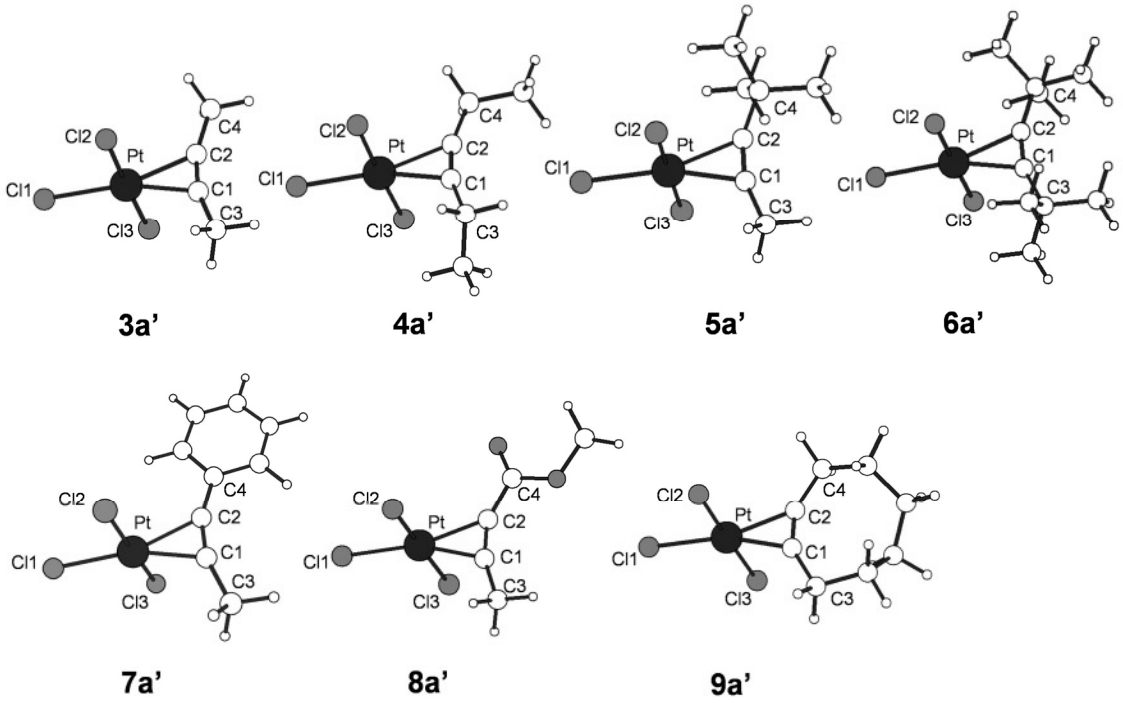

Figure 2. Calculated structures of the complex anions $[PtCl_3(RC{\equiv}CR')]^-$ (R/R′ = Me/Me, **3a′**; Et/Et, **4a′**; Me/*t*-Bu, **5a′**; *t*-Bu/*t*-Bu, **6a′**; Me/COOMe, **8a′**; and RC≡CR′ = COC, **9a′**).

Table 3. Calculated Structural Parameters of $[PtCl_3(RC{\equiv}CR')]^-$ (3a′–9a′) (interatomic distances in Å, angles in deg)

	3a′	4a′	5a′	6a′	7a′	8a′	9a′
R/R′	Me/Me	Et/Et	Me/*t*-Bu	*t*-Bu/*t*-Bu	Me/Ph	Me/CO_2Me	COC
Pt–C1	2.143	2.141	2.136	2.147	2.119	2.103	2.118
Pt–C2	2.143	2.141	2.150	2.147	2.136	2.110	2.118
Pt–Cl1	2.348	2.347	2.349	2.349	2.343	2.341	2.352
Pt–Cl2	2.365	2.365	2.365	2.366	2.362	2.363	2.365
Pt–Cl3	2.365	2.365	2.365	2.366	2.362	2.363	2.365
C1–C2[a]	1.243	1.244	1.245	1.248	1.251	1.254	1.246
	(1.203)	(1.205)	(1.204)	(1.206)	(1.206)	(1.204)	(1.205)
α(C2–C1–C3)	18.0	18.2	18.2	21.5	18.9	20.7	27.5
α(C1–C2–C4)	18.0	18.2	21.9	21.5	22.2	27.9	27.5
Cl1–Pt–Cl3	91.0	91.0	90.6	90.1	90.7	90.7	90.8
Cl2–Pt–Cl3	178.0	178.0	177.4	179.7	178.2	178.0	178.4
Cl1–Pt–Cl2	91.0	91.0	90.6	90.1	90.7	90.7	90.8

[a]The values for the corresponding noncoordinated alkynes are given in parentheses.

As expected, NBO analyses show a depopulation of the bonding π orbitals and a population of the antibonding π^* orbitals of the alkyne ligands in the complex anions **3a′–9a′** compared to the noncoordinated alkynes (Table 4). A remarkable difference can be seen between complexes bearing alkynes with alkyl substituents (R/R′ = Me/Me, **3a′**; Et/Et, **4a′**; Me/*t*-Bu, **5a′**; *t*-Bu/*t*-Bu, **6a′**) and those with electron-withdrawing substituents and the COC ligand (R/R′ = Me/Ph, **7a′**; Me/CO_2Me, **8a′**; COC, **9a′**). In the latter ones a significantly higher population of the antibonding π^* orbitals (P_{π^*}: 0.297–0.307, **3a′–6a′** versus 0.322–0.377, **7a′–9a′**) can be observed, indicating a larger back-donation. This is also reflected by the total charge of the alkyne ligands, q_{alkyne}, which was found to be slightly positive for **3a′–6a′** (0.001 to 0.024 e) and slightly negative for **7a′–9a′** (−0.021 to −0.071 e).

2.4. On Ligand (Olefin/Alkyne) Substitution Reactions in Zeise's Salt Type Complexes. The equilibrium positions of the substitution reactions (according to Scheme 5) were determined NMR spectroscopically in sealed NMR tubes in chloroform at 27 °C. These equilibrium constants give insight into the relative stability of olefin and alkyne complexes of Zeise's type. Values of K_{NMR} between 0.0055 (**8a**) and 0.47 (**4a**) were observed for the formation of alkyne complexes $[PtCl_3(RC{\equiv}CR')]^-$ (R/R′ = Me/Me, Et/Et, Me/*t*-Bu, *t*-Bu/*t*-Bu, Me/Ph, Me/CO_2Me; Table 5) from $[PtCl_3(cis\text{-MeHC}{=}CHMe)]^-$ (**2a**). In contrast, the reaction of the but-2-ene complex **2a** with cyclooctyne resulted in a complete degree of conversion (K_{NMR} estimated to be >500). Thus, the Gibbs free energies, $\Delta_r G^\circ$, for the ligand substitution reactions (but-2-ene versus alkyne) according to Scheme 2 were found to be slightly positive, except for cyclooctyne, which was found to be strongly negative (Table 5). Furthermore, the standard Gibbs free energies of the investigated alkyne complexes (**3a′–9a′**), the olefin complex $[PtCl_3(cis\text{-MeHC}{=}CHMe)]^-$ (**2a′**), the

dx.doi.org/10.1021/om200767q | Organometallics 2011, 30, 5919–5927

Organometallics Article

Scheme 4

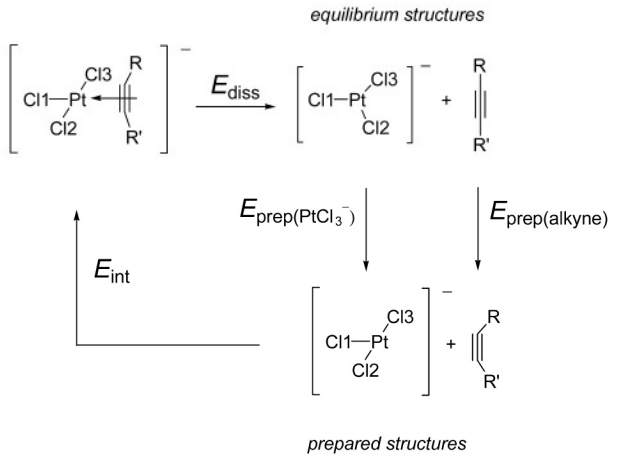

Scheme 5

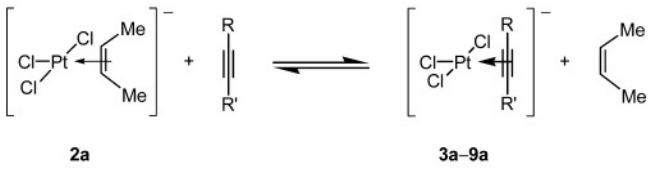

	3a	4a	5a	6a	7a	8a	9a
R/R'	Me/Me	Et/Et	Me/*t*-Bu	*t*-Bu/*t*-Bu	Me/Ph	Me/CO_2Me	COC

noncoordinated alkynes, and *cis*-but-2-ene were calculated at the DFT level of theory. On the basis of these calculations (Section 2.3) the standard Gibbs free energies for the substitution equilibria between $[PtCl_3(cis\text{-}MeHC{=}CHMe)]^-$ (**2a′**) and $[PtCl_3(RC{\equiv}CR')]^-$ (**3a′–9a′**) (Scheme 5) were determined both in the gas phase and with consideration of solvent effects ($CHCl_3$), modeled according to Tomasi's polarized continuum model (Table 5).[22] The solvent influence on the free energy of the substitution reactions was found to be of minor importance for most alkyne complexes, except for the complex $[PtCl_3(MeC{\equiv}CCO_2Me)]^-$ (**8a′**), bearing a polar substituent on the alkyne ligand. Considering a margin of error of the DFT method in the range 1–2 kcal/mol, the calculated values were found to be in good agreement with the experimentally determined values. This demonstrates the capability of the employed DFT model to represent properly the alkyne bonding in Zeise's type complexes.

2.5. On Dissociation Constants of Zeise's Salt Type Complexes. To get insight into the dissociation of Zeise's salt type complexes in solution, conductivity measurements of the *cis*-but-2-ene and the 5,5-dimethylpent-2-yne complex [K(18C6)][$PtCl_3$(*cis*-MeHC=CHMe)] (**2**) and [K(18-C-6)][$PtCl_3$(MeC≡C*t*-Bu)] (**5**), respectively, were performed in chloroform, the same solvent that was used for the ligand substitution reactions. At room temperature the plot of molar conductivity, Λ_M, as a function of the square root of the concentration $\sqrt{c}$ gave proof that [K(18C6)][$PtCl_3$(*cis*-MeHC=CHMe)] (**2**) and [K(18C6)][$PtCl_3$(MeC≡C*t*-Bu)] (**5**) are weak electrolytes (Figure 3a).

From the graph of $1/\Lambda_M$ against the specific conductivity $\kappa = c{\cdot}\Lambda_M$ in the concentration range 1×10^{-4} to 3×10^{-3} mol/L (Figure 3b) the molar conductivity at infinite dilution, Λ_0, was determined by extrapolation against $\kappa \rightarrow 0$. From the obtained values of Λ_0 the dissociation constants K_d of the two complexes were estimated to be about 2×10^{-6} mol/L (**2**) and 6×10^{-5} mol/L (**5**), respectively. Both values correspond to a degree of dissociation α in the range of ≈2% for (**2**) and ≈14% for (**5**) in diluted chloroform solutions ($c = 3 \times 10^{-2}$ mol/L) used in the NMR experiments. Thus, conductivity measurements show a significant dissociation of the ion pairs in diluted $CHCl_3$ solutions, indicating the absence of strongly directed cation–anion interactions. Therefore, it can be assumed that the cation influence on the (olefin/alkyne) substitution reactions is of minor importance.

2.6. Conclusion. We have described a straightforward synthesis for a series of alkyne platinum(II) complexes via ligand substitution (olefin versus alkyne) according to Scheme 2. Furthermore, the equilibria of these reactions were studied both by NMR spectroscopic measurements and by quantum chemical calculations at the DFT level of theory. The following conclusions can be drawn:

Table 4. Bond Characteristics of Alkynes in the Complex Anions $[PtCl_3(RC{\equiv}CR')]^-$ (3a′–9a′): Results of the Energy Decomposition Analysis (EDA) (ΔE_{diss} = bond dissociation energy, ΔE_{int} = instantaneous interaction energy, ΔE_{prep} = preparation energy; all energies in kcal/mol) and NBO Analysis (P_π/P_{π^*} = population of the π/π^* orbitals of the alkyne complexes/noncoordinated alkynes; q_{alkyne} = ligand charge; values in electrons)

	3a′	4a′	5a′	6a′	7a′	8a′	9a′
R/R′	Me/Me	Et/Et	Me/*t*-Bu	*t*-Bu/*t*-Bu	Me/Ph	Me/CO_2Me	COC
ΔE_{diss} [a]	26.5	26.6	26.0	25.0	26.0	28.3	38.0
ΔE_{int} [a]	−37.9	−37.7	−39.2	−39.4	−39.8	−42.6	−44.8
ΔE_{prep} [b]	11.4	11.1	13.2	14.5	13.8	14.3	6.9
$\Delta E_{prep(alkyne)}$	8.1	7.8	9.5	10.8	10.3	11.0	3.3
$\Delta E_{prep(PtCl_3^-)}$	3.3	3.3	3.7	3.7	3.5	3.3	3.6
NBO analysis							
alkyne complexes							
P_π	1.642	1.648	1.642	1.645	1.642	1.631	1.625
P_{π^*}	0.301	0.297	0.301	0.307	0.322	0.377	0.365
q_{alkyne}	0.024	0.012	0.011	0.001	−0.021	−0.071	−0.036
noncoordinated alkynes							
P_π	1.962	1.962	1.963	1.963	1.917	1.905	1.955
P_{π^*}	0.063	0.055	0.054	0.046	0.092	0.061	0.060

[a] With consideration of the BSSE, obtained by counterpoise calculations (BSSE = 1.71–2.56 kcal/mol). [b] $\Delta E_{prep} = \Delta E_{prep(alkyne)} + \Delta E_{prep(PtCl_3^-)}$.

dx.doi.org/10.1021/om200767q | *Organometallics* 2011, 30, 5919–5927

Table 5. Standard Gibbs Free Energies, $\Delta_r G°$ (in kcal/mol), and Equilibrium Constants, K_{NMR}, of the Ligand Substitution Reaction According to Scheme 5, Obtained from NMR Spectroscopic Measurements and Quantum Chemical Calculations, Respectively

	R/R′	K_{NMR}	$\Delta_r G°_{NMR}$	$\Delta_r G°_{gp}{}^a$	$\Delta_r G°_{CHCl_3}{}^b$
3a	Me/Me	0.25	0.8	1.5	1.1
4a	Et/Et	0.47	0.5	0.8	0.6
5a	Me/*t*-Bu	0.26	0.8	1.8	1.9
6a	*t*-Bu/*t*-Bu	0.020	2.3	2.3	3.0
7a	Me/Ph	0.061	1.7	2.0	4.1
8a	Me/CO_2Me	0.0055	3.1	−0.3	3.4
9a	COC	>500[c]	<−3.7[c]	−10.9	−9.8

[a]Calculated Gibbs free energies under gas phase conditions. [b]Calculated Gibbs free energies considering solvent effects ($CHCl_3$). [c]The absence of any signal of noncoordinated COC in the ^{1}H NMR spectrum indicates a degree of formation toward **9a** greater than 0.96.

(1) Structural investigations of alkyne Pt(II) complexes of Zeise's type and DFT calculations of the corresponding anions exhibited that the coordination-induced lengthening of the alkyne C≡C bond and the back bending of its substituents are much smaller than in alkyne Pt(0) complexes. This can be attributed to a, in general, smaller capability for π back-donation in Pt(II) compared to Pt(0) complexes.

(2) NMR spectroscopic investigations and DFT calculations ascertained that the substitution of *cis*-but-2-ene in Zeise's type complexes (Schemes 2 and 5) by alkynes bearing alkyl, aryl, and methoxycarbonyl substituents is endergonic. Thus, the platinum−alkyne bond has to be regarded as slightly less stable than the platinum−olefin bond. An exceptional case was found for the cyclooctyne (COC) ligand. Here, the analogous substitution reaction was found to be distinctly exergonic, demonstrating an unusually strong platinum−alkyne bond.

(3) An energy decomposition analysis gave further insights into the alkyne bonding and clarified that the exceptionally higher dissociation energy by 10−14 kcal/mol of the COC ligand can be attributed both to a reduced preparation energy, ΔE_{prep}(alkyne), due to the already "prebended" alkyne and an increased interaction energy, ΔE_{int}, in the COC complex in about equal amounts. NBO analyses made clear that the COC complex and the complexes bearing alkynes with electron-withdrawing substituents (Ph, CO_2Me) exhibit significantly more back-donation than the complexes bearing alkynes with alkyl substituents (Me, Et, *t*-Bu).

Thus, both the presented experimental and theoretical investigations give insight how subtly the stability of alkyne−platinum(II) complexes depends on the substitution pattern of the alkyne and the ring strain in cyclic alkynes. Furthermore, due to the applicability of the synthesis method for a wide range of alkynes, the diversity of alkyne−platinum(II) complexes could be significantly expanded.

3. EXPERIMENTAL SECTION

3.1. General Procedures. All reactions were performed under an Ar atmosphere using standard Schlenk techniques. Solvents were dried (Et_2O and *n*-pentane over Na benzophenone; $CHCl_3$, $CDCl_3$, CH_2Cl_2, and CD_2Cl_2 over CaH_2; acetone over molecular sieve 3 Å) and distilled prior to use. ^{1}H, ^{13}C, and ^{195}Pt NMR spectra were recorded on Varian Gemini 200, VXR 400, and Unity 500 NMR spectrometers. Chemical shifts are relative to $CHCl_3$ (δ = 7.24) and $CDCl_3$ (δ = 77.0 ppm) as internal references. ^{195}Pt NMR spectra were calibrated with external H_2PtCl_6 (δ_{Pt} 0.0 ppm). Microanalyses were performed by the University of Halle microanalytical laboratory using CHNS-932 (LECO) and Vario EL (Elementar Analysensysteme) elemental analyzers. The starting compounds cyclooctyne (COC), 2,2,5,5-tetramethylhex-3-yne, $[K(18C6)]_2[Pt_2Cl_6]$ (**1**), and $[K(18C6)][PtCl_3(cis\text{-}MeHC{=}CHMe)]$ (**2**) were synthesized according to published methods.[7,23,24] All other chemicals were commercially available.

*Synthesis of [K(18C6)][PtCl$_3$(RC≡CR′)] (R/R′ = Me/Me, **3**; Et/Et, **4**; Me/t-Bu, **5**; Me/Ph, **7**).* To a solution of **2** (126 mg, 0.190 mmol) in CH_2Cl_2 (4 mL) was added the corresponding alkyne (1.14 mmol), and the solution was stirred for 24 h at room temperature, whereby from time to time the liberated volatile olefin was removed by short evaporation of some solvent in vacuo. Then the intense yellow-colored solution was concentrated by evaporation in vacuo to 1−2 mL, and diethyl ether (2 mL) was added. The precipitate was filtered off, washed with Et_2O (2·1 mL), and dried briefly in vacuo. The crude product was purified by dissolving in CH_2Cl_2/acetone and layering with Et_2O.

R/R′ = Me/Me (**3**): Yield 67 mg, 54%. Anal. Calcd for $C_{16}H_{30}Cl_3KO_6Pt$ (658.94): C, 29.16; H, 4.59; Cl, 16.14. Found: C, 28.89; H, 4.86; Cl, 16.07. ^{1}H NMR (200 MHz, 300 K, $CDCl_3$): δ 2.11 (s+d, $^3J_{Pt,H}$ = 33 Hz, 3H, CH_3), 3.66 (s, 24H, OCH_2). ^{13}C NMR (101 MHz, 300 K, CD_2Cl_2): δ 7.7 (s+d, $^2J_{Pt,C}$ = 27 Hz, CH_3), 67.3 (s+d, $^1J_{Pt,C}$ = 173 Hz, ≡CCH_3), 70.0 (s, OCH_2).

R/R′ = Et/Et (**4**): Yield 91 mg, 70%. Anal. Calcd for $C_{18}H_{34}Cl_3KO_6Pt$ (686.99): C, 31.47; H, 4.99; Cl, 15.48. Found: C, 32.02; H, 5.56; Cl, 16.07. ^{1}H NMR (200 MHz, 300 K, $CDCl_3$): δ 1.34 (t, $^3J_{H,H}$ = 7.5 Hz, 6H, CH_3), 2.48 (q, $^3J_{H,H}$ = 7.5 Hz, 4H, CH_2), 3.65

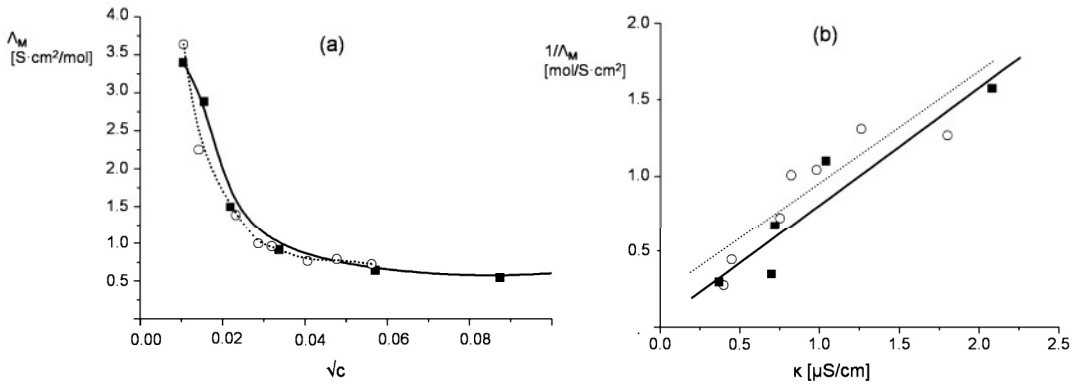

Figure 3. Plot of molar conductivity, Λ_M, as a function of the square root of concentration $\sqrt{c}$ (a) and plot of reciprocal molar conductivity $1/\Lambda_M$ against specific conductivity κ (b) for solutions of **2** (■) and **5** (○) in $CHCl_3$.

dx.doi.org/10.1021/om200767q | *Organometallics* 2011, 30, 5919−5927

(s, 24H, OCH_2). ^{13}C NMR (101 MHz, 300 K, CD_2Cl_2): δ 12.7 (s+d, $^3J_{Pt,C}$ = 27 Hz, CH_3), 15.6 (s+d, $^2J_{Pt,C}$ = 20 Hz, CH_2), 70.4 (s, OCH_2), 72.6 (s+d, $^1J_{Pt,C}$ = 188 Hz, $\equiv CCH_2$).

R/R′ = Me/*t*-Bu (**5**): Yield 120 mg, 90%. Anal. Calcd for $C_{19}H_{36}Cl_3KO_6Pt$ (701.02): C, 32.55; H, 5.18; Cl, 15.17. Found: C, 32.62; H, 5.56; Cl, 15.31. ^1H NMR (200 MHz, 300 K, $CDCl_3$): δ 1.42 (s, 9H, $C(CH_3)_3$), 2.15 (s+d, $^3J_{Pt,H}$ = 32 Hz, 3H, $\equiv CCH_3$), 3.63 (s, 24H, OCH_2). ^{13}C NMR (101 MHz, 300 K, CD_2Cl_2): δ 7.7 (s+d, $^2J_{Pt,C}$ = 27 Hz, $\equiv CCH_3$), 29.1 (s+d, $^2J_{Pt,C}$ = 17 Hz, $C(CH_3)_3$), 30.4 (s+d, $^3J_{Pt,C}$ = 19 Hz, $C(CH_3)_3$), 68.1 (s+d, $^1J_{Pt,C}$ = 176 Hz, $\equiv CCH_3$), 70.0 (s, OCH_2), 77.7 (s+d, $^1J_{Pt,C}$ = 223 Hz, $\equiv C(CH_3)_3$).

R/R′ = Me/Ph (**7**): Yield 115 mg, 84%. Anal. Calcd for $C_{21}H_{32}Cl_3KO_6Pt$ (721.01): C, 34.98; H, 4.47; Cl, 14.75. Found: C, 34.80; H, 4.66; Cl, 15.01. ^1H NMR (200 MHz, 300 K, $CDCl_3$): δ 2.44 (s+d, $^3J_{Pt,H}$ = 31 Hz, 3H, CH_3), 3.63 (s, 24H, OCH_2), 7.33−7.38 (m, 3H, *p*-H/*m*-H), 7.96−8.01 (m, 2H, *o*-H). ^{13}C NMR (50 MHz, 300 K, CD_2Cl_2): δ 8.8 (s+d, $^2J_{Pt,C}$ = 27 Hz, $\equiv CCH_3$), 68.2 (s+d, $^1J_{Pt,C}$ = 172 Hz, $\equiv CCH_3$), 70.4 (s, OCH_2), 76.6 (s+d, $^1J_{Pt,C}$ = 180 Hz, $\equiv CPh$), 123.4 (s+d, $^2J_{Pt,C}$ = 28 Hz, $CC\equiv CCH_3$), 128.6 (s+d, $^2J_{Pt,C}$ = 20 Hz, *m*-*C*), 131.4 (s, o-C), 131.7 (s, p-C).

*Synthesis of [K(18C6)][PtCl$_3$(t-BuC≡Ct-Bu)] (**6**).* To a solution of **2** (200 mg, 0.303 mmol) in $CHCl_3$ (3 mL) was added 2,2,5,5-tetramethylhex-3-yne (167 mg, 1.21 mmol), resulting in an intense yellow-colored solution. After stirring the solution for 24 h at room temperature the solvent and the volatile olefin were removed by evaporating the solution to dryness in vacuo. Then the residue was redissolved in $CHCl_3$ (3 mL), a new batch of 2,2,5,5-tetramethylhex-3-yne (167 mg, 1.21 mmol) was added, and the resulting solution was treated as mentioned above. After eight repetitions of this procedure a nearly complete degree of conversion (>96%) was observed by NMR spectroscopy. Finally, the residue was washed with Et_2O (2·1 mL) and purified by dissolving in CH_2Cl_2/acetone and layering with Et_2O. Yield: 180 mg, 80%. Anal. Calcd for $C_{22}H_{42}Cl_3KO_6Pt$ (743.10): C, 35.56; H, 5.70. Found: C, 35.58; H, 5.71. ^1H NMR (200 MHz, 300 K, $CDCl_3$): δ 1.44 (s, 18H, $C(CH_3)_3$), 3.64 (s, 24H, OCH_2). ^{13}C NMR (101 MHz, 300 K, CD_2Cl_2): δ 28.8 (s+d, $^2J_{Pt,C}$ = 14 Hz, $C(CH_3)_3$), 30.7 (s+d, $^3J_{Pt,C}$ = 20 Hz, $C(CH_3)_3$), 70.5 (s, OCH_2), 78.8 (s+d, $^1J_{Pt,C}$ = 216 Hz, $\equiv Ct$-Bu).

*Synthesis of [K(18C6)][PtCl$_3$(MeC≡CCO$_2$Me)] (**8**).* At −30 °C to a solution of **2** (190 mg, 0.287 mmol) in $CHCl_3$ (3 mL) was added methyl but-2-ynoate (1.41 g, 14.4 mmol), resulting in an intense yellow-colored solution. After stirring the solution for 1 h at −30 °C the solvent and the volatile olefin were removed by evaporating the solution to the dryness in vacuo at this temperature and stirring for another 3 h applying a vacuum (0.1 bar, −30 °C). Finally the product was precipitated by layering with Et_2O/*n*-pentane (3 mL) and washed with *n*-pentane (2 × 3 mL). This product had to be recrystallized from $CHCl_3$ (2 mL) by layering with Et_2O/*n*-pentane (3 mL) and washing with *n*-pentane (2 × 3 mL). Yield: 121 mg, 60%. Anal. Calcd for $C_{17}H_{30}Cl_3KO_8Pt$ (702.95): C, 29.05; H, 4.30. Found: C, 28.90; H, 4.46. ^1H NMR (200 MHz, 300 K, CD_2Cl_2): δ 2.28 (s+d, $^3J_{Pt,H}$ = 33 Hz, 3H, $\equiv CCH_3$), 3.62 (s, 24H, OCH_2), 3.83 (s, 3H, OCH_3).

*Synthesis of [K(18C6)][PtCl$_3$(COC)] (**9**).* To a solution of **2** (260 mg, 0.393 mmol) in CH_2Cl_2 (4 mL) was added cyclooctyne (63.8 mg, 0.590 mmol). After stirring the solution for 30 min at room temperature the intense yellow-colored solution was filtered, concentated in vacuo to 1 mL, and layered with *n*-pentane (2 mL). The precipitate was filtered off, dried briefly in vacuo, and purified by dissolving in CH_2Cl_2/acetone and layering with Et_2O/*n*-pentane. Yield: 269 mg, 96%. Anal. Calcd for $C_{20}H_{36}Cl_3KO_6Pt$ (713.03): C, 33.69; H, 5.09. Found: C, 33.69; H, 5.08. ^1H NMR (200 MHz, 300 K, CD_2Cl_2): δ 1.65 (m, $\equiv CCH_2CH_2CH_2$, 4H), 1.66 (m, $\equiv CCH_2CH_2$, 4H), 2.57 (m, $\equiv CCH_2CH_2$, 4H), 3.65 (s, OCH_2, 24H). ^{13}C NMR (50 MHz, 300 K, CD_2Cl_2): δ 22.4 (s+d, $^2J_{Pt,C}$ = 11 Hz, $\equiv CCH_2CH_2$), 28.9 (s, $\equiv CCH_2CH_2CH_2$), 30.2 (s+d, $^3J_{Pt,C}$ = 42 Hz, $\equiv CCH_2CH_2$), 70.4 (s, OCH_2), 76.6 (s+d, $^1J_{Pt,C}$ = 236 Hz, $\equiv CCH_2$). ^{195}Pt NMR (107 MHz, 300 K, CD_2Cl_2): δ −2078.7 (s).

*Reaction of [K(18C6)][PtCl$_3$(MeHC═CHMe)] (**2**) with Alkynes.* In a typical experiment complex **2** (15 mg, 0.023 mmol) was placed into an NMR tube, and a solution of the requisite alkyne RC≡CR′ in $CDCl_3$ (0.7 mL) was added at −80 °C. Then the NMR tube was closed by melting and warmed to room temperature. ^1H NMR spectroscopic measurements revealed that in all cases the equilibrium composition was reached within 10 min. The positions of the equilibria were calculated from signals of nonsuperimposed protons; see Supporting Information. The equilibrium constants given in Table 5 were obtained from at least two independent experiments using different stoichiometric ratios (Table S3).

X-ray Structure Determinations. Crystals suitable for X-ray diffraction analyses were grown at room temperature from solutions of complexes in CH_2Cl_2/acetone by slow addition of diethyl ether (**5**−**7**) and diethyl ether/*n*-pentane (**9**), respectively. Intensity data were collected on a STOE IPDS diffractometer at 200(2) K (**9**) and a STOE STADI IV diffractometer at 293(1) K (**5**−**7**), with Mo Kα radiation (λ = 0.71073 Å, graphite monochromator). Crystallographic data and data collection parameters are given in Table S1. Absorption corrections were applied using Ψ-scans for **5** (T_{min}/T_{max} 0.16/0.26), **6** (T_{min}/T_{max} 0.21/0.42), and **7** (T_{min}/T_{max} 0.21/0.42) and numerically for **9** (T_{min}/T_{max} 0.28/0.88). The structures were solved by direct methods with SHELXS-97 and refined using full-matrix least-squares routines against F^2 with SHELXL-97.[25] Non-hydrogen atoms were refined with anisotropic displacement parameters and hydrogen atoms with isotropic displacement parameters. Hydrogen atoms were added to their calculated positions and refined according to the riding model.

Computational Details. DFT calculations were carried out by the Gaussian03 program package[26] using the hybrid functional B3LYP. The 6-311G(d,p)[27] basis sets as implemented in Gaussian03 were employed for C, H, O, and Cl atoms, while the relativistic pseudopotential of the Ahlrichs group and related basis functions of TZVPP quality[28] were employed for Pt atoms. The appropriateness of the functional in combination with the basis sets and effective core potential used for reliable interpretation of structural and energetic aspects of related platinum complexes has been demonstrated.[29] All systems were fully optimized without any symmetry restrictions. The resulting geometries were characterized as equilibrium structures by the analysis of the force constants of normal vibrations. Solvent effects were considered according to the polarized continuum model.[22] Basis set superposition errors (BSSE) were calculated according to the counterpoise method as implemented in Gaussian03.[30] The atom coordinates as well as energies of all calculated equilibrium structures are given in the Supporting Information (S4). Energy decomposition analyses were performed on the basis of the optimized structures of the complexes and fragments, as given in the literature.[21] The NBO analyses were performed with the NBO module as implemented in Gaussian03.[31]

■ ASSOCIATED CONTENT

Ⓢ Supporting Information

CIF files giving crystallographic data for **5**−**7**, **9** (CCDC 838514−839517), crystallographic and structure refinement data for **5**−**7**, **9** (S1), description of crown ether conformations in **5**−**7**, **9** (S2), details of equilibrium constants of substitution reactions (S3), as well as energies and atom coordinates of all calculated equilibrium structures (S4). This material is available free of charge via the Internet at http://pubs.acs.org.

■ AUTHOR INFORMATION

Corresponding Author

*E-mail: dirk.steinborn@chemie.uni-halle.de.

■ REFERENCES

(1) (a) Zeise, W. C. *Overs K. Dan. Vidensk. Selsk. Forh.* **1825−1826**, 13. (b) Zeise, W. C. *Pogg. Ann. Phys.* **1827**, *9*, 632.

(2) (a) Liebig, J. *Ann. Pharm.* **1834**, *9*, 1. (b) Zeise, W. C. *Ann. Pharm.* **1837**, *23*, 1. (c) Griess, P.; Martius, C. A. *Ann. Pharm.* **1861**, *120*, 324. (d) Birnbaum, K. *Liebigs Ann. Chem.* **1868**, *145*, 67.

(3) (a) Dewar, M. J. S. *Bull. Soc. Chim. Fr.* **1951**, *18*, C71−C79. (b) Chatt, J.; Duncanson, L. A. *J. Chem. Soc.* **1953**, 2939.

(4) (a) Wunderlich, J. A.; Mellor, D. P. *Acta Crystallogr.* **1954**, *7*, 130. (b) Love, R. A.; Koetzle, T. F.; Williams, G. J. B.; Andrews, L. C.; Bau, R. *Inorg. Chem.* **1975**, *14*, 2653.
(5) (a) Beauchamp, A. L.; Rochon, F. D.; Theophanides, T. *Can. J. Chem.* **1973**, *51*, 126. (b) Dubey, R. J. *Acta Crystallogr.* **1976**, *B32*, 199.
(6) (a) Chatt, J.; Duncanson, L. A.; Guy, R. G. *Chem. Ind.* **1959**, 430. (b) Chatt, J.; Guy, R. G.; Duncanson, L. A. *J. Chem. Soc.* **1961**, 827. (c) Chatt, J.; Guy, R. G.; Duncanson, L. A.; Thompson, D. T. *J. Chem. Soc.* **1963**, 5170.
(7) (a) Steinborn, D.; Potechin, V. V.; Gerisch, M.; Bruhn, C.; Schmidt, H. *Trans. Met. Chem.* **1999**, *24*, 67. (b) Schwieger, S.; Wagner, C.; Bruhn, C.; Schmidt, H.; Steinborn, D. *Z. Anorg. Allg. Chem.* **2005**, *631*, 2696.
(8) (a) Steinborn, D.; Tschoerner, M.; von Zweidorf, A.; Sieler, J.; Bögel, H. *Inorg. Chim. Acta* **1995**, *234*, 47. (b) Gerisch, M.; Heinemann, F. W.; Bögel, H.; Steinborn, D. *J. Organomet. Chem.* **1997**, *548*, 247.
(9) Albano, V. G.; Demartin, F.; De Felice, V.; Morelli, G.; Vitagliano, A. *Gazz. Chim. Ital.* **1987**, *117*, 437.
(10) Boag, N. M.; Green, M.; Grove, D. M.; Howard, J. A. K.; Spencer, J. L.; Stone, F. G. A. *J. Chem. Soc., Dalton Trans.* **1980**, 2170.
(11) De Felice, V.; De Renzi, A.; Giordano, F.; Tesauro, D. *J. Chem. Soc., Dalton Trans.* **1993**, 1927.
(12) Fanizzi, F. P.; Natile, G.; Lanfranchi, M.; Tiripicchio, A.; Pacchioni, G. *Inorg. Chim. Acta* **1998**, *275*−*276*, 500.
(13) Cg(C1/C2): Center of gravity between the two acetylenic C atoms.
(14) Landolt-Börnstein. *Numerical Data and Functional Relationships in Science and Technology*; Springer: Berlin, 1976, 1987, 1992, 1995; Vols. *7, 15, 21, 23*.
(15) *Cambridge Structural Database (CSD)*, Version 5.29; Cambridge University Chemical Laboratory: Cambridge, 2007.
(16) (a) Rochon, F. D.; Melanson, R.; Doyon, M. *Can. J. Chem.* **1989**, *67*, 2209. (b) Davies, G. R.; Hewertson, W.; Mais, R. H. B.; Owston, P. G.; Patel, C. G. *J. Chem. Soc. A* **1970**, 1873.
(17) (a) Gröger, G.; Behrens, U.; Olbrich, F. *Organometallics* **2000**, *19*, 3354. (b) Manojlović-Muir, L.; Muir, K. W.; Walker, R. *Acta Crystallogr.* **1979**, *B35*, 2416.
(18) Robertson, G. B.; Whimp, P. O. *Aust. J. Chem.* **1980**, *33*, 1373.
(19) Landolt-Börnstein. *Numerical Data and Functional Relationship in Science and Technology*; Springer: Berlin, 1987, 1998; Vols. *15, 25*.
(20) Anions are designated with the letter "**a**" and calculated structures with a prime " ′ ".
(21) (a) Frenking, G.; Fröhlich, N. *Chem. Rev.* **2000**, *100*, 717. (b) Frenking, G.; Wichmann, K.; Fröhlich, N.; Loschen, C.; Lein, M.; Frunzke, J.; Rayón, V. M. *Coord. Chem. Rev.* **2003**, *238*−*239*, 55.
(22) (a) Mennucci, B.; Tomasi, J. *J. Chem. Phys.* **1997**, *106*, 5151. (b) Cancès, E.; Mennucci, B.; Tomasi, J. *J. Chem. Phys.* **1997**, *107*, 3032. (c) Cossi, M.; Barone, V.; Mennucci, B.; Tomasi, J. *Chem. Phys. Lett.* **1998**, *286*, 253.
(23) Capozzi, G.; Romeo, G.; Marcuzzi, F. *J. Chem. Soc., Chem. Commun.* **1982**, 959.
(24) Tietze, L.-F.; Eicher, T. In *Reaktionen und Synthesen im Organisch-Chemischen Praktikum*: Georg Thieme Verlag: Stuttgart, 1981.
(25) (a) Sheldrick, G. M. *SHELXS-97 Program for Crystal Structures Solutions*; University of Göttingen: Göttingen, Germany, 1990. (b) Sheldrick, G. M. *SHELXL-97 Program for the Refinement of Crystal Structures*; University of Göttingen: Göttingen, Germany, 1997.
(26) Frisch, M. J.; et al. *Gaussian 03*, revision B.04; Gaussian, Inc.: Wallingford, CT, 2004.
(27) (a) Dewar, M. J. S.; Reynolds, C. H. *J. Comput. Chem.* **1986**, *7*, 140. (b) Raghavachari, K.; Pople, J. A.; Replogle, E. S.; Head-Gordon, M. *J. Phys. Chem.* **1990**, *94*, 5579.
(28) (a) Weigend, F.; Häser, M.; Patzelt, H.; Ahlrichs, R. *Chem. Phys. Lett.* **1998**, *294*, 143. (b) Leininger, T.; Nicklass, A.; Küchle, W.; Stoll, H.; Dolg, M.; Bergner, A. *Chem. Phys. Lett.* **1996**, *255*, 274. (c) Andrae, D.; Häussermann, U.; Dolg, M.; Stoll, H.; Preuss, H. *Theor. Chim. Acta.* **1990**, *77*, 123.
(29) (a) Steinborn, D.; Schwieger, S. *Chem.—Eur. J.* **2007**, *13*, 9668. (b) Werner, M.; Lis, T.; Bruhn, C.; Lindner, R.; Steinborn, D. *Organometallics* **2006**, *25*, 5946. (c) Vetter, C.; Kaluderović, G. N.; Paschke, R.; Gómez-Ruiz, S.; Steinborn, D. *Polyhedron* **2009**, *28*, 3699. (d) Schwieger, S.; Heinemann, F. W.; Wagner, C.; Kluge, R.; Damm, C.; Israel, G.; Steinborn, D. *Organometallics* **2009**, *28*, 2485.
(30) (a) Simon, S.; Duran, M.; Dannenberg, J. J. *J. Chem. Phys.* **1996**, *105*, 11024. (b) Boys, S. F.; Bernardi, F. *Mol. Phys.* **1970**, *19*, 553.
(31) (a) Glendening, E. D.; Badenhoop, J. K.; Reed, A. E.; Carpenter, J. E.; Bohmann, J. A.; Morales, C. M.; Weinhold, F. *NBO 5.0*; Theoretical Chemistry Institute, University of Wisconsin: Madison, WI, 2001. (b) Weinhold, F.; Landis, C. R. *Chem. Ed.: Res. Pract.* **2001**, *2*, 91. (c) Foster, J. P.; Weinhold, F. *J. Am. Chem. Soc.* **1980**, *102*, 7211. (d) Reed, A. E.; Weinhold, F. *J. Chem. Phys.* **1983**, *78*, 4066. (e) Reed, A. E.; Weinstock, R. B.; Weinhold, F. *J. Chem. Phys.* **1985**, *83*, 735.

View Online / Journal Homepage / Table of Contents for this issue
Dynamic Article Links

Dalton Transactions

Cite this: *Dalton Trans.*, 2012, **41**, 7156

www.rsc.org/dalton

PAPER

On the isomerization of cyclooctyne into cycloocta-1,3-diene: synthesis, characterization and structure of a dinuclear platinum(II) complex with a μ-η²:η²-1,3-COD ligand†

Anja König, Christoph Wagner, Martin Bette and Dirk Steinborn*

Received 13th December 2011, Accepted 12th April 2012
DOI: 10.1039/c2dt12405j

The Zeise's salt type cyclooctyne compound $[K(18C6)][PtCl_3(COC)]$ (**1**; COC = cyclooctyne; 18C6 = 18-crown-6) was found to react in chloroform solution at room temperature within several weeks yielding the dinuclear cyclooctadiene compound $[K(18C6)]_2[(PtCl_3)_2(\mu\text{-}\eta^2\text{:}\eta^2\text{-}1,3\text{-COD})]$ (**2**; 1,3-COD = cycloocta-1,3-diene) and non-coordinated cycloocta-1,3-diene. The identity of **2** was confirmed by microanalysis, NMR spectroscopy (^1H, ^{13}C) and electrospray ionization mass spectrometry (ESI-MS). A single-crystal X-ray diffraction analysis of **2** exhibited a bridging μ-η²:η²-cycloocta-1,3-diene ligand with non-conjugated double bonds each coordinated to a $PtCl_3$ fragment. On the basis of DFT calculations as well as energy decomposition analyses (EDA), charge decomposition analyses (CDA) and natural bond orbital (NBO) analyses the peculiarities of the nature of the Pt–C bonds in the dinuclear complex anion $[(PtCl_3)_2(\mu\text{-}\eta^2\text{:}\eta^2\text{-}1,3\text{-COD})]^{2-}$ (**2a′**) compared with those in mononuclear olefin complexes of Zeise's salt type $[PtCl_3L]^-$ (L = η²-1,3-COD, **3a′**; *cis*-but-2-ene, **4a′**; COE, **5a′**; COE = cyclooctene) are discussed. Furthermore, the driving force for the strongly exergonic reaction with formation of the cyclooctadiene complex **2a′** was found to be a significant release of ring strain of the cyclooctyne ligand in the starting compound **1**.

Introduction

Isomerization reactions of alkynes under triple bond migration[1] as well as formation of allenes[2] or 1,3-dienes[3] are of particular interest in organic synthesis. The latter isomerization reaction has been at first described to proceed under strongly basic or acidic conditions as well as by heterogeneous catalysts. However, harsh reaction conditions (temperature 100–400 °C) and low selectivity are typical of these reactions.[4] As exemplified by the isomerization of butyne (see Fig. 1), the driving force for this kind of reaction is the higher stability of the 1,3-diene.

The first example for a transition metal catalyzed homogeneous reaction was found in 1980 with the hydrido-ruthenium catalyzed isomerization of acetylenic silyl ethers into dienol silyl ethers.[5] In the following, isomerization reactions of alkynes RC≡CR′ (R = alkyl) activated with electron withdrawing α substituents (R′ = C(O)R, C(O)OR, $C(O)NR_2$) were reported under formation of the corresponding conjugated (*E*,*E*)-dienones, (*E*,*E*)-dienoates and (*E*,*E*)-dienamides, catalyzed by Co, Rh, Ir, Ru, Re, Pd metal complexes.[6–10] Although the underlying mechanism of this isomerization has not yet been fully understood, allene-like intermediates are postulated.[10,11,17] Such intermediates are also discussed in analogous isomerization reactions performed with (metal-free) phosphane catalysts.[11,12]

Furthermore, alkynes RC≡CR′ (R = alkyl) with other electron-withdrawing substituents (R′ = $(CF_2)_nCl$, *n* = 2, 4, 8; aryl) and also those functionalized at the β position (R′ = $CH_2C(CO_2Me)_2Me$) were found to undergo a rhodium or palladium catalyzed isomerization into the corresponding dienes.[13,14] Finally, alkynes bearing vinylogous carbonyl groups can be isomerized by ruthenium and iridium catalysts into conjugated (*E*,*E*,*E*)-trienones.[15]

In contrast, isomerization reactions of non-functionalized alkynes into 1,3-dienes are significantly less common and are restricted to a narrow substrate scope. Thus, cyclododecyne was

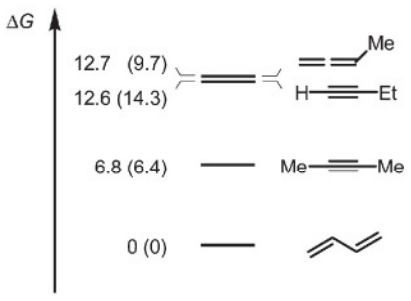

Fig. 1 Relative Gibbs-free energies Δ*G* (in kcal mol^{-1}) of several butyne isomers based on calorimetric measurements[1,38] and calculations on the DFT level of theory (in parentheses), respectively.

Institut für Chemie – Anorganische Chemie, Martin-Luther-Universität Halle-Wittenberg, Kurt-Mothes-Straße 2, D-06120 Halle, Germany

† Electronic supplementary information (ESI) available. CCDC 858731. For ESI and crystallographic data in CIF or other electronic format see DOI: 10.1039/c2dt12405j

found to isomerize to the corresponding (*E*,*Z*)-cyclododeca-1,3-diene as the main product using a rhodium catalyst.[16] Furthermore, simple internal alkynes such as oct-4-yne were found to react with electron-deficient olefins like MeO_2C–CH═CH–CO_2Me in a ruthenium-catalyzed formal [4 + 2] cycloaddition yielding cyclohexenedicarboxylates. As a first reaction step, the isomerization of the alkyne into a 1,3-diene followed by a Diels–Alder reaction is discussed.[17]

Here, we describe the isomerization of a cyclic alkyne ligand of a platinum(II) complex of Zeise's salt type, [K(18C6)]-[$PtCl_3$(COC)] (**1**), into a dinuclear complex bearing a bridging cycloocta-1,3-diene ligand.

Results and discussion

2.1. Synthesis and spectroscopic characterization

In an earlier work we described the synthesis of a cyclooctyne compound of Zeise's salt type, [K(18C6)][$PtCl_3$(COC)] (**1**), *via* a ligand substitution reaction starting from the corresponding *cis*-but-2-ene compound (Scheme 1a).[18] At room temperature, solutions of the cyclooctyne complex **1** in chloroform–acetone were found to undergo within several weeks a transformation into a cycloocta-1,3-diene (1,3-COD) compound, [K(18C6)]$_2$-[($PtCl_3$)$_2$(μ-η^2:η^2-1,3-COD)]·Me_2CO (**2**·Me_2CO), with concomitant formation of non-coordinated cycloocta-1,3-diene (Scheme 1b). After 8 weeks, the degree of conversion was found to be >90%. The reaction proved to be highly selective; the only side product are small amounts of platinum. Compound **2**·Me_2CO could be isolated as yellow, slightly air-sensitive crystals in yields of 60%. The identity was confirmed by microanalysis, ESI-MS and NMR spectroscopic measurements. The coordination induced shifts (CIS; $\Delta\delta = \delta_{complex} - \delta_{noncoord.ligand}$)[19] of the olefinic carbon atoms ═*C*H are −41.9 and −47.7 ppm. Thus, they are in the same range (−40 to −55 ppm) as those of olefinic *C* atoms in olefin platinum(II) complexes.[20]

The $^1J_{Pt,C}$ coupling constants in compound **2** were found to be 204 and 259 Hz. These values differ slightly from those found in platinum(II) compounds of the type M^I[$PtCl_3$(R_2C═CR_2')] (M^I = [K(18C6)], [N(*n*-Bu)$_4$], PPh_4; R/R′ = H, alkyl, aryl) ($^1J_{Pt,C}$ = 180–193 Hz) whereas in complexes of the types [$PtCl_2L_2$] and [{$PtCl_2L$}$_2$] (L = ethylene, 1,5-COD) coupling constants of $^1J_{Pt,C}$ = 131–152 Hz were observed.[20–22]

An ESI mass spectrum of compound **2** was obtained by the direct injection ESI-MS technique using a solution of the compound in dry CH_2Cl_2 (Fig. 2). The parent peak at *m*/*z* 1012.9 represents the anion [K(18C6)][($PtCl_3$)$_2$(μ-η^2:η^2-1,3-COD)]$^-$; its observed isotope pattern is in good agreement with the calculated values. Furthermore, platinum-containing mass peaks of lower intensities such as [$PtCl_3$]$^-$ (*m*/*z* 301.5), [$PtCl_3$(1,3-COD)]$^-$ (*m*/*z* 409.2) and [Pt_2Cl_4(1,3-COD$_{-H}$)]$^-$ (*m*/*z* 639.1) were also detected. As shown NMR spectroscopically, these species are not present in the original solution, but formed by thermal decomposition during the ionization process.

2.2. Structural investigations

The molecular structure of **2**, obtained by a single-crystal X-ray diffraction analysis of **2**·Me_2CO, is shown in Fig. 3; selected structural parameters are given in Table 1. The dinuclear platinum(II) complex dianion is built up by a bridging μ-η^2:η^2-cycloocta-1,3-diene ligand in which each of the two double bonds is coordinated to a $PtCl_3$ fragment. Thus, the platinum atoms are square-planar coordinated by three chlorido ligands and an olefinic double bond. Analogous to Zeise's salt type compounds, the olefinic double bond is oriented almost perpendicularly to the coordination plane (interplanar angles $PtCl_3$–PtC_2 88.9(3)/89.6(3)°). The dihedral angle C1═C2–C3═C4 of the diene fragment amounts to 59.7(9)° (for comparison: 37.8(1)° in non-coordinated COD[23]) which excludes any π conjugation. Thus, the two double bonds have to be regarded to be isolated ones.

2·Me_2CO is the first crystallographically characterized compound bearing a μ-1,3-COD ligand.[24] In structurally characterized complexes with bridging acyclic 1,3-diene ligands the double-bond system is conjugated in most cases. Thus, *e.g.*, in butadiene platinum complexes [($PtCl_2L_2$)$_2$(μ-η^2:η^2-C_4H_6)] (L_2 = 2 PMe_2Ph, 2,3-butanedione-*N*,*N*-bis(dimethylhydrazone)) C═CH–CH═C dihedral angles of 180° were found.[25] The C═C bonds in **2**·Me_2CO (1.412(9)/1.394(9) Å) are of the same length (1.391(7)–1.399(6) Å) as those in compounds of Zeise's salt type, M^I[$PtCl_3$(COE)] (M^I = [PPh_4], [NBu_4], COE = cyclooctene).[26] Thus, the coordination-induced bond lengthening of 5–6 pm is in the same range as for Zeise's type complexes with cyclic monoolefin ligands.

In crystals of **2**·Me_2CO contact ion pairs of **2** and solvate molecules (Me_2CO) without unusual interactions between them were found. The [($PtCl_3$)$_2$(μ-1,3-COD)]$^{2-}$ and [K(18C6)]$^+$ ions form contact ion pairs. Noteworthy, only one of the two $PtCl_3$ fragments is involved. The shortest K···Cl contacts (3.132(2)–3.453 (3) Å; Table 1) are in the range of the K···Cl distance in {KCl}$_s$ (*CN*(K) = 6; 3.146 Å), but are significantly longer than those in gaseous mono- and dinuclear {(KCl)$_n$}$_g$ (*CN*(K) = 1, *n* = 1, 2.667 Å; *CN*(K) = 2, *n* = 2, 2.950 Å).[27]

To prove additionally the identity and the phase purity of the bulk material obtained in the synthesis of [K-(18C6)]$_2$[($PtCl_3$)$_2$(μ-η^2:η^2-1,3-COD)]·Me_2CO (**2**·Me_2CO), an X-ray diffraction (XRD) pattern of the solid material of **2**·Me_2CO was measured. As shown in the ESI (S2†), the XRD pattern confirms the pattern calculated from the single-crystal X-ray data, thus indicating the phase purity of the bulk material.

2.3. Quantum chemical calculations

To get further insight into the thermodynamics of the formation of the COD complex **2a′** and into the platinum olefin bonding, DFT calculations were performed. The equilibrium structure of [($PtCl_3$)$_2$(μ-η^2:η^2-1,3-COD)]$^{2-}$ (**2a′**)‡ as well as selected structural parameters are given in Fig. 4 and Table 1. The comparison between the calculated values (representing the structure of the dianion **2a′** in the gas phase) and the corresponding values in crystals of **2**·Me_2CO reveals a good agreement. An inspection of the structural parameters of cycloocta-1,3-diene shows that also the non-coordinated molecule exhibits a significantly non-planar

‡ Anions are designated with the letter "**a**" and calculated structures with a dash " ′ ".

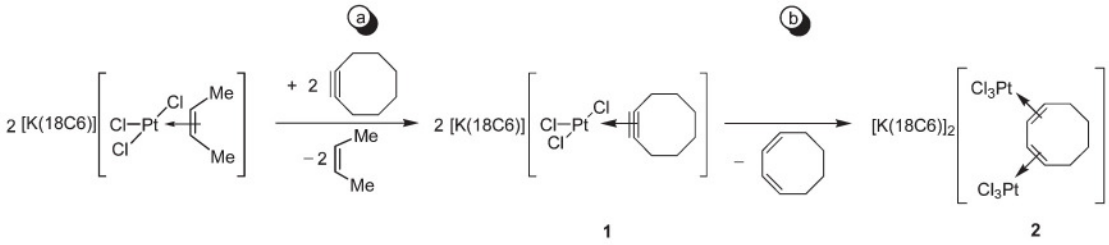

Scheme 1 Syntheses of compounds **1** and **2**.

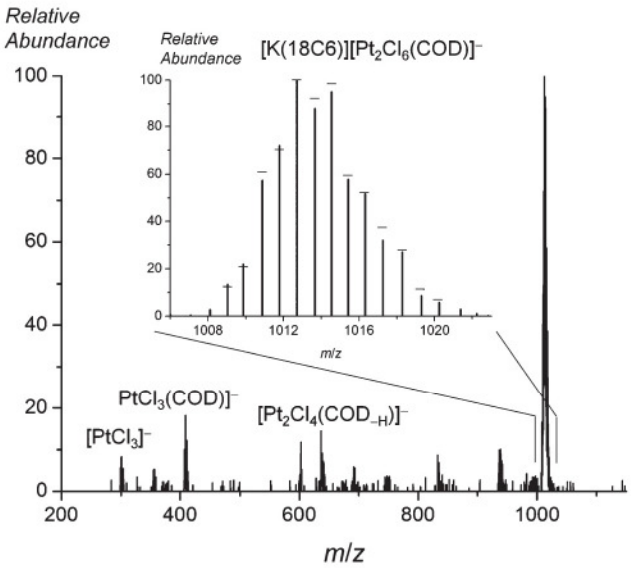

Fig. 2 ESI mass spectrum obtained from $[K(18C6)]_2[(PtCl_3)_2(\mu\text{-}\eta^2\text{:}\eta^2\text{-}1,3\text{-COD})]\cdot Me_2CO$ (**2**·Me_2CO) (negative ion mode, solvent CH_2Cl_2). The inset shows an expansion of the isotope pattern for a $[K(18C6)][(PtCl_3)_2(\mu\text{-}\eta^2\text{:}\eta^2\text{-}1,3\text{-COD})]^-$ species at *m*/*z* 1012.9 (calculated intensities are shown by horizontal bars).

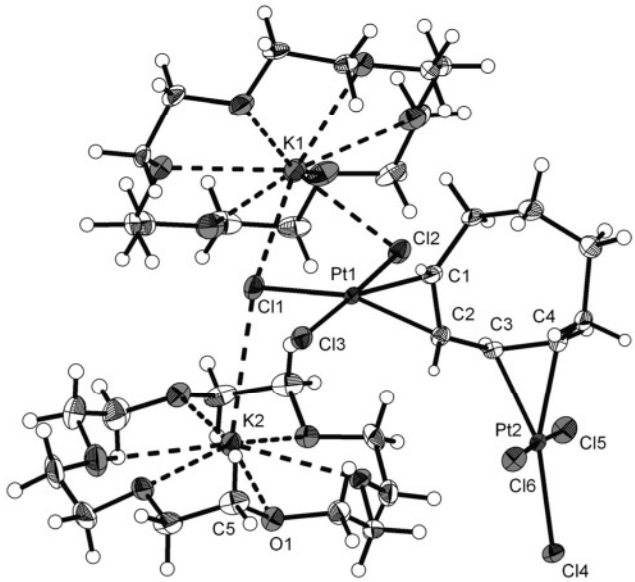

Fig. 3 Structure of $[K(18C6)]_2[(PtCl_3)_2(\mu\text{-}\eta^2\text{:}\eta^2\text{-}1,3\text{-COD})]$ (**2**) in crystals of **2**·Me_2CO. Displacement ellipsoids are drawn at 30% probability.

conformation which is close to that of the coordinated COD in the platinum complex (Cl═C2–C3═C4 55.9° in **2a′** *versus* 51.8° in non-coordinated 1,3-COD).

Furthermore, the Gibbs free energy of the formation of the COD complex **2a′** from the cyclooctyne complex **1a′** according to Scheme 2a was found to depend strongly on solvent effects. In the gas phase the reaction is endergonic ($\Delta_rG°_{gp}$ = 16.5 kcal mol^{-1}), but considering solvent effects ($CHCl_3$), within the framework of the polarized continuum model (PCM),[28] the Gibbs free energy proved to be strongly exergonic ($\Delta_rG°_{CHCl3}$ = −15.9 kcal mol^{-1}). This is probably attributable to a strong solvation of the complex dianion **2a′**.

Energy decomposition analysis (EDA) allows to investigate the metal–ligand bond strength. According to the EDA, the energy for the [M]–L bond formation ([M] + L → [M]–L, $-E_{diss}$) can formally be split up into the contribution of two processes: (i) the preparation energy, which is required to promote the two isolated fragments [M] and L from their equilibrium structures to the structures which they acquire in the complex ([M] + L → [M]* + L*, E_{prep}); and (ii) the interaction energy, which is the instantaneous interaction energy of the two "prepared" fragments ([M]* + L* → [M]–L, E_{int}). Thus, the equation $-E_{diss} = E_{int} + E_{prep}$ holds. For a brief explanation of these fundamental steps, see ref. 29. The results of the energy decomposition analysis of the platinum–olefin bonds of complex **2a′** are shown in Scheme 3 and in Table 2.

In the gas phase, the dissociation of the first $PtCl_3^-$ fragment was found to be exergonic by −12.9 kcal mol^{-1} and that of the second $PtCl_3^-$ fragment endergonic by 28.2 kcal mol^{-1} (Scheme 3). The exergonic character of the first dissociation step is a consequence of the separation of two charges of the same sign which is—in the gas phase—usually an energy providing process. In contrast, in chloroform solution (in accordance with the experimental findings), both values were found to be endergonic and in the following we will discuss only energies which were corrected by the solvent influence. The two dissociation steps exhibit significantly different values: the first one requires much less energy (14.6 kcal mol^{-1}) than the second one (23.0 kcal mol^{-1}). The latter value is in the range of the dissociation energies of olefin complexes of the Zeise's salt type $[PtCl_3L]^-$ (L = COE, E_{diss} = 26.7 kcal mol^{-1}; L = *cis*-but-2-ene, E_{diss} = 26.4 kcal mol^{-1}) which are included in Table 2 for comparison.

Evaluation of the preparation energies shows that the preparation of the $PtCl_3^-$ fragment from the equilibrium structure

Table 1 Selected interatomic distances (in Å) and angles (in °) in crystals of $[K(18C6)]_2[(PtCl_3)_2(\mu\text{-}\eta^2\text{:}\eta^2\text{-}1,3\text{-COD})]\cdot Me_2CO$ (**2**·Me_2CO) as well as the corresponding parameters obtained by DFT calculations of the complex anion $[(PtCl_3)_2(\mu\text{-}\eta^2\text{:}\eta^2\text{-}1,3\text{-COD})]^{2-}$ (**2a′**) and of the non-coordinated 1,3-COD

	2	**2a′**
Pt1–C1	2.149(6)	2.172
Pt1–C2	2.152(6)	2.210
Pt2–C3	2.153(7)	2.210
Pt2–C4	2.174(7)	2.172
Pt1–Cl1	2.324(2)	2.369
Pt1–Cl2	2.313(2)	2.367
Pt1–Cl3	2.303(2)	2.368
Pt2–Cl4	2.338(2)	2.369
Pt2–Cl5	2.318(2)	2.368
Pt2–Cl6	2.301(2)	2.367
C1–C2[b]	1.412(9) (1.347(5))	1.408 (1.340)
C2–C3[b]	1.513(9) (1.47(1))	1.501 (1.465)
C3–C4[b]	1.394(9) (1.347(5))	1.408 (1.340)
K1···Cl1	3.323(3)	
K2···Cl1	3.453(3)	
K2···Cl2	3.132(2)	
Cl1–Pt1–Cl3	88.87(7)	89.4
Cl2–Pt1–Cl3	177.43(7)	177.5
Cl1–Pt1–Cl2	88.67(7)	88.2
Cl4–Pt2–Cl5	88.98(7)	88.2
Cl4–Pt2–Cl6	88.31(6)	89.4
Cl5–Pt2–Cl6	177.17(7)	177.5
Cl1–Pt–Cg1[a]	176.64(4)	176.3
Cl4–Pt–Cg2[a]	176.89(5)	176.3
Cl–C2–C3–C4[b]	59.7(9) (37.8(1))	55.9 (51.8)
$\Phi 1$[c]	88.9(3)	
$\Phi 2$[c]	89.6(3)	

[a] Cg: center of gravity between the two olefinic C atoms (C1–C2; C3–C4). [b] The values for the corresponding non-coordinated 1,3-COD are given in parentheses. [c] Φ: Angle between the Pt1,Cl1,Cl2,Cl3 and Pt1, C1,C2 plane, respectively, between the Pt2,Cl4,Cl5,Cl6 and the Pt2,C3, C4 plane.

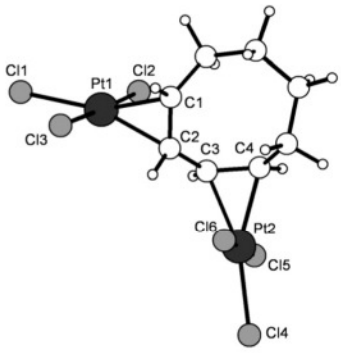

Fig. 4 Calculated structure of $[(PtCl_3)_2(\mu\text{-}\eta^2\text{:}\eta^2\text{-}1,3\text{-COD})]^{2-}$ (**2a′**).

(Cl2/5–Pt–Cl3/6 166.3°) into the "prepared" T-shaped structures (Cl2/5–Pt–Cl3/6 177.5/178.2°; Scheme 3) requires less energy (−0.3/−1.0 kcal mol^{-1}) than the preparation of the $[PtCl_3(1,3\text{-COD})]^-$ (10.3 kcal mol^{-1}) and of 1,3-COD (10.3 kcal mol^{-1}). Furthermore, the comparison of the preparation energy of 1,3-COD with those of COE and *cis*-but-2-ene in the olefin complexes $[PtCl_3L]^-$ shows that the preparation energies of all these olefin/diene ligands are similar (Table 2).

From all this follows that an analogous difference as found in the dissociation energies ΔE_{diss} of the two $PtCl_3^-$ fragments (8.4 kcal mol^{-1}) will also be found in the interaction energies ΔE_{int} (7.7 kcal mol^{-1}). Thus, the ease of the dissociation of $PtCl_3^-$ from **2a′** and the relatively low interaction energy forming **2a′** is likely due to repulsive Coulomb interaction between the two singly negatively charged $PtCl_3^-$ and $[PtCl_3(1,3\text{-COD})]^-$ (**3a′**) fragments. These results also indicate that the driving force for the isomerization of $[PtCl_3(COC)]^-$ (**1a′**) according to Scheme 2a is not an extraordinarily high Pt–C bond strength in **2a′**, but the significant release of ring strain of the cyclooctyne ligand, represented by the energy balance of the isomerization reaction of the non-coordinated alkyne COC → 1,3-COD ($\Delta_r G°_{CHCl3}$ = −27.0 kcal mol^{-1}, Scheme 2b).

To evaluate the mode of bonding of 1,3-COD in $[(PtCl_3)_2(\mu\text{-}\eta^2\text{:}\eta^2\text{-}1,3\text{-COD})]^{2-}$ (**2a′**) and $[PtCl_3(\eta^2\text{-}1,3\text{-COD})]^-$ (**3a′**) complexes as well as of *cis*-but-2-ene and COE ligands in $[PtCl_3L]^-$ (L = *cis*-but-2-ene, **4a′**; COE, **5a′**) complexes, charge decomposition analyses (CDA)[30] of Frenking and natural bond orbital analyses (NBO)[31] were performed (Table 2). The low residual terms (−0.017 to −0.020) allow to discuss the complexes in terms of the Dewar–Chatt–Duncanson model.[32] The ratio *d*/*b* (*d* = donation, *b* = back donation) proved to be significantly higher in the complex **2a′** compared to complexes **3a′–5a′** (1.205 *versus* 0.864–1.011), thus indicating in the dinuclear μ-1,3-COD complex **2a′** a higher olefin→Pt donation (0.300 *versus* 0.228–0.278) combined with a smaller back donation (0.249 *versus* 0.264–0.289) compared with those in the mononuclear $[PtCl_3L]^-$ complexes **3a′–5a′**. An NBO analysis, which measures the depopulation of the bonding π orbital and the population of the corresponding antibonding π* orbitals of an olefin at complex formation, gives, in principle, the same result: the values P_π (1.621, **2a′** *versus* 1.626–1.636, **3a′–5a′**) and P_{π^*} (0.327, **2a′** *versus* 0.348–0.351, **3a′–5a′**) indicate a slightly larger donation and a smaller back donation of the μ-1,3-COD ligand in the dinuclear complex **2a′** as compared to the mono-anionic Zeise salt type complexes **3a′–5a′**.

2.4. Summary

To the best of our knowledge, the reaction COC → 1,3-COD in [K(18C6)][$PtCl_3$(COC)] (**1**) presented within this work is the first isomerization of a cyclooctyne ligand into cyclooctadiene. Unexpectedly, the reaction was found to result in the formation both of non-coordinated cycloocta-1,3-diene and of a dinuclear platinum complex bearing a bridging cycloocta-1,3-diene ligand. The driving force for the isomerization COC → 1,3-COD was found to be primarily the release of ring strain of cyclooctyne. Structural data from crystallographic and quantum chemical investigations give proof that the double bonds in the μ-1,3-COD ligand are not conjugated but isolated. In accordance with that, CDA and NBO analyses exhibit that the nature of the platinum–carbon bonds both in the dinuclear and the mononuclear cyclooctadiene complexes $[(PtCl_3)_2(\mu\text{-}\eta^2\text{:}\eta^2\text{-}1,3\text{-COD})]^{2-}$ (**2a′**) and $[PtCl_3(\eta^2\text{-}1,3\text{-COD})]^-$ (**3a′**) can be described within the framework of the Dewar–Chatt–Duncanson model.[32] A higher *d*/*b* ratio (mainly due to a lower back donation) is found in the dinuclear complex **2a′** with the bridging $\mu\text{-}\eta^2\text{:}\eta^2$-1,3-COD ligand

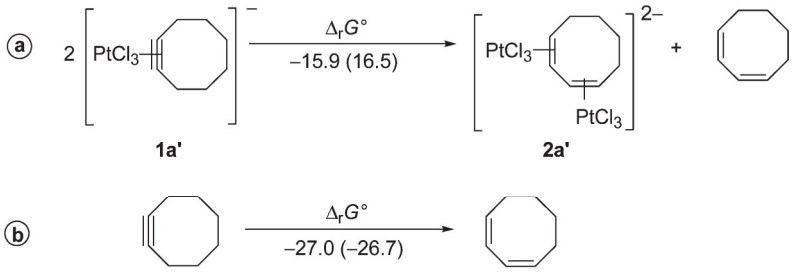

Scheme 2 Gibbs free energy of the formation of the COD complex **2a′** from the cyclooctyne complex **1a′**. The energies are given in kcal mol^{-1} in $CHCl_3$ as solvent. The corresponding values for the gas phase are given in parentheses.

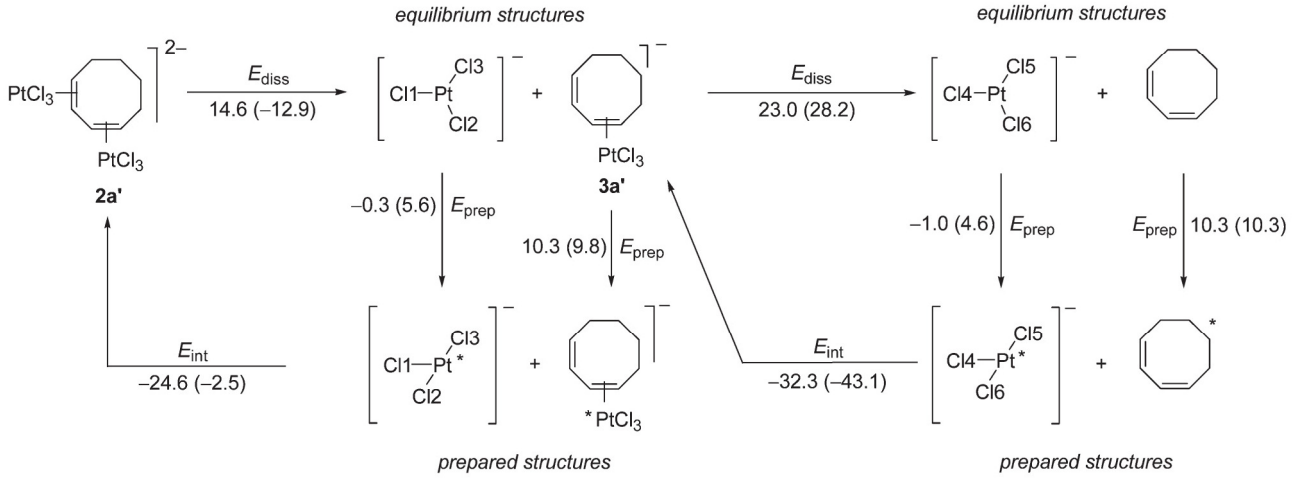

Scheme 3 Results of the energy decomposition analysis of the platinum–olefin bonds of complex **2a′**. The energies are given in kcal mol^{-1} in $CHCl_3$ as solvent. The corresponding values for the gas phase are given in parentheses.

Table 2 Bond characteristics of the complex anions $[(PtCl_3)_2(\mu\text{-}\eta^2\text{:}\eta^2\text{-}1,3\text{-COD})]^{2-}$ (**2a′**), $[PtCl_3(\eta^2\text{-}1,3\text{-COD})]^-$ (**3a′**), and $[PtCl_3L]^-$ (L = *cis*-but-2-ene, **4a′**; COE, **5a′**)

	2a′	**3a′**	**4a′**	**5a′**
L	η^2,η^2-1,3-COD	η^2-1,3-COD	*cis*-but-2-ene	COE
EDA				
ΔE_{diss} [a]	14.6 (12.9)	23.0 (28.2)	26.4 (30.4)	26.7 (31.7)
ΔE_{prep} ($PtCl_3^-$)[a]	−0.3 (5.6)	−1.0 (4.6)	−0.8 (4.9)	−0.8 (5.0)
ΔE_{prep} (L)[a]	10.3 (9.8)	10.3 (10.3)	9.5 (9.6)	9.2 (9.3)
ΔE_{int}[a]	−24.6 (−2.5)	−32.3 (−43.1)	−35.2 (−44.9)	−35.1 (−46.0)
CDA				
Donation (*d*)	0.300	0.278	0.228	0.278
Back donation (*b*)	0.249	0.275	0.264	0.289
Repulsive polarization	−0.667	−0.689	−0.702	−0.705
Residual term	−0.020	−0.017	−0.018	−0.019
d/*b*	1.205	1.011	0.864	0.962
NBO analysis				
Olefin complexes				
P_π	1.621/1.621	1.636/1.950	1.626	1.628
P_{π^*}	0.327/0.327	0.351/0.056	0.348	0.349
q_{PtCl3^-}	−1.011	−0.965	−0.999	−0.981
Non-coordinated olefins				
P_π	1.950	1.931/1.931	1.961	1.964
P_{π^*}	0.056	0.075/0.075	0.066	0.052

Results of the energy decomposition analysis (EDA) (ΔE_{diss} = bond dissociation energy, ΔE_{int} = instantaneous interaction energy, ΔE_{prep} = preparation energy; all energies in kcal mol^{-1}), of charge decomposition analysis CDA (*d* = donation, *b* = back donation; values in electrons), and of NBO analysis (P_π/P_{π^*} = population of the π/π^* orbitals of the olefin complexes/non-coordinated olefins, q_{PtCl3^-} = charge of the $PtCl_3^-$ fragment; values in electrons).[a] Values are corrected by the solvent effect of $CHCl_3$ (PCM); values for the gas phase are given in parentheses.

compared with those found in mononuclear Zeise salt type complexes **3a′–5a′**.

3. Experimental

3.1. General procedures

All reactions were performed under argon atmosphere using standard Schlenk techniques. Solvents were dried (Et_2O and *n*-pentane over Na benzophenone; $CHCl_3$ over CaH_2; acetone over molecular sieve 3 Å) and distilled prior to use. ^1H and ^{13}C NMR spectra were recorded on Varian Gemini 200, VXR 400, and Unity 500 NMR spectrometers. Chemical shifts are relative to $CHCl_3$ (δ = 7.24) and $CDCl_3$ (δ = 77.0 ppm) as internal references. Microanalyses were performed by the University of Halle microanalytical laboratory using CHNS-932 (LECO) and Vario EL elemental analyzers. The ESI mass spectrum (negative ion polarity mode) was recorded on a Finnigan LCQ spectrometer (Thermo Electron) using the following conditions: solvent, CH_2Cl_2; solvent flow, 8 µl min^{-1}; ESI spray voltage, 4.1 kV; capillary temperature, 120 °C; capillary voltage, −4 or +4 V; tube lens offset, −3 or +3 V; sheath gas N_2; damping gas He. The starting compound [K(18C6)][$PtCl_3(\eta^2$-COC)] (**1**) was synthesized according to the published method.[18] All other chemicals were commercially available.

3.2. Synthesis of [K(18C6)]$_2$[$(PtCl_3)_2(\mu$-η^2:η^2-1,3-COD)]·Me_2CO (2·Me_2CO)

Compound **2**·Me_2CO was obtained by layering a solution of **1** (143 mg, 0.2 mmol) in chloroform or methylene chloride or in a mixture with acetone (4 mL) with diethyl ether/*n*-pentane (4 mL) for 8 weeks. The microcrystalline precipitate was filtered off, washed with *n*-pentane (2 mL) and dried *in vacuo*. Yield: 60%. Anal. Calcd (found) for $C_{35}H_{66}Cl_6K_2O_{13}Pt_2$ (1376.0): C 30.54 (30.86), H 4.83 (4.89). ^{1}H-NMR (200 MHz, 300 K, CD_2Cl_2): δ 1.36 (m,=CHCH$_2$CH_2, 2 H), 1.88 (m,=CHCH$_2$CH_2, 2 H), 2.12 (s, OC(CH_3)$_2$, 6 H), 2.18 (m,=CHCH_2, 2 H), 2.34 (m,=CHCH_2, 2 H), 3.70 (s, OCH_2, 48 H), 5.12 (m,=C*H*CH$_2$, 2 H), 5.94 (m, C*H*=CHCH$_2$, 2 H). ^{13}C-NMR (50.3 MHz, 300 K, CD_2Cl_2): δ 27.3 (s,=CHCH$_2$C*H*$_2$), 30.6 (s, OC(*C*H$_3$)$_2$), 31.1 (s,=CH*C*H$_2$), 70.6 (s, O*C*H$_2$), 78.4 (s + d, ^1J(Pt,C) = 204 Hz, *C*H=CHCH$_2$), 89.3 (s + d, ^1J(Pt,C) = 259 Hz,=*C*HCH$_2$). ESI-MS *m*/*z* (obsd/calcd, %) $[Pt_2Cl_6KC_{20}H_{36}O_6]^-$ 1009.0 (13/12), 1009.9 (28/26), 1010.9 (51/56), 1011.9 (77/73), 1012.9 (100/100), 1013.7 (98/96), 1014.5 (93/100), 1015.9 (63/75), 1016.9 (38/64), 1017.9 (26/38), 1018.9 (11/29), 1019.9 (9/14), 1020.9 (4/9).

To determine the degree of conversion towards **2** and to identify the formation of non-coordinated 1,3-COD, the reaction was followed in an NMR tube closed by melting in CD_2Cl_2 as solvent. Apart from the ^{1}H and ^{13}C NMR signals of **2**, those of non-coordinated COD were found: δ_H 1.51 (m,=CHCH$_2$CH_2, 4 H), 2.19 (m,=CHCH_2, 4 H), 5.66 (m,=C*H*CH$_2$, 2 H), 5.82 (m, C*H*=CHCH$_2$, 2 H). δ_C 23.3 (s,=CHCH$_2$C*H*$_2$), 28.2 (s,=CH*C*H$_2$), 126.1 (s, CH=*C*HCH$_2$), 131.2 (s, *C*H=CHCH$_2$).

3.3. X-Ray structure determination

Crystals of **2**·Me_2CO suitable for X-ray diffraction analysis were grown at room temperature from solutions of **1** in $CHCl_3$/acetone by slow addition diethyl ether/*n*-pentane. Intensity data were collected on a STOE IPDS diffractometer at 220(2) K with Mo Kα radiation (λ = 0.71073 Å, graphite monochromator). Crystallographic data and data collection parameters are given in the ESI (S1†). Absorption corrections were applied numerically (T_{min}/T_{max} 0.25/0.54). The structure was solved by direct methods with SHELXS-97 and refined using full-matrix least square routines against F^2 with SHELXL-97.[33] Non-hydrogen atoms were refined with anisotropic displacement parameters and hydrogen atoms with isotropic displacement parameters. Hydrogen atoms were added to their calculated positions and refined according to the riding model.

3.4. Computational details

DFT calculations were carried out by the Gaussian 03 program package[34] using the hybrid functional B3LYP. The 6-311G(d,p)[35] basis sets, as implemented in Gaussian03, were employed for C, H, O and Cl atoms, while the relativistic pseudopotential of the Ahlrichs group and related basis functions of TZVPP quality[36] were employed for Pt atoms. The appropriateness of the functional in combination with the basis sets and effective core potential used for reliable interpretation of structural and energetic aspects of the related platinum complexes has been demonstrated.[37] All systems were fully optimized without any symmetry restrictions. The resulting geometries were characterized as equilibrium structures by the analysis of the force constants of normal vibrations. Solvent effects were considered according to the polarized continuum model.[28]

Acknowledgements

We are thankful to Dr R. Kluge (Univ. Halle) for ESI measurements.

References

1 (*a*) *Methoden der Organischen Chemie (Houben-Weyl)*, Thieme Verlag, Stuttgart, 1977, Vol. 5/2a, p. 282; (*b*) B. J. Barry, W. J. Beale, M. D. Carr, S.-K. Hei and I. Reid, *J. Chem. Soc., Chem. Commun.*, 1973, 177.
2 (*a*) A. J. L. Pombeiro, *J. Organomet. Chem.*, 1984, **358**, 273; (*b*) S. Patai, *Supplement C2: the Chemistry of Triple Bonded Functional Groups*, Thieme, Verlag, Stuttgart, 1994, Vol. 2, pp. 485; (*c*) *Methoden der Organischen Chemie (Houben-Weyl)*, Thieme Verlag, Stuttgart, 1993, Vol. 15/3, p. 2959.
3 C. K.-W. Kwong, M. Y. Fu, C. S.-L. Lam and P. H. Toy, *Synthesis*, 2008, **15**, 2307.
4 *Methoden der Organischen Chemie (Houben-Weyl)*, Thieme Verlag, Stuttgart, 1970, Vol. 5/1c, p. 353.
5 K. Hirai, H. Suzuki, Y. Moro-Oka and T. Ikawa, *Tetrahedron Lett.*, 1980, **21**, 3413.
6 (*a*) B. Trost and T. Schmidt, *J. Am. Chem. Soc.*, 1988, **110**, 2301; (*b*) D. Ma, Y. Lin and X. Lu, *Tetrahedron Lett.*, 1988, **29**, 1045; (*c*) Y. Inoue and S. Imaizumi, *J. Mol. Catal.*, 1988, **49**, L19.
7 D. Ma, Y. Yu and X. Lu, *J. Org. Chem.*, 1989, **54**, 1105.
8 C. Guo and X. Lu, *Synlett*, 1992, 405.
9 D. Ma and X. Lu, *Tetrahedron Lett.*, 1989, **30**, 843.

10 (*a*) D. Ma and X. Lu, *Tetrahedron*, 1990, **46**, 3189; (*b*) C. Guo and X. Lu, *Tetrahedron Lett.*, 1991, **32**, 7549; (*c*) X. Lu and D. Ma, *Pure Appl. Chem.*, 1990, **62**, 723.
11 (*a*) B. Trost and U. Kazmaier, *J. Am. Chem. Soc.*, 1992, **114**, 7933; (*b*) B. Trost and C.-J. Li, *J. Am. Chem. Soc.*, 1994, **116**, 10819.
12 C. Guo and X. Lu, *J. Chem. Soc., Perkin Trans. 1*, 1993, 1921.
13 R. Shintani, W.-L. Duan, S. Park and T. Hayashi, *Chem. Commun.*, 2006, 3646–3647.
14 Z. Wang and X. Lu, *Tetrahedron*, 1995, **51**, 11765.
15 X. Lu, C. Guo and D. Ma, *Synlett*, 1990, 357.
16 H. Yasui, H. Yorimitsu and K. Oshima, *Synlett*, 2006, **11**, 1783.
17 M. Shiotsuki, Y. Ura, T. Ito, K. Wada, T. Kondo and T. Mitsudo, *J. Organomet. Chem.*, 2004, **689**, 3168.
18 A. König, M. Bette, C. Wagner, R. Lindner and D. Steinborn, *Organometallics*, 2011, **30**, 5919.
19 R. E. Rülke, J. M. Ernsting, A. L. Spek, C. J. Elsevier, P. W. N. M. van Leeuwen and K. Vrieze, *Inorg. Chem.*, 1993, **32**, 5769.
20 D. Steinborn, V. V. Potechin, M. Gerisch, C. Bruhn and H. Schmidt, *Transition Met. Chem.*, 1999, **24**, 67.
21 S. Otto, A. Roodt and L. I. Elding, *Inorg. Chem. Commun.*, 2006, **9**, 764.
22 A. Singh and P. R. Sharp, *Organometallics*, 2006, **25**, 678.
23 M. Trætteberg, *Acta Chem. Scand.*, 1970, **24**, 2285.
24 To the structure of a tetranuclear ruthenium complex with a bridging doubly deprotonated 1,3-COD ligand see: D. Braga, F. Grepioni, D. B. Brown, B. F. G. Johnson and M. J. Calhorda, *Organometallics*, 1996, **15**, 5723.
25 (*a*) V. G. Albano, F. Demartin, V. De Felice, G. Morelli and A. Vitagliano, *Gazz. Chim. Ital.*, 1987, **437**, 117; (*b*) J. R. Briggs, C. Crocker, W. S. McDonald and B. L. Shaw, *J. Chem. Soc., Dalton Trans.*, 1982, 457.
26 S. Otto, A. Roodt and L. I. Elding, *Dalton Trans.*, 2003, 2519.
27 *Landolt-Börnstein: Numerical Data and Functional Relationships in Science and Technology*, Springer, Berlin, 1997, Vol. 25, p. 139/151.
28 (*a*) B. Mennucci and J. Tomasi, *J. Chem. Phys.*, 1997, **106**, 5151; (*b*) E. Cancès, B. Mennucci and J. Tomasi, *J. Chem. Phys.*, 1997, **107**, 3032; (*c*) M. Cossi, V. Barone, B. Mennucci and J. Tomasi, *Chem. Phys. Lett.*, 1998, **286**, 253.
29 (*a*) G. Frenking and N. Fröhlich, *Chem. Rev.*, 2000, **100**, 717; (*b*) G. Frenking, K. Wichmann, N. Fröhlich, C. Loschen, M. Lein, J. Frunzke and V. M. Rayón, *Coord. Chem. Rev.*, 2003, **238–239**, 55.
30 S. Dapprich and G. Frenking, *J. Phys. Chem.*, 1995, **99**, 9352.
31 (*a*) E. D. Glendening, J. K. Badenhoop, A. E. Reed, J. E. Carpenter, J. A. Bohmann, C. M. Morales and F. Weinhold, *NBO 5.0*, Theoretical Chemistry Institute, University of Wisconsin, Madison, WI, 2001; (*b*) F. Weinhold and C. R. Landis, *Chemistry Education Research and Practice*, 2001, **2**, 91; (*c*) J. P. Foster and F. Weinhold, *J. Am. Chem. Soc.*, 1980, **102**, 7211; (*d*) A. E. Reed and F. Weinhold, *J. Chem. Phys.*, 1983, **78**, 4066; (*e*) A. E. Reed, R. B. Weinstock and F. Weinhold, *J. Chem. Phys.*, 1985, **83**, 735.
32 (*a*) M. J. S. Dewar, *Bull. Soc. Chim. Fr.*, 1951, **18**, C71; (*b*) J. Chatt and L. A. Duncanson, *J. Chem. Soc.*, 1953, 2939.
33 G. M. Sheldrick, *Acta Crystallogr., Sect. A: Found. Crystallogr.*, 2007, **64**, 112.
34 M. J. Frisch *et al.*, *Gaussian 03, revision B.04*, Gaussian, Inc., Wallingford, CT, 2004.
35 (*a*) M. J. S. Dewar and C. H. Reynolds, *J. Comput. Chem.*, 1986, **7**, 140; (*b*) K. Raghavachari, J. A. Pople, E. S. Replogle and M. Head-Gordon, *J. Phys. Chem.*, 1990, **94**, 5579.
36 (*a*) F. Weigend, M. Häser, H. Patzelt and R. Ahlrichs, *Chem. Phys. Lett.*, 1998, **294**, 143; (*b*) T. Leininger, A. Nicklass, W. Küchle, H. Stoll, M. Dolg and A. Bergner, *Chem. Phys. Lett.*, 1996, **255**, 274; (*c*) D. Andrae, U. Häußermann, M. Dolg, H. Stoll and H. Preuss, *Theor. Chim. Acta*, 1990, **77**, 123.
37 (*a*) D. Steinborn and S. Schwieger, *Chem.–Eur. J.*, 2007, **13**, 9668; (*b*) M. Werner, T. Lis, C. Bruhn, R. Lindner and D. Steinborn, *Organometallics*, 2006, **25**, 5946; (*c*) C. Vetter, G. N. Kaluderović, R. Paschke, S. Gómez-Ruiz and D. Steinborn, *Polyhedron*, 2009, **28**, 3699; (*d*) S. Schwieger, F. W. Heinemann, C. Wagner, R. Kluge, C. Damm, G. Israel and D. Steinborn, *Organometallics*, 2009, **28**, 2485.
38 H. Zeise, *Thermodynamik*, Hirzel Verlag, Leipzig, 1954, vol. 3/1.

EurJIC European Journal of Inorganic Chemistry

FULL PAPER

DOI: 10.1002/ejic.201200744

Dinuclear Olefin and Alkyne Complexes of Platinum(II)

Anja König,[a] Martin Bette,[a] Clemens Bruhn,[b] and Dirk Steinborn*[a]

Keywords: Platinum / Alkyne ligands / Alkene ligands / Isomerization / Density functional calculations

Bis(olefin) complexes of Zeise's dimer type – [{$PtCl_2$(*cis*-MeHC=CHMe)}$_2$] (**2**) or [{$PtCl_2$(*c*-Hex)}$_2$] (**3**, *c*-Hex = cyclohexene) – were prepared by treatment of $K_2[PtCl_4]$ in the presence of $SnCl_2$ or K[$PtCl_3$(*cis*-MeHC=CHMe)] with the corresponding olefin. Zeise's dimer, [{$PtCl_2(H_2C=CH_2)$}$_2$] (**1**), was found to react in chloroform or dichloromethane with the internal alkynes RC≡C*t*Bu (R = Me, *t*Bu), provided that the cleaved-off ethene was removed, to yield bis(alkyne) complexes of Zeise's dimer type [{$PtCl_2$(RC≡C*t*Bu)}$_2$] (R = Me, **11**; *t*Bu, **12**). Without removal of the ethene, mononuclear mixed ethene/alkyne complexes *cis*-[$PtCl_2(H_2C=CH_2)$(RC≡C*t*Bu)] (R = Me, **8**; *t*Bu, **9**) and *cis*-[$PtCl_2(H_2C=CH_2)_2$] (**10**) were formed. Analogous reactions with alkynes RC≡CR′ bearing sterically less demanding substituents (R, R′ = Me, Et, *n*Pr, Ph) led to (cyclobutadiene)platinum(II) complexes [$PtCl_2(C_4R_2R'_2)$] (R/R′ = Me/Me **4**; Et/Et **5**; Me/*n*Pr **6**) and [$PtCl_2(C_4Me_2Ph_2)$] (**7**). Furthermore, use of acetone (instead of $CHCl_3/CH_2Cl_2$) as solvent in the reactions between **1** and sterically undemanding substituted alkynes resulted in bridge cleavage of Zeise's dimer (**1**) and in aldol addition and condensation reactions, thereby confirming why Chatt et al. in his analogous classical experiments (1961) observed only decomposition. Complexes **2**–**7** and **11**/**12** were isolated in pure states and fully characterized by elemental analysis, NMR spectroscopy, and X-ray diffraction measurements (**2**, **11**, **12**). For the dinuclear bis(olefin) (**1**–**3**) and bis(alkyne) complexes (**11**, **12**) solvent-dependent equilibria between the *transoid* and *cisoid* isomers were observed, and these could even be ascertained crystallographically for complex [{$PtCl_2$(*t*BuC≡C*t*Bu)}$_2$] (**12**), which crystallized both as the *transoid* isomer **12a** and as the *cisoid* isomer **12b**·$CHCl_3$. Furthermore, consistent with DFT calculations, NMR measurements provided evidence of fast rotation and of hindered rotation of olefin and alkyne ligands, respectively, resulting in conformational isomers in **8** and **11**.

Introduction

The synthesis of the first organotransition metal compound, Zeise's salt K[$PtCl_3(H_2C=CH_2)$]·H_2O, in 1825 is a milestone both in coordination chemistry and in organometallic chemistry.[1] Shortly after (1830/1831), Zeise considered that he had obtained the compound known today as Zeise's dimer [{$PtCl_2(H_2C=CH_2)$}$_2$].[2] It was prepared in a pure state and recognized as a dinuclear chlorido-bridged complex by Anderson in 1934.[3] Substitution of the ethene ligand in Zeise's dimer by other olefins resulted in the formation of analogous dinuclear olefin complexes [{$PtCl_2$(RHC=CHR′)}$_2$] (R, R′ = alkyl, aryl).[4,5] The equilibria and kinetics relating to the bridge cleavage in [{$PtCl_2$(cot)}$_2$] (cot = cyclooctene) with neutral nucleophiles L (such as MeOH, MeCN, cot) and anionic nucleophiles X (such as Br, I, N_3, SCN) with formation of neutral and anionic mononuclear complexes of the type [$PtCl_2$(cot)L] and [$PtCl_2$X(cot)]$^-$, respectively, were investigated in detail by multinuclear NMR and UV/Vis spectroscopy.[4,6] In general, the thermodynamic balances of these reactions were found to be significantly dependent on the approaching ligands: anionic ligands led to complete conversions, whereas σ-donating neutral ligands such as MeCN and MeOH and π ligands such as cot were found to result in equilibrium reactions.[4,6]

Alkyne complexes of platinum(II) are less common than those of platinum(0). When starting from $M^I_2[PtX_4]$ (M^I = K, Na, [PPh_4]; X = Cl, Br) or K[$PtCl_3(H_2C=CH_2)$]·H_2O, by halide or ethene displacement, respectively, alkyne complexes M^I[PtX_3(RC≡CR′)] (M^I = K, Na, [PPh_4]; X = Cl, Br) of the Zeise's salt type were thus only accessible with alkyne ligands bearing sterically demanding or oxygen-functionalized substituents [such as *t*Bu, $C(OH)R_2$] or with phenyl-substituted alkynes.[7–9] On the other hand, when starting from the crown ether adducts [K(18C6)][$PtCl_3$L] (L = but-2-ene, but-2-yne) or [K(18C6)]$_2$[Pt_2Cl_6], complexes of the [K(18C6)][$PtCl_3$(RC≡CR′)] type (R, R′ = H, alkyl, aryl) were obtained with a wide scope of alkynes, terminal alkynes among them.[10,11]

Alkyne complexes [{$PtCl_2$(RC≡C*t*Bu)}$_2$] (R = Et, *i*Pr, *t*Bu, CMe_2R') of the Zeise's dimer type were synthesized either from $Na_2[PtCl_4]$ or directly from Zeise's dimer, but only with alkynes bearing sterically demanding substituents.[7] From the historical point of view, it is of interest

[a] Institut für Chemie – Anorganische Chemie,
Martin-Luther-Universität,
Kurt-Mothes-Straße 2, 06120 Halle, Germany
E-mail: steinborn@chemie.uni-halle.de
Homepage: www.chemie.uni-halle.de
[b] Institut für Chemie, Universität Kassel,
Heinrich-Plett-Straße 40, 34132 Kassel, Germany

Supporting information for this article is available on the WWW under http://dx.doi.org/10.1002/ejic.201200744.

to clarify why analogous reactions with alkynes RC≡CR′ bearing sterically less demanding substituents R/R′ [such as H, Me, Et, *n*Pr, *i*Pr, *n*Bu, Ph, C(OH)Me_2, $CMe_2OC(O)Ph$] resulted only in decomposition.[7,8] Furthermore, (cyclobutadiene)platinum(II) complexes are accessible through reactions between internal alkynes and $H_2[PtCl_6]·6H_2O$[12] or $[PtCl_2L_2]$ (L = CO, MeCN).[13]

Here we present corresponding investigations into reactions of $[\{PtCl_2(RHC=CHR)\}_2]$ (R = H, Me) with alkynes RC≡CR′ (R, R′ = Me, Et, *n*Pr, Ph, *t*Bu) resulting in alkyne complexes of Zeise's dimer type and in mononuclear mixed (olefin)(alkyne)- and (cyclobutadiene)platinum(II) complexes. The influence of the alkyne substituents R/R′ on the courses of these reactions is the subject of this study, which permits, with the aid of DFT calculations, conclusions about the relative stabilities of olefin and alkyne complexes.

Results and Discussion

Synthesis and Spectroscopic Characterization of Dinuclear Olefin Complexes

The synthesis of the dinuclear ethene complex $[\{PtCl_2(H_2C=CH_2)\}_2]$ (Zeise's dimer) from $K_2[PtCl_4]$ and ethene is described in the literature (Scheme 1a).[14] Here, however, we observed that the analogous reaction with *cis*-but-2-ene was very slow and required a reaction time of several weeks. The formation of Zeise's salt from $K_2[PtCl_4]$ with ethene was reported to be catalyzed by $SnCl_2$ in HCl_{aq},[15] so it was felt that reactions with higher olefins yielding complexes of the Zeise's dimer type might be catalyzed by $SnCl_2$ as well. The synthesis of the neutral dinuclear bis(olefin) complex $[\{PtCl_2(MeHC=CHMe)\}_2]$ (**2**) by this approach was found to be significantly accelerated by addition of catalytic amounts of $SnCl_2$ (Scheme 1b). On the other hand, the synthesis of the complex $[\{PtCl_2(c\text{-Hex})\}_2]$ (**3**) could be performed by substitution of *cis*-but-2-ene in $K[PtCl_3(MeHC=CHMe)]$ by the less volatile cyclohexene (Scheme 1c).

Complexes **2** and **3** were isolated in good (75%) and moderate yields (60%), respectively, and characterized unambiguously by microanalysis and NMR spectroscopy, as well as by X-ray diffraction measurement in the case of **2**. Selected NMR spectroscopic parameters for complexes **2** and **3** are given in Table 1. Additionally, the parameters of the corresponding ethene complex **1** (Zeise's dimer) are presented for comparison. Closer inspection of the ^{13}C and ^{195}Pt NMR spectra of the dinuclear complexes **1**–**3** shows two sets of signals with very similar chemical shifts for the olefinic C atoms (except for **1**) and Pt atoms, indicating the presence of two configurational isomers (*transoid*/*cisoid*) in

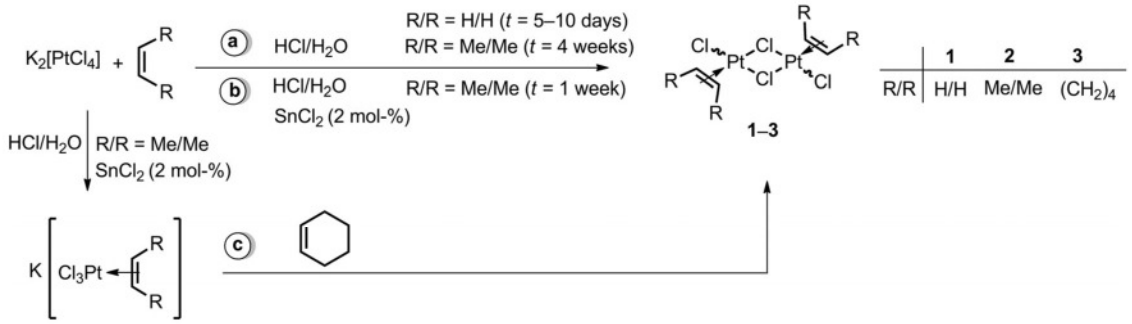

Scheme 1.

Table 1. Selected ^1H, ^{13}C, and ^{195}Pt NMR spectroscopic data (δ in ppm, J in Hz) for (olefin)- and (olefin)(alkyne)platinum(II) complexes.

Olefin	$\delta(=CH)$	$\Delta\delta$[a]	$^2J_{Pt,H}$	$\delta(=CH)$	$\Delta\delta$[a]	$^1J_{Pt,C}$	$\delta(^{195}Pt)$
Neutral dinuclear olefin complexes $[\{PtCl_2(olefin)\}_2]$							
1 (ethene)	4.82	–0.46	74	72.1	–51.2	199	–2490[c]
(2.2:1)[d,f]							–2495[b]
2 (*cis*-but-2-ene)	5.55	0.10	71	86.9[b]	–37.3	190	–2426[b]
(3.0:1)[d,f]				87.4[c]	–36.8	182	–2405[c]
3 (cyclohexene)	5.96	0.30	81	91.5[b]	–35.8	196	–2298[b]
(12.6:1)[d,f]				90.9[c]	–36.4	[e]	–2374[c]
Anionic olefin complexes $M^I[PtCl_3(olefin)]$ (M^I = K, [K(18C6)])							
cis-But-2-ene	5.13	–0.32	76	84.2	–40.0	183	
cis-But-2-ene[g]	5.17	–0.28	75	82.8	–41.4	182	
Ethene[g]	4.46	–0.82	64	68.0	–55.3	192	
Neutral olefin complexes $[PtCl_2(olefin)(RC{\equiv}CtBu)]$ (R = Me, **8**; *t*Bu, **9**), $[PtCl_2(olefin)_2]$ (**10**)							
8 (ethene)	4.56	–0.77	60	80.2	–43.1	141	–3145
9 (ethene)	4.55	–0.78	55	80.4	–42.9	138	–3143
10 (ethene)	4.70	–0.57	56	84.3	–39.0	131	–3642

[a] $\Delta\delta = \delta_{complex} - \delta_{noncoord.ligand}$. [b] Major isomer. [c] Minor isomer. [d] Ratio of isomers in parentheses. [e] Not found for reasons of intensity. [f] Measured in CD_2Cl_2. [g] Values taken from ref.[16,17]

solution in each case (Scheme 2). The chemically induced shifts (CISs: $\Delta\delta = \delta_{complex} - \delta_{noncoord.\,ligand}$) of the olefinic carbon atoms of the dinuclear olefin complexes **1**–**3** (–35.8 to –51.2 ppm) and the $^1J_{Pt,C}$ coupling constants (182–199 Hz) are of the same order of magnitude as those found in complexes of the Zeise's salt type $M^I[PtCl_3(R_2C{=}CR'_2)]$ {M^I = K, [K(18C6)], (PPh_4), [N(nBu)$_4$]; R, R′ = H, alkyl, aryl} [$\Delta\delta$(=CH) = –40 to –55 ppm; $^1J_{Pt,C}$ = 180–195 Hz].[4,16,6,17] On the other hand, significantly smaller coupling constants ($^1J_{Pt,C}$ = 131–152 Hz) are observed in neutral mononuclear *cis*-configured complexes of the $[PtCl_2L_2]$ type (L = ethene, 1,5-cod), indicating weaker Pt–C interaction in these complexes.[18,19] Furthermore, the ^{195}Pt chemical shifts of complexes **1**–**3** were found to be in the range from –2298 to –2495 ppm.

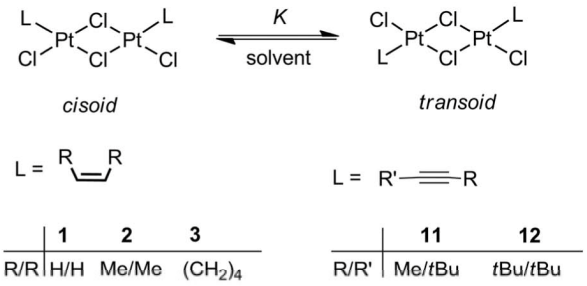

Scheme 2.

Molecular Structure of [{PtCl$_2$(*cis*-MeHC=CHMe)}$_2$] (2)

Crystals of the dinuclear olefin complex **2** suitable for X-ray diffraction analysis were obtained from $CHCl_3/Et_2O$ solutions. In crystals of **2**, discrete dinuclear molecules without unusual intermolecular interactions were found. The molecular structure, depicted in Figure 1, shows crystallographically imposed inversion symmetry. Selected structural parameters are given in Table 2. The central $Pt_2(\mu\text{-}Cl)_2$ unit is precisely planar. The platinum atoms are square-planar coordinated to a good approximation, as shown by the angles between *trans*-disposed ligands $Cl_{term.}$–Pt–μ-Cl [174.5(1)°] and Cg–Pt–μ-Cl [179.70(8)°] (Cg = center of gravity of the two olefinic C atoms). The olefin ligand is oriented almost perpendicularly to the $PtCl_3$ coordination plane as measured by the interplanar angle $\Phi(PtCl_3/PtC_2)$ = 88.1(6)°. Furthermore, comparison of the C1=C2 double bond in **2** [1.40(2) Å] with that in noncoordinated *cis*-but-2-ene [1.346(3) Å[20]] shows a coordination-induced bond lengthening of 0.054 Å, as would be anticipated for (olefin)-platinum(II) complexes. The terminal Pt–Cl2 bond [2.278(3) Å] is significantly shorter than the two bridging Pt–Cl1/Pt–Cl1′ bonds [2.378(3)/2.338(3) Å]. Furthermore, the Pt–Cl bond *trans* to the olefin was found to be longer than that *trans* to the terminal chlorido ligand [2.378(3) vs. 2.338(3) Å]. All of these structural features are in the range of those of Zeise's dimer complexes [{$PtCl_2L$}$_2$] with various olefin ligands L (cyclopentene, cycloheptene, cyclooctene, ethene;[4,5,21,22] cf. S2 in the Supporting Information).

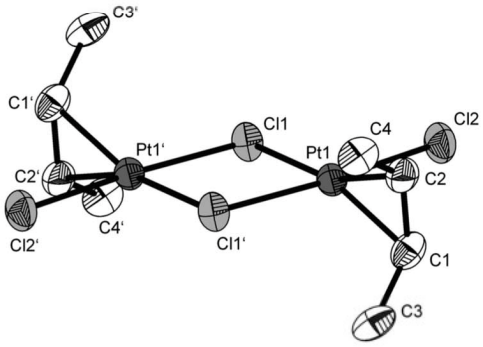

Figure 1. Structure of [{$PtCl_2$(*cis*-MeHC=CHMe)}$_2$] (**2**). Displacement ellipsoids are drawn at 50% probability. H atoms have been omitted for clarity.

Synthesis and Spectroscopic Characterization of Alkyne Complexes of the Zeise's Dimer Type and of Cyclobutadiene Complexes

Reactions between the dinuclear ethene complex [{$PtCl_2(H_2C{=}CH_2)$}$_2$] (**1**) and stoichiometric amounts of alkynes RC≡CtBu (R = Me, tBu) with removal of the cleaved-off ethene in CH_2Cl_2 or $CHCl_3$ as solvent resulted in the formation of dinuclear alkyne complexes [{$PtCl_2$(RC≡CtBu)}$_2$] (R = Me, **11**; tBu, **12**; Scheme 3a), which were isolated as deep red powders in good yields (90, 95%). When alkynes RC≡CR′ with sterically less demanding substituents (R/R′ = Me/Me, Et/Et, Me/nPr) were

Table 2. Selected bond lengths [Å] and angles [°] in crystals of [{$PtCl_2$(MeHC=CHMe)}$_2$] (**2**) and calculated values for the same complex **2a′**.

	2	**2a′**		**2**	**2a′**
C1–C2	1.40(2) (1.346(3))[a]	1.410 (1.334)[a]	Cl2–Pt–Cl1′	174.5(1)	173.94
Pt–C1	2.18(2)	2.175	Cl2–Pt–Cl1	91.0(1)	90.91
Pt–C2	2.16(2)	2.175	Cl1–Pt–Cl1′	83.6(1)	83.03
Pt–Cl2	2.278(3)	2.305	Pt–Cl1–Pt′	96.4(1)	96.97
Pt–Cl1′	2.338(3)[b]	2.405	Cl2–Pt–Cg[b]	88.81(9)	89.07
Pt–Cl1	2.378(3)[b]	2.429	Cg–Pt–Cl1[b]	179.70(8)	179.98
			$\Phi(PtCl_3/PtC_2)$[c]	88.1(6)	90.0

[a] For comparison, values (measured by electron diffraction[20] and obtained by DFT calculation, respectively) for non-coordinated *cis*-but-2-ene in parentheses. [b] Cg: Center of gravity of the two olefinic C atoms (C1–C2). [c] $\Phi(PtCl_3/PtC_2)$: angle between the planes defined by Pt,Cl1,Cl1′,Cl2 and Pt,C1,C2.

used, [2+2] cycloadditions were observed with formation of neutral mononuclear cyclobutadiene complexes [$PtCl_2$-($C_4R_2R'_2$)] (**4**–**6**, Scheme 3b), which were isolated as yellow microcrystals in 73–81% yields. The corresponding reaction with MeC≡CPh also led to a cyclobutadiene complex: compound **7** (Scheme 3c), which proved to be, most likely, dinuclear. Notably, in the case of complex **6**, bearing an unsymmetrically Me-/*n*Pr-substituted cyclobutadiene ligand, the two regioisomeric cyclobutadienes (1,2-dimethyl-3,4-dipropyl, *cis*; 1,3-dimethyl-2,4-dipropyl, *trans*), were formed in a 1:1 ratio, so the cycloaddition did not proceed regioselectively. On the other hand, the coupling of MeC≡CPh to yield complex **7** proceeded regioselectively: both the cyclobutadiene ligands and their substituents of the same kind are believed to be in a mutual *trans* position.

All complexes were characterized unambiguously by microanalysis and NMR spectroscopy, and in the cases of **11** and **12** also by X-ray diffraction measurements. Selected NMR spectroscopic parameters of the complexes are given in Table 3. The CISs ($\Delta\delta = \delta_{complex} - \delta_{noncoord.\,ligand}$) of the alkyne carbon atoms of the dinuclear alkyne complexes **11** and **12** (–3.7 to –8.6 ppm) and the $^1J_{Pt,C}$ coupling constants (190–231 Hz) are of the same order of magnitude as those found in complexes of the Zeise's salt type with alkyne ligands [K(18C6)][$PtCl_3$(RC≡CR′)] (R, R′ = H, alkyl, aryl; $\Delta\delta$ = –5.6 to –17.8 ppm, $^1J_{Pt,C}$ = 173–236 Hz).[10,11] Moreover, all of these values differ from those found in neutral homoleptic mononuclear bis(alkyne)platinum(0) complexes of the type [Pt(RC≡CR′)$_2$] (R, R′ = Me, *t*Bu, Ph; $\Delta\delta$ = 35.2–41.6 ppm, $^1J_{Pt,C}$ = 266–311 Hz).[23]

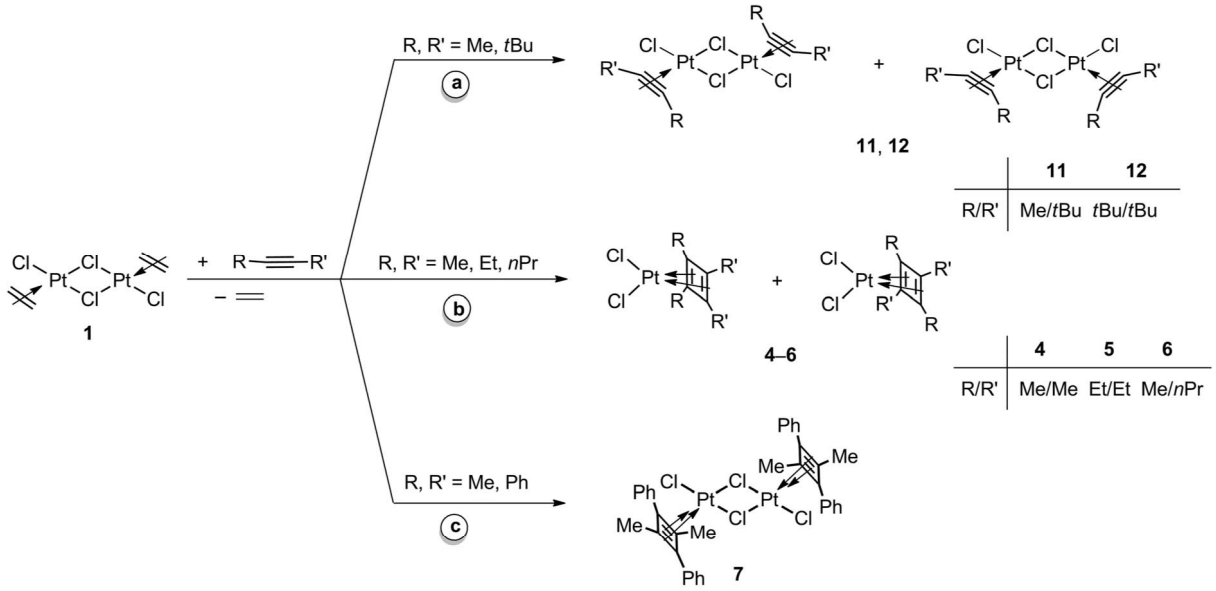

Scheme 3.

Table 3. Selected ^{13}C and ^{195}Pt NMR spectroscopic data (δ in ppm, J in Hz) for (cyclobutadiene)- and (alkyne)platinum(II) complexes.

R/R′	δ(*C*R)/(*C*R′)	$\Delta\delta$[a]	$^1J_{Pt,C}$	$\delta(^{195}Pt)$
Cyclobutadiene complexes [$PtCl_2(C_4R_2R'_2)$]				
4 (Me/Me)	104.1	29.5	145	–3168
5 (Et/Et)	106.3	25.3	150	–3265
6 (Me/*n*Pr)	99.2/103.3	23.7/23.5	[e]/159	–3180
(1:1)[d]	102.8/106.9	27.8/27.7	148/158	–3186
7 (Me/Ph)	101.5/110.0	21.7/10.0	150/156	–1672
16 (Me/*t*Bu)	107.8/98.7	33.2/11.2	153/132	[e]
Mononuclear alkyne complexes [$PtCl_2(H_2C{=}CH_2)$(RC≡CR′)]				
8 (Me/*t*Bu)	74.9/84.8	1.2/–3.2	115/156	–3145
9 (*t*Bu/*t*Bu)	85.9	–1.6	151	–3143
Dinuclear alkyne complexes [{$PtCl_2$(RC≡CR′)}$_2$]				
11 (Me/*t*Bu)	70.0/80.0[b]	–3.7/–8.0	190/224	–1960[b]
(5.5:1:1.2)[d]	69.7/79.5[c]	–4.0/–8.5	[e]/228	–1955
	69.4/79.4[c]	–4.3/–8.6	[e]	–1971[c]
12 (*t*Bu/*t*Bu)	80.7[b]	–6.4	221	–1968[b]
(2.7:1)[d]	80.6[c]	–6.5	231	–2005[c]

[a] $\Delta\delta = \delta_{complex} - \delta_{noncoord.\,alkyne}$. [b] Major isomer. [c] Minor isomer. [d] Ratio of isomers in parentheses. [e] Not found for reasons of intensity.

EurJIC European Journal of Inorganic Chemistry

In cyclobutadiene complexes of the type [$PtCl_2$-($C_4R_2R'_2$)] (**4**–**7**; R, R′ = Me, Et, *n*Pr, Ph), significantly smaller coupling constants ($^1J_{Pt,C}$ = 145–159 Hz) and downfield shifts between δ = 10.0 and 29.5 ppm relative to the non-coordinated alkynes are observed for the C ring atoms. Apart from the ^{13}C NMR spectroscopic data already discussed, the ^{195}Pt NMR shifts offer a straightforward method to distinguish between the different kinds of complexes: for the dinuclear bis(alkyne) complexes ^{195}Pt NMR shifts between δ = –1955 and –2005 ppm (**11**, **12**) are found, whereas the cyclobutadiene complexes (**4**–**6**) exhibit shifts from δ = –3168 to –3265 ppm. The significant difference from these values in the ^{195}Pt NMR shift of complex **7** (δ = –1672 ppm) indicates a dinuclear structure (Scheme 3c).

Molecular Structures of [{$PtCl_2$(RC≡C*t*Bu)}$_2$] (R = Me, **11**; *t*Bu, **12**)

Crystals of the dinuclear bis(alkyne) complexes **11** and **12** suitable for X-ray diffraction analysis were obtained from $CHCl_3$/Et_2O/*n*-pentane solutions. Complex **12** was found to crystallize as two configurational isomers, with the two alkyne ligands either in a mutual *transoid* (**12a**) configuration or in a *cisoid* configuration (**12b**·$CHCl_3$). In all crystals, discrete dinuclear complexes were found without unusual intermolecular interactions. In the crystals of **12a**, two symmetry-independent molecules of very similar structure were found. The molecular structures are depicted in Figures 2, 3, and 4; selected structural parameters are given in the figure captions.

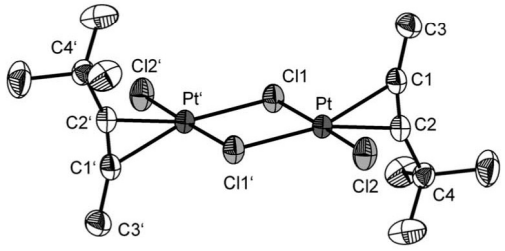

Figure 2. Molecular structure of [{$PtCl_2$(MeC≡C*t*Bu)}$_2$] (**11**). Displacement ellipsoids are drawn at 50% probability. H atoms have been omitted for clarity. Selected structural parameters (distances in Å, angles in °): Pt–C1 2.147(5), Pt–C2 2.143(5), Pt–Cl1 2.341(1), Pt–Cl1′ 2.354(1), Pt–Cl2 2.267(1), C1–C2 1.254(7); C2–C1–C3 163.0(5), C1–C2–C4 159.8(5), Cl1–Pt–Cl2 176.67(4), Cl1–Pt–Cl1′ 84.92(4), Cl1′–Pt–Cl2 91.88(4); Φ($PtCl_3$/PtC_2)[a] 87.5(2). [a] Angle between the planes defined by Pt,Cl1,Cl1′,Cl2 and Pt,C1,C2.

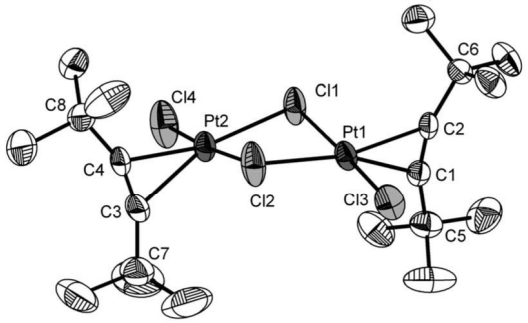

Figure 3. One of the two symmetry-independent molecules of [{$PtCl_2$(*t*BuC≡C*t*Bu)}$_2$] (*transoid* configuration) in crystals of **12a**. Displacement ellipsoids are drawn at 50% probability. H atoms have been omitted for clarity. Selected structural parameters (distances in Å, angles in °; the values for the two symmetry-independent molecules are separated by slashes): Pt1–C1 2.142(4)/2.130(4), Pt1–C2 2.126(4)/2.140(4), Pt2–C3 2.135(5)/2.132(4), Pt2–C4 2.135(4)/2.133(4), Pt1–Cl3 2.262(1)/2.263(1), Pt1–Cl1 2.347(1)/2.349(1), Pt1–Cl2 2.351(1)/2.346(1), Pt2–Cl1 2.349(1)/2.353(1), Pt2–Cl2 2.337(1)/2.330(1), Pt2–Cl4 2.263(1)/2.267(1), C1–C2 1.244(6)/1.238(6), C3–C4 1.229(7)/1.226(6); C1–C2–C6 159.3(4)/161.4(4), C2–C1–C5 161.1(5)/159.2(5), C3–C4–C8 159.2(5)/160.7(5), C4–C3–C7 159.9(5)/160.5(5), Cl1–Pt1–Cl3 176.04(4)/175.67(4), Cl4–Pt2–Cl2 175.11(5)/176.08(5), Cl1–Pt1–Cl2 84.57(4)/84.53(4), Cl1–Pt2–Cl2 84.84(4)/84.80(4), Cl3–Pt1–Cl2 91.58(5)/91.20(5), Cl4–Pt2–Cl1 90.41(4)/91.51(4); Φ($Pt1Cl_3$/$Pt1C_2$)[a] 89.7(3)/89.8(2), Φ($Pt2Cl_3$/$Pt2C_2$)[b] 89.5(3)/89.0(2). [a] Angle between the planes defined by Pt1, Cl1, Cl2, Cl3 and Pt, C1, C2. [b] Angle between the planes defined by Pt2, Cl1, Cl2, Cl4 and Pt2, C3, C4.

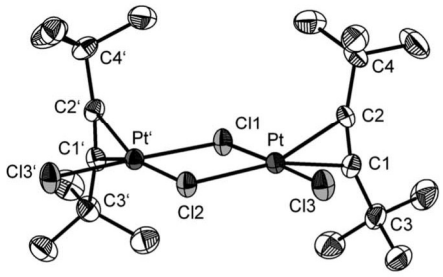

Figure 4. Molecular structure of [{$PtCl_2$(*t*BuC≡C*t*Bu)}$_2$] (**12b**, *cisoid* configuration) in crystals of **12b**·$CHCl_3$. Displacement ellipsoids are drawn at 50% probability. H atoms have been omitted for clarity. Selected structural parameters (distances in Å, angles in °): Pt–C1 2.135(4), Pt–C2 2.144(4), Pt–Cl1 2.3394(9), Pt–Cl2 2.3779(8), Pt–Cl3 2.272(1), C1–C2 1.258(5); C2–C1–C3 159.8(4), C1–C2–C4 160.8(4), Cl1–Pt–Cl3 177.55(4), Cl1–Pt–Cl2 84.93(3) Cl2–Pt–Cl3 92.72(3); Φ($PtCl_3$/PtC_2)[a] 89.7(2). [a] Angle between the planes defined by Pt, Cl1, Cl2, Cl3 and Pt, C1, C2.

Molecules of complex **11** and of the *cisoid* complex **12b** exhibit crystallographically imposed inversion and mirror symmetry, respectively. In each of these two complexes, the central $Pt_2(\mu\text{-}Cl)_2$ unit is precisely (**11**) or nearly planar [Pt–Cl1···Cl2–Pt′ 177.00(5)°, **12b**]. In complex **12a** the central four-membered ring is more folded [Pt1–Cl1···Cl2–Pt2 152.51(5)/153.35(6)°].[1] The platinum atoms are square-planar coordinated to a good approximation, as shown by the angles between the *trans*-disposed ligands $Cl_{term.}$–Pt–μ-Cl and Cg–Pt–μ-Cl (Cg = center of gravity of the two alkyne C atoms), which were found to be between 175.05(3) and 177.88(3)°.

The alkyne ligands are orientated almost perpendicular to the $PtCl_3$ coordination planes, as measured by the interplanar angles Φ($PtCl_3$/PtC_2) = 87.5(2) to 89.8(2)°. The terminal Pt–$Cl_{term.}$ bonds [2.262(1) to 2.272(1) Å] are significantly shorter than the bridging Pt–μ-Cl bonds [2.330(1) to 2.3779(9) Å] (cf. S3 in the Supporting Information).

Furthermore, in the *cisoid*-configured complex **12b**, the Pt–μ-Cl bond *trans* to the alkyne ligand is significantly longer than the corresponding bond *trans* to the chlorido ligand [2.3779(9) vs. 2.3394(9) Å].

In the complexes **11** and **12a/b**, the Pt–C bonds [2.126(4) to 2.147(5) Å] were found to be of lengths comparable to those in complexes of the type $M^{I}[PtCl_3(RC{\equiv}CR')]$ {M^{I} = K, [K(18C6)], (PPh_4); R, R′ = alkyl, phenyl}.[9] Furthermore, bond lengthening of the C≡C bonds in complexes **12a** and **12b** relative to non-coordinated bis(*tert*-butyl)-acetylene can be observed [1.226(6) to 1.258(5) vs. 1.202(1) Å[24]]. This finding and the "bending back" of the substituents R/R′, as measured by the angle α [α = 180 – γ(C≡C–C); 17.0(5) to 20.8(4)°], reflect a degree of back-donation as would be anticipated for Pt^{II} complexes. Analogous values [C≡C 1.22(1) to 1.24(2) Å; α = 16(1)° to 21(1)°] were found in neutral mononuclear alkyne complexes $[PtCl_2(RC{\equiv}CR)L]$ (R = CMe_2OH, *t*Bu; L = $NMeH_2$, toluidine) and in alkyne complexes $[K(18C6)][PtCl_3(RC{\equiv}CR')]$ (R/R′ = Me, *t*Bu) of the Zeise's salt type[10,11,25,26] (cf. S3 in the Supporting Information).

Reactivity of Zeise's Dimer Toward Sterically Demanding Alkynes

As already described, reactions between $[\{PtCl_2(H_2C{=}CH_2)\}_2]$ (**1**) and stoichiometric amounts of alkynes RC≡C*t*Bu (R = Me, *t*Bu) resulted in the formation of $[\{PtCl_2(RC{\equiv}Ct\text{Bu})\}_2]$ (R = Me, **11**; *t*Bu, **12**, Scheme 4, path a). When these reactions were monitored by ^{1}H NMR spectroscopy in sealed NMR tubes (i.e., without removal of cleaved-off ethene), within 7 d the formation of mononuclear complexes of the type $[PtCl_2(H_2C{=}CH_2)(RC{\equiv}Ct\text{Bu})]$ (R = Me, **8**; *t*Bu, **9**) as main products, according to Scheme 4, paths b/c, was observed. As side products, apart from small amounts of $[PtCl_2(H_2C{=}CH_2)_2]$ (**10**), the dinuclear complex $[\{PtCl_2(t\text{BuC}{\equiv}Ct\text{Bu})\}_2]$ (**12**, Scheme 4, path b) was formed in the case of *t*BuC≡C*t*Bu, whereas in that of MeC≡C*t*Bu traces of the cyclobutadiene complex $[PtCl_2(C_4Me_2t\text{Bu}_2)]$ (**16**, path c) were observed. Notably, the coupling of the alkynes proceeded regioselectively, yielding only the *trans* isomer of complex **16**. Furthermore, it was shown with complex **12** as an example that the use of a tenfold excess of bis(*tert*-butyl)acetylene does not lead to bridge cleavage in complex **12** to yield the bis(*tert*-butyl)-acetylene complexes *trans*-**19** and/or *cis*-**19** (Scheme 4, path d).

Selected ^{1}H, ^{13}C, and ^{195}Pt NMR spectroscopic parameters of the complexes formed in these reactions are given in Tables 1 and 3. The identity of $[PtCl_2(H_2C{=}CH_2)_2]$ (**10**) was confirmed by comparison with data given in ref.[19] The cyclobutadiene complex **16** showed chemical shifts and coupling constants typical of mononuclear cyclobutadiene complexes of the same type (**4**–**6**). Although the isolation of the mixed olefin/alkyne complexes $[PtCl_2(H_2C{=}CH_2)$-$(RC{\equiv}Ct\text{Bu})]$ (R = Me, **8**; *t*Bu, **9**) failed, their identities could be determined unambiguously by ^{1}H and ^{13}C NMR spectroscopy. The ^{1}H NMR signal of the methyl group in **8** (δ_H = 2.26 ppm; Figure 5) shows a $^3J_{Pt,H}$ coupling constant of 31 Hz, typical for Pt^{II} complexes bearing methyl-substituted alkyne ligands (≡CCH_3: δ_H = 2.10–2.44 ppm; $^3J_{Pt,H}$ = 30–33 Hz).[10,11] Selective irradiation at the resonance frequency of the methyl protons was found to result in small intensity enhancements of the two signals at δ = 4.50 and 1.40 ppm (see NOE difference spectrum in Figure 5). This indicates a distance of less than 5 Å between the irradiated protons and the protons of the ethene ligand, thus demonstrating a mononuclear complex.[27] At ambient

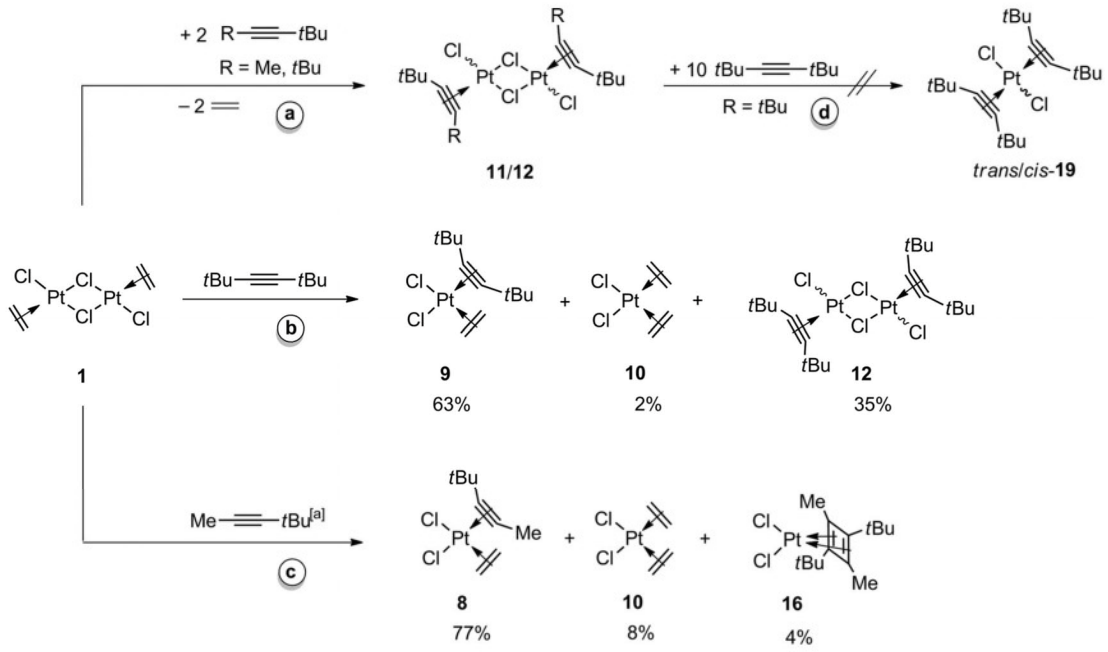

Scheme 4. [a] Additionally, the reaction mixture contained 11% of the starting complex **1**.

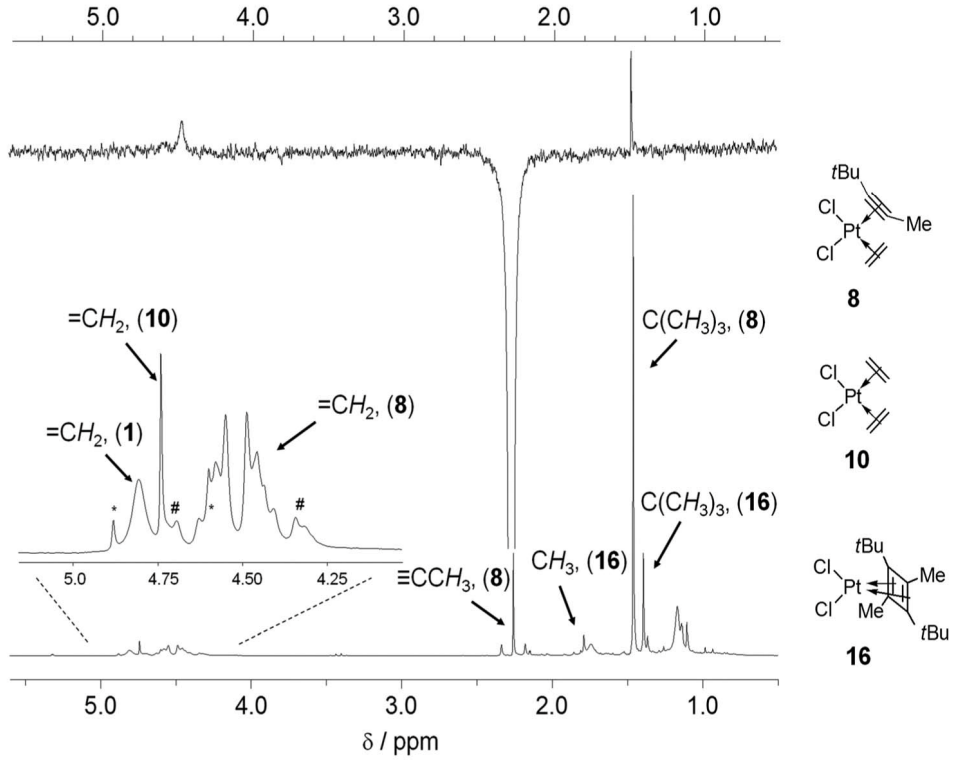

Figure 5. ^{1}H NMR spectrum (300 K, 200 MHz in CD_2Cl_2) of the reaction mixture of [{$PtCl_2(H_2C{=}CH_2)$}$_2$] (**1**) with MeC≡C*t*Bu (bottom) and NOE difference spectrum (top). In the expanded spectrum, platinum satellites are assigned with crosses and stars for the complexes [$PtCl_2(H_2C{=}CH_2)$(*t*BuC≡C*t*Bu)] (**8**) and [$PtCl_2(H_2C{=}CH_2)_2$] (**10**), respectively.

temperature, in complex **8** a highly complex ethene signal (=CH_2; δ = 4.56 ppm) was found, simulation of which resulted in an AA′BB′ spin system (see S1 in the Supporting Information). At –80 °C the spin system was found to change to an ABCD system with four chemically nonequivalent protons (Figure 6). These findings give confirmation both of the *cis* configuration of complex **8** and of a fast rotation of the ethene ligand at ambient temperature. The temperature dependence of the rotation of the olefin, as well as the alkyne ligand, is discussed in the following section.

The CISs ($\Delta\delta = \delta_{complex} - \delta_{noncoord.ligand}$) of the ethene carbon atoms of the mononuclear complexes [$PtCl_2$-($H_2C{=}CH_2$)(RC≡C*t*Bu)] (R = Me, **8**; *t*Bu, **9**) [$\Delta\delta$(=*C*H) = –43.1/–42.9 ppm, **8/9**] are in the same range as those found in complexes of the Zeise's dimer type [{$PtCl_2$(RHC=CHR)}$_2$] (R = H, alkyl) and of the Zeise's salt type M^I[$PtCl_3(R_2C{=}CR'_2)$] {M^I = K, [K(18C6)], (PPh_4), [N(*n*Bu)$_4$]; R, R′ = H, alkyl, aryl} [$\Delta\delta$(=*C*H) = –40 to –55 ppm].[4,16,6,17] The $^1J_{Pt,C}$ coupling constants of ethene in the ethene/alkyne complexes [$PtCl_2(H_2C{=}CH_2)$-(RC≡C*t*Bu)] (R = Me, **8**; *t*Bu, **9**; $^1J_{Pt,C}$ = 141/138 Hz) are of the same order of magnitude as those of neutral mononuclear bis(olefin) complexes [$PtCl_2L_2$] (2 L = ethene, 1,5-COD; $^1J_{Pt,C}$ = 131/152 Hz).[18,19] On the other hand, significantly larger coupling constants are found in Zeise's complexes [{$PtCl_2$(RHC=CHR′)}$_2$] (R, R′ = H, alkyl; $^1J_{Pt,C}$ = 182–199 Hz) and M^I[$PtCl_3(R_2C{=}CR'_2)$] {M^I = K, [K(18C6)], (PPh_4), [N(*n*Bu)$_4$]; R, R′ = H, alkyl, aryl; $^1J_{Pt,C}$ = 180–195 Hz}.[4,16,6,17] The same trend can be observed for the $^1J_{Pt,C}$ coupling constants of the alkyne ligands (Table 3): values between 115 and 156 Hz are found for [$PtCl_2(H_2C{=}CH_2)$(RC≡C*t*Bu)] (R = Me, **8**; *t*Bu, **9**), and these are significantly smaller than those in the neutral dinuclear complexes [{$PtCl_2$(RC≡C*t*Bu)}$_2$] (R = Me, *t*Bu; $^1J_{Pt,C}$ = 190–231 Hz) and anionic mononuclear complexes [K(18C6)][$PtCl_3$(RC≡CR′)] (R, R′ = H, alkyl, aryl; $^1J_{Pt,C}$ = 173–236 Hz).[10,11]

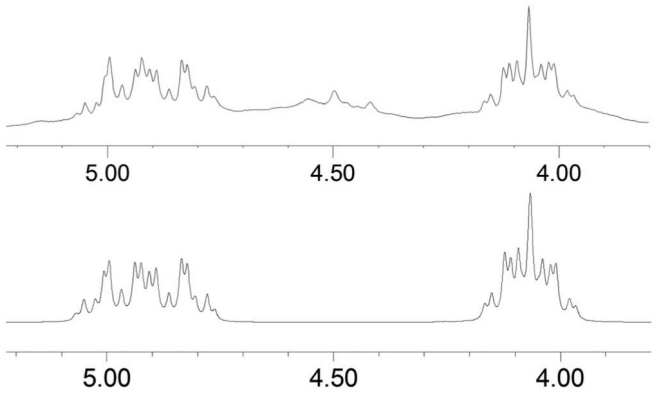

Figure 6. Experimentally measured (193 K, 200 MHz in CD_2Cl_2; top) and simulated (bottom) ^{1}H NMR spectrum of the ethene protons of [$PtCl_2(H_2C{=}CH_2)$(*t*BuC≡C*t*Bu)] (**8**). Coupling constants ($J_{H,H}$) from higher-order multiplets (given in S1 in the Supporting Information) were obtained by use of the PERCH NMR software package.[37]

Reactivity of Zeise's Dimer Toward Sterically Less Demanding Alkynes

As described above, reactions between [{$PtCl_2$-(H_2C=CH_2)}$_2$] (**1**) and stoichiometric amounts of alkynes RC≡CR′ bearing sterically less demanding substituents (R, R′ = Me, Et, *n*Pr, Ph) in chloroform or dichloromethane resulted – if the cleaved-off ethene was removed from the reaction mixtures – in the formation (Scheme 3, paths b/c) of cyclobutadiene complexes [$PtCl_2$($C_4R_2R'_2$)] (**4**–**6**) and [{$PtCl_2$($C_4R_2R'_2$)}$_2$] (**7**). As a representative example, the reaction between **1** and but-2-yne was carried out in a sealed NMR tube (i.e., without the removal of the cleaved-off ethene). Apart from the formation of the cyclobutadiene complex **4** as main product, smaller amounts of the bis-(ethene) complex **10** were produced. Furthermore, on a small scale, a cyclotrimerization yielding hexamethylbenzene took place (Scheme 5, path a). In contrast with these reactions (solvent: $CHCl_3$, CH_2Cl_2), in the classical work of Chatt et al.,[7,8] decomposition was observed on addition of stoichiometric amounts of internal or terminal alkynes bearing only sterically less demanding substituents to Zeise's dimer in acetone as solvent. In order to clarify the reason for this observation, corresponding NMR experiments were performed. Dissolution of Zeise's dimer in acetone resulted immediately in a change of color from orange to yellow. ^{195}Pt NMR spectroscopic data indicated the formation of the mononuclear complex *trans*-[$PtCl_2$(Me_2CO)(H_2C=CH_2)] (**18**) and of one unidentified complex. Furthermore, the solvent acetone underwent both aldol addition and condensation reactions (Scheme 5, path b). After several days, the formation of higher acetone condensation products containing Me–(MeC=CH)$_n$–C(O)Me (n = 5–7) units was observed.[28]

Addition of but-2-yne to a freshly prepared solution of Zeise's dimer in acetone resulted immediately in a change in color from yellow to red. ^{13}C and ^{195}Pt NMR spectroscopic data indicated the formation of the mononuclear complex *trans*-[$PtCl_2$(Me_2CO)(H_2C=CH_2)] (**18**, Scheme 5, path c) and after several days the formation of the cyclobutadiene complex [$PtCl_2$(C_4Me_4)] (**4**) and [$PtCl_2$-(H_2C=CH_2)$_2$] (**10**), analogously to the reaction performed in chloroform. The decomposition of the solvent, especially the formation of higher condensation products of acetone (see above), led – after removal of all volatile components in vacuo – to black oils, as also described by Chatt et al.[7,8]

Configurational and Conformational Isomers of Alkyne and Olefin Complexes of the Zeise's Dimer Type

To obtain insight into the structures of the dinuclear (olefin)- and (alkyne)platinum(II) complexes, in particular into the stabilities of the configurational and conformational isomers, quantum-chemical calculations at the DFT level of theory were performed. The structures and relative energies of these isomers, together with selected structural parameters, are given in Figures 7 and 8 and in Tables 2 and 4. In all these complexes, inspection of the Gibbs free energies of the different isomers shows that, in general, the *transoid* isomer was found to be only slightly more stable (maximum 1.6 kcal mol^{-1}) than the corresponding *cisoid* isomer. This difference is even less pronounced when solvent effects are considered (Table 6, below).

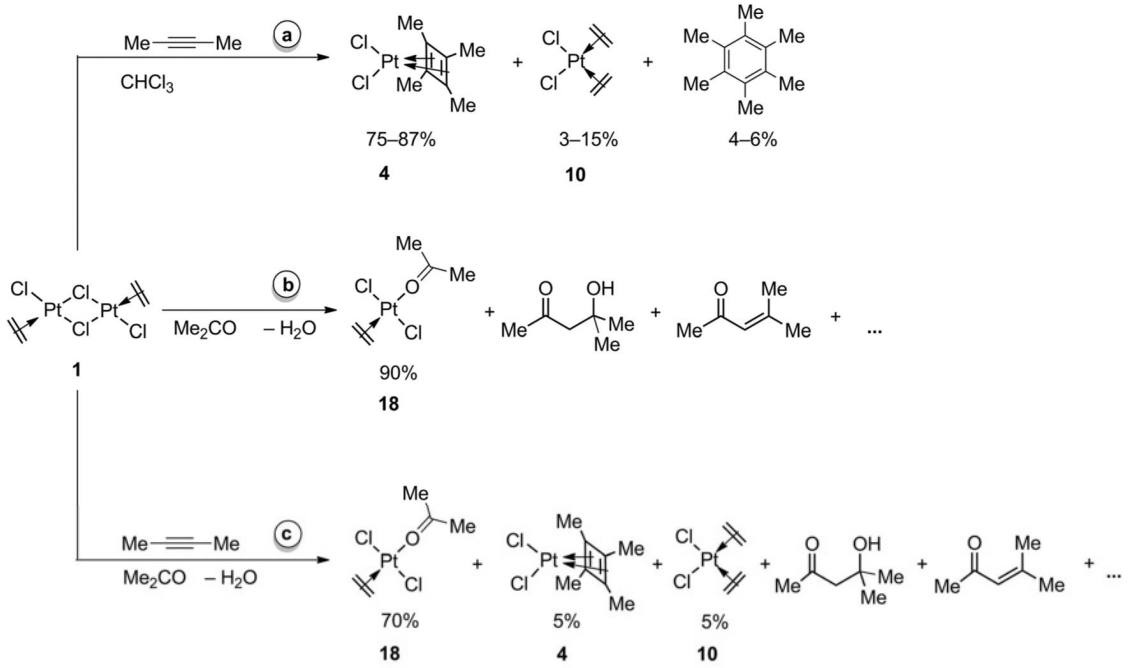

Scheme 5.

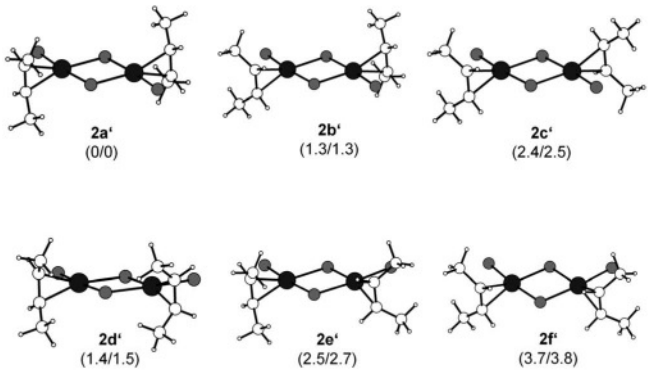

Figure 7. Calculated structures of [{$PtCl_2$(*cis*-MeHC=CHMe)}$_2$] (**2a′**–**2f′**) along with the standard Gibbs free energies (kcal mol^{-1}) in parentheses relative to the most stable isomer **2a′**. Values for the gas phase and in $CHCl_3$ as solvent are separated by slashes. DFT calculations: B3LYP/6-311G(d,p) for main-group atoms; for details, see Experimental Section.

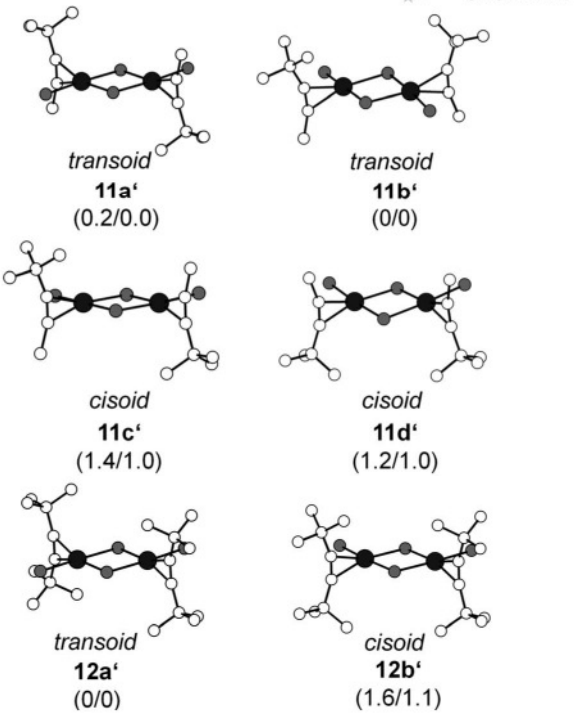

Figure 8. Calculated configurational (R = Me: **11a′**/**11c′**, **11b′**/**11d′**; R = *t*Bu: **12a′**/**12b′**) and conformational (R = Me: **11a′**/**11b′**, **11c′**/**11d′**) isomers of [{$PtCl_2$(RC≡C*t*Bu)}$_2$] along with the Gibbs free energies (kcal mol^{-1}) in parentheses relative to the most stable isomers (**11b′**, **12a′**). Values for the gas phase and in $CHCl_3$ as solvent are separated by slashes. H atoms have been omitted for clarity. DFT calculations: B3LYP/6-311G(d,p) for main-group atoms; for details, see Experimental Section.

The rates of rotation around the platinum–olefin/alkyne bonds were calculated (Table 5) for the dinuclear complexes [{$PtCl_2$(*cis*-MeHC=CHMe)}$_2$] (**2a′**) and [{$PtCl_2$-(MeC≡C*t*Bu)}$_2$] (**11a′**) and for the mixed mononuclear complex *cis*-[$PtCl_2$(H_2C=CH_2)(MeC≡C*t*Bu)] (**8′**). Under standard conditions, the activation barriers ($\Delta G^{\ddagger}$) for the rotation of the olefin ligands (13.4/12.1 kcal mol^{-1}, **2a′**/**8′**) proved to be significantly lower than those of the *tert*-butyl-substituted alkyne ligands (20.6/23.9 kcal mol^{-1}, **11a′**/**8′**), which seems to be mainly for steric reasons. These values fit well with the activation barriers found experimentally for rotations of olefin ligands in platinum(II) complexes (10.0–15.0 kcal mol^{-1}).[29] As far as is known, and in good agreement with this work, in olefin and alkyne complexes with the same structure, higher barriers (by 3–6 kcal mol^{-1}) were found for rotations of alkynes.[30] One exception was observed in the five-coordinate platinum complexes [PtI_2-(Me_2phen)L] (L = MeC≡CH, MeHC=CH_2; Me_2phen = 2,9-dimethyl-1,10-phenanthroline), in which the alkyne ligand was found to be associated with a lower barrier (by about 3 kcal mol^{-1}) than the olefin ligand, which might be interpreted in terms of a dissociative/associative process instead of an intramolecular rotation.[31]

Furthermore, the DFT calculations are in good agreement with the experimental findings relating to the fast and (with respect to the NMR timescale) the frozen rotations of the ethene ligand in complex **8** at room temperature and at –80 °C, respectively. In addition, in accordance with the NMR spectroscopic investigations of complex **8** and **11**, the calculations give confirmation that the alkyne ligands both

Table 4. Calculated structural parameters of selected isomers of complexes [{$PtCl_2$(MeC≡C*t*Bu)}$_2$] (**11a′**/**11c′**) and [{$PtCl_2$(*t*BuC≡C*t*Bu)}$_2$] (**12a′**/**12b′**).

	11a′[a] (*transoid*)[b]	**11c′** (*cisoid*)[b]	**12a′**[a] (*transoid*)	**12b′**[a] (*cisoid*)
Pt–C[c]	2.156/2.135	2.158/2.138	2.150	2.153
Pt–$Cl_{term.}$	2.300	2.296	2.301	2.296
Pt–μ-$Cl_{trans\ C\equiv C}$[d]	2.409	2.402	2.412	2.404
Pt–μ-$Cl_{trans\ Cl}$[d]	2.412	2.421	2.412	2.423
C≡C[e]	1.247 (1.204)	1.247 (1.204)	1.250 (1.206)	1.250 (1.206)
C≡C–C[c]	159.3/161.9	159.3/161.9	159.5	159.4
Cg–Pt–$Cl_{term.}$	91.0	90.8	91.8	91.6
Cg–Pt–μ-$Cl_{trans\ C\equiv C}$[d]	176.9	177.2	176.7	177.0
Cg–Pt–μ-$Cl_{trans\ Cl}$[d]	92.5	92.8	92.5	92.9

[a] Corresponding values obtained experimentally by X-ray diffraction measurements in the captions of Figures 2, 3, and 4. [b] Head-to-tail arrangement of the two alkyne ligands. [c] Values for the *tert*-butyl- and methyl-substituted carbon atoms separated by slashes. [d] M–$Cl_{trans\ C\equiv C}$/μ-$Cl_{trans\ Cl}$: μ-chlorido ligand *trans* to the alkyne and to the terminal chlorido ligand, respectively. Cg = center of gravity of the two alkyne C atoms. [e] Values for the corresponding non-coordinated alkynes in parentheses.

Table 5. Calculated standard Gibbs free energies of activation (kcal mol^{-1}) and corresponding first-order rate constants (s^{-1}) for the rotation of π ligands in complexes of the Zeise's dimer type [{$PtCl_2$(MeHC=CHMe)}$_2$] (**2**) and [{$PtCl_2$(MeC≡C*t*Bu)}$_2$] (**11**), and in the mononuclear complex [$PtCl_2$(H_2C=CH_2)(MeC≡C*t*Bu)] (**8**).

	Olefin	$\Delta G^{\ddagger}$	k		Alkyne	$\Delta G^{\ddagger}$	k
2a′	*cis*-but-2-ene	13.4	9.1×10^{2}	**11′a**	MeC≡C*t*Bu	20.6	4.7×10^{-3}
8′	ethene	12.1	8.2×10^{3}	**8′**	MeC≡C*t*Bu	23.9	1.8×10^{-5}
8′[a]	ethene	11.8	1.7×10^{-1}	**8′**[a]	MeC≡C*t*Bu[a]	22.9	4.5×10^{-14}

[a] T = 193 K.

in the mononuclear complex **8** and in the dinuclear complexes **11/12** do not rotate even at room temperature.

In summary, these findings give further support for the complexity of the NMR spectra of the dinuclear olefin complex **2** and of the alkyne complexes **11** and **12** being due to the presence of configurational/conformational isomers.

On the Equilibria Between *cisoid* and *transoid* Isomers

The ^{13}C and ^{195}Pt NMR spectra of the dinuclear olefin complexes **1**–**3** each showed two sets of signals for the olefinic ^{13}C atoms (except in the case of **1**) and ^{195}Pt atoms. These findings can be explained in terms of the presence in each case (in solution) of two configurational isomers: namely a *transoid* and a *cisoid* configuration (Scheme 2). The major isomers were assigned as the *transoid* complexes, on the basis of single-crystal and powder diffraction measurements (**2**, S5 in the Supporting Information) and the thermodynamic stabilities predicted by DFT calculations. The relative intensities of the two signal sets were found to depend on the solvent. From these values, equilibrium constants for the isomerization were obtained (K_{NMR} = 1.5–12.6), corresponding to standard Gibbs free energies from –0.2 to –1.5 kcal mol^{-1} (Table 6 and Table 1). In general, more polar solvents give rise to smaller energy differences between the two isomers, which can be understood in terms of the different dipole moments of the isomers.

Table 6. Solvent dependence of the equilibrium constants for the *cisoid*/*transoid* interconversion as shown in Scheme 2 derived from ^{13}C and ^{195}Pt NMR spectra (K_{NMR}), together with the corresponding standard Gibbs free energies (kcal mol^{-1}) obtained from K_{NMR} (ΔG_{NMR}) and DFT calculations (ΔG_{DFT}). Relative dielelctric constants $\varepsilon/\varepsilon_0$ given are taken from ref.[47]

Solvent	CH_3NO_2	CH_2Cl_2	$CHCl_3$	CCl_4	Et_2O	C_6H_6	Gas phase
$\varepsilon/\varepsilon_0$	38.6	8.9	4.8	2.2	4.3	2.3	
[{$PtCl_2$(H_2C=CH_2)}$_2$] (**1**)							
K_{NMR}		2.2	1.7			6.8	
ΔG_{NMR}		–0.5	–0.3			–1.1	
ΔG_{DFT}	–0.5	–0.7	–0.8	–1.0		–1.0	–1.1
[{$PtCl_2$(*cis*-MeHC=CHMe)}$_2$] (**2**)							
K_{NMR}	1.5	3.0	4.7	7.5			
ΔG_{NMR}	–0.2	–0.7	–0.9	–1.2			
ΔG_{DFT}	–0.8	–0.9	–1.5	–1.4		–1.5	–1.4
[{$PtCl_2$(*t*BuC≡C*t*Bu)}$_2$] (**12**)							
K_{NMR}		2.7	2.5		2.2	5.1	
ΔG_{NMR}		–0.6	–0.5		–0.4	–1.0	
ΔG_{DFT}		–0.2	–1.1		–0.4	–0.6	–1.6

In the ^{1}H, ^{13}C, and ^{195}Pt NMR spectra of the dinuclear alkyne complex **12**, with the coordinated symmetrically substituted *t*BuC≡C*t*Bu alkyne, two sets of signals were observed, whereas in the analogous complex **11**, with the coordinated unsymmetrically substituted MeC≡C*t*Bu alkyne, three sets of signals were found. These findings for the two complexes (**11** and **12**) can be explained in terms of the presence of two configurational isomers (*cisoid*/*transoid*), and for complex **11**, additionally, by the presence of conformational isomers as shown in Figure 8. As in the cases of the olefin complexes, in the NMR spectra the major isomers of the dinuclear alkyne complexes were assigned as the *transoid* complexes, on the basis of X-ray diffraction measurements (**11** and **12**; see S6/S7 in the Supporting Information) and DFT calculations. It remains unclear whether the signal of the *transoid* or of the *cisoid* isomer is split into **11a′**/**11b′** and **11c′**/**11d′**, respectively.

Ligand Substitution and Bridge Cleavage Reactions of Complexes of the Zeise's Dimer Type

In the literature, only relatively few examples of mononuclear complexes bearing two monodentately bound olefin ligands have been reported. One of the first examples was the reaction between Zeise's dimer [{$PtCl_2$(H_2C=CH_2)}$_2$] and ethene to yield a yellow, unstable complex, postulated to be *trans*-[$PtCl_2$(H_2C=CH_2)$_2$],[14] which has also been assumed to exist as a short-lived intermediate in the ethene exchange reaction of [$PtCl_3$(H_2C=CH_2)]$^-$.[32] Furthermore, for cleavage reactions between dinuclear chlorido-bridged complexes [($PtCl_2L)_2$] (L = ethene, styrene, cot) and nucleophiles (L = ethene, styrene, cot) to yield *trans*-[$PtCl_2L_2$] (L = styrene, cot, ethene) chemical equilibria [K = 0.0235 ± 0.0003 (styrene), 2.05 ± 0.06 (cot), and 6.8 ± 0.6 M^{-1} (ethene)] corresponding to ΔG values between 2.2 and –1.1 kcal mol^{-1} were observed.[19,4,33]

To address the stabilities of various mono- and dinuclear olefin and alkyne complexes in this study, further DFT calculations were performed. For this purpose, the thermodynamic balances of ligand substitution and bridge cleavage reactions as shown in Scheme 6 were calculated with consideration of solvent effects ($CHCl_3$); the values for the gas phase are given in the Supporting Information (S8). The substitution of ethene in Zeise's dimer by *tert*-butyl-substituted alkynes RC≡C*t*Bu (R = Me, *t*Bu) resulting in the formation of [{$PtCl_2$(RC≡C*t*Bu)}$_2$] (R = Me, **11b′**; *t*Bu, **12a′**; Scheme 6, reaction path a) was found to be endergonic (ΔG_{solv} = 8.4/7.9 kcal mol^{-1} for R = Me/*t*Bu), pointing to a

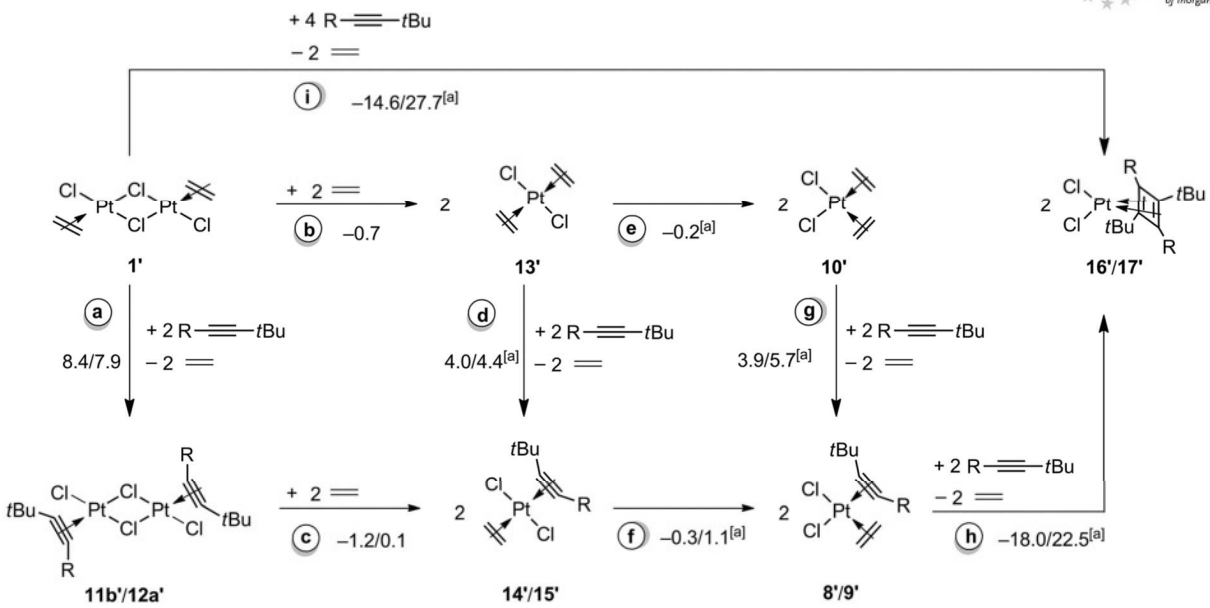

Scheme 6. Figures given are standard Gibbs free energies [kcal mol^{-1}] with consideration of $CHCl_3$ as solvent (ΔG_{solv}). The values for R = Me and R = *t*Bu are separated by slashes. [a] ΔG_{solv} refers to the formation of 1 mol complex.

stronger binding of ethene to platinum than of the alkyne. It can thus be understood that in the synthesis of complexes **11** and **12** the removal of ethene through evaporation is crucial for significant conversion.

The bridge cleavage in complexes [{$PtCl_2(H_2C{=}CH_2)$}$_2$] (**1′**) and [{$PtCl_2(RC{\equiv}CtBu)$}$_2$] (R = Me, **11b′**; *t*Bu, **12a′**) with formation of [$PtCl_2(H_2C{=}CH_2)_2$] (**13′**) and *trans*-[$PtCl_2(H_2C{=}CH_2)(RC{\equiv}CtBu)$] (R = Me, **14′**; *t*Bu, **15′**), respectively, was found to be nearly thermoneutral (ΔG_{solv} = –1.2 to 0.1 kcal mol^{-1}; reaction paths b/c), indicating the presence of chemical equilibria in these reactions. Notably, for the bridge cleavage reaction path b of Zeise's dimer by ethene a Gibbs free energy of –0.7 kcal mol^{-1} was calculated, which fits well with the experimentally measured value (–1.1 kcal mol^{-1}) obtained by Elding et al.,[19] demonstrating the appropriateness of the quantum-chemical model used.

The isomerization of the mononuclear *trans*-configured complexes [$PtCl_2(H_2C{=}CH_2)(RC{\equiv}CtBu)$] (R = Me, **14′**; *t*Bu, **15′**) and [$PtCl_2(H_2C{=}CH_2)_2$] (**13′**) into the analogous *cis* complexes **8′**–**10′** was found to be almost thermoneutral (ΔG_{solv} = –0.3 to 1.1 kcal mol^{-1}; reaction paths e/f). The substitution of one ethene ligand in the mononuclear complexes *cis*/*trans*-[$PtCl_2(H_2C{=}CH_2)_2$] (**10′**/**13′**) by an alkyne to yield *cis*/*trans*-[$PtCl_2(H_2C{=}CH_2)(RC{\equiv}CtBu)$] (R = Me, **8′**/**14′**; *t*Bu, **9′**/**15′**) was found to be only moderately endergonic (ΔG_{solv} = 3.9–5.7 kcal mol^{-1}; reaction paths g/d).

Furthermore, the [2+2] cycloaddition of MeC≡C*t*Bu as in the reaction paths h and i (Scheme 6) to yield the cyclobutadiene complexes [$PtCl_2(C_4R_2tBu_2)$] (R = Me, **16′**; *t*Bu, **17′**) could proceed via precursor complexes [$PtCl_2(RC{\equiv}CtBu)_2$] (R = Me, **20′**; *t*Bu, **19′**; see the Supporting Information). The formation of complex **16′** (R = Me) is strongly exergonic (ΔG_{solv} = –18.0 kcal mol^{-1}). In contrast, the analogous reactions with a sterically more demanding alkyne (*t*BuC≡C*t*Bu) to yield [$PtCl_2(C_4tBu_4)$] (**17′**) proved to be endergonic (ΔG_{solv} = 22.5 kcal mol^{-1}). Although the formation of **16′** was calculated to be strongly exergonic, only small amounts of this complex were observed spectroscopically, whereas the formation of **17′** was not observed, even in traces.

Conclusions

This work presents a straightforward method for the preparation of mono- and dinuclear (alkyne)platinum(II) complexes by ligand substitution and bridge cleavage reactions. The following conclusions can be drawn:

(1) Zeise's dimer was found to react smoothly with alkynes bearing *tert*-butyl substituents RC≡C*t*Bu (R = Me, *t*Bu) to yield complexes [{$PtCl_2(RC{\equiv}CtBu)$}$_2$] if ethene was removed from the reaction mixture, but to yield *cis*-[$PtCl_2(H_2C{=}CH_2)(RC{\equiv}CtBu)$] without removal of ethene. Although the complexes *cis*-[$PtCl_2(H_2C{=}CH_2)(RC{\equiv}CtBu)$] (R = Me, *t*Bu) were not isolated as solids, they could be unambiguously characterized in solution by NMR spectroscopy. Consistent with the NMR spectroscopic investigations, DFT calculations indicate unhindered rotation of the ethene ligand around the Pt–C bond at room temperature, whereas the analogous rotation of the alkyne ligand is frozen under these conditions.

(2) Olefin complexes of the Zeise's dimer type [{$PtCl_2(RHC{=}CHR)$}$_2$] (R = H, Me, *c*-Hex) and analogous alkyne complexes [{$PtCl_2(RC{\equiv}CtBu)$}$_2$] (R = Me, *t*Bu) exist in solvent-dependent equilibria between the *transoid* and *cisoid* isomers (cf. Scheme 2). This configurational isomerism is described for the first time in this work and could even be structurally established (Figures 3 and 4). In accordance with the experiments, DFT calculations gave con-

firmation of the equilibria between the *transoid* and *cisoid* isomers.

(3) Zeise's dimer reacts with alkynes RC≡CR′ bearing sterically less demanding substituents (R, R′ = Me, Et, *n*Pr, Ph) with formation of (cyclobutadiene)platinum(II) complexes $[PtCl_2(C_4R_2R'_2)]$. Notably, these [2+2] cycloadditions proceed under very mild reaction conditions (room temp.), whereas the formation of (cyclobutadiene)platinum(II) complexes by starting from $H_2[PtCl_6]\cdot 6H_2O$[34] or from $[PtCl_2L_2]$ (L = CO, MeCN)[35] requires harsher reaction conditions. Furthermore, with regard to the experimental findings, it can be deduced from DFT calculations that the formation of the complexes $[PtCl_2(C_4tBu_4)]$ and $[PtCl_2(C_4Me_2tBu_2)]$ is thermodynamically and kinetically, respectively, hampered.

(4) From the historical point of view, it is of interest to clarify why Chatt et al.,[7,8] on the one hand, succeeded in the synthesis of $[\{PtCl_2(RC{\equiv}CtBu)\}_2]$ by treatment of Zeise's dimer or $Na_2[PtCl_4]$ with sterically demanding substituted alkynes RC≡C*t*Bu, whereas – on the other hand – analogous reactions with alkynes RC≡CR′ bearing sterically less demanding substituents (such as R, R′ = H, Me, Et, *n*Pr, *i*Pr, *n*Bu, ...) resulted in decomposition. Apart from the much more sophisticated spectroscopic and preparative methods available today, the following reasons can be named:

(a) Chatt's experiments were performed in acetone (Gutmann's donor number *DN* = 17.0), which might act concurrently as a donor for the olefins and alkynes; this is not the case in dichloromethane (*DN* = 1)[36] or chloroform (*DN* = 4)[36] used in this study.

(b) In these reactions acetone is not inert, but undergoes aldol coupling and condensation reactions, giving rise to the formation of, among others, at least oligomeric products containing $Me{-}(MeC{=}CH)_n{-}C(O)Me$ (n = 5–7) units.

To sum up, for reactions between Zeise's dimer and alkynes, which have been known for 50 years, both the experimental and the theoretical investigations presented here give insight for the first time into how subtly the courses of these reactions depend on the substitution patterns of the alkynes and on the solvent, thus opening a way to targeted syntheses of (cyclobutadiene)- and (alkyne)platinum(II) complexes starting from Zeise's dimer.

Experimental Section

General Procedures: All reactions were performed under Ar with use of standard Schlenk techniques. Solvents were dried (Et_2O, *n*-pentane, and benzene with Na benzophenone; $CHCl_3$, $CDCl_3$, and CH_2Cl_2 with CaH_2; acetone with molecular sieves, 3 Å) and distilled prior to use. NMR spectra were recorded with Varian Gemini 200, VXR 400, and Unity 500 NMR spectrometers. ^1H and ^{13}C chemical shifts are relative to solvent signals. ^{195}Pt NMR spectra were calibrated with external $H_2[PtCl_6]$ (δ_{Pt} = 0.0 ppm). Coupling constants ($J_{H,H}$) from higher-order multiplets ("m") were obtained by use of the PERCH NMR software package.[37] Microanalyses were performed by the University of Halle microanalytical laboratory with a CHNS-932 (LECO) elemental analyzer. Bis(*tert*-butyl)-acetylene was synthesized according to published methods[38] and $K[PtCl_3(MeHC{=}CHMe)]$ as described in ref.[15] but with use of *cis*-but-2-ene instead of ethene. All other chemicals were commercially available.

Synthesis of $[\{PtCl_2(RHC{=}CHR)\}_2]$ (R/R = H/H, 1; R/R = Me/Me, 2): An aqueous HCl solution (1.1 M, 25 mL) of $K_2[PtCl_4]$ (2.10 g, 5.06 mmol) and $SnCl_2$ (22.8 mg, 0.10 mmol) was purged with the requisite olefin at –30 °C, stirred for 1–2 h, and allowed to warm to room temperature. The purging was repeated three or four times over 6–7 d until an orange-colored solution had formed and the precipitation of a yellow solid was observed. The solvent was removed by evaporation, and the yellow solid residue was dried with $MgCl_2$ in vacuo. The resulting residue was extracted with a mixture of EtOH (30 mL) and HCl (12 M, 4 mL), the non-dissolved KCl was filtered off, and the filtrate was concentrated to dryness. The resulting residue was extracted with dry chloroform (50 mL), and after filtration of some yellowish solid $K[PtCl_3(RHC{=}CHR)]$/KCl the solution was taken to dryness under vacuum. The residue was dissolved in CH_2Cl_2 (40 mL). The solution was reduced to half of its volume, and the same volume of diethyl ether was added, resulting in precipitation of the complex. This was filtered off, washed with diethyl ether (2 × 2 mL), and dried in vacuo.

Compound 1 (R/R = H/H): Yield: 1.11 g, 68%. ^1H NMR (200 MHz, 300 K, CD_2Cl_2): δ = 4.82 (s, d, $^2J_{Pt,H}$ = 74 Hz, 8 H, =C*H*$_2$) ppm. ^{13}C NMR (50.29 MHz, 300 K, CD_2Cl_2): δ = 72.1 (s, d, $^1J_{Pt,C}$ = 199 Hz, =*C*H$_2$) ppm. ^{195}Pt NMR (107 MHz, 300 K, $CDCl_3$): δ = –2490 (s), –2495 (s) ppm. $C_4H_8Cl_4Pt_2$ (588.08): calcd. C 8.17, H 1.37; found C 8.08, H 1.40.

Compound 2 (R/R = Me/Me): Yield: 1.22 g, 75%. ^1H NMR (200 MHz, 300 K, CD_2Cl_2): δ = 1.55 (m, dm, $^3J_{Pt,H}$ = 38 Hz, 12 H, C*H*$_3$), 5.55 (m, dm, $^2J_{Pt,H}$ = 71 Hz, 2 H, =C*H*) ppm. ^{13}C NMR (50.29 MHz, 300 K, CD_2Cl_2): δ = 15.5 (s, d, $^2J_{Pt,C}$ = 24 Hz, *C*H$_3$), 86.9 (s, d, $^1J_{Pt,C}$ = 190 Hz, =*C*HMe), 87.4 (s, d, $^1J_{Pt,C}$ = 182 Hz, =*C*HMe) ppm. ^{195}Pt NMR (107 MHz, 300 K, $CDCl_3$): δ = –2426 (s), –2405 (s) ppm. $C_8H_{16}Cl_4Pt_2$ (644.19): calcd. C 14.91, H 2.50; found C 15.00, H 2.62.

Synthesis of $[\{PtCl_2(c\text{-}Hex)_2\}]$ (3): Cyclohexene (2.05 g, 25.2 mmol) was added to a solution of $K[PtCl_3(MeHC{=}CHMe)]$ (500 mg, 1.26 mmol) in EtOH (15 mL)/HCl (12 M, 2 mL). After the mixture had been stirred at room temperature for 24 h, the solvent was removed in vacuo. The resulting residue was extracted with dry chloroform (50 mL), and the non-dissolved KCl was filtered off. The filtrate was then concentrated to dryness, and the residue was redissolved in CH_2Cl_2 (40 mL). The solution was reduced to half of its volume, and the same volume of diethyl ether was added, resulting in precipitation of **3**, which was filtered off, washed with diethyl ether (2 × 2 mL), and dried in vacuo. Yield: 263 mg, 60%. ^1H NMR (200 MHz, 300 K, $CDCl_3$): δ = 1.41–1.50 (m, 4 H, =CHCH$_2$CH*H*), 1.62–1.72 (m, 4 H, =CHCH$_2$CH*H*), 1.98–2.07 (m, 4 H, =CHCH*H*), 2.22–2.32 (m, 4 H, =CHC*H*H), 5.96 (m, dm, $^2J_{Pt,H}$ = 81 Hz, 4 H, =C*H*) ppm. ^{13}C NMR (50.29 MHz, 300 K, $CDCl_3$): δ = 20.9 (s, *C*H$_2$), 27.2 (s, =CH*C*H$_2$), 90.9 (s, =*C*HCH$_2$), 91.5 (s, d, $^1J_{Pt,C}$ = 196 Hz, =*C*HCH$_2$) ppm. ^{195}Pt NMR (107 MHz, 300 K, $CDCl_3$): δ = –2298 (s), –2374 (s) ppm. $C_{12}H_{20}Cl_4Pt_2$ (696.26): calcd. C 20.7, H 2.89; found C 19.90, H 2.93.

Synthesis of $[PtCl_2(C_4R_2R'_2)]$ (R/R′ = Me/Me, 4; R/R′ = Et/Et, 5; R/R′ = Me/*n*Pr, 6) and $[\{PtCl_2(C_4Me_2Ph_2)_2\}]$ (7): The requisite alkyne (0.51 mmol) was added at room temperature to a suspension of $[\{PtCl_2(H_2C{=}CH_2)\}_2]$ (**1**, 50 mg, 0.085 mmol) in $CHCl_3$ (5 mL). After the orange-colored solution had been stirred at room temperature for 5 d, its volume was reduced to about 2 mL. Layering with diethyl ether (2 mL) resulted in precipitation of the complex,

EurJIC European Journal of Inorganic Chemistry

which was filtered off, washed with diethyl ether (2 × 2 mL), and dried in vacuo.

R/R′ = Me/Me (4): Yield 52 mg, 81%. ^{1}H NMR (200 MHz, 300 K, CD_2Cl_2): δ = 1.61 (s, d, $^3J_{Pt,H}$ = 18.7 Hz, 12 H, CH_3) ppm. ^{13}C NMR (50.29 MHz, 300 K, $CDCl_3$): δ = 8.8 (s, d, $^2J_{Pt,C}$ = 15 Hz, *C*H$_3$), 104.1 (s, d, $^1J_{Pt,C}$ = 145 Hz, *C*$_4$) ppm. ^{195}Pt NMR (107 MHz, 300 K, $CDCl_3$): δ = –3168 (s) ppm. $C_8H_{12}Cl_2Pt$ (374.17): calcd. C 25.68, H 3.23, Cl 18.95; found C 25.56, H 3.52, Cl 19.02.

R/R′ = Et/Et (5): Yield 56 mg, 76%. ^{1}H NMR (200 MHz, 300 K, CD_2Cl_2): δ = 1.28 (t, $^3J_{H,H}$ = 7.47 Hz, 12 H, CH$_2$CH_3), 2.01 (q, $^3J_{H,H}$ = 7.47 Hz, 8 H, CH_2CH$_3$) ppm. ^{13}C NMR (50.29 MHz, 300 K, $CDCl_3$): δ = 10.9 (s, d, $^3J_{Pt,C}$ = 14.9 Hz, CH$_2$*C*H$_3$), 18.1 (s, d, $^2J_{Pt,C}$ = 12.6 Hz, *C*H$_2$CH$_3$), 106.3 (s, d, $^1J_{Pt,C}$ = 150 Hz, *C*$_4$) ppm. ^{195}Pt NMR (107 MHz, 300 K, $CDCl_3$): δ = –3265 (s) ppm. $C_{12}H_{20}Cl_2Pt$ (430.27): calcd. C 33.49, H 4.68, Cl 16.48; found C 33.00, H 4.84, Cl 16.43.

R/R′ = Me/*n*Pr (6): Yield 51 mg, 73%. ^{1}H NMR (200 MHz, 300 K, CD_2Cl_2): δ = 0.98 (t, $^3J_{H,H}$ = 7.32 Hz, 6 H, CH$_2$CH_3), 0.99 (t, $^3J_{H,H}$ = 7.32 Hz, 6 H, CH$_2$CH_3), 1.62 (s, 6 H, CH_3), 1.63 (s, 6 H, CH_3), 1.66 (m, 8 H, CH_2CH$_3$), 1.90 (m, 8 H, CH_2CH$_2$) ppm. ^{13}C NMR (50.29 MHz, 300 K, $CDCl_3$): δ = 9.26 (s, d, $^3J_{Pt,C}$ = 12.8 Hz, *C*H$_3$), 9.38 (s, d, $^3J_{Pt,C}$ = 14.4 Hz, *C*H$_3$), 14.41 (s, *C*H$_3$), 14.49 (s, *C*H$_3$), 19.48 (s, d, $^3J_{Pt,C}$ = 16.0 Hz, *C*H$_2$), 19.78 (s, d, $^3J_{Pt,C}$ = 15.3 Hz, *C*H$_2$), 25.86 (s, d, $^2J_{Pt,C}$ = 11.6 Hz, *C*H$_2$), 26.18 (s, d, $^2J_{Pt,C}$ = 11.6 Hz, *C*H$_2$), 99.2 (s, *C*$_4$), 102.8 (s, d, $^1J_{Pt,C}$ = 148 Hz, *C*$_4$), 103.3 (s, d, $^1J_{Pt,C}$ = 159 Hz, *C*$_4$), 106.9 (s, d, $^1J_{Pt,C}$ = 158 Hz, *C*$_4$) ppm. ^{195}Pt NMR (107 MHz, 300 K, $CDCl_3$): δ = –3180 (s), –3186 (s) ppm. $C_{12}H_{20}Cl_2Pt$ (430.27): calcd. C 33.49, H 4.68, Cl 16.48; found C 33.13, H 4.89, Cl 16.45.

R/R′ = Me/Ph (7): Yield 51 mg, 60%. ^{1}H NMR (200 MHz, 300 K, CD_2Cl_2): δ = 1.90 (s, d, $^3J_{Pt,H}$ = 20 Hz, 12 H, CH_3), 7.30–7.49 (m, 12 H, *m*-H/*p*-H), 7.53–7.77 (m, 8 H, *o*-*H*) ppm. ^{13}C NMR (50.29 MHz, 300 K, $CDCl_3$): δ = 3.1 (s, d, $^2J_{Pt,C}$ = 16 Hz, *C*H$_3$), 101.5 (s, d, $^1J_{Pt,C}$ = 150 Hz, *C*$_4$), 110.0 (s, d, $^1J_{Pt,C}$ = 156 Hz, *C*$_4$), 131.9 (s, d, $^2J_{Pt,C}$ = 21 Hz, *i*-*C*), 135.9 (s, *m*-*C*), 136.8 (s, d, $^3J_{Pt,C}$ = 21 Hz, *o*-*C*), 138.7 (s, *p*-*C*) ppm. ^{195}Pt NMR (107 MHz, 300 K, $CDCl_3$): δ = –1672 (s) ppm.

Reaction between [{PtCl$_2$(H$_2$C=CH$_2$)}$_2$] (1) and RC≡C*t*Bu (R = Me, *t*Bu): A solution of the requisite alkyne (0.36 mmol) in CD_2Cl_2 (0.7 mL) was added at –80 °C to [{PtCl$_2$(H$_2$C=CH$_2$)}$_2$] (**1**, 97 mg, 0.165 mmol) and benzene (5 µL) as standard in an NMR tube. The NMR tube was then sealed by melting and allowed to warm to room temperature. The courses of the reactions were monitored for up to several months by means of ^{1}H and ^{13}C NMR spectroscopic measurements showing the formation of [PtCl$_2$(H$_2$C=CH$_2$)-(RC≡C*t*Bu)] (R = Me, **8**; *t*Bu, **9**) as the main products and of [PtCl$_2$(H$_2$C=CH$_2$)$_2$] (**10**) as well as [{PtCl$_2$(*t*BuC≡C*t*Bu)}$_2$] (**12**) and [PtCl$_2$(C$_4$Me$_2$*t*Bu$_2$)] (**16**), respectively, as sideproducts.

Reaction with MeC≡C*t*Bu: ^{1}H NMR (200 MHz, 300 K, CD_2Cl_2): δ = 1.39 [s, C(CH_3)$_3$, 18 H, **16**], 1.47 [s, 9 H, C(CH_3)$_3$, **8**], 1.77 (s, d, $^3J_{Pt,H}$ = 21 Hz, 6 H, CH_3, **16**), 2.26 (s, d, $^3J_{Pt,H}$ = 31 Hz, 3 H, CH_3, **8**), 4.47–4.56 (m, dm, $^2J_{Pt,H}$ = 60 Hz, 4 H, =CH_2, **8**), 4.70 (s, d, $^2J_{Pt,H}$ = 56 Hz, 8 H, =CH_2, **10**) ppm. ^{13}C NMR (50.3 MHz, 300 K, $CDCl_3$): δ = 8.5 (s, d, $^3J_{Pt,C}$ = 24 Hz, ≡CCH_3, **8**), 11.0 (s, *C*H$_3$, **16**), 28.2 [s C(*C*H$_3$)$_3$, **16**], 30.6 [s, d, $^2J_{Pt,C}$ = 28 Hz, *C*(CH$_3$)$_3$, **8**], 31.1 [s, d, $^3J_{Pt,C}$ = 17 Hz, C(*C*H$_3$)$_3$, **8**], 74.9 (s, d, $^1J_{Pt,C}$ = 115 Hz, ≡*C*, **8**), 80.2 (s, d, $^1J_{Pt,C}$ = 141 Hz, =*C*H$_2$, **8**), 84.3 (s, d, $^1J_{Pt,C}$ = 131 Hz, =*C*H$_2$, **10**), 84.8 (s, d, $^1J_{Pt,C}$ = 156 Hz, ≡*C*), 98.7 (s, d, $^1J_{Pt,C}$ = 132 Hz, =*C*t*Bu, **16**), 107.8 (s, d, $^1J_{Pt,C}$ = 153 Hz, =*C*Me, **16**) ppm. ^{195}Pt NMR (86.0 MHz, 300 K, CD_2Cl_2): δ = –3145 (s, **8**), –3642 (s, **10**) ppm.

Reaction with *t*BuC≡C*t*Bu: ^{1}H NMR (200 MHz, 300 K, CD_2Cl_2): δ = 1.48 [s, 36 H, C(CH_3)$_3$, **12**], 1.51 [s, 36 H, C(CH_3)$_3$, **12**], 1.47 [s, 9 H, C(CH_3)$_3$, **9**], 4.55 (s, d, $^2J_{Pt,H}$ = 55 Hz, 4 H, =CH_2, **9**), 4.70 (s, d, $^2J_{Pt,H}$ = 56 Hz, 8 H, =CH_2, **10**) ppm. ^{13}C NMR (50.3 MHz, 300 K, $CDCl_3$): δ = 27.9 [s, *C*(CH$_3$)$_3$], 30.4 [s, C(*C*H$_3$)$_3$, **12**], 31.4 [s, C(*C*H$_3$)$_3$, **12**], 31.7 [s, C(*C*H$_3$)$_3$, **9**], 80.4 (s, d, $^1J_{Pt,C}$ = 138 Hz, =*C*H$_2$, **9**), 80.7 (s, d, $^1J_{Pt,C}$ = 221 Hz, =*C*, **12**), 80.6 (s, d, $^1J_{Pt,C}$ = 231 Hz, ≡*C*, **12**), 84.3 (s, **10**, =*C*H$_2$), 85.9 (s, d, $^1J_{Pt,C}$ = 151 Hz, ≡*C*, **9**) ppm. ^{195}Pt NMR (86.0 MHz, 300 K, CD_2Cl_2): δ = –1958 (s, **12**), –1995 (s, **12**), –3143 (s, **9**) ppm.

Synthesis of [{PtCl$_2$(RC≡C*t*Bu)}$_2$] (R = Me, 11; R = *t*Bu, 12): The requisite alkyne (0.76 mmol) was added at room temperature to a suspension of [{PtCl$_2$(H$_2$C=CH$_2$)}$_2$] (**1**, 186 mg, 0.316 mmol) in $CHCl_3$ (3 mL), resulting in a deep red solution. After having been stirred at room temperature for 24 h, the solution was reduced to 1 mL and layered with diethyl ether (1 mL)/*n*-pentane (2–3 mL), resulting in precipitation of the requisite complex, which was filtered off, washed with small amounts of *n*-pentane, and dried in vacuo.

R/R′ = Me/*t*Bu (11): Yield 206 mg, 90%. ^{1}H NMR (200 MHz, 300 K, CD_2Cl_2): δ = 1.61 [s, 18 H, C(CH_3)$_3$], 2.26 (s, d, $^3J_{Pt,H}$ = 32 Hz, 6 H, CH_3) ppm. ^{13}C NMR (50.29 MHz, 300 K, $CDCl_3$): δ = 7.9 (s, d, $^2J_{Pt,C}$ = 22 Hz, *C*H$_3$), 26.9 [s, *C*(CH$_3$)$_3$], 30.0 [s, C(*C*H$_3$)$_3$], 69.4 (s, ≡*C*), 69.7 (s, ≡*C*), 70.0 (s, d, $^1J_{Pt,C}$ = 190 Hz, ≡*C*), 79.4 (s, ≡*C*), 79.5 (s, d, $^1J_{Pt,C}$ = 228 Hz, ≡*C*), 79.7 (s, d, $^1J_{Pt,C}$ = 224 Hz, ≡*C*) ppm. ^{195}Pt NMR (107 MHz, 300 K, CD_2Cl_2): δ = –1971 (s), –1960 (s), –1955 (s) ppm. $C_{14}H_{24}Cl_4Pt_2$ (724.31): calcd. C 23.21, H 3.34; found C 23.63, H 3.58.

R/R′ = *t*Bu/*t*Bu (12): Yield 242 mg, 95%. ^{1}H NMR (200 MHz, 300 K, CD_2Cl_2): δ = 1.48 [s, 36 H, C(CH_3)$_3$], 1.51 [s, 36 H, C(CH_3)$_3$] ppm. ^{13}C NMR (50.29 MHz, 300 K, $CDCl_3$): δ = 29.8 [s, *C*(CH$_3$)$_3$], 29.9 [s, d, $^2J_{Pt,C}$ = 21 Hz, *C*(CH$_3$)$_3$], 30.3 [s, d, $^3J_{Pt,C}$ = 21 Hz, C(*C*H$_3$)$_3$], 30.4 [s, C(*C*H$_3$)$_3$], 81.1 (s, d, $^1J_{Pt,C}$ = 230.8 Hz, ≡*C*), 81.2 (s, ≡*C*) ppm. ^{195}Pt NMR (107 MHz, 300 K, $CDCl_3$): δ = –1968 (s), –2005 (s) ppm. $C_{20}H_{36}Cl_4Pt_2$ (808.47): calcd. C 29.71, H 4.49; found C 29.76, H 4.81.

Reaction between [{PtCl$_2$(H$_2$C=CH$_2$)}$_2$] (1) and But-2-yne in CDCl$_3$: [{PtCl$_2$(H$_2$C=CH$_2$)}$_2$] (**1**, 18 mg, 0.03 mmol) was placed in an NMR tube and dissolved in $CDCl_3$ (0.7 mL), and but-2-yne (6 mg, 0.12 mmol) was added. The course of the reaction was monitored for up to several days by ^{1}H and ^{13}C NMR spectroscopic measurements and showed the formation of [PtCl$_2$(C$_4$Me$_4$)] (**4**) as main product, and hexamethylbenzene and [PtCl$_2$(H$_2$C=CH$_2$)$_2$] (**10**) as sideproducts. ^{1}H NMR (200 MHz, 300 K, $CDCl_3$): δ = 1.63 (s, d, $^3J_{Pt,H}$ = 20 Hz, 12 H, CH_3, **4**), 2.22 [s, 18 H, C$_6$(CH_3)$_6$], 4.70 (s, d, $^2J_{Pt,H}$ = 56.0 Hz, 8 H, **10**), 5.07 (br., =CH_2) ppm. ^{13}C NMR (50.3 MHz, 300 K, $CDCl_3$, after two weeks): δ = 8.9 (s, *C*H$_3$, **4**), 16.2 [s, C$_6$(*C*H$_3$)$_6$], 84.3 (s, =*C*H$_2$, **10**), 104.1 (s, *C*$_4$, **4**) ppm.

Reaction between [{PtCl$_2$(H$_2$C=CH$_2$)}$_2$] (1) and Acetone: [{PtCl$_2$(H$_2$C=CH$_2$)}$_2$] (**1**, 18 mg, 0.03 mmol) was placed in an NMR tube and dissolved in [D$_6$]acetone (0.7 mL). The course of the reaction was monitored for up to several days by ^{13}C and ^{195}Pt NMR spectroscopic measurements and showed the formation of [PtCl$_2$(Me$_2$CO)(H$_2$C=CH$_2$)] (**18**) as main product and of 4-hydroxy-4-methylpentan-2-one, 4-methylpent-3-en-2-one, and higher condensation products of acetone containing Me–(MeC=CH)$_n$–C(O)Me (n = 5–7) units, as side products, as well as an unidentified platinum complex. ^{13}C NMR [50.3 MHz, 300 K, (CD$_3$)$_2$CO]: δ = 20.6 (s, =CCH_3), 27.6 (s, =CCH_3), 29.3 [s, =C(*C*H$_3$)$_2$OH], 31.6 (s, H$_3$*C*CO), 31.8 (s, H$_3$*C*CO), 54.6 (s, *C*H$_2$), 69.3 (s, *C*Me$_2$OH), 89.0 (br., =*C*H$_2$, **18**), 124.8 (s, =*C*HCO), 154.3 (s, =*C*Me$_2$), 198.3 (s, =CH*C*O), 210.0 (s, CH$_2$*C*O) ppm. ^{195}Pt NMR [86 MHz, 300 K,

$(CD_3)_2CO$]: δ = –2245 (s), –2719 (s, **18**) ppm. The δ_{Pt} value of complex **18** is in the range (δ_{Pt}: –2696/–2892 ppm) of other *trans*-[$PtCl_2L(COE)$] (L = MeOH, MeCN) complexes,[4] thus showing the constitution of **18**.

Me–(MeC=CH)$_5$–C(O)Me: HRMS (ESI): calcd. for $[C_{18}H_2D_{25}O]^+$ 284.36256 $[M]^+$; found 284.36269.

Me–(MeC=CH)$_6$–C(O)Me: HRMS (ESI): calcd. for $[C_{21}D_{31}O]^+$ 330.43152 $[M]^+$; found 330.43131.

Me–(MeC=CH)$_7$–C(O)Me: HRMS (ESI): calcd. for $[C_{24}D_{35}O]^+$ 374.48793 $[M]^+$; found 374.48747.

Me–(MeC=CH)$_6$–C(OH)MeCH$_2$C(O)Me: HRMS (ESI): calcd. for $[C_{24}H_2D_{35}O_2]^+$ 392.49849 $[M]^+$; found 392.49779.

Me–(MeC=CH)$_7$–C(OH)MeCH$_2$C(O)Me: HRMS (ESI): calcd. for $[C_{27}H_2D_{39}O_2]^+$ 436.55490 $[M]^+$; found 436.55428.

Reaction between [{PtCl$_2$(H$_2$C=CH$_2$)}$_2$] (1) and But-2-yne in Acetone: [{$PtCl_2(H_2C=CH_2)$}$_2$] (**1**, 18 mg, 0.03 mmol) was placed in an NMR tube and dissolved in [D_6]acetone (0.7 mL), and but-2-yne (83 mg, 1.54 mmol) was added. The course of the reaction was monitored for up to several days by ^{13}C and ^{195}Pt NMR spectroscopic measurements and showed the formation of [$PtCl_2(Me_2CO)(H_2C=CH_2)$] (**18**) as main product and of 4-hydroxy-4-methylpentan-2-one, 4-methylpent-3-en-2-one, higher condensation products of acetone, [$PtCl_2(C_4Me_4)$] (**4**), and [$PtCl_2(H_2C=CH_2)_2$] (**10**) as sideproducts, as well as an unidentified platinum complex. ^{13}C NMR [50.3 MHz, 300 K, $(CD_3)_2CO$]: δ = 8.8 (s, d, $^2J_{Pt,C}$ = 15 Hz, CH_3, **4**), 20.6 (s, =CCH_3), 27.6 (s, =CCH_3), 29.3 [s, =C(CH_3)$_2$OH], 31.6 (s, H_3CCO), 31.8 (s, H_3CCO), 54.6 (s, CH_2), 69.3 (s, CMe_2OH), 84.3 (s, d, $^1J_{Pt,C}$ = 131 Hz, =CH_2, **10**), 89.0 (br., =CH_2, **18**), 104.1 (s, d, $^1J_{Pt,C}$ = 145 Hz, C_4, **4**), 124.8 (s, =CHCO), 154.3 (s, =CMe_2), 198.3 (s, =CHCO), 210.0 (s, CH_2CO) ppm. ^{195}Pt NMR [86 MHz, 300 K, $(CD_3)_2CO$]: δ = –2244.9 (s), –2719 (s, **18**), –3648 (s, **10**), –3168 (s, **4**) ppm.

X-ray Structure Determinations: Crystals suitable for X-ray diffraction analyses were grown at room temperature from solutions of complexes **2**, **11a**, **12a**, and **12b** in $CHCl_3$ by slow addition of either diethyl ether (**2**) or diethyl ether/*n*-pentane (**11a**, **12a** and **12b**). Intensity data were collected with a STOE IPDS diffractometer at 203(2) K (**2**), 200(2) K (**11a**, **12a**), or 173(2) K (**12b**) with Mo-K_α radiation (λ = 0.71073 Å, graphite monochromator). Crystallographic data and data collection parameters are given in S4 in the Supporting Information. Absorption corrections were applied empirically with the PLATON program package[39] (0.02/0.09, **11a**), numerically (T_{min}/T_{max}0.12/0.69, **12a**) and by integration[40] (T_{min}/T_{max} 0.19/0.39, **2**; T_{min}/T_{max} 0.10/0.56, **12b**). The structures were solved by direct methods with SHELXS-97 and refined by full-matrix, least-squares routines against F^2 with SHELXL-97.[41] Non-hydrogen atoms were refined with anisotropic displacement parameters and hydrogen atoms with isotropic displacement parameters. Hydrogen atoms were added to their calculated positions and refined according to the riding model.

Computational Details: DFT calculations were carried out with the aid of the Gaussian 03 program package[42] and use of the B3LYP hybrid functional. The 6-311G(d,p) basis sets[43] as implemented in Gaussian 03 were employed for C, H, and Cl atoms, whereas the relativistic pseudopotential of the Ahlrichs group and related basis functions of TZVPP quality were employed for Pt atoms.[44] The appropriateness of the functional in combination with the basis sets and effective core potential used for reliable interpretation of structural and energetic aspects of related platinum complexes has been demonstrated.[45] All systems were fully optimized without any symmetry restrictions. The resulting geometries were characterized as equilibrium and transition-state structures, respectively, by analysis of the force constants of normal vibrations. Solvent effects were considered according to the polarized continuum model.[46]

Supporting Information (see footnote on the first page of this article): NMR spectroscopic data of **8** obtained by spectra simulation, comparison of structural parameters of Zeise's dimer type complexes, crystallographic data for **2**, **11**, **12a** and **12b**, powder diffraction data of **2**, **11** and **12**, a detailed route according to Scheme 6 including calculated values for the gas phase, and Cartesian coordinates and energies of the calculated molecules are presented.

Acknowledgment

We are thankful to Dr. J. Schmidt (Leibniz Institute of Plant Biochemistry, Halle) for the HRMS ESI measurements.

[1] a) W. C. Zeise, *Overs. K. Dan. Vidensk. Selsk. Forh.* **1825–1826**, 13; b) D. Seyferth, *Organometallics* **2001**, *20*, 2.
[2] W. C. Zeise, *Ann. Phys. Chem.* **1831**, *21*, 497.
[3] J. S. Anderson, *J. Chem. Soc.* **1934**, 971.
[4] S. Otto, A. Roodt, L. I. Elding, *Dalton Trans.* **2003**, 2519.
[5] J. Bordner, D. W. Wertz, *Inorg. Chem.* **1974**, *13*, 1639.
[6] S. Otto, L. I. Elding, *J. Chem. Soc., Dalton Trans.* **2002**, 2354.
[7] J. Chatt, R. G. Guy, L. A. Duncanson, *J. Chem. Soc.* **1961**, 827.
[8] J. Chatt, R. G. Guy, L. A. Duncanson, D. T. Thompson, *J. Chem. Soc.* **1963**, 5170.
[9] a) A. L. Beauchamp, F. D. Rochon, T. Theophanides, *Can. J. Chem.* **1973**, *51*, 126; b) R. J. Dubey, *Acta Crystallogr., Sect. B* **1976**, *32*, 199; c) R. Spagna, L. Zambonelli, *Acta Crystallogr., Sect. B* **1973**, *29*, 2302.
[10] A. König, M. Bette, C. Wagner, R. Lindner, D. Steinborn, *Organometallics* **2011**, *30*, 5919.
[11] a) D. Steinborn, M. Tschoerner, A. v. Zweidorf, J. Sieler, H. Bögel, *Inorg. Chim. Acta* **1995**, *234*, 47; b) M. Gerisch, F. W. Heinemann, H. Bögel, D. Steinborn, *J. Organomet. Chem.* **1997**, *548*, 247.
[12] a) D. Steinborn, M. Gerisch, F. W. Heinemann, J. Scholz, *Z. Anorg. Allg. Chem.* **1995**, *621*, 1421; b) M. Gerisch, D. Steinborn, *Z. Anorg. Allg. Chem.* **1995**, *621*, 1426; c) D. Steinborn, R. Nünthel, J. Sieler, R. Kempe, *Chem. Ber.* **1993**, *126*, 2393.
[13] a) F. Canziani, P. Chini, A. Quarta, A. Di Martino, *J. Organomet. Chem.* **1971**, *26*, 285; b) F. Canziani, F. Galimberti, L. Garlaschelli, M. C. Malatesta, A. Albinati, *Gazz. Chim. Ital.* **1982**, *112*, 323; c) F. Canziani, C. Allevi, L. Garlaschelli, M. C. Malatesta, A. Albinati, F. Ganazzoli, *J. Chem. Soc., Dalton Trans.* **1984**, 2637; d) J. Moreto, P. M. Maitlis, *J. Chem. Soc., Dalton Trans.* **1980**, 1368.
[14] J. Chatt, M. L. Searle, *Inorg. Synth.* **1957**, *5*, 210.
[15] P. B. Chock, J. Halpern, F. E. Paulik, *Inorg. Synth.* **1973**, *14*, 90.
[16] D. Steinborn, V. V. Potechin, M. Gerisch, C. Bruhn, H. Schmidt, *Transition Met. Chem.* **1999**, *24*, 67.
[17] S. Schwieger, C. Wagner, C. Bruhn, H. Schmidt, D. Steinborn, *Z. Anorg. Allg. Chem.* **2005**, *631*, 2696.
[18] A. Singh, P. R. Sharp, *Organometallics* **2006**, *25*, 678.
[19] S. Otto, A. Roodt, L. I. Elding, *Inorg. Chem. Commun.* **2006**, *9*, 764.
[20] Landolt–Börnstein, *Numerical Data and Functional Relationships in Science and Technology*, Springer, Berlin, **1976**, vol. 7.
[21] T. G. Hewitt, J. J. De Boer, *J. Chem. Soc. A* **1971**, 817.
[22] N. M. Boag, M. S. Ravetz, *Acta Crystallogr., Sect. E* **2007**, *63*, m3103.
[23] N. M. Boag, M. Green, D. M. Grove, J. A. K. Howard, J. L. Spencer, F. G. A. Stone, *J. Chem. Soc., Dalton Trans.* **1980**, 2170.

[24] R. Boese, D. Bläser, R. Latz, A. Bäumen, *Acta Crystallogr., Sect. C: Cryst. Struct. Commun.* **1999**, *55*, IUC9900016.
[25] F. D. Rochon, R. Melanson, M. Doyon, *Can. J. Chem.* **1989**, *67*, 2209.
[26] G. R. Davies, W. Hewertson, R. H. B. Mais, P. G. Owston, C. G. Patel, *J. Chem. Soc. A* **1970**, 1873.
[27] T. D. W. Claridge, *High-Resolution NMR Techniques in Organic Chemistry*, 1st ed., Elsevier, Oxford, **1999**, vol. 19.
[28] a) J. Clayden, N. Greeves, S. Warren, P. Wothers, *Organic Chemistry*, Oxford University Press, Oxford, **2001**; b) J. I. Di Cosima, C. R. Apesteguía, *J. Mol. Catal. A* **1998**, *130*, 177.
[29] D. M. Roundhill, in *Comprehensive Coordination Chemistry* (Eds.: G. Wilkinson, R. D. Gillard, J. A. McCleverty), Pergamon, Oxford, **1987**, vol. 5, p. 407.
[30] a) D. L. Reger, C. J. Coleman, *Inorg. Chem.* **1979**, *18*, 3270; b) J. J. Kowalczyk, A. M. Arif, J. A. Gladysz, *Organometallics* **1991**, *10*, 1079; c) N. M. Boag, M. Green, D. M. Grove, J. A. K. Howard, J. L. Spencer, F. G. A. Stone, *J. Chem. Soc., Dalton Trans.* **1980**, 2170; d) J. H. Nelson, J. J. R. Reed, H. B. Jonassen, *J. Organomet. Chem.* **1971**, *29*, 163.
[31] a) F. P. Fanizzi, G. Natile, M. Lanfranchi, A. Tiripicchio, G. Pacchioni, *Inorg. Chim. Acta* **1998**, *275–276*, 500; b) F. P. Fanizzi, F. P. Intini, L. Maresca, G. Natile, M. Lanfranchi, A. Tiripicchio, *J. Chem. Soc., Dalton Trans.* **1991**, 1007.
[32] a) R. Cramer, *Inorg. Chem.* **1965**, *4*, 445; b) M. R. Plutino, S. Otto, A. Roodt, L. I. Elding, *Inorg. Chem.* **1999**, *38*, 1233.
[33] S. S. Hupp, G. Dahlgren, *Inorg. Chem.* **1976**, *15*, 2349.
[34] a) D. Steinborn, M. Gerisch, F. W. Heinemann, J. Scholz, *Z. Anorg. Allg. Chem.* **1995**, *621*, 1421; b) M. Gerisch, D. Steinborn, *Z. Anorg. Allg. Chem.* **1995**, *621*, 1426; c) D. Steinborn, R. Nünthel, J. Sieler, R. Kempe, *Chem. Ber.* **1993**, *126*, 2393.
[35] a) F. Canziani, P. Chini, A. Quarta, A. Di Martino, *J. Organomet. Chem.* **1971**, *26*, 285; b) F. Canziani, F. Galimberti, L. Garlaschelli, M. C. Malatesta, A. Albinati, *Gazz. Chim. Ital.* **1982**, *112*, 323; c) F. Canziani, C. Allevi, L. Garlaschelli, M. C. Malatesta, A. Albinati, F. Ganazzoli, *J. Chem. Soc., Dalton Trans.* **1984**, 2637; d) J. Moreto, P. M. Maitlis, *J. Chem. Soc., Dalton Trans.* **1980**, 1368.
[36] Y. Marcus, *J. Solution Chem.* **1984**, *13*, 599.
[37] *PERCH NMR Software*, Version 1/2000, University of Kuopio, Finland, **2000**.
[38] G. Capozzi, G. Romeo, F. Marcuzzi, *J. Chem. Soc., Chem. Commun.* **1982**, 959.
[39] a) *MULscanABS*, PLATON for Windows v. 1.15, University of Glasgow, **2008**; b) A. L. Spek, *J. Appl. Crystallogr.* **2003**, *36*, 7.
[40] *X-RED: Program for Numerical Absorption Correction*, V. 1.06, Stoe & Cie GmbH, Darmstadt, **2004**.
[41] a) G. M. Sheldrick, *SHELXS-97 Program for Crystal Structures Solutions*, University of Göttingen, Göttingen, Germany, **1998**; b) G. M. Sheldrick, *SHELXL-97 Program for the Refinement of Crystal Structures*, University of Göttingen, Göttingen, Germany, **1997**.
[42] M. J. Frisch, G. W. Trucks, H. B. Schlegel, G. E. Scuseria, M. A. Robb, J. R. Cheeseman, V. G. Zakrzewski, J. A. Montgomery Jr., R. E. Stratmann, J. C. Burant, S. Dapprich, J. M. Millam, A. D. Daniels, K. N. Kudin, M. C. Strain, O. Farkas, J. Tomasi, V. Barone, M. Cossi, R. Cammi, B. Mennucci, C. Pomelli, C. Adamo, S. Clifford, J. Ochterski, G. A. Petersson, P. Y. Ayala, Q. Cui, K. Morokuma, D. K. Malick, A. D. Rabuck, K. Raghavachari, J. B. Foresman, J. Cioslowski, J. V. Ortiz, B. B. Stefanov, G. Liu, A. Liashenko, P. Piskorz, I. Komaromi, R. Gomperts, R. L. Martin, D. J. Fox, T. Keith, M. A. Al-Laham, C. Y. Peng, A. Nanayakkara, C. Gonzalez, M. Challacombe, P. M. W. Gill, B. Johnson, W. Chen, M. W. Wong, J. L. Andres, C. Gonzalez, M. Head-Gordon, E. S. Replogle, J. A. Pople, *Gaussian 03*, Revision B.04, Gaussian, Inc., Wallingford, CT, **2004**.
[43] a) M. J. S. Dewar, C. H. Reynolds, *J. Comput. Chem.* **1986**, *7*, 140; b) K. Raghavchari, J. A. Pople, E. S. Replogle, M. Head-Gordon, *J. Phys. Chem.* **1990**, *94*, 5579.
[44] a) F. Weigend, M. Häser, H. Patzelt, R. Ahlrichs, *Chem. Phys. Lett.* **1998**, *294*, 143; b) T. Leininger, A. Nicklass, W. Küchle, H. Stoll, M. Dolg, A. Bergner, *Chem. Phys. Lett.* **1996**, *255*, 274; c) D. Andrae, U. Häussermann, M. Dolg, H. Stoll, H. Preuss, *Theor. Chim. Acta* **1990**, *77*, 123.
[45] a) D. Steinborn, S. Schwieger, *Chem. Eur. J.* **2007**, *13*, 9668; b) M. Werner, T. Lis, C. Bruhn, R. Lindner, D. Steinborn, *Organometallics* **2006**, *25*, 5946; c) C. Vetter, G. N. Kaluderović, R. Paschke, S. Gómez-Ruiz, D. Steinborn, *Polyhedron* **2009**, *28*, 3699; d) S. Schwieger, F. W. Heinemann, C. Wagner, R. Kluge, C. Damm, G. Israel, D. Steinborn, *Organometallics* **2009**, *28*, 2485.
[46] a) B. Mennucci, J. Tomasi, *J. Chem. Phys.* **1997**, *106*, 5151; b) E. Cancès, B. Mennucci, J. Tomasi, *J. Chem. Phys.* **1997**, *107*, 3032; c) M. Cossi, V. Barone, B. Mennucci, J. Tomasi, *Chem. Phys. Lett.* **1998**, *286*, 253.
[47] V. Gutmann, *The Donor-Acceptor Approach to Molecular Interactions*, Plenum Press, New York, **1978**.

Received: July 4, 2012
Published Online: October 17, 2012

nicht publizierte Ergebnisse -

Dinukleare Olefinkomplexe als Präkatalysatoren in Hydroaminierungsreaktionen

Alle Reaktionen wurden unter sorgfältigem Ausschluss von Luftfeuchtigkeit und Sauerstoff durch Verwendung von Argon als Schutzgas mittels Schlenk-Technik ausgeführt. Das als Schutzgas eingesetzte Argon der Qualität 4.6 (Fa. Linde) wurde mittels Molsieb (4A) und Phosphorpentoxid (Scicapent® mit Indikator, Fa. Merck) getrocknet. Toluol wurde über Na/Benzophenon entwässert und frisch destilliert.

Reaktion von Styrol mit Benzamid

Eine Lösung von Benzamid (244 mg, 2.0 mmol), Styrol (208 mg, 2.0 mmol) und [{$PtCl_2$(MeHC=CHMe)}$_2$] (**C2**) (13 mg, 0.02 mmol) in Toluol (1.0 mL) wurde bei 110 °C für 24 h unter Rückfluß erhitzt, auf Raumtemperatur abgekühlt und chromatographiert (SiO_2; Hexan/Essigsäureethylester = 4:1). Nach dem Entfernen der Lösungsmittel im Vakuum wurden die *N*-(Phenyllethyl)benzamide **I** und **II** als Feststoffe isoliert und NMR-spektroskopisch untersucht.

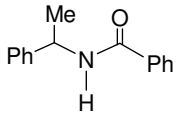

I

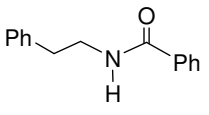

II

^{1}H-NMR (200 MHz, $CDCl_3$): 1.35 (m, 2H, PhCH_2, **II**), 1.56 (d, $^3J_{H,H}$ = 6.8 Hz, 3H, CH_3, **I**), 3.67 (m, 2H, NCH_2, **II**), 5.31 (m, 1H, C*H*, **I**), 6.37 (m, 1H, C*H*, **I**), 7.44–7.40 (m, 10H, C_6H_5, **I**), 7.27–7.47 (m, 2H), 7.51–7.47 (m, 1H), 7.44–7.40 (m, 2H), 7.29 (d, J = 8.0 Hz, 2H).^{13}C-NMR (50 MHz, $CDCl_3$): 21.7 (s, CH_3, **I**), 35.6 (s, CH_2, **II**), 41.1 (s, CH_2, **II**), 49.2 (s, *C*H, **I**), 126.2 (s, **I**) 126.6 (s, **II**) 126.8 (s, **II**), 126.9 (s, **I**), 127.4 (s, **II**), 127.9 (s, **II**), 128.5 (s, **I**), 128.7 (s, **I**), 131.4 (s, **I**), 133.0 (s, **II**), 134.6 (s, **I**).

Reaktion von Styrol mit Pentafluoranilin

Eine Lösung von Pentafluoranilin (366 mg, 2.0 mmol), Styrol (208 mg, 2.0 mmol) und [{$PtCl_2$(MeHC=CHMe)}$_2$] (**C2**) (13 mg, 0.02 mmol) in Toluol (1.0 mL) wurde bei 110 °C für 24 h unter Rückfluß erhitzt, auf Raumtemperatur abgekühlt und chromatographiert (SiO_2; Hexan/Essigsäureethylester = 4:1). Nach dem Entfernen der Lösungsmittel im Vakuum wurde der Rückstand NMR-spektroskopisch untersucht.

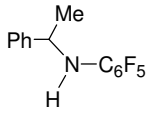

I

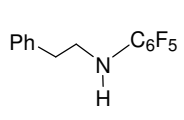

II

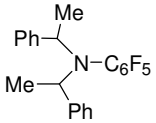

III

^{1}H-NMR (200 MHz, $CDCl_3$): 1.51 (d, $^3J_{H,H}$ = 6.6 Hz, 3H, CH_3, **I**), 1.56 (m, 2H, PhCH_2, **II**), 3.81 (s br, 2H, NCH_2, **II**), 4.77 (m, 1H, C*H*, **I**), 7.44–7.40 (m, 10H, C_6H_5, **I**), 7.20–7.77 (m, 10 H). ^{19}F-NMR

(188.1 MHz, $CDCl_3$) : −146.3 (d, *o*-C–*F*, **II**), −157.8 (d, *o*-C–*F*, **III**), −158.2 (d, *o*-C–*F*, **I**), −164.7 (m, *m*-C–*F*, **I**), −170.8 (t·t, *p*-C–*F*, **I**). ^{13}C-NMR (50 MHz, $CDCl_3$): 24.2 (s, *C*H_3, **I**), 55.3 (s+d, $^4J_{C,F}$ = 8 Hz, *C*H, **I**), 126.2 (s, **I**) 126.6 (s, **II**) 126.8 (s, **II**), 126.9 (s, **I**), 127.4 (s, **II**), 127.9 (s, **II**), 128.5 (s, **I**), 128.7 (s, **I**), 131.4 (s, **I**), 133.0 (s, **II**), 134.6 (s, **I**).

SUPPORTING INFORMATION

On the Equilibrium Between Alkyne and Olefin Platinum(II) Complexes of Zeise's Salt Type: Syntheses and Characterization of $[K(18C6)][PtCl_3(RC{\equiv}CR')]$

Anja König, Martin Bette, Christoph Wagner, Ronald Lindner, and Dirk Steinborn*

Institut für Chemie –Anorganische Chemie, Martin-Luther-Universität, Kurt-Mothes-Strasse 2, D-06120 Halle, Germany

S1. Crytallographic and Structure Refinement Data for 5–7, 9.

	5	**6**	**7**	**9**
Empirical formula	$C_{19}H_{36}Cl_3KO_6Pt$	$C_{22}H_{42}Cl_3KO_6Pt$	$C_{21}H_{28}Cl_3KO_6Pt$	$C_{20}H_{36}Cl_3KO_6Pt$
M_r	701.02	743.10	716.97	713.03
Crystal system	monoclinic	monoclinic	orthorhombic	orthorhombic
Space group	$P2_1/c$	$P2_1/c$	$P2_12_12_1$	$P2_12_12_1$
a/Å	14.32(2)	16.957(2)	9.804(1)	8.257(1)
b/Å	8.68(2)	8.706(1)	9.850(1)	12.165(1)
c/Å	23.30(2)	22.118(1)	28.336(2)	26.975(2)
β	104.5(1)	110.63(1)	-	-
V/Å^3	2805(9)	3055.8(6)	2736.4(3)	2709.6(3)
Z	4	4	4	4
D_{calc}/g·cm^{-1}	1.660	1.615	1.740	1.748
M(Mo Kα)/mm^{-1}	0.71073	0.71073	0.71073	0.71073
T/K	293(1)	293(1)	293(1)	200(2)
μ (mm^{-1})	5.464	5.021	5.604	5.659
F(000)	1384	1480	1400	1408
Θ range/°	1.81–26.04	1.93–25.04	2.19–25.28	2.58–28.00
Refln. collected	5785	7080	10051	27980
Refln. Obs. [$I > 2\sigma$ (I)]	3630	3857	3948	5855
Refln. Independent (R_{int})	5455	5412	4913	6518
Data/restraints/parameters	5455/0/271	5412/0/298	4913/0/291	6518/0/281
Goodness-of-fit on F^2	1.289	1.114	1.068	1.052
R_1 [$I > 2\sigma(I)$]	0.0560	0.0520	0.0384	0.0392
wR_2 (all data)	0.0900	0.1224	0.0834	0.0971
Largest difference peak and hole /e · Å^{-3}	1.011/–1.270	1.443/–1.252	0.590/–0.504	1.549/–0.961
T_{min}/T_{max}	0.16/0.26	0.21/0.42	0.21/0.42	0.28/0.88

S2. Description of Conformations of Crown Ethers in Complexes 5–7, 9

The K^+ ions were found to be located slightly outside the mean plane of the crown ether defined by its six O atoms; the distances of the K atoms and the mean plane of crown ethers are 0.709(2)–0.780(3) Å. The crown ethers itself exhibit a conformation showing D_{3d} symmetry in very rough approximation. The torsion angles (absolute values) are in the ranges of 172(1)–180(1)° for C–C–O–C and 60(1)–68(1)° for O–C–C–O units; the conformation of the macrocycles is characterized by an alternating sequence (*ap*, +*sc*, *ap*) and (*ap*, –*sc*, *ap*) of the O–C–C–O subunits.

S3. Equilibrium Constants of Substitution Reactions

entry	R/R'	*m* mg (*n*/mmol)	ratio[a)]	*K*	*K*[b)]
1	Me/Me	1.24 (0.023)	1/0.65	0.25	0.25
		3.73 (0.069)	1/3.3	0.24	
		7.46 (0.138)	1/5.7	0.25	
2	Et/Et	1.9 (0.023)	1/1.0	0.47	0.47
		5.7 (0.069)	1/2.8	0.48	
3	Me/*t*-Bu	4.4 (0.046)	1/2.3	0.27	0.26
		6.5 (0.068)	1/3.1	0.26	
4	*t*-Bu/ *t*-Bu	3.2 (0.023)	1/1.0	0.020	0.020
		9.5 (0.069)	1/2.5	0.019	
5	Me/Ph	5.3 (0.046)	1/1.8	0.062	0.06
		16.0 (0.138)	1/6.6	0.060	
6	Me/CO_2Me	2.3 (0.023)	1/0.7	0.005	0.006
		6.8 (0.069)	1/3.3	0.006	
7	COC		1/1	–	–

a) Ratio of **2**/RC≡CR' determined by ^{1}H NMR spectroscopically.
b) Averaged equilibrium constants.

S4. Energies and Atom Coordinates of All Calculated Structures

The following section contains potential energy, sum of electronic and zero-point energies, Gibbs free energy (298.15 K), solvation energy (in $CHCl_3$, 298.15 K), and Cartesian coordinates of atom positions of all structures calculated within this work as well as the BSSE for the platinum–alkyne bonds.

cis-but-2-ene (L2')

(file: cis-but-2-ene.log / cis-but-2-ene_PCM.log)

E(RB+HF–LYP)	–157.271121 a.u.
Sum of electronic and zero-point energies	–157.163567 a.u.
Sum of electronic and thermal Gibbs free energies (298.15 K)	–157.190749 a.u.
ΔG_{solv} (PCM, 298.15 K)	3.4 kcal/mol

	x	*y*	*z*
C	0.00000	0.66722	0.66328
H	0.00000	1.16469	1.63122
C	0.00000	–0.66722	0.66328
H	0.00000	–1.16469	1.63122
C	0.00000	1.59027	–0.52163
H	–0.87804	2.24577	–0.50298
H	0.87804	2.24577	–0.50298
H	0.00000	1.06063	–1.47513
C	0.00000	–1.59027	–0.52163
H	0.87804	–2.24577	–0.50298
H	–0.87804	–2.24577	–0.50298
H	0.00000	–1.06063	–1.47513

but-2-yne (L3')

(file: but-2-yne.out / but-2-yne_PCM.log)

E(RB+HF–LYP)	–156.024934 a.u.
Sum of electronic and zero-point energies	–155.941161 a.u.
Sum of electronic and thermal Gibbs free energies (298.15 K)	–155.969948 a.u.
ΔG_{solv}(PCM, 298.15 K)	3.9 kcal/mol

	x	*y*	*z*
C	0.60148	–0.00014	0.00003
C	–0.60148	–0.00014	0.00003
C	2.06017	0.00007	–0.00001

H	2.45633	–0.66522	–0.77311
H	2.45606	1.00233	–0.18969
H	2.45633	–0.33671	0.96273
C	–2.06017	0.00007	–0.00001
H	–2.45633	–0.66519	–0.77314
H	–2.45633	–0.33675	0.96272
H	–2.45606	1.00234	–0.18965

hex-3-yne (L4')

(file: hex-3-yne.out / hex-3-yne_PCM.log)

E(RB+HF–LYP)	–234.673131 a.u.
Sum of electronic and zero-point energies	–234.531652 a.u.
Sum of electronic and thermal Gibbs free energies (298.15 K)	–234.564858 a.u.
ΔG_{solv}(PCM, 298.15 K)	4.5 kcal/mol

	x	*y*	*z*
C	0.00585	0.60228	–0.32716
C	–0.00585	–0.60228	–0.32716
C	–0.00585	2.06467	–0.31705
C	–1.16580	2.65903	0.50167
H	–0.06090	2.43158	–1.34857
H	0.94765	2.42913	0.08245
H	–1.13061	3.75143	0.47845
H	–2.12901	2.33750	0.09958
H	–1.11106	2.33525	1.54331
C	0.00585	–2.06467	–0.31705
C	1.16580	–2.65903	0.50167
H	0.06090	–2.43158	–1.34857
H	–0.94765	–2.42913	0.08245
H	1.13061	–3.75143	0.47845
H	2.12901	–2.33750	0.09958
H	1.11106	–2.33525	1.54331

4,4-dimethylpent-2-yne (L5')

(file: 4,4-Dimethylpent-2-yne.out / 4,4-Dimethylpent-2-yne_PCM.log)

E(RB+HF–LYP)	–273.998081 a.u.
Sum of electronic and zero-point energies	–273.829829 a.u.
Sum of electronic and thermal Gibbs free energies (298.15 K)	–273.864477 a.u.
ΔG_{solv}(PCM, 298.15 K)	6.5 kcal/mol

	x	*y*	*z*
C	0.57852	–0.00002	–0.00007

C	1.78292	–0.00002	–0.00005
C	–0.89395	0.00002	–0.00002
C	–1.40738	–0.92947	–1.12345
C	–1.40722	–0.50824	1.36669
C	–1.40726	1.43773	–0.24316
H	–1.05582	–0.58972	–2.10044
H	–1.05527	–1.95266	–0.97297
H	–2.50165	–0.93935	–1.13484
H	–1.05538	0.13386	2.17754
H	–2.50149	–0.51360	1.38089
H	–1.05526	–1.52406	1.56103
H	–2.50153	1.45273	–0.24561
H	–1.05527	2.11394	0.53940
H	–1.05544	1.81890	–1.20466
C	3.24173	–0.00001	–0.00001
H	3.63763	–0.35829	0.95502
H	3.63768	–0.64794	–0.78778
H	3.63766	1.00621	–0.16722

2,2,5,5-tetramethylhex-3-yne (L6')

(file: 2,2,5,5-tetramethylhex-3-yne.out / 2,2,5,5-tetramethylhex-3-yne_PCM.log)

E(RB+HF–LYP)	–391.971216 a.u.
Sum of electronic and zero-point energies	–391.718579 a.u.
Sum of electronic and thermal Gibbs free energies (298.15 K)	–347.707185 a.u.
ΔG_{solv}(PCM, 298.15 K)	2.5 kcal/mol

	x	*y*	*z*
C	0.77737	–1.47347	–0.07843
C	–0.41808	–1.54756	–0.21171
C	0.54934	1.30582	–0.57654
C	–1.78471	–1.03016	–0.18820
C	–0.92025	1.47693	–0.09689
C	–1.72093	0.32758	0.56289
H	–2.17193	–0.89790	–1.20547
H	0.56008	0.70447	–1.48958
H	–1.48681	1.82884	–0.96821
H	0.86949	2.30756	–0.88334
H	–2.47847	–1.70311	0.32614
H	–0.94469	2.30848	0.61816
H	–2.74403	0.69410	0.71042
H	–1.32043	0.12492	1.56087
C	2.02563	–0.73101	0.08987
H	2.62421	–0.76218	–0.82773
H	2.65489	–1.13271	0.88993

C	1.60840	0.73747	0.40699
H	1.22951	0.77161	1.43337
H	2.50751	1.36238	0.38746

1-phenylprop-1-yne (L7')

(file: 1-phenylprop-1-yne.out / 1-phenylprop-1-yne_PCM.log)

E(RB+HF–LYP)	–347.808799 a.u.
Sum of electronic and zero-point energies	–347.671502 a.u.
Sum of electronic and thermal Gibbs free energies (298.15 K)	–347.707185 a.u.
ΔG_{solv}(PCM, 298.15 K)	1.7 kcal/mol

	x	*y*	*z*
C	–1.39386	0.00066	–0.00012
C	–2.60027	0.00056	–0.00021
C	–4.05678	–0.00029	–0.00006
H	–4.45090	–0.72181	–0.72207
H	–4.45167	–0.26611	0.98548
H	–4.45130	0.98555	–0.26274
C	0.03427	0.00037	0.00000
C	0.75073	–1.20914	0.00005
C	0.75146	1.20944	0.00005
C	2.14084	–1.20561	0.00004
H	0.20456	–2.14474	0.00017
C	2.14156	1.20507	0.00004
H	0.20593	2.14541	0.00017
C	2.84166	–0.00049	0.00001
H	2.67933	–2.14676	0.00009
H	2.68061	2.14589	0.00009
H	3.92572	–0.00081	0.00004

methyl but-2-ynoate (L8')

(file: Methyl but-2-ynoat.log / Methyl but-2-ynoat_PCM.log)

E(RB+HF–LYP)	–312.079357 a.u.
Sum of electronic and zero-point energies	–311.899786 a.u.
Sum of electronic and thermal Gibbs free energies (298.15 K)	–311.931275 a.u.
ΔG_{solv}(PCM, 298.15 K)	1.3 kcal/mol

	x	*y*	*z*
C	0.77737	–1.47347	–0.07843
C	–0.41808	–1.54756	–0.21171
C	0.54934	1.30582	–0.57654
C	–1.78471	–1.03016	–0.18820

C	–0.92025	1.47693	–0.09689
C	–1.72093	0.32758	0.56289
H	–2.17193	–0.89790	–1.20547
H	0.56008	0.70447	–1.48958
H	–1.48681	1.82884	–0.96821
H	0.86949	2.30756	–0.88334
H	–2.47847	–1.70311	0.32614
H	–0.94469	2.30848	0.61816
H	–2.74403	0.69410	0.71042
H	–1.32043	0.12492	1.56087
C	2.02563	–0.73101	0.08987
H	2.62421	–0.76218	–0.82773
H	2.65489	–1.13271	0.88993
C	1.60840	0.73747	0.40699
H	1.22951	0.77161	1.43337
H	2.50751	1.36238	0.38746

cylooctyne (L9')

(file: COC.out / COC_PCM.log)

E(RB+HF–LYP)	–312.079357 a.u.
Sum of electronic and zero-point energies	–311.899786 a.u.
Sum of electronic and thermal Gibbs free energies (298.15 K)	–311.931275 a.u.
ΔG_{solv}(PCM, 298.15 K)	1.3 kcal/mol

	x	*y*	*z*
C	0.77737	–1.47347	–0.07843
C	–0.41808	–1.54756	–0.21171
C	0.54934	1.30582	–0.57654
C	–1.78471	–1.03016	–0.18820
C	–0.92025	1.47693	–0.09689
C	–1.72093	0.32758	0.56289
H	–2.17193	–0.89790	–1.20547
H	0.56008	0.70447	–1.48958
H	–1.48681	1.82884	–0.96821
H	0.86949	2.30756	–0.88334
H	–2.47847	–1.70311	0.32614
H	–0.94469	2.30848	0.61816
H	–2.74403	0.69410	0.71042
H	–1.32043	0.12492	1.56087
C	2.02563	–0.73101	0.08987
H	2.62421	–0.76218	–0.82773
H	2.65489	–1.13271	0.88993
C	1.60840	0.73747	0.40699
H	1.22951	0.77161	1.43337

H	2.50751	1.36238	0.38746

[$PtCl_3$(*cis*-MeHC=CHMe)]$^-$ (2a')

(file: PtCl3(cis-MeHC=CHMe).out / PtCl3(cis-MeHC=CHMe)_PCM.log)

E(RB+HF–LYP)	–1657,588982 a.u.
Sum of electronic and zero-point energies	–1657,475276 a.u.
Sum of electronic and thermal Gibbs free energies (298.15 K)	–1657,514871 a.u.
ΔG_{solv}(PCM, 298.15 K)	–35.3 kcal/mol
BSSE	1.80 kcal/mol

	x	*y*	*z*
C	–1.55199	–1.01459	0.70389
H	–1.12659	–1.89691	1.17347
C	–1.55201	–1.01469	–0.70370
H	–1.12666	–1.89709	–1.17316
C	–2.50372	–0.24755	1.58673
H	–3.37389	–0.88049	1.81203
H	–2.02649	0.00717	2.53624
H	–2.85002	0.67845	1.13256
C	–2.50377	–0.24776	–1.58660
H	–2.02659	0.00677	–2.53618
H	–3.37399	–0.88069	–1.81175
H	–2.84999	0.67833	–1.13257
Pt	0.23867	0.00558	–0.00002
Cl	1.31199	–2.10466	0.00013
Cl	–0.77927	2.14474	–0.00003
Cl	2.33828	1.07147	–0.00015

[$PtCl_3$(MeC≡CMe)]$^-$ (3a')

(file: PtCl3(MeCCMe).out / PtCl3(MeCCMe)_PCM.log)

E(RB+HF–LYP)	–1656.339254 a.u.
Sum of electronic and zero-point energies	–1656.250308 a.u.
Sum of electronic and thermal Gibbs free energies (298.15 K)	–1656.291609 a.u.
ΔG_{solv}(PCM, 298.15 K)	–35.2 kcal/mol
BSSE	1.71 kcal/mol

	x	*y*	*z*
C	–1.85066	0.00006	–0.62128
C	–1.85059	–0.00007	0.62134

C	–2.30418	0.00027	–2.01539
H	–1.92961	–0.88487	–2.53662
H	–3.39893	0.00024	–2.06445
H	–1.92967	0.88562	–2.53632
C	–2.30403	–0.00028	2.01548
H	–1.92949	–0.88563	2.53640
H	–1.92943	0.88486	2.53670
H	–3.39877	–0.00024	2.06460
Pt	0.20037	0.00000	–0.00003
Cl	0.15962	2.36474	0.00010
Cl	0.15963	–2.36474	–0.00025
Cl	2.54803	0.00000	0.00020

$[PtCl_3(EtC{\equiv}CEt)]^-$ (4a')

(file: PtCl3(EtCCEt).log / PtCl3(EtCCEt)_PCM.log)

E(RB+HF–LYP)	–1734.987811 a.u.
Sum of electronic and zero-point energies	–1734.841789 a.u.
Sum of electronic and thermal Gibbs free energies (298.15 K)	–1734.88773 a.u.
ΔG_{solv}(PCM, 298.15 K)	–34.3 kcal/mol
BSSE	1.78 kcal/mol

	x	*y*	*z*
C	–1.48002	0.01007	0.62221
C	–1.48006	–0.00953	–0.62219
Pt	0.56886	–0.00002	–0.00001
Cl	0.52794	–2.36424	0.03352
Cl	0.52868	2.36424	–0.03365
Cl	2.91555	–0.00036	0.00003
C	–1.93918	0.03240	2.01853
C	–3.47112	0.03827	2.14522
H	–1.51531	0.91598	2.50742
H	–1.51965	–0.83805	2.53406
H	–3.76725	0.05515	3.19850
H	–3.89927	0.91684	1.65601
H	–3.90408	–0.85250	1.68305
C	–1.93935	–0.03173	–2.01849
C	–3.47131	–0.03839	–2.14504
H	–1.51510	–0.91498	–2.50764
H	–1.52032	0.83906	–2.53385
H	–3.76751	–0.05517	–3.19831
H	–3.89892	–0.91730	–1.65600
H	–3.90470	0.85204	–1.68262

[$PtCl_3$(MeC≡C*t*-Bu)]$^-$ (5a')

(file: PtCl3(MeCCt-Bu).out / PtCl3(MeCCt-Bu)_PCM.log)

E(RB+HF–LYP)	–1774.311969 a.u.
Sum of electronic and zero-point energies	–1774.138985 a.u.
Sum of electronic and thermal Gibbs free energies (298.15 K)	–1774.185777 a.u.
ΔG_{solv}(PCM, 298.15 K)	–32.0 kcal/mol
BSSE	1.95 kcal/mol

	x	*y*	*z*
C	–1.48720	–0.00012	0.37950
C	–0.93459	–0.00062	1.49573
Pt	0.63756	0.00001	0.05016
Cl	0.63576	2.36457	0.10466
Cl	0.63585	–2.36461	0.10329
C	–2.59765	0.00023	–0.61149
C	–3.92662	–0.00102	0.17839
C	–2.52171	1.26230	–1.49627
C	–2.52062	–1.26025	–1.49844
H	–4.00196	–0.88836	0.81253
H	–4.00267	0.88510	0.81414
H	–4.77446	–0.00073	–0.51487
H	–1.58231	1.29022	–2.04968
H	–3.35459	1.26353	–2.20828
H	–2.56965	2.16980	–0.89109
H	–3.35358	–1.26105	–2.21036
H	–1.58126	–1.28631	–2.05202
H	–2.56761	–2.16883	–0.89482
C	–0.72803	–0.00132	2.94770
H	–0.16156	0.88357	3.25018
H	–1.68905	–0.00132	3.47403
H	–0.16200	–0.88677	3.24936
Cl	2.75011	0.00037	–0.97634

[$PtCl_3$(*t*-Bu≡C*t*-Bu)]$^-$ (6a')

(file: PtCl3(t-BuCCt-Bu).out / PtCl3(t-BuCCt-Bu)_PCM.log)

E(RB+HF–LYP)	–1892.283862 a.u.
Sum of electronic and zero-point energies	–1892.026805 a.u.
Sum of electronic and thermal Gibbs free energies (298.15 K)	–1892,079201 a.u.
ΔG_{solv}(PCM, 298.15 K)	–28.6 kcal/mol
BSSE	2.16 kcal/mol

	x	*y*	*z*
C	–1.24111	0.62414	–0.01166
C	–1.24117	–0.62414	0.01142
Pt	0.81282	–0.00003	–0.00001
Cl	0.80725	0.05809	2.36484
Cl	0.80711	–0.05788	–2.36491
C	–1.78642	2.01150	–0.02747
C	–3.29002	1.92954	–0.37693
C	–1.61405	2.65575	1.36544
C	–1.05973	2.86682	–1.08601
H	–3.43620	1.48563	–1.36484
H	–3.83155	1.32640	0.35631
H	–3.72582	2.93430	–0.38244
H	–0.56313	2.67907	1.65518
H	–2.00425	3.67956	1.34815
H	–2.15147	2.08781	2.12852
H	–1.50253	3.86853	–1.11507
H	0.00101	2.95708	–0.84769
H	–1.13323	2.41333	–2.07598
Cl	3.16190	–0.00019	–0.00004
C	–1.78656	–2.01144	0.02747
C	–1.60866	–2.65844	–1.36344
C	–1.06415	–2.86469	1.09061
C	–3.29157	–1.92877	0.37071
H	–2.14250	–2.09171	–2.12990
H	–0.55654	–2.68286	–1.64870
H	–1.99941	–3.68203	–1.34579
H	–1.14189	–2.40943	2.07945
H	–1.50688	–3.86644	1.11965
H	–0.00240	–2.95515	0.85694
H	–3.72740	–2.93352	0.37645
H	–3.44175	–1.48293	1.35715
H	–3.83010	–1.32708	–0.36590

[$PtCl_3$(MeC≡CPh)]$^-$ (7a')

(file: PtCl3(MeCCPh).out / PtCl3(MeCCPh_PCM).out)

E(RB+HF–LYP)	–1848.122554 a.u.
Sum of electronic and zero-point energies	–1847.980759 a.u.
Sum of electronic and thermal Gibbs free energies (298.15 K)	–1848.028150 a.u.
ΔG_{solv}(PCM, 298.15 K)	–34.8 kcal/mol
BSSE	1.84 kcal/mol

	x	*y*	*z*
C	–1.01904	0.81375	0.14699

C	–0.19923	1.74254	0.32249
C	0.34989	3.07717	0.57486
H	0.97291	3.06533	1.47362
H	0.97409	3.39274	–0.26592
H	–0.45474	3.80760	0.71192
Pt	0.94506	–0.01177	–0.00159
Cl	0.96380	0.48193	–2.31204
Cl	0.90983	–0.43531	2.32235
Cl	2.74708	–1.48602	–0.27190
C	–2.30089	0.17479	0.02769
C	–2.41631	–1.21135	–0.15578
C	–3.47529	0.94718	0.09730
C	–3.66947	–1.80457	–0.26434
H	–1.51219	–1.80425	–0.20911
C	–4.72355	0.34729	–0.01176
H	–3.39527	2.01934	0.23571
C	–4.82767	–1.03233	–0.19323
H	–3.74006	–2.87779	–0.40543
H	–5.61913	0.95776	0.04377
H	–5.80304	–1.49955	–0.27903

$[PtCl_3(MeC{\equiv}CCO_2Me)]^-$ (8a')

(file: PtCl3(MeCCCOOMe).log / PtCl3(MeCCCOOMe_PCM).log)

E(RB+HF–LYP)	–1844.946229 a.u.
Sum of electronic and zero-point energies	–1844.842296 a.u.
Sum of electronic and thermal Gibbs free energies (298.15 K)	–1844.888489 a.u.
ΔG_{solv}(PCM, 298.15 K)	–32.5 kcal/mol
BSSE	2.56 kcal/mol

	x	*y*	*z*
C	–1.34907	0.70107	0.00049
Pt	0.64138	–0.00055	0.00001
Cl	0.63184	0.03789	2.36299
Cl	0.63196	0.04142	–2.36292
Cl	2.55434	–1.35044	–0.00096
C	–2.66143	0.08756	0.00004
C	–0.59377	1.70156	0.00124
C	–0.18066	3.10466	0.00225
H	–1.05601	3.76142	0.00276
H	0.42746	3.31160	0.88700
H	0.42739	3.31288	–0.88226
O	–3.70165	0.71076	0.00048
C	–3.85798	–1.93246	–0.00144
H	–3.61715	–2.99350	–0.00222
H	–4.43695	–1.67128	0.88718

H	–4.43693	–1.66996	–0.88968
O	–2.59666	–1.25741	–0.00093

$[PtCl_3(COC)]^-$ (9a')

(file: PtCl3(COC).out / PtCl3(COC_PCM).log)

E(RB+HF–LYP)	–1812.412183 a.u.
Sum of electronic and zero-point energies	–1812.227827 a.u.
Sum of electronic and thermal Gibbs free energies (298.15 K)	–1812.272828 a.u.
ΔG_{solv}(PCM, 298.15 K)	–36.2 kcal/mol
BSSE	1.85 kcal/mol

	x	*y*	*z*
C	1.05024	0.07768	0.70837
C	1.07986	0.35242	–0.50906
C	3.76516	–0.89645	0.39552
C	1.83896	0.70331	–1.71773
C	4.20488	–0.02564	–0.80669
C	3.28143	1.09747	–1.32588
H	1.83594	–0.14084	–2.41877
H	2.97388	–1.57852	0.07454
H	4.41967	–0.70880	–1.63854
H	4.62378	–1.53055	0.64493
H	1.35641	1.54088	–2.23169
H	5.16433	0.44696	–0.55629
H	3.76976	1.53749	–2.20426
H	3.21479	1.89806	–0.58224
C	1.77508	–0.27559	1.93678
H	1.52153	–1.30564	2.21386
H	1.47270	0.36236	2.77374
C	3.29832	–0.15309	1.67474
H	3.55873	0.90895	1.61197
H	3.82705	–0.54665	2.54973
Pt	–0.93762	–0.01229	–0.00186
Cl	–1.19996	2.29940	0.41159
Cl	–3.27139	–0.28558	–0.12798
Cl	–0.60912	–2.32004	–0.41470

Electronic Supplementary Material (ESI) for Dalton Transactions

SUPPORTING INFORMATION

On the isomerization of cyclooctyne into cycloocta-1,3-diene: Synthesis, characterization and structure of a dinuclear platinum(II) complex with a μ-η^2:η^2-1,3-COD ligand

Anja König, Christoph Wagner, Martin Bette, Dirk Steinborn

Institut für Chemie –Anorganische Chemie, Martin-Luther-Universität, Kurt-Mothes-Straße 2, D-06120 Halle, Germany

S1. Crystallographic and structure refinement data of $[K(18C6)]_2[(PtCl_3)_2(\mu\text{-}\eta^2\text{:}\eta^2\text{-}1,3\text{-COD})]\cdot Me_2CO$ (**2**·Me_2CO).

Empirical formula	$C_{35}H_{66}Cl_6K_2O_{13}Pt_2$
M_r	1375.96
Crystal system	monoclinic
Space group	$P2_1/n$
a/Å	13.553(1)
b/Å	20.363(2)
c/Å	18.689(2)
β	98.39(1)
V/Å^3	5102.7(8)
Z	4
D_{calc}/g·cm^{-1}	1.791
M(Mo Kα)/mm^{-1}	0.71073
T/K	220(2)
μ (mm^{-1})	6.007
F(000)	2704
Θ range/°	1.95–25.9
Refln. Collected	34509
Refln. Obs. [$I > 2\sigma(I)$]	6642
Refln. Independent (R_{int})	9756
Data/restraints/parameters	9756/59/564
Goodness-of-fit on F^2	0.887
R_1 [$I > 2\sigma(I)$]	0.0349
wR_2 (all data)	0.0690
Largest difference peak and hole /e · Å^{-3}	1.293/–0.916
T_{min}/T_{max}	0.2488/0.5409

S2. Comparison of calculated XRD pattern obtained from single X-ray data (black vertical lines) and an experimentally measured XRD pattern of $[K(18C6)]_2[(PtCl_3)_2(\mu\text{-}\eta^2\text{:}\eta^2\text{-}1,3\text{-}COD)]\cdot Me_2CO$ (**2**·Me_2CO).

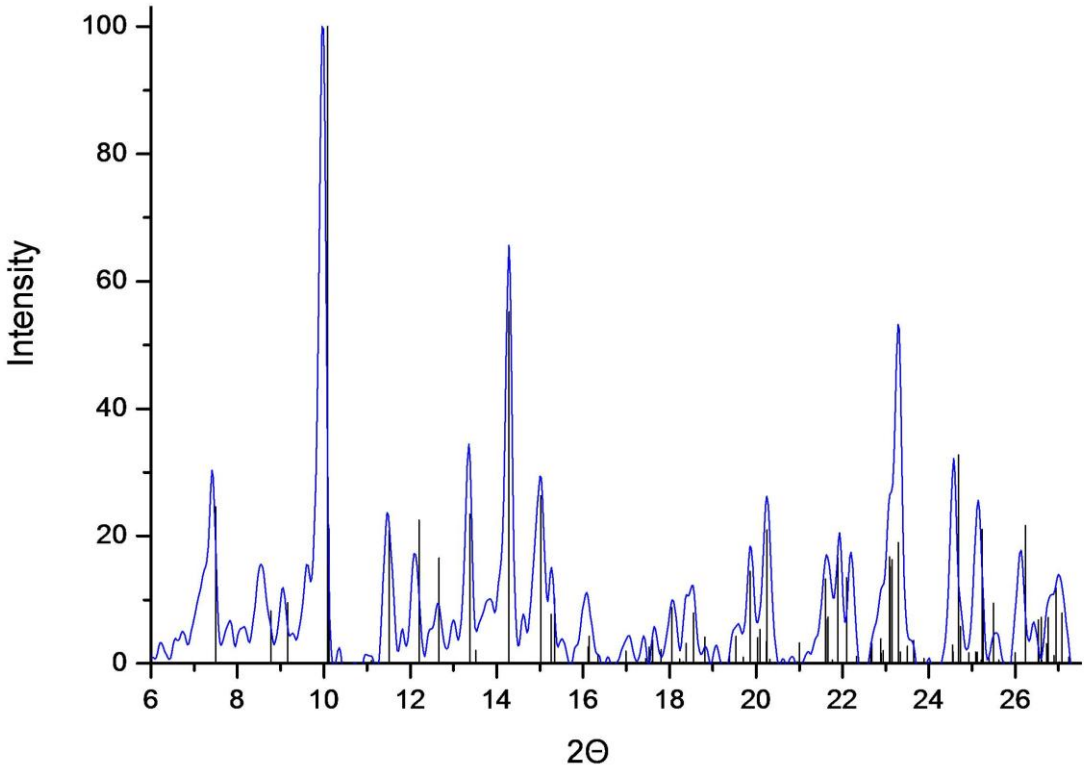

S3. DFT calculations

The following section contains potential energies, sum of electronic and zero-point energies, Gibbs free energies (298.15 K), solvation energies (in $CHCl_3$, 298.15 K), calculated BSSE for the platinum–alkyne bonds and Cartesian coordinates of all structures calculated within this work.

cylooctyne (L1')

(file: COC.out / COC_PCM.out)

E(RB+HF–LYP)	–312.079357 a.u.
Sum of electronic and zero-point energies	–311.899786 a.u.
Sum of electronic and thermal Gibbs free energies (298.15 K)	–311.931275 a.u.
ΔG_{solv}(PCM, 298.15 K)	1.3 kcal/mol

	x	*y*	*z*
C	0.77737	–1.47347	–0.07843
C	–0.41808	–1.54756	–0.21171
C	0.54934	1.30582	–0.57654
C	–1.78471	–1.03016	–0.18820
C	–0.92025	1.47693	–0.09689
C	–1.72093	0.32758	0.56289
H	–2.17193	–0.89790	–1.20547
H	0.56008	0.70447	–1.48958
H	–1.48681	1.82884	–0.96821
H	0.86949	2.30756	–0.88334
H	–2.47847	–1.70311	0.32614
H	–0.94469	2.30848	0.61816
H	–2.74403	0.69410	0.71042
H	–1.32043	0.12492	1.56087
C	2.02563	–0.73101	0.08987
H	2.62421	–0.76218	–0.82773
H	2.65489	–1.13271	0.88993
C	1.60840	0.73747	0.40699
H	1.22951	0.77161	1.43337
H	2.50751	1.36238	0.38746

cycloocta-1,3-diene (L2')

(file: COD.out / COD_PCM.out)

E(RB+HF–LYP)	–312.122953 a.u.
Sum of electronic and zero-point energies	–311.943283 a.u.
Sum of electronic and thermal Gibbs free energies (298.15 K)	–311.973799 a.u.
ΔG_{solv}(PCM, 298.15 K)	1.0 kcal/mol

	x	*y*	*z*
C	–1.34143	0.83189	–0.75658
H	–2.40840	1.00995	–0.87378
C	–0.71012	0.17933	–1.74247
C	–0.71012	1.41842	0.48104
H	–1.27923	–0.08401	–2.63259
C	0.71012	–0.17933	–1.74247
C	–0.60492	0.47043	1.70117
H	–1.30391	2.28903	0.77671
H	0.29289	1.78735	0.24093
H	1.27923	0.08401	–2.63259
C	1.34143	–0.83189	–0.75658
C	0.60492	–0.47043	1.70117
H	–0.55269	1.08351	2.60739
H	–1.52665	–0.11781	1.78235
H	2.40840	–1.00995	–0.87378
C	0.71012	–1.41842	0.48104
H	0.55269	–1.08351	2.60739
H	1.52665	0.11781	1.78235
H	1.30391	–2.28903	0.77671
H	–0.29289	–1.78735	0.24093

cis-but-2-ene (L4')

(file: butene.out / butene_PCM.out)

E(RB+HF–LYP)	–157.271117 a.u.
Sum of electronic and zero-point energies	–157.163588 a.u.
Sum of electronic and thermal Gibbs free energies (298.15 K)	–157.191471 a.u.
ΔG_{solv}(PCM, 298.15 K)	3.4 kcal/mol

	x	*y*	*z*
C	0.66718	0.66372	–0.00001
H	1.16515	1.63144	0.00003
C	–0.66718	0.66372	–0.00001
H	–1.16515	1.63144	0.00003
C	1.58945	–0.52190	0.00000
H	2.24537	–0.50346	–0.87776
H	2.24455	–0.50408	0.87839
H	1.05869	–1.47485	–0.00058
C	–1.58945	–0.52190	0.00000
H	–2.24455	–0.50408	0.87839
H	–2.24538	–0.50345	–0.87776
H	–1.05869	–1.47485	–0.00058

cyclooctene (L5')

(file: COE.out / COE_PCM.out)

E(RB+HF–LYP)	–313.339279 a.u.
Sum of electronic and zero-point energies	–313.136222 a.u.
Sum of electronic and thermal Gibbs free energies (298.15 K)	–313.168584 a.u.
ΔG_{solv}(PCM, 298.15 K)	1.7 kcal/mol

	x	*y*	*z*
C	–1.93703	–0.14017	–0.20148
C	–1.35749	–1.33062	–0.03537
C	1.20640	1.22640	0.40175
C	0.00903	–1.59985	0.54569
C	1.97192	–0.00257	–0.12197
C	1.15085	–1.26323	–0.45715
H	0.14854	–1.03149	1.47147
H	0.92844	1.06442	1.44925
H	2.72654	–0.25936	0.63137
H	1.92225	2.05516	0.42420
H	0.06957	–2.65357	0.82889
H	2.53391	0.28211	–1.01930
H	1.84482	–2.10697	–0.52632
H	0.71126	–1.15672	–1.45267
C	–1.41251	1.21747	0.21422
H	–1.34600	1.27026	1.30917
H	–2.16695	1.95789	–0.06626
C	–0.05119	1.68285	–0.37246
H	0.01491	1.39132	–1.42607
H	–0.06566	2.77741	–0.36551
H	–1.89214	–2.20144	–0.40878
H	–2.90934	–0.13075	–0.68891

buta-1,3-diene

(file: but-1,3-diene.out)

E(RB+HF–LYP)	–156.038506 a.u.
Sum of electronic and zero-point energies	–155.953728 a.u.
Sum of electronic and thermal Gibbs free energies (298.15 K)	–155.980177 a.u.

	x	*y*	*z*
C	–1.84487	0.10956	0.00015
H	–2.01570	1.18160	0.00044
H	–2.72232	–0.52570	0.00059
C	–0.60866	–0.39940	–0.00031
H	–0.47637	–1.47961	–0.00009
C	0.60867	0.39941	–0.00031
H	0.47637	1.47966	–0.00008
C	1.84487	–0.10957	0.00015
H	2.01569	–1.18161	0.00044
H	2.72232	0.52569	0.00059

buta-1,2-diene

(file: but-1,2-diene.out)

E(RB+HF–LYP)	–156.021362 a.u.
Sum of electronic and zero-point energies	–155.937787 a.u.
Sum of electronic and thermal Gibbs free energies (298.15 K)	–155.964724 a.u.

	x	*y*	*z*
C	1.93686	–0.21452	0.00054
C	0.69249	0.17499	–0.00195
C	–0.55355	0.56008	0.00046
H	2.48117	–0.38211	–0.92442
H	2.47629	–0.38343	0.92813
H	–0.75973	1.62953	0.00231
C	–1.74557	–0.36550	–0.00002
H	–1.43479	–1.41104	–0.00188
H	–2.37133	–0.19293	0.88185
H	–2.37303	–0.19032	–0.88015

but-1-yne

(file: but-1-yne.out)

E(RB+HF–LYP)	–156.014867 a.u.
Sum of electronic and zero-point energies	–155.930458 a.u.
Sum of electronic and thermal Gibbs free energies (298.15 K)	–155.957304 a.u.

	x	*y*	*z*
C	1.96012	–0.26253	0.00000
C	0.83379	0.15635	0.00000
C	–0.54226	0.64731	0.00000
H	–0.69120	1.28811	0.87614
H	–0.69120	1.28811	–0.87614
C	–1.58857	–0.48275	0.00000
H	–1.47666	–1.11458	0.88369
H	–2.59850	–0.06484	0.00000
H	–1.47666	–1.11458	–0.88369
H	2.95568	–0.63248	0.00000

but-2-yne

(file: but-2-yne.out)

E(RB+HF–LYP)	–156.024934 a.u.
Sum of electronic and zero-point energies	–155.941161 a.u.
Sum of electronic and thermal Gibbs free energies (298.15 K)	–155.969948 a.u.

	x	*y*	*z*
C	0.60148	–0.00014	0.00003
C	–0.60148	–0.00014	0.00003
C	2.06017	0.00007	–0.00001
H	2.45633	–0.66522	–0.77311
H	2.45606	1.00233	–0.18969
H	2.45633	–0.33671	0.96273
C	–2.06017	0.00007	–0.00001
H	–2.45633	–0.66519	–0.77314
H	–2.45633	–0.33675	0.96272
H	–2.45606	1.00234	–0.18965

$[PtCl_3(COC)]^-$ (1a')

(file: PtCl3(COC).out / PtCl3(COC)_PCM.out)

E(RB+HF–LYP)	–1812.412183 a.u.
Sum of electronic and zero-point energies	–1812.227827 a.u.
Sum of electronic and thermal Gibbs free energies (298.15 K)	–1812.272828 a.u.
ΔG_{solv}(PCM, 298.15 K)	–36.2 kcal/mol

	x	*y*	*z*
C	1.05024	0.07768	0.70837
C	1.07986	0.35242	–0.50906
C	3.76516	–0.89645	0.39552
C	1.83896	0.70331	–1.71773
C	4.20488	–0.02564	–0.80669
C	3.28143	1.09747	–1.32588
H	1.83594	–0.14084	–2.41877
H	2.97388	–1.57852	0.07454
H	4.41967	–0.70880	–1.63854
H	4.62378	–1.53055	0.64493
H	1.35641	1.54088	–2.23169
H	5.16433	0.44696	–0.55629
H	3.76976	1.53749	–2.20426
H	3.21479	1.89806	–0.58224
C	1.77508	–0.27559	1.93678
H	1.52153	–1.30564	2.21386
H	1.47270	0.36236	2.77374
C	3.29832	–0.15309	1.67474
H	3.55873	0.90895	1.61197
H	3.82705	–0.54665	2.54973
Pt	–0.93762	–0.01229	–0.00186
Cl	–1.19996	2.29940	0.41159
Cl	–3.27139	–0.28558	–0.12798
Cl	–0.60912	–2.32004	–0.41470

$[(PtCl_3)_2(COD)]^{2-}$ (2a')

(file: $(PtCl_3)_2$(COD).out / $(PtCl_3)_2$(COD)_PCM.out)

E(RB+HF–LYP)	–3312.686094 a.u.
Sum of electronic and zero-point energies	–3312.495855 a.u.
Sum of electronic and thermal Gibbs free energies (298.15 K)	–3312.549985 a.u.
ΔG_{solv}(PCM, 298.15 K)	–106.5 kcal/mol

	x	*y*	*z*
C	–1.45480	1.42916	0.68017
H	–1.85073	1.57313	1.68227
C	–0.52759	0.37881	0.53405
C	–1.58274	2.64595	–0.21240
Pt	–2.56148	–0.32201	0.02660
H	–0.31344	–0.21028	1.41727
C	0.52760	0.37881	–0.53405
C	–0.72753	3.84809	0.24608
H	–2.63692	2.94210	–0.20478
H	–1.34823	2.39317	–1.24681
Cl	–4.42988	–1.67608	–0.51317
Cl	–2.31363	0.12889	–2.28579
Cl	–2.90201	–0.80998	2.31814
H	0.31344	–0.21028	–1.41727
C	1.45481	1.42916	–0.68017
Pt	2.56148	–0.32201	–0.02660
C	0.72754	3.84809	–0.24609
H	–1.20696	4.76741	–0.11559
H	–0.73694	3.91106	1.34226
H	1.85073	1.57314	–1.68227
C	1.58274	2.64595	0.21241
Cl	4.42988	–1.67608	0.51316
Cl	2.90201	–0.80998	–2.31814
Cl	2.31363	0.12889	2.28579
H	1.20696	4.76741	0.11558
H	0.73695	3.91105	–1.34226
H	2.63692	2.94210	0.20478
H	1.34823	2.39317	1.24681

$[PtCl_3(COD)]^-$ (3a')

(file: $PtCl_3$ (COD).out / $PtCl_3$(COD)_PCM.out)

E(RB+HF–LYP)	–1812.437260 a.u.
Sum of electronic and zero-point energies	–1812.252305 a.u.
Sum of electronic and thermal Gibbs free energies (298.15 K)	–1812.295071 a.u.
ΔG_{solv}(PCM, 298.15 K)	–36.4 kcal/mol

	x	*y*	*z*
C	–3.108334	–0.495805	–1.586269
H	–3.591396	–1.278096	–2.169205
C	–1.774670	–0.430832	–1.616544
C	–4.035336	0.423010	–0.823773
H	–1.222228	–1.133566	–2.230621
C	–0.990973	0.588293	–0.874938
C	–4.339612	–0.007749	0.631863
H	–4.983366	0.474909	–1.371273
H	–3.632611	1.441763	–0.812027
H	–0.687660	1.452354	–1.462788
C	–1.058046	0.763315	0.521057
Pt	0.919227	0.012856	–0.016173
C	–3.308319	0.428346	1.684418
H	–5.311412	0.411415	0.922276
H	–4.452288	–1.097959	0.664938
H	–0.825376	1.757806	0.892387
C	–1.864436	–0.085845	1.478553
Cl	3.167134	–0.629754	0.216343
Cl	1.586589	2.279295	–0.185147
Cl	0.309520	–2.268847	0.106251
H	–3.660371	0.071876	2.659967
H	–3.301894	1.524702	1.749055
H	–1.348963	–0.070409	2.443875
H	–1.878949	–1.125752	1.152074

[$PtCl_3$(cis-but-2-ene)]$^-$ (4a')

(file: PtCl3(butene).out / PtCl3(butene)_PCM.out)

E(RB+HF–LYP)	–1657.588982 a.u.
Sum of electronic and zero-point energies	–1657.475276 a.u.
Sum of electronic and thermal Gibbs free energies (298.15 K)	–1657.514871 a.u.
ΔG_{solv}(PCM, 298.15 K)	–35.3 kcal/mol

	x	*y*	*z*
C	–1.55199	–1.01459	0.70389
H	–1.12659	–1.89691	1.17347
C	–1.55201	–1.01469	–0.70370
H	–1.12666	–1.89709	–1.17316
C	–2.50372	–0.24755	1.58673
H	–3.37389	–0.88049	1.81203
H	–2.02649	0.00717	2.53624
H	–2.85002	0.67845	1.13256
C	–2.50377	–0.24776	–1.58660
H	–2.02659	0.00677	–2.53618
H	–3.37399	–0.88069	–1.81175
H	–2.84999	0.67833	–1.13257
Pt	0.23867	0.00558	–0.00002
Cl	1.31199	–2.10466	0.00013
Cl	–0.77927	2.14474	–0.00003
Cl	2.33828	1.07147	–0.00015

$[PtCl_3(COE)]^-$ (5a')

(file: PtCl3(COE).out / PtCl3(COE)_PCM.out)

E(RB+HF–LYP)	–1813.659112 a.u.
Sum of electronic and zero-point energies	–1813.450212 a.u.
Sum of electronic and thermal Gibbs free energies (298.15 K)	–1813.493844 a.u.
ΔG_{solv}(PCM, 298.15 K)	–36.0 kcal/mol

	x	*y*	*z*
C	0.91127	0.77996	0.80288
C	0.93545	0.84870	–0.60232
C	4.06401	–0.62995	0.57013
C	1.88017	0.08432	–1.50150
C	4.39963	0.06840	–0.76215
C	3.26326	0.79592	–1.51087
H	1.97028	–0.95499	–1.18835
H	3.51763	–1.55558	0.36390
H	4.82224	–0.69826	–1.42392
H	5.02122	–0.94855	1.00071
H	1.46151	0.06280	–2.51096
H	5.20799	0.79171	–0.59199
H	3.59368	0.95368	–2.54361
H	3.14229	1.79946	–1.08881
C	1.75198	–0.12895	1.67642
H	1.58887	–1.17482	1.41474
H	1.39290	–0.01145	2.70339
C	3.27845	0.16189	1.64349
H	3.46340	1.23871	1.54487
H	3.68023	–0.11895	2.62336
H	0.62304	1.80097	–1.02457
H	0.57622	1.68402	1.30338
Pt	0.96431	–0.00186	0.00015
Cl	1.80418	2.20472	0.14650
Cl	–3.16584	–0.82636	–0.12685
Cl	–0.19180	–2.23752	–0.16614

SUPPORTING INFORMATION

Dinuclear Olefin and Alkyne Complexes of Platinum(II)

Anja König, Martin Bette, Clemens Bruhn, Dirk Steinborn

S1. Selected NMR spectroscopical data of $[PtCl_2(H_2C{=}CH_2)(RC{\equiv}Ct\text{-}Bu)]$ (**8**). Coupling constants $J_{H;H}$ from higher order multiplets ('m') were obtained by using the PERCH NMR software package. [37]

H	δ/ppm	(−80°C)				*H*	δ/ppm	(27°C)			
		H_A	H_B	H_C	H_D			H_A	$H_{A'}$	H_B	$H_{B'}$
H_A	4.1	–	8.8	1.7	15.0	H_A	4.46	–	17.2	2.9	7.0
H_B	4.0	8.8	–	15.1	1.6	$H_{A'}$	4.46	17.2	–	8.3	1.8
H_C	4.8	1.7	15.1	–	8.8	H_B	4.57	2.9	8.3	–	19.0
H_D	5.0	15.0	1.6	8.8	–	$H_{B'}$	4.57	7.0	1.8	19.0	–

S2.Selected bond lengths (in Å) in dinuclear olefin complexes $[\{PtCl_2L\}_2]$.

L	$Pt–Cl_{term.}$	$Pt–\mu\text{-}Cl_{tr\ C=C}$[a]	$Pt–\mu\text{-}Cl_{tr\ Cl}$[a]	Pt–C	C=C
cis-but-2-ene	2.278(3)	2.378(3)	2.338(3)	2.18(2)/2.16(2)	1.40(2)
cyclopentene[b]	2.264(6)	2.349(5)	2.320(5)	2.20(2)	1.40(2)
cycloheptene[b]	2.257(6)	2.362(6)	2.328(6)	2.14(2)/2.10(2)	1.38(3)
ethene[b]	2.257(5)–2.274(5)	2.363(4)–2.376(4)	2.324(4)–2.328(4)	2.11(2)–2.16(2)	1.38(3) – 1.41(3)
cyclooctene[b]	2.265(4)	2.371(3)	2.340(3)	2.13(1)/2.14(1)	1.41(2)

[a] $\mu\text{-}Cl_{tr\ C=C}/\mu\text{-}Cl_{tr\ Cl}$: μ-Chlorido ligand *trans* to the olefin and to the terminal chlorido ligand, respectively. [b] Values taken from Ref [4, 5, 21, 22].

S3.Selected structural parameters (distances in Å, angles in °) in alkyne platinum(II) complexes.

R	$Pt–Cl_{term.}$	$Pt–\mu\text{-}Cl_{tr\ C\equiv C}$[a]	$Pt–\mu\text{-}Cl_{tr\ Cl}$[a]	Pt–C	C≡C	α[b]
neutral dinuclear alkyne complexes [{PtCl₂(RC≡Ct-Bu)}₂]						
11 (Me)	2.267(1)	2.354(1)	2.341(1)	2.143(5)/2.147(5)	1.254(7)	17.0(5)/20.2(5)
12a (*t*-Bu)	2.262(1)–2.267(1)	2.346(1)–2.353(1)	2.330(1)–2.349(1)	2.126(4)–2.142(4)	1.226(6–1.244(6)	18.6(4)/20.8(4)
12b (*t*-Bu)	2.272(1)	2.3779(9)	2.3395(9)	2.135(4)/2.144(4)	1.258(5)	19.2(3)/20.2(4)
neutral mononuclear complexes [PtCl₂(RC≡CR)L][c] (L = NMeH₂, toluidine)						
CMe_2OH/CMe_2OH		2.300(3)		2.143(5)/2.147(5)	1.22(1)	19.8(9)/18.8(9)
t-Bu/*t*-Bu			2.300(2)	2.14(1)/2.18(1)	1.24(2)	18(1)/15(1)
anionic mononuclear complexes [K(18C6)][PtCl₃(RC≡Ct-Bu)][c]						
Me		2.316(5)	2.301(3)/2.314(3)	2.10(1)/2.13(1)	1.24(1)	16(1)/18(1)
t-Bu		2.310(3)	2.309(3)/2.299(3)	2.141(9)/2.130(9)	1.24(1)	20(1)/21(1)

[a] $\mu\text{-}Cl_{tr\ C=C}/\mu\text{-}Cl_{tr\ Cl}$: μ-Chlorido ligand *trans* to the alkyne and to the terminal chlorido ligand, respectively.[b] Back bending of the substituents R/R' measured by the angle α = 180 – γ(C≡C–C).[c] Values taken from Ref [10, 25, 26].

S4. Crystallographic and structure refinement data of [{$PtCl_2$(MeHC=CHMe)}$_2$] (**2**), [{($PtCl_2$(MeC≡C*t*-Bu)}$_2$] (**11**), *trans*-[{($PtCl_2$(*t*-BuC≡C*t*-Bu)}$_2$] (**12a**) and *cis*-[{($PtCl_2$(*t*-BuC≡C*t*-Bu)}$_2$] (**12b**·$CHCl_3$).

	2	**11**	**12a**	**12b**·$CHCl_3$
Empirical formula	$C_8H_{16}Cl_4Pt_2$	$C_{14}H_{24}Cl_4Pt_2$	$C_{20}H_{36}Cl_4Pt_2$	$C_{21}H_{37}Cl_7Pt_2$
M_r	644.19	724.31	808.47	927.84
Crystal system	monoclinic	monoclinic	monoclinic	orthorhombic
Space group	$P2_1/n$	$P2_1/n$	$P2_1/c$	*Pnma*
a/Å	7.8428(6)	7.6845(3)	12.5306(4)	15.9015(10)
b/Å	8.3011(6)	11.2117(6)	15.3461(5)	22.8923(11)
c/Å	11.2676(9)	12.0147(5)	28.1017(8)	8.4366(4)
β	105.690(6)	108.268(3)	90.331(2)	
V/Å^3	706.23(9)	982.97(8)	5403.7(3)	3071.1(3)
Z	2	2	8	4
D_{calc}/g·cm^{-1}	3.029	2.447	1.987	2.007
M(Mo Kα)/mm^{-1}	0.71073	0.71073	0.71073	0.71073
T/K	203(2)	200(2)	200(2)	173(2)
μ/mm^{-1}	20.507	14.749	10.743	9.718
F(000)	576	664	3040	1752
θ range/°	1.88–25.65	2.55–29.18	2.55–27.00	2.56–25.58
Refln. collected	4319	18343	65058	12952
Refln. Obs. [$I > 2\sigma(I)$]	1204	2195	8984	2217
Refln. Independent (R_{int})	1232 (0.0907)	2652 (0.0644)	11758 (0.0627)	2791 (0.0437)
Data/restraints/parameters	1232/2/67	2652/0/95	11758/0/494	2791/0/149
Goodness-of-fit on F^2	1.315	0.986	0.887	0.905
$R_1[I > 2\sigma(I)]$	0.0470	0.0243	0.0246	0.0189
wR_2 (all data)	0.1297	0.0530	0.0511	0.0398
T_{min}/T_{max}	0.19/0.39	0.019/0.09	0.12/0.69	0.10/0.56
Largest difference peak and hole/e · Å^{-3}	5.334/–2.005	0.931/–2.195	0.928/–1.399	0.868/–0.560

S5. Comparison of calculated XRD pattern (blue lines) obtained from single-crystal X-ray data of [{$PtCl_2$(MeHC=CHMe)}$_2$] (**2**) and an experimentally measured XRD pattern (black lines) of [{$PtCl_2$(MeHC=CHMe)}$_2$] (**2**).

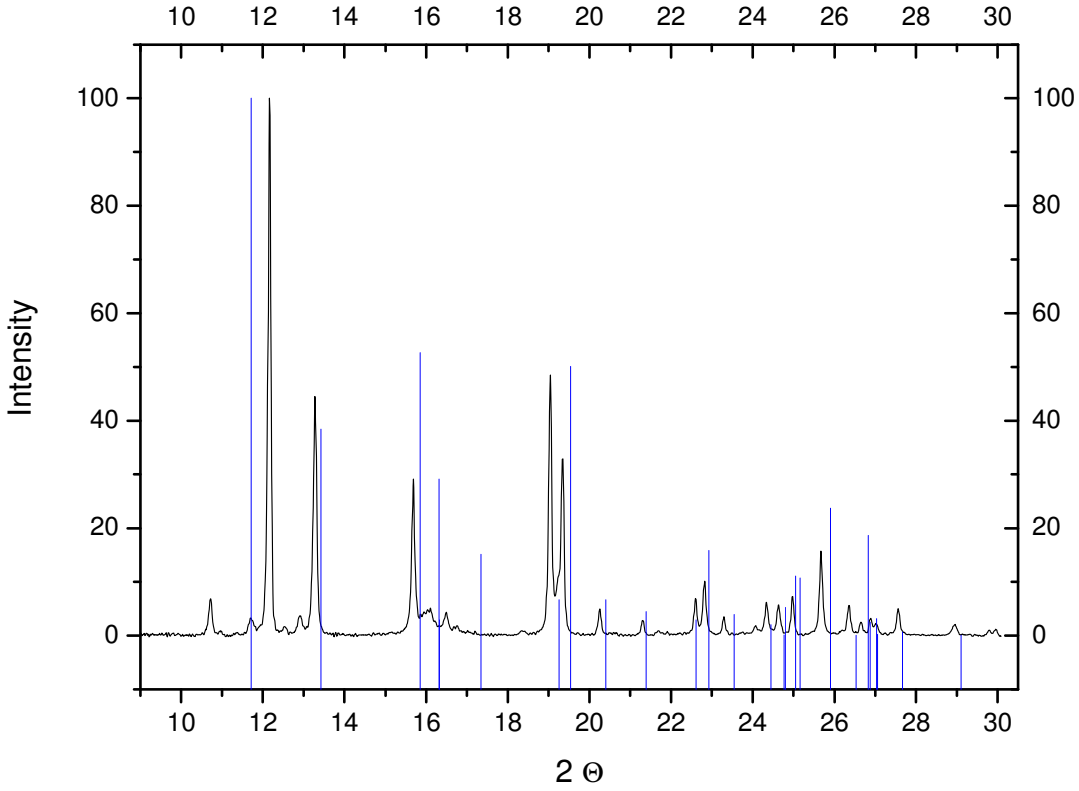

S6. Comparison of calculated XRD pattern (blue lines) obtained from single-crystal X-ray data of *trans*-[{($PtCl_2$(MeC≡C*t*-Bu)}$_2$] (**11**) and an experimentally measured XRD pattern (black lines) of [{($PtCl_2$(MeC≡C*t*-Bu)}$_2$] (**11**).

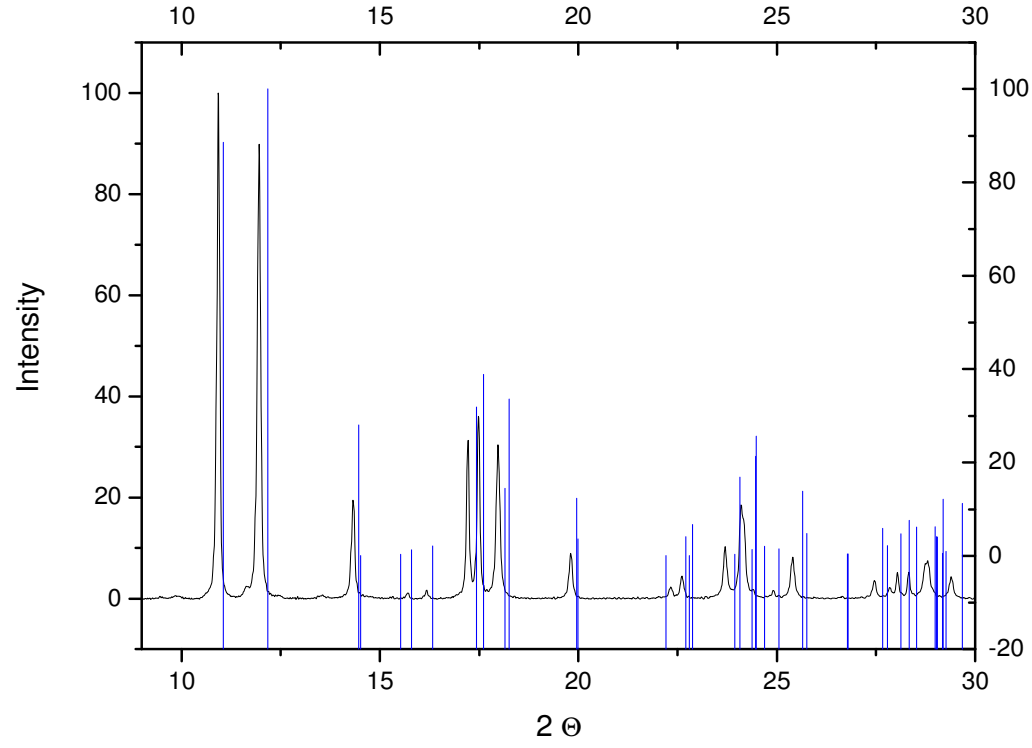

S7. Comparison of calculated XRD pattern (blue lines **12a**; red lines **12b**·$CHCl_3$) obtained from single-crystal X-ray data of *trans*-[{($PtCl_2$(*t*-BuC≡C*t*-Bu)}$_2$] (**12a**) and *cis*-[{($PtCl_2$(*t*-BuC≡C*t*-Bu)}$_2$] (**12b**·$CHCl_3$) and an experimentally measured XRD pattern (black lines) of **12**.

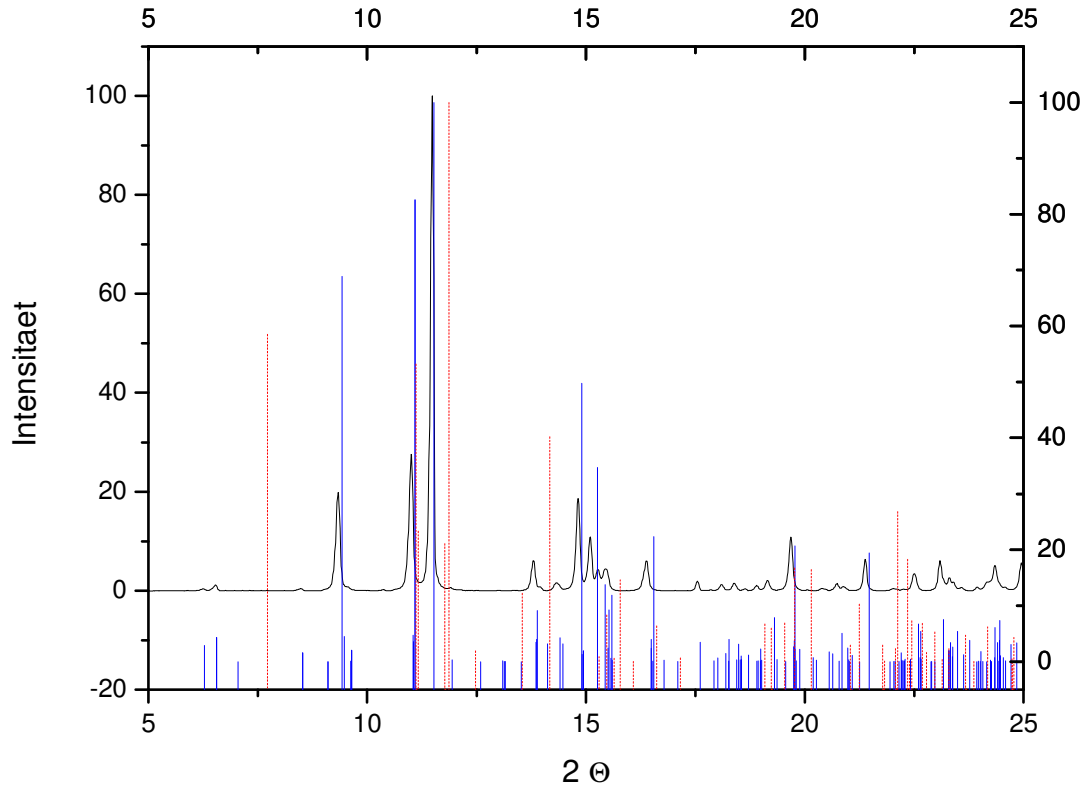

S8. DFT Calculations (Gas Phase Values According to Scheme 6).

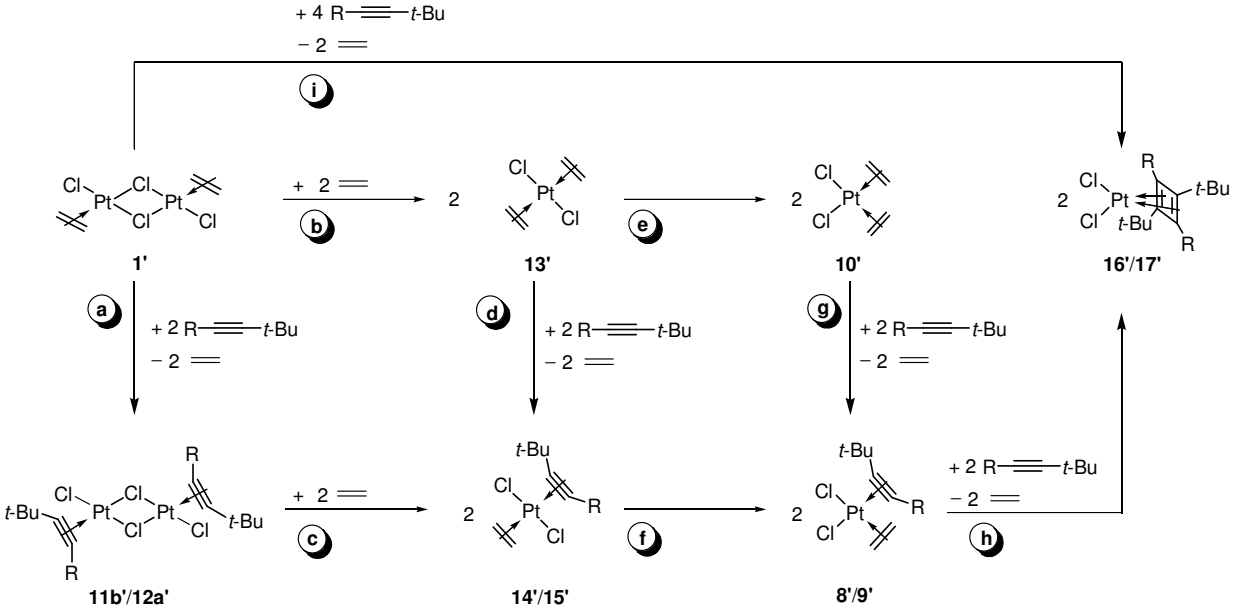

	a	b	c	d	e	f	g	h	i
R = Me	5.4		5.5	3.1[a)]		2.8[a)]	6.0[a)]	−14.4[a)]	−6.2[a)]
t-Bu	6.1		6.9	4.2[a)]		4.5[a)]	8.7[a)]	28.5[a)]	39.5[a)]
C_2H_4		4.7			3.4[a)]				

[a] ΔG_{solv} given refers to the formation of 1 mol complex.

S9. DFT Calculations (Detailed Route According to Scheme 6).

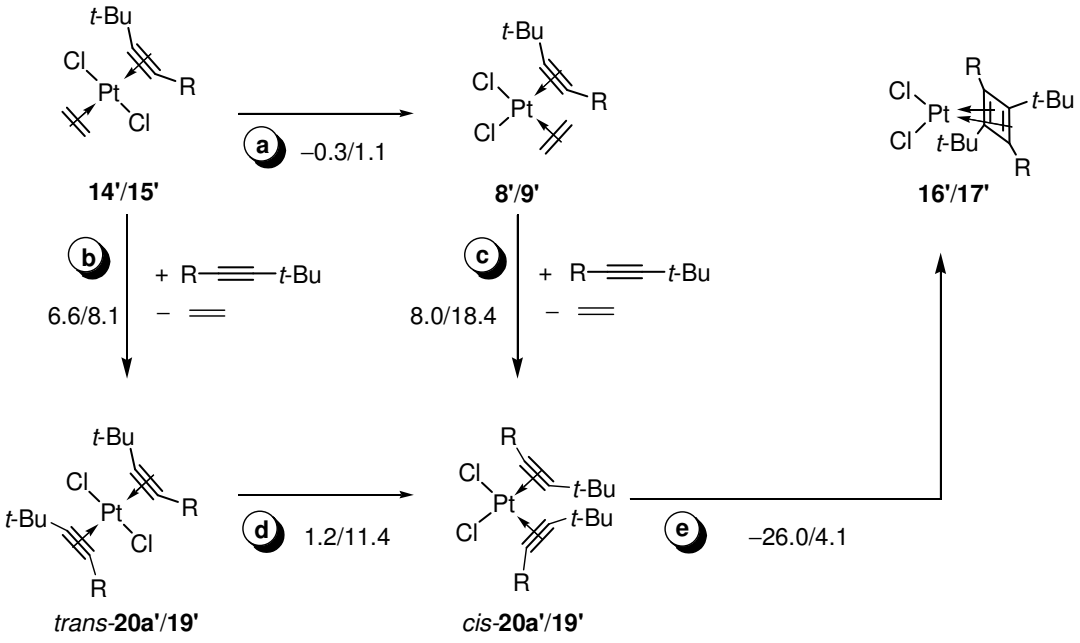

Figures given are standard Gibbs free energies in kcal/mol with consideration of $CHCl_3$ as solvent (ΔG_{solv}). The values for R = Me and R = *t*-Bu are separated by a slash.

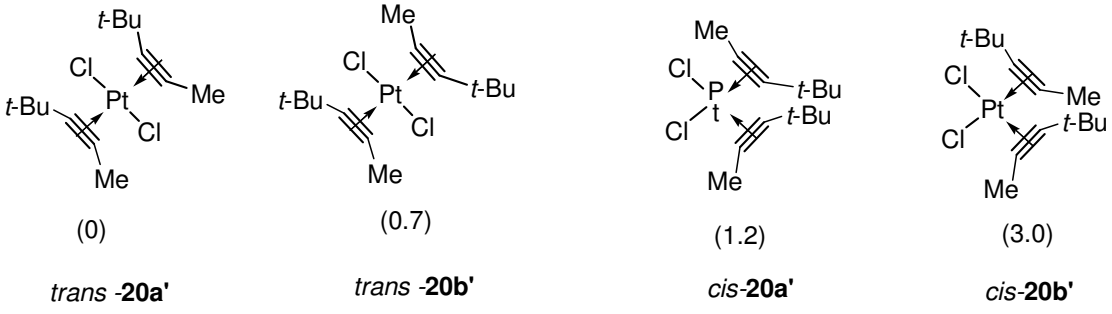

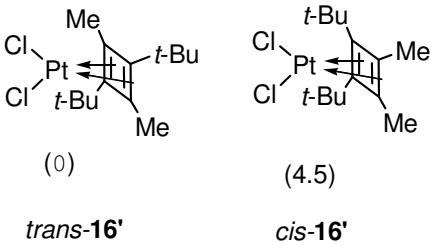

The energies given for complexes *trans*/*cis*-**20a'**in the reaction scheme above refer to the most stable conformer. Energies of less stable conformers (*trans*/*cis*-**20b'**) are given here. Furthermore, the energies of the two regioisomers *trans*/*cis*-**16'** are given.

S10. DFT Calculations (Coordinates and Energies).

The following section contains potential energies, sum of electronic and zero-point energies, Gibbs free energies (298.15 K) and solvation energies (in $CHCl_3$, 298.15 K).

C_2H_4

(file: C2H4.out / C2H4_PCM.out)

E(RB+HF–LYP)	–78.613979 a.u.
Sum of electronic and zero-point energies	–78.563175 a.u.
Sum of electronic and thermal Gibbs free energies (298.15 K)	–78.585352 a.u.
ΔG_{solv}(PCM, 298.15 K)	2.3 kcal/mol

	x	*y*	*z*
C	–0.66348	0.00000	–0.00003
H	–1.23469	0.92245	0.00006
H	–1.23454	–0.92263	0.00011
C	0.66346	–0.00001	–0.00001
H	1.23487	–0.92241	0.00003
H	1.23449	0.92265	0.00008

4,4-dimethylpent-2-yne

(file: 4,4-Dimethylpent-2-yne.out / 4,4-Dimethylpent-2-yne_PCM.out)

E(RB+HF–LYP)	–273.998081 a.u.
Sum of electronic and zero-point energies	–273.829829 a.u.
Sum of electronic and thermal Gibbs free energies (298.15 K)	–273.864477 a.u.
ΔG_{solv}(PCM, 298.15 K)	6.5 kcal/mol

	x	*y*	*z*
C	0.57852	–0.00002	–0.00007
C	1.78292	–0.00002	–0.00005
C	–0.89395	0.00002	–0.00002
C	–1.40738	–0.92947	–1.12345
C	–1.40722	–0.50824	1.36669
C	–1.40726	1.43773	–0.24316
H	–1.05582	–0.58972	–2.10044
H	–1.05527	–1.95266	–0.97297
H	–2.50165	–0.93935	–1.13484
H	–1.05538	0.13386	2.17754
H	–2.50149	–0.51360	1.38089

H	–1.05526	–1.52406	1.56103
H	–2.50153	1.45273	–0.24561
H	–1.05527	2.11394	0.53940
H	–1.05544	1.81890	–1.20466
C	3.24173	–0.00001	–0.00001
H	3.63763	–0.35829	0.95502
H	3.63768	–0.64794	–0.78778
H	3.63766	1.00621	–0.16722

2,2,5,5-tetramethylhex-3-yne

(file: 2,2,5,5-tetramethylhex-3-yne.out / 2,2,5,5-tetramethylhex-3-yne_PCM.out)

E(RB+HF–LYP) –391.971216 a.u.

Sum of electronic and zero-point energies –391.718579 a.u.

Sum of electronic and thermal Gibbs free energies (298.15 K) –347.707185 a.u.

ΔG_{solv}(PCM, 298.15 K) 2.5 kcal/mol

	x	*y*	*z*
C	0.77737	–1.47347	–0.07843
C	–0.41808	–1.54756	–0.21171
C	0.54934	1.30582	–0.57654
C	–1.78471	–1.03016	–0.18820
C	–0.92025	1.47693	–0.09689
C	–1.72093	0.32758	0.56289
H	–2.17193	–0.89790	–1.20547
H	0.56008	0.70447	–1.48958
H	–1.48681	1.82884	–0.96821
H	0.86949	2.30756	–0.88334
H	–2.47847	–1.70311	0.32614
H	–0.94469	2.30848	0.61816
H	–2.74403	0.69410	0.71042
H	–1.32043	0.12492	1.56087
C	2.02563	–0.73101	0.08987
H	2.62421	–0.76218	–0.82773
H	2.65489	–1.13271	0.88993
C	1.60840	0.73747	0.40699
H	1.22951	0.77161	1.43337
H	2.50751	1.36238	0.38746

***trans*-[{$PtCl_2(C_2H_4)$}$_2$] (1a')**

(file: PtCl2C2H4_dimer_1a.out / PtCl2C2H4_dimer_1a_PCM.out)

E(RB+HF–LYP) –2237.160831 a.u.

Sum of electronic and zero-point energies –2237.045013 a.u.

Sum of electronic and thermal Gibbs free energies (298.15 K) –2237.091933 a.u.

ΔG_{solv}(PCM, 298.15 K) 2.4 kcal/mol

	x	*y*	*z*
C	3.16831	–1.55270	0.70098
H	3.95178	–1.03978	1.24584
C	3.16848	–1.55284	–0.70056
H	3.95208	–1.04002	–1.24532
Pt	1.78134	–0.07611	–0.00009
Cl	3.44333	1.50915	–0.00004
Cl	–0.05441	–1.62349	–0.00023
Cl	0.05441	1.62349	–0.00042
Pt	–1.78134	0.07611	0.00003
Cl	–3.44333	–1.50915	0.00034
C	–3.16858	1.55281	–0.70030
H	–3.95226	1.03998	–1.24494
C	–3.16822	1.55273	0.70123
H	–3.95161	1.03983	1.24622
H	–2.61094	2.30055	–1.25325
H	–2.61027	2.30039	1.25398
H	2.61045	–2.30035	1.25383
H	2.61076	–2.30059	–1.25340

***cis*-[{$PtCl_2(C_2H_4)$}$_2$] (1b')**

(file: PtCl2C2H4_dimer_1b.out / PtCl2C2H4_dimer_1b_PCM.out)

E(RB+HF–LYP) –2237.159217 a.u.

Sum of electronic and zero-point energies –2237.043435 a.u.

Sum of electronic and thermal Gibbs free energies (298.15 K) –2237.090245 a.u.

ΔG_{solv}(PCM, 298.15 K) 2.1 kcal/mol

	x	*y*	*z*
C	–3.23782	1.45502	0.69978
H	–3.99652	0.90706	1.24539
C	–3.23773	1.45498	–0.70016
H	–3.99635	0.90698	–1.24584
Pt	–1.78234	0.03775	–0.00005
Cl	–3.37477	–1.61012	–0.00011
Cl	0.00000	1.66511	0.00006
Cl	0.00000	–1.58258	0.00014
Pt	1.78234	0.03775	0.00002
Cl	3.37476	–1.61012	–0.00003
H	3.99655	0.90714	–1.24532
C	3.23784	1.45507	–0.69970
C	3.23771	1.45493	0.70024
H	3.99632	0.90689	1.24591

H	–2.71328	2.22584	1.25346
H	–2.71310	2.22576	–1.25383
H	2.71307	2.22568	1.25395
H	2.71331	2.22593	–1.25334

***trans*-[{PtCl$_2$(MeHC=CHMe)}$_2$] (2a')**

(file: PtCl2butene_dimer_2a.out / PtCl2butene_dimer_2a_PCM.out)

E(RB+HF–LYP)	–2394.472101 a.u.
Sum of electronic and zero-point energies	–2394.244737 a.u.
Sum of electronic and thermal Gibbs free energies (298.15 K)	–2394.298753 a.u.
ΔG_{solv}(PCM, 298.15 K)	5.4 kcal/mol

	x	*y*	*z*
C	3.54244	–0.74718	0.70613
H	4.10961	0.05040	1.17713
C	3.54332	–0.74730	–0.70414
H	4.11107	0.05022	–1.17456
C	3.29509	–1.93788	1.59137
H	4.26563	–2.37853	1.85129
H	2.81647	–1.63721	2.52542
H	2.68638	–2.71107	1.12599
C	3.29713	–1.93816	–1.58950
H	2.81959	–1.63768	–2.52416
H	4.26801	–2.37877	–1.84818
H	2.68794	–2.71134	–1.12471
Pt	1.78195	0.31706	–0.00020
Cl	3.00585	2.26976	0.00053
Cl	0.29681	–1.57439	–0.00126
Cl	–0.29682	1.57437	–0.00161
Pt	–1.78195	–0.31707	–0.00031
Cl	–3.00588	–2.26975	0.00065
C	–3.54350	0.74726	–0.70390
H	–4.11144	–0.05023	–1.17413
C	–3.54223	0.74727	0.70637
H	–4.10921	–0.05035	1.17755
C	–3.29489	1.93805	1.59149
H	–2.68646	2.71136	1.12594
H	–4.26550	2.37846	1.85156
H	–2.81601	1.63754	2.52546
C	–3.29730	1.93804	–1.58938
H	–4.26813	2.37887	–1.84789
H	–2.68782	2.71110	–1.12479
H	–2.82005	1.63739	–2.52414

***trans*-[{PtCl$_2$(MeHC=CHMe)}$_2$] (2b')**

(file: PtCl2butene_dimer_2b.out / PtCl2butene_dimer_2b_PCM.out)

E(RB+HF–LYP)	–2394.470022 a.u.
Sum of electronic and zero-point energies	–2394.242705 a.u.
Sum of electronic and thermal Gibbs free energies (298.15 K)	–2394.296727 a.u.
ΔG_{solv}(PCM, 298.15 K)	5.3 kcal/mol

	x	*y*	*z*
C	3.55150	0.87117	–0.70447
H	4.16637	0.10934	–1.17480
C	3.55073	0.87092	0.70628
H	4.16506	0.10890	1.17702
C	3.23549	2.04538	–1.58974
H	4.17911	2.54135	–1.84913
H	2.77574	1.71736	–2.52405
H	2.58284	2.78208	–1.12479
C	3.23367	2.04475	1.59165
H	2.77291	1.71632	2.52532
H	4.17698	2.54066	1.85229
H	2.58149	2.78160	1.12628
Pt	1.85937	–0.29766	–0.00023
Cl	3.19915	–2.17200	0.00034
Cl	0.26779	1.50931	–0.00109
Cl	–0.13999	–1.69151	–0.00065
Pt	–1.71646	0.11547	–0.00017
Cl	–3.03061	2.01384	0.00016
C	–3.29127	–1.21692	–0.70487
H	–2.70647	–2.00048	–1.18074
C	–3.29068	–1.21705	0.70568
H	–2.70544	–2.00063	1.18097
C	–4.35804	–0.63604	1.59148
H	–4.90347	0.18228	1.12830
H	–5.06647	–1.43641	1.83993
H	–3.93108	–0.27601	2.52934
C	–4.35931	–0.63569	–1.58971
H	–5.06720	–1.43630	–1.83889
H	–4.90520	0.18170	–1.12542
H	–3.93292	–0.27420	–2.52727

***trans*-[{PtCl$_2$(MeHC=CHMe)}$_2$] (2c')**

(file: PtCl2butene_dimer_2c.out / PtCl2butene_dimer_2c_PCM.out)

E(RB+HF–LYP)	–2394.467989 a.u.

Sum of electronic and zero-point energies	–2394.240746 a.u.
Sum of electronic and thermal Gibbs free energies (298.15 K)	–2394.294877 a.u.
ΔG_{solv}(PCM, 298.15 K)	5.2 kcal/mol

	x	*y*	*z*
C	3.29466	1.28034	0.70568
H	2.67471	2.03697	1.18062
C	3.29503	1.27990	–0.70539
H	2.67570	2.03650	–1.18124
C	4.38727	0.74905	1.59180
H	5.05653	1.58196	1.84199
H	3.97671	0.36824	2.52878
H	4.97132	–0.04193	1.12830
C	4.38851	0.74872	–1.59056
H	3.97875	0.36708	–2.52755
H	5.05731	1.58195	–1.84088
H	4.97292	–0.04160	–1.12639
Pt	1.78505	–0.12288	–0.00010
Cl	3.18536	–1.95774	–0.00032
Cl	0.13281	1.61983	–0.00040
Cl	–0.13269	–1.61963	0.00044
Pt	–1.78517	0.12298	0.00003
Cl	–3.18526	1.95797	–0.00037
C	–3.29440	–1.28053	–0.70533
H	–2.67425	–2.03684	–1.18050
C	–3.29450	–1.28023	0.70576
H	–2.67442	–2.03636	1.18133
C	–4.38800	–0.74923	1.59098
H	–4.97152	0.04198	1.12718
H	–5.05762	–1.58212	1.84019
H	–3.97839	–0.36871	2.52849
C	–4.38775	–0.74987	–1.59094
H	–5.05736	–1.58284	–1.83990
H	–4.97131	0.04156	–1.12755
H	–3.97798	–0.36975	–2.52854

***cis*-[{$PtCl_2$(MeHC=CHMe)}$_2$] (2d')**

(file: PtCl2butene_dimer_2d.out / PtCl2butene_dimer_2d_PCM.out)

E(RB+HF–LYP)	–2394.469727 a.u.
Sum of electronic and zero-point energies	–2394.242386 a.u.
Sum of electronic and thermal Gibbs free energies (298.15 K)	–2394.296466 a.u.
ΔG_{solv}(PCM, 298.15 K)	5.0 kcal/mol

	x	*y*	*z*
C	–3.35940	1.11320	0.70377
H	–4.05733	0.42805	1.17572
C	–3.35906	1.11302	–0.70463
H	–4.05679	0.42776	–1.17674
C	–2.90538	2.24126	1.58971
H	–3.78083	2.84963	1.84847
H	–2.48945	1.85976	2.52435
H	–2.16756	2.89283	1.12423
C	–2.90459	2.24084	–1.59065
H	–2.48794	1.85908	–2.52487
H	–3.77994	2.84898	–1.85024
H	–2.16719	2.89266	–1.12486
Pt	–1.80875	–0.24590	0.00011
Cl	–3.35849	–1.94378	–0.00015
Cl	0.00007	1.36195	0.00044
Cl	0.00008	–1.84254	0.00088
Pt	1.80871	–0.24590	–0.00021
Cl	3.35862	–1.94371	–0.00064
H	4.05698	0.42833	–1.17636
C	3.35913	1.11331	–0.70404
C	3.35927	1.11291	0.70437
H	4.05705	0.42749	1.17613
C	2.90486	2.24165	–1.58952
H	2.16701	2.89294	–1.12372
H	3.78018	2.85023	–1.84819
H	2.48885	1.86044	–2.52425
C	2.90501	2.24055	1.59070
H	2.16704	2.89211	1.12546
H	2.48915	1.85861	2.52520
H	3.78032	2.84901	1.84968

***cis*-[{PtCl$_2$(MeHC=CHMe)}$_2$] (2e')**

(file: PtCl2butene_dimer_2e.out / PtCl2butene_dimer_2e_PCM.out)

E(RB+HF–LYP)	–2394.467729 a.u.
Sum of electronic and zero-point energies	–2394.240503 a.u.
Sum of electronic and thermal Gibbs free energies (298.15 K)	–2394.294696 a.u.
ΔG_{solv}(PCM, 298.15 K)	5.1 kcal/mol

	x	y	z
C	3.08205	1.45509	0.70497

H	2.38381	2.13940	1.18131
C	3.08248	1.45544	–0.70381
H	2.38451	2.13992	–1.18027
C	4.22368	1.04127	1.59253
H	4.80108	1.93900	1.84714
H	3.85447	0.61438	2.52691
H	4.88921	0.31822	1.12788
C	4.22475	1.04217	–1.59081
H	3.85626	0.61547	–2.52555
H	4.80205	1.94016	–1.84475
H	4.89021	0.31917	–1.12596
Pt	1.72138	–0.10216	–0.00019
Cl	3.31084	–1.76791	–0.00031
Cl	–0.12525	1.45117	–0.00029
Cl	–0.01262	–1.77315	–0.00081
Pt	–1.87329	–0.23092	0.00018
Cl	–3.35876	–1.98313	0.00087
H	–4.14413	0.36165	1.17624
C	–3.47195	1.07192	0.70403
C	–3.47200	1.07144	–0.70441
H	–4.14417	0.36081	–1.17611
C	–3.05943	2.21581	1.58989
H	–2.34847	2.89598	1.12360
H	–3.95721	2.78960	1.85105
H	–2.62716	1.84995	2.52338
C	–3.05949	2.21466	–1.59113
H	–2.34862	2.89524	–1.12532
H	–2.62714	1.84810	–2.52431
H	–3.95731	2.78816	–1.85279

***cis*-[{PtCl$_2$(MeHC=CHMe)}$_2$] (2f')**

(file: PtCl2butene_dimer_2f.out / PtCl2butene_dimer_2f_PCM.out)

E(RB+HF–LYP)	–2394.465761 a.u.
Sum of electronic and zero-point energies	–2394.292838 a.u.
Sum of electronic and thermal Gibbs free energies (298.15 K)	–2394.238616 a.u.
ΔG_{solv}(PCM, 298.15 K)	5.0 kcal/mol

	x	y	z
C	–3.20328	–1.42652	0.70462
H	–2.52996	–2.13547	1.18074
C	–3.20394	–1.42629	–0.70420
H	–2.53093	–2.13501	–1.18112
C	–4.32922	–0.97231	1.59240

H	–4.93807	–1.84903	1.84691
H	–3.94488	–0.55914	2.52683
H	–4.96881	–0.22607	1.12797
C	–4.33063	–0.97193	–1.59092
H	–3.94709	–0.55848	–2.52556
H	–4.93959	–1.84865	–1.84516
H	–4.96994	–0.22590	–1.12578
Pt	–1.78790	0.08173	–0.00008
Cl	–3.31461	1.80282	0.00060
Cl	–0.00006	–1.54812	–0.00168
Cl	0.00008	1.70075	–0.00033
Pt	1.78778	0.08176	–0.00027
Cl	3.31483	1.80251	0.00012
H	2.53153	–2.13533	–1.18069
C	3.20436	–1.42644	–0.70377
C	3.20335	–1.42627	0.70500
H	2.52984	–2.13506	1.18110
C	4.33114	–0.97214	–1.59041
H	4.97101	–0.22683	–1.12487
H	4.93948	–1.84908	–1.84538
H	3.94769	–0.55779	–2.52468
C	4.32898	–0.97190	1.59310
H	4.96867	–0.22564	1.12885
H	3.94429	–0.55874	2.52739
H	4.93778	–1.84859	1.84782

***trans*-[{($PtCl_2$(MeC≡C*t*-Bu)}$_2$] (11a')**

(file: PtCl2MeCCtBu_dimer_11a.out / PtCl2MeCCtBu_dimer_11a_PCM.out)

E(RB+HF–LYP)	–2627.920410 a.u.
Sum of electronic and zero-point energies	–2627.574579 a.u.
Sum of electronic and thermal Gibbs free energies (298.15 K)	–2627.641287 a.u.
ΔG_{solv}(PCM, 298.15 K)	13.9 kcal/mol

	x	y	z
C	–3.27355	0.37468	1.42376
C	–4.34338	–1.24616	–0.44006
C	–3.35153	1.06219	2.71744
Pt	–1.67168	0.62388	0.03397
Cl	–2.71496	2.47136	–0.85498
Cl	–0.43782	–1.23016	0.95911
Cl	0.43768	1.22958	–0.95987
Pt	1.67175	–0.62408	–0.03416
Cl	2.71519	–2.47110	0.85549
C	3.56391	0.32834	–0.43503

C	3.27380	–0.37450	–1.42353
C	4.34296	1.24656	0.44048
C	3.35251	–1.06179	–2.71730
C	3.50616	2.49176	0.80059
H	3.18224	3.02680	–0.09458
H	2.61742	2.21772	1.37170
H	4.10963	3.17026	1.40952
C	5.59182	1.67124	–0.36920
H	6.20211	2.34764	0.23524
H	6.20278	0.80522	–0.63395
H	5.30968	2.19350	–1.28641
C	4.77802	0.51321	1.72688
H	5.36846	–0.37513	1.49568
H	5.38383	1.18748	2.33865
H	3.91360	0.19573	2.31172
C	–3.50797	–2.49304	–0.79764
H	–2.61806	–2.22100	–1.36787
H	–3.18606	–3.02754	0.09858
H	–4.11165	–3.17135	–1.40660
C	–5.59386	–1.66803	0.36860
H	–6.20437	–2.34433	–0.23574
H	–5.31361	–2.18956	1.28681
H	–6.20388	–0.80079	0.63151
C	–4.77580	–0.51373	–1.72786
H	–5.36496	0.37592	–1.49847
H	–3.91019	–0.19850	–2.31218
H	–5.38207	–1.18778	–2.33941
H	–3.37397	2.14443	2.57039
H	–4.26466	0.75847	3.23768
H	–2.49290	0.81631	3.34627
H	4.26677	–0.75925	–3.23622
H	3.37323	–2.14411	–2.57055
H	2.49505	–0.81451	–3.34720

***trans*-[{($PtCl_2$(MeC≡C*t*-Bu)}$_2$] (11b')**

(file: PtCl2MeCCtBu_dimer_11b.out / PtCl2MeCCtBu_dimer_11b_PCM.out)

E(RB+HF–LYP)	–2627.920423 a.u.
Sum of electronic and zero-point energies	–2627.574599 a.u.
Sum of electronic and thermal Gibbs free energies (298.15 K)	–2627.641562 a.u.
ΔG_{solv}(PCM, 298.15 K)	14.0 kcal/mol

	x	y	z
C	3.46853	0.54113	–1.01482
C	3.52754	0.55353	0.23081

C	3.81398	0.72078	–2.42925
C	4.05935	0.81202	1.59719
Pt	1.71898	–0.47547	–0.33287
Cl	2.82510	–2.48836	–0.46266
Cl	0.43018	1.56172	–0.26550
Cl	–0.43011	–1.56208	–0.26336
Pt	–1.71895	0.47500	–0.33355
Cl	–2.82508	2.48769	–0.46605
C	–3.52744	–0.55314	0.23158
C	–3.46845	–0.54261	–1.01407
C	–4.05949	–0.80970	1.59824
C	–3.81384	–0.72439	–2.42825
C	–3.04566	–1.62236	2.43025
H	–2.80467	–2.57204	1.94789
H	–2.11623	–1.06761	2.57014
H	–3.47103	–1.83310	3.41514
C	–5.36176	–1.62610	1.41664
H	–5.79525	–1.83904	2.39748
H	–6.09749	–1.06899	0.83211
H	–5.16561	–2.57728	0.91622
C	–4.37310	0.52528	2.30627
H	–5.08463	1.12061	1.73138
H	–4.80278	0.31910	3.29053
H	–3.47016	1.12277	2.43968
C	3.04618	1.62756	2.42719
H	2.80659	2.57659	1.94288
H	2.11600	1.07424	2.56774
H	3.47139	1.83967	3.41185
C	5.36272	1.62646	1.41455
H	5.16796	2.57690	0.91217
H	5.79605	1.84081	2.39515
H	6.09800	1.06729	0.83143
C	4.37104	–0.52196	2.30795
H	3.46728	–1.11801	2.44228
H	5.08197	–1.11935	1.73446
H	4.80068	–0.31437	3.29194
H	3.03480	1.27518	–2.95718
H	4.75310	1.27635	–2.50769
H	3.93788	–0.24971	–2.91527
H	–4.75276	–1.28041	–2.50591
H	–3.93810	0.24536	–2.91565
H	–3.03446	–1.27925	–2.95539

***trans*-[{($PtCl_2$(MeC≡C*t*-Bu)}$_2$] (11b')**

(file: PtCl2MeCCtBu_dimer_11b.out / PtCl2MeCCtBu_dimer_11b_PCM.out)

E(RB+HF–LYP) –2627.920423 a.u.

Sum of electronic and zero-point energies	–2627.574599 a.u.
Sum of electronic and thermal Gibbs free energies (298.15 K)	–2627.641562 a.u.
ΔG_{solv}(PCM, 298.15 K)	14.0 kcal/mol

	x	y	Z
C	3.46853	0.54113	–1.01482
C	3.52754	0.55353	0.23081
C	3.81398	0.72078	–2.42925
C	4.05935	0.81202	1.59719
Pt	1.71898	–0.47547	–0.33287
Cl	2.82510	–2.48836	–0.46266
Cl	0.43018	1.56172	–0.26550
Cl	–0.43011	–1.56208	–0.26336
Pt	–1.71895	0.47500	–0.33355
Cl	–2.82508	2.48769	–0.46605
C	–3.52744	–0.55314	0.23158
C	–3.46845	–0.54261	–1.01407
C	–4.05949	–0.80970	1.59824
C	–3.81384	–0.72439	–2.42825
C	–3.04566	–1.62236	2.43025
H	–2.80467	–2.57204	1.94789
H	–2.11623	–1.06761	2.57014
H	–3.47103	–1.83310	3.41514
C	–5.36176	–1.62610	1.41664
H	–5.79525	–1.83904	2.39748
H	–6.09749	–1.06899	0.83211
H	–5.16561	–2.57728	0.91622
C	–4.37310	0.52528	2.30627
H	–5.08463	1.12061	1.73138
H	–4.80278	0.31910	3.29053
H	–3.47016	1.12277	2.43968
C	3.04618	1.62756	2.42719
H	2.80659	2.57659	1.94288
H	2.11600	1.07424	2.56774
H	3.47139	1.83967	3.41185
C	5.36272	1.62646	1.41455
H	5.16796	2.57690	0.91217
H	5.79605	1.84081	2.39515
H	6.09800	1.06729	0.83143
C	4.37104	–0.52196	2.30795
H	3.46728	–1.11801	2.44228
H	5.08197	–1.11935	1.73446
H	4.80068	–0.31437	3.29194
H	3.03480	1.27518	–2.95718
H	4.75310	1.27635	–2.50769
H	3.93788	–0.24971	–2.91527

H	–4.75276	–1.28041	–2.50591
H	–3.93810	0.24536	–2.91565
H	–3.03446	–1.27925	–2.95539

***cis*-[{($PtCl_2$(MeC≡C*t*-Bu)}$_2$] (11c')**

(file: PtCl2MeCCtBu_dimer_11c.out / PtCl2MeCCtBu_dimer_11c_PCM.out)

E(RB+HF–LYP)	–2627.918914 a.u.
Sum of electronic and zero-point energies	–2627.573020 a.u.
Sum of electronic and thermal Gibbs free energies (298.15 K)	–2627.639287 a.u.
ΔG_{solv}(PCM, 298.15 K)	13.8 kcal/mol

	x	y	Z
C	–3.03370	1.01209	1.30756
C	–3.30338	1.03970	0.09072
C	–3.07836	1.26419	2.75220
C	–3.98611	1.42148	–1.17619
Pt	–1.74312	–0.42148	0.38492
Cl	–3.28341	–2.07289	0.79921
Cl	0.00001	1.21362	0.00018
Cl	–0.00007	–2.02835	–0.00015
Pt	1.74306	–0.42146	–0.38489
Cl	3.28337	–2.07280	–0.79941
C	3.03364	1.01208	–1.30749
C	3.30330	1.03970	–0.09064
C	3.07823	1.26440	–2.75210
C	3.98630	1.42131	1.17618
C	4.74210	0.20856	1.75926
H	5.46748	–0.18577	1.04556
H	4.05486	–0.59881	2.01588
C	4.99100	2.54171	0.81533
H	5.52293	2.85625	1.71727
H	5.72813	2.19023	0.08985
H	4.47950	3.41284	0.39894
C	2.96416	1.94817	2.20484
H	2.41364	2.80674	1.81388
H	2.24254	1.17456	2.47321
H	3.48925	2.25786	3.11246
H	5.27251	0.51567	2.66496
C	–2.96385	1.94956	–2.20411
H	–2.41412	2.80832	–1.81246
H	–2.24158	1.17659	–2.47255
H	–3.48875	2.25935	–3.11182
C	–4.99172	2.54101	–0.81519

H	–4.48099	3.41226	–0.39809
H	–5.52343	2.85571	–1.71721
H	–5.72895	2.18865	–0.09025
C	–4.74084	0.20854	–1.76025
H	–4.05295	–0.59820	–2.01709
H	–5.46622	–0.18672	–1.04706
H	–5.27113	0.51580	–2.66598
H	2.10718	1.59784	–3.12498
H	3.82027	2.03937	–2.96557
H	3.35796	0.35323	–3.28597
H	–3.35801	0.35289	3.28590
H	–2.10737	1.59768	3.12518
H	–3.82052	2.03903	2.96577

***cis*-[{(PtCl$_2$(MeC≡C*t*-Bu)}$_2$] (11d')**

(file: PtCl2MeCCtBu_dimer_11d.out / PtCl2MeCCtBu_dimer_11d_PCM.out)

E(RB+HF–LYP)	–2627.918821 a.u.
Sum of electronic and zero-point energies	–2627.572993 a.u.
Sum of electronic and thermal Gibbs free energies (298.15 K)	–2627.639619 a.u.
ΔG_{solv}(PCM, 298.15 K)	13.7 kcal/mol

	x	y	Z
C	–3.21397	0.20781	1.41993
C	–3.27201	0.97063	0.43559
C	–3.50455	–0.43256	2.70756
C	–3.73061	2.08910	–0.43377
Pt	–1.78399	–0.53495	0.01472
Cl	–3.37265	–1.94822	–0.85141
Cl	0.00001	0.83206	0.91451
Cl	0.00000	–1.78512	–0.99650
Pt	1.78398	–0.53496	0.01472
Cl	3.37274	–1.94822	–0.85125
C	3.27198	0.97065	0.43556
C	3.21394	0.20785	1.41991
C	3.73060	2.08911	–0.43380
C	3.50451	–0.43248	2.70757
C	4.36923	1.53291	–1.72408
H	5.20262	0.86582	–1.49720
H	3.64353	0.97038	–2.31309
H	4.74026	2.36419	–2.33010
C	4.78822	2.87402	0.37875
H	5.15966	3.70943	–0.22082
H	4.36021	3.27790	1.29939

H	5.63668	2.23701	0.63864
C	2.55057	3.01735	–0.78883
H	2.07925	3.42215	0.10953
H	2.91412	3.85175	–1.39464
H	1.78982	2.48392	–1.36138
C	–2.55056	3.01732	–0.78879
H	–2.07923	3.42211	0.10957
H	–1.78983	2.48388	–1.36135
H	–2.91410	3.85174	–1.39459
C	–4.78821	2.87402	0.37879
H	–4.36020	3.27790	1.29944
H	–5.15965	3.70945	–0.22078
H	–5.63668	2.23703	0.63868
C	–4.36925	1.53292	–1.72404
H	–3.64356	0.97038	–2.31306
H	–5.20265	0.86584	–1.49716
H	–4.74027	2.36421	–2.33006
H	2.61108	–0.48306	3.33397
H	3.87221	–1.44893	2.54914
H	4.27135	0.14089	3.23668
H	–3.87230	–1.44899	2.54910
H	–2.61113	–0.48321	3.33395
H	–4.27136	0.14083	3.23670

***trans*-[{($PtCl_2$(*t*-BuC≡C*t*-Bu)}$_2$] (12a')**

(file: PtCl2tBuCCtBu_dimer_12a.out / PtCl2tBuCCtBu_dimer_12a_PCM.out)

E(RB+HF–LYP)	–2863.863893 a.u.
Sum of electronic and zero-point energies	–2863.349712 a.u.
Sum of electronic and thermal Gibbs free energies (298.15 K)	–2863.428599 a.u.
ΔG_{solv}(PCM, 298.15 K)	18.4 kcal/mol

	x	y	Z
C	–3.53167	0.62837	–0.33356
C	–3.53698	–0.62162	–0.33274
C	–3.99933	2.02682	–0.55464
C	–4.01636	–2.01628	–0.55239
Pt	–1.69213	–0.00371	0.58237
Cl	–2.64961	0.00266	2.67452
Cl	–0.52645	–0.01087	–1.52930
Cl	0.52651	–0.01109	1.52944
Pt	1.69208	–0.00362	–0.58229
Cl	2.64959	0.00322	–2.67444
C	3.53694	–0.62174	0.33261
C	3.53181	0.62825	0.33355

C	4.01626	–2.01646	0.55202
C	3.99952	2.02663	0.55477
C	2.95226	2.82752	1.35679
H	2.73995	2.35589	2.31852
H	2.01379	2.91113	0.80601
C	5.31614	1.94056	1.36282
H	5.69397	2.95041	1.54404
H	5.15760	1.45676	2.32916
H	6.08033	1.38431	0.81576
C	4.26560	2.71946	–0.79873
H	5.00479	2.17091	–1.38536
H	3.35425	2.78903	–1.39372
H	4.64258	3.72995	–0.61745
C	2.98100	–2.82312	1.36382
H	2.77392	–2.35169	2.32681
H	2.03842	–2.91342	0.82121
H	3.36890	–3.82872	1.54739
C	5.33877	–1.91995	1.34918
H	5.72477	–2.92687	1.52943
H	6.09474	–1.35982	0.79468
H	5.18496	–1.43512	2.31577
C	4.27621	–2.70982	–0.80237
H	5.00594	–2.15667	–1.39643
H	4.66263	–3.71697	–0.62237
H	3.36035	–2.78787	–1.38934
H	3.33211	3.83582	1.54239
C	–2.98215	–2.82209	–1.36639
H	–2.77677	–2.34994	–2.32939
H	–2.03868	–2.91246	–0.82535
H	–3.37003	–3.82768	–1.55002
C	–5.34011	–1.91944	–1.34746
H	–5.18793	–1.43370	–2.31385
H	–5.72608	–2.92631	–1.52804
H	–6.09539	–1.36004	–0.79129
C	–4.27412	–2.71075	0.80184
H	–3.35732	–2.78925	1.38727
H	–5.00291	–2.15812	1.39753
H	–4.66078	–3.71776	0.62161
C	–2.95082	2.82865	–1.35406
H	–2.01341	2.91210	–0.80144
H	–2.73656	2.35785	–2.31576
H	–3.33063	3.83698	–1.53956
C	–5.31442	1.94101	–1.36520
H	–5.69223	2.95088	–1.54628
H	–5.15392	1.45806	–2.33165
H	–6.07946	1.38406	–0.82005
C	–4.26813	2.71850	0.79893

H	–5.00820	2.16922	1.38376
H	–3.35791	2.78803	1.39562
H	–4.64520	3.72897	0.61772

***cis*-[{($PtCl_2$(*t*-BuC≡C*t*-Bu)}$_2$] (12b')**

(file: PtCl2tBuCCtBu_dimer_12b.out / PtCl2tBuCCtBu_dimer_12b_PCM.out)

E(RB+HF–LYP)	–2863.862091 a.u.
Sum of electronic and zero-point energies	–2863.347927 a.u.
Sum of electronic and thermal Gibbs free energies (298.15 K)	–2863.426085 a.u.
ΔG_{solv}(PCM, 298.15 K)	17.2 kcal/mol

	x	y	Z
C	3.25258	0.62594	0.83910
C	3.25292	–0.62361	0.83938
C	3.63652	2.02251	1.19364
C	3.64027	–2.01975	1.19224
Pt	1.79106	0.00028	–0.61222
Cl	3.36343	–0.00081	–2.28546
Cl	0.00006	0.00135	1.01945
Cl	–0.00006	–0.00183	–2.21569
Pt	–1.79103	–0.00114	–0.61216
Cl	–3.36357	–0.00365	–2.28524
C	–3.25226	–0.62460	0.84032
C	–3.25304	0.62494	0.83847
C	–3.63654	–2.02066	1.19649
C	–3.64021	2.02160	1.18936
C	–4.32950	2.70142	–0.01304
H	–5.21063	2.14169	–0.33182
H	–3.65527	2.77428	–0.86705
C	–4.63047	1.93327	2.37469
H	–4.94092	2.94166	2.66140
H	–5.52359	1.36713	2.10195
H	–4.16881	1.45791	3.24312
C	–2.40045	2.83757	1.61116
H	–1.88867	2.37455	2.45766
H	–1.68844	2.92347	0.78856
H	–2.71102	3.84446	1.90291
C	–4.30014	–2.71628	–0.01120
H	–5.17820	–2.16470	–0.35181
H	–3.60998	–2.79412	–0.85198
H	–4.61080	–3.72362	0.28013
C	–4.64782	–1.92869	2.36365
H	–4.95539	–2.93669	2.65482
H	–4.20512	–1.44133	3.23529

H	–5.54038	–1.37232	2.06978
C	–2.39850	–2.82389	1.64714
H	–1.90574	–2.35032	2.49911
H	–2.70673	–3.83081	1.94131
H	–1.67089	–2.91073	0.83843
H	–4.64051	3.70996	0.27375
C	2.39961	–2.83802	1.60678
H	1.88212	–2.37606	2.45038
H	1.69250	–2.92510	0.78007
H	2.71034	–3.84438	1.90016
C	4.62362	–1.93008	2.38322
H	4.15602	–1.45608	3.24922
H	4.93441	–2.93800	2.67120
H	5.51718	–1.36205	2.11593
C	4.33751	–2.69791	–0.00653
H	3.66845	–2.77098	–0.86457
H	5.21984	–2.13686	–0.31965
H	4.64810	–3.70626	0.28140
C	2.40021	2.82149	1.65655
H	1.66496	2.90706	0.85465
H	1.91671	2.34542	2.51243
H	2.70807	3.82900	1.94912
C	4.65843	1.93154	2.35159
H	4.96556	2.93995	2.64180
H	4.22505	1.44133	3.22630
H	5.54997	1.37837	2.04867
C	4.28744	2.72195	–0.01868
H	5.16347	2.17300	–0.36856
H	3.58933	2.79998	–0.85287
H	4.59849	3.72941	0.27179

***cis*-[$PtCl_2(C_2H_4)_2$] (10')**

(file: cis_PtCl2ethene2.out / cis_PtCl2ethene2_PCM.out)

E(RB+HF–LYP)	–1197.197813 a.u.
Sum of electronic and zero-point energies	–1197.085694 a.u.
Sum of electronic and thermal Gibbs free energies (298.15 K)	–1197.122194 a.u.
ΔG_{solv}(PCM, 298.15 K)	–2.8 kcal/mol

	x	y	Z
Pt	–0.00001	0.07175	–0.00001
Cl	–1.64126	–1.57490	–0.00002
C	–1.56248	1.47396	0.69408
H	–2.26378	0.85797	1.24242
H	–1.10403	2.28354	1.24893

C	–1.56245	1.47400	–0.69403
H	–1.10401	2.28352	–1.24879
H	–2.26382	0.85808	–1.24241
C	1.56223	1.47418	–0.69407
H	2.26366	0.85833	–1.24242
H	1.10369	2.28364	–1.24887
C	1.56220	1.47420	0.69404
H	1.10369	2.28368	1.24881
H	2.26364	0.85837	1.24241
Cl	1.64153	–1.57463	0.00003

***trans*-[$PtCl_2(C_2H_4)_2$] (13')**

(file: trans_PtCl2ethene2.out / trans_PtCl2ethene_PCM.out)

E(RB+HF–LYP)	–1197.200610 a.u.
Sum of electronic and zero-point energies	–1197.089597 a.u.
Sum of electronic and thermal Gibbs free energies (298.15 K)	–1197.127607 a.u.
ΔG_{solv}(PCM, 298.15 K)	0.7 kcal/mol

	x	y	Z
Pt	–0.00001	0.00000	0.03906
Cl	–2.33749	0.00000	0.05737
Cl	2.33749	0.00001	0.05737
C	0.00005	–2.19130	0.53320
H	0.92707	–2.34752	1.07217
H	–0.92696	–2.34756	1.07220
C	0.00002	–2.09252	–0.84036
H	–0.92595	–2.14961	–1.39995
H	0.92596	–2.14956	–1.39999
C	0.00004	2.09252	–0.84036
H	0.92600	2.14957	–1.39995
H	–0.92591	2.14960	–1.39999
C	0.00001	2.19131	0.53320
H	–0.92702	2.34756	1.07217
H	0.92701	2.34752	1.07221

***cis*-[$PtCl_2(C_2H_4)$(MeC≡C*t*-Bu)] (8')**

(file: cis_PtCl2ethene_MeCCtBu.out / cis_PtCl2ethene_MeCCtBu_PCM.out)

E(RB+HF–LYP)	–1392.57779452 a.u.
Sum of electronic and zero-point energies	–1392.350636 a.u.
Sum of electronic and thermal Gibbs free energies (298.15 K)	–1392.397248 a.u.

ΔG_{solv}(PCM, 298.15 K) 2.8 kcal/mol

	x	y	Z
C	–1.53235	–0.07918	0.43677
C	–0.97286	0.10838	1.52708
Pt	0.65646	–0.03674	0.04845
Cl	0.47664	2.26862	–0.23458
Cl	2.75388	–0.02342	–0.95413
C	–2.64423	–0.16158	–0.55995
C	–3.40687	–1.49059	–0.35537
C	–3.58881	1.03043	–0.26940
C	–2.13263	–0.06525	–2.01027
H	–2.77255	–2.35458	–0.56759
H	–3.77816	–1.58138	0.66802
H	–4.26267	–1.52899	–1.03487
H	–3.06169	1.97808	–0.39025
H	–4.43109	1.00646	–0.96673
H	–3.98508	0.98122	0.74775
H	–2.98508	–0.09556	–2.69412
H	–1.58810	0.86533	–2.17499
H	–1.46958	–0.89633	–2.25963
C	–0.70591	0.45678	2.92692
H	–0.23680	1.44226	2.97960
H	–1.64733	0.48467	3.48321
H	–0.04070	–0.26302	3.40936
C	0.58650	–2.20630	–0.31172
H	–0.44777	–2.51733	–0.39001
H	1.20997	–2.37737	–1.18023
C	1.15835	–1.98363	0.93429
H	2.23453	–1.98070	1.05399
H	0.57220	–2.12009	1.83551

***trans*-[$PtCl_2(C_2H_4)$(MeC≡C*t*-Bu)] (14')**

(file: trans_PtCl2ethene_MeCCtBu.out / trans_PtCl2ethene_MeCCtBu_PCM.out)

E(RB+HF−LYP) –1392.579774 a.u.

Sum of electronic and zero-point energies –1392.401792 a.u.

Sum of electronic and thermal Gibbs free energies (298.15 K) –1392.353338 a.u.

ΔG_{solv}(PCM, 298.15 K) 5.9 kcal/mol

	x	y	Z
C	–1.59581	–0.06856	0.52701
C	–0.95550	–0.18135	1.56963
Pt	0.68958	0.00619	0.01877

Cl	0.66309	2.33592	0.23644
Cl	0.76136	–2.32952	–0.12857
C	–2.65456	0.03563	–0.50630
C	–3.98849	–0.26089	0.22652
C	–2.69380	1.45928	–1.10049
C	–2.43707	–1.00521	–1.62422
H	–3.98973	–1.26712	0.65089
H	–4.16636	0.45819	1.02927
H	–4.81255	–0.18712	–0.48810
H	–1.75967	1.70311	–1.60743
H	–3.51188	1.52399	–1.82325
H	–2.85485	2.20801	–0.32267
H	–3.27388	–0.95809	–2.32634
H	–1.51486	–0.80612	–2.17231
H	–2.37287	–2.01644	–1.21936
C	–0.50195	–0.34304	2.95361
H	0.08815	0.51914	3.27141
H	–1.37374	–0.43107	3.60863
H	0.10569	–1.24452	3.05651
C	2.14742	0.15912	–1.65571
H	1.99470	–0.73321	–2.25084
H	1.94381	1.11370	–2.12619
C	2.85015	0.09882	–0.46679
H	3.21213	1.00533	0.00303
H	3.26095	–0.84209	–0.12064

***cis*-[$PtCl_2(C_2H_4)$(*t*-BuC≡C*t*-Bu)] (9')**

(file: cis_PtCl2ethene_tBuCCtBu.out / cis_PtCl2ethene_tBuCCtBu_PCM.out)

E(RB+HF–LYP)	–1510.547325 a.u.
Sum of electronic and zero-point energies	–1510.287031 a.u.
Sum of electronic and thermal Gibbs free energies (298.15 K)	–1510.235656 a.u.
ΔG_{solv}(PCM, 298.15 K)	4.7 kcal/mol

	x	y	Z
Pt	–0.84809	–0.02853	–0.04433
Cl	–3.16726	–0.09401	0.15533
Cl	–0.64935	0.06622	2.27577
C	1.24825	0.63772	–0.16855
C	1.29926	–0.60514	–0.16729
C	1.76106	2.04350	–0.08096
C	2.58560	2.34809	–1.35277
H	1.96392	2.31317	–2.25088
H	3.01487	3.35115	–1.27916

H	3.40351	1.63458	–1.47538
C	2.67746	2.11263	1.16499
H	3.08071	3.12454	1.26479
H	2.11731	1.86802	2.06872
H	3.51576	1.41774	1.07703
C	1.89928	–1.96856	–0.04168
C	0.62997	3.07900	0.07066
H	1.06885	4.07575	0.16621
H	–0.03288	3.08715	–0.79679
H	0.02916	2.87979	0.95886
C	–1.10646	–0.71340	–2.12763
H	–0.21403	–1.23631	–2.44230
H	–2.02847	–1.28098	–2.13046
C	–1.13154	0.67336	–2.11145
H	–2.07199	1.20996	–2.10058
H	–0.25675	1.23665	–2.41208
C	1.31780	–2.96784	–1.06046
H	1.80055	–3.93903	–0.92588
H	0.24454	–3.10409	–0.91618
H	1.49943	–2.64635	–2.08941
C	3.41698	–1.80198	–0.30042
H	3.60887	–1.41521	–1.30415
H	3.86805	–1.12352	0.42660
H	3.90872	–2.77418	–0.20832
C	1.67578	–2.50967	1.38791
H	2.07799	–1.82599	2.13678
H	0.61516	–2.64562	1.60064
H	2.17964	–3.47544	1.48672

***trans*-[$PtCl_2(C_2H_4)$(*t*-BuC≡C*t*-Bu)] (15')**

(file: trans_PtCl2ethene_tBuCCtBu.out / trans_PtCl2ethene_tBuCCtBu_PCM.out)

E(RB+HF−LYP)	–1510.550562 a.u.
Sum of electronic and zero-point energies	–1510.240040 a.u.
Sum of electronic and thermal Gibbs free energies (298.15 K)	–1510.294142 a.u.
ΔG_{solv}(PCM, 298.15 K)	8.0 kcal/mol

	x	y	Z
Pt	0.85499	–0.00319	–0.00021
Cl	0.87890	0.16105	–2.33704
Cl	0.87994	–0.17019	2.33636
C	–1.35841	–0.61292	–0.02457
C	–1.35838	0.61869	0.02328
C	–1.79096	–2.03707	–0.07021
C	–3.28861	–2.01827	–0.46703

H	–3.42812	–1.57473	–1.45515
H	–3.66514	–3.04446	–0.49349
H	–3.88272	–1.45548	0.25642
C	–1.63051	–2.68583	1.32132
H	–1.98468	–3.71969	1.27822
H	–0.58852	–2.68498	1.64211
H	–2.21165	–2.15078	2.07516
C	–1.78312	2.04454	0.07058
C	–0.99224	–2.83354	–1.12218
H	–1.39530	–3.84796	–1.18539
H	–1.05346	–2.36718	–2.10660
H	0.06207	–2.89956	–0.84780
C	2.97541	0.69375	0.05935
H	3.08941	1.32093	–0.81673
H	3.09088	1.16232	1.02921
C	2.98066	–0.68147	–0.05936
H	3.09990	–1.30742	0.81691
H	3.10052	–1.14912	–1.02911
C	–1.59141	2.70482	–1.31134
H	–1.94297	3.73946	–1.26641
H	–0.54296	2.70335	–1.61024
H	–2.15799	2.17841	–2.08206
C	–3.28885	2.03055	0.43673
H	–3.87108	1.47776	–0.30384
H	–3.45099	1.57901	1.41774
H	–3.66001	3.05862	0.46491
C	–1.00170	2.82693	1.14595
H	–1.08680	2.35273	2.12483
H	0.05858	2.88795	0.89474
H	–1.39945	3.84345	1.20932

***trans*-[$PtCl_2(C_4Me_2t\text{-}Bu_2)$] (16')**

(file: PtCl2C4Me2tBu2.out / PtCl2C4Me2tBu2.out)

E(RB+HF–LYP)	–1587.993580 a.u.
Sum of electronic and zero-point energies	–1587.647168 a.u.
Sum of electronic and thermal Gibbs free energies (298.15 K)	–1587.699383 a.u.
ΔG_{solv}(PCM, 298.15 K)	3.6 kcal/mol

	x	y	z
Pt	0.00004	0.78428	–0.00003
C	–0.14168	–1.09244	–1.03044
C	–1.03962	–1.10024	0.09842
Cl	–1.27053	2.39987	–1.13743
Cl	1.27086	2.39968	1.13739

C	–2.52003	–1.32872	0.30208
C	1.03949	–1.10040	–0.09832
C	0.14156	–1.09235	1.03055
C	–2.69697	–2.81868	0.69081
H	–2.17956	–3.05661	1.62381
H	–3.75906	–3.03585	0.83212
H	–2.31853	–3.48293	–0.09097
C	–3.06744	–0.43194	1.43284
H	–4.13537	–0.62701	1.56196
H	–2.58027	–0.63085	2.38918
H	–2.93991	0.62507	1.19268
C	–3.30925	–1.03753	–0.98871
H	–3.14919	–0.01156	–1.32699
H	–3.03732	–1.72418	–1.79359
H	–4.37704	–1.16797	–0.79483
C	2.51989	–1.32895	–0.30203
C	2.69669	–2.81881	–0.69120
H	2.17928	–3.05642	–1.62428
H	3.75877	–3.03604	–0.83255
H	2.31818	–3.48325	0.09038
C	3.30914	–1.03821	0.98884
H	4.37691	–1.16869	0.79491
H	3.14918	–0.01232	1.32741
H	3.03715	–1.72508	1.79351
C	–0.29407	–1.25238	–2.50487
H	0.53224	–0.78087	–3.03616
H	–0.30579	–2.31581	–2.77037
H	–1.22053	–0.80005	–2.85419
C	0.29385	–1.25206	2.50501
H	–0.53192	–0.77948	3.03620
H	0.30438	–2.31544	2.77079
H	1.22082	–0.80068	2.85418
C	3.06739	–0.43188	–1.43253
H	4.13527	–0.62712	–1.56178
H	2.58012	–0.63036	–2.38892
H	2.94007	0.62507	–1.19200

***cis*-[$PtCl_2(C_4Me_2$*t*-$Bu_2)$] (16')**

(file: cis_cyclobutadien_MeTBA.out / cis_cyclobutadien_MeTBA_PCM.out)

E(RB+HF–LYP)	–1587.986233 a.u.
Sum of electronic and zero-point energies	–1587.639522 a.u.
Sum of electronic and thermal Gibbs free energies (298.15 K)	–1587.691152 a.u.
ΔG_{solv}(PCM, 298.15 K)	2.8 kcal/mol

	x	*y*	*z*
C	1.04790	0.77857	0.39693
C	1.06410	–0.68035	0.47456
Pt	–0.88416	–0.01496	–0.16238
Cl	–1.17427	–0.32335	–2.47054
Cl	–3.20086	0.09356	0.22150
C	1.86950	–1.85907	–0.04021
C	0.09065	0.81610	1.55982
C	0.11172	–0.61047	1.63759
C	2.98033	–2.14008	1.00466
H	2.56153	–2.37710	1.98609
H	3.57678	–2.99733	0.68112
H	3.65157	–1.28519	1.11693
C	0.96286	–3.10482	–0.16220
H	1.55766	–3.94583	–0.52765
H	0.53599	–3.40106	0.79707
H	0.14847	–2.93142	–0.86791
C	2.51385	–1.60399	–1.41236
H	1.76214	–1.34300	–2.15928
H	3.26621	–0.81521	–1.36984
H	3.01843	–2.51573	–1.74272
C	1.83378	1.89477	–0.27615
C	–0.44235	–1.56018	2.64195
H	–0.83589	–2.46309	2.17594
H	0.33823	–1.85503	3.35225
H	–1.25283	–1.08745	3.19871
C	–0.50136	1.84464	2.46147
H	–1.31791	1.40538	3.03676
H	0.25369	2.21682	3.16288
H	–0.89986	2.69310	1.90733
C	1.87003	1.78063	–1.81387
H	0.86426	1.80822	–2.23422
H	2.43775	2.62521	–2.21445
H	2.34738	0.86690	–2.15739
C	3.27447	1.86070	0.29266
H	3.79486	0.94106	0.01868
H	3.84530	2.70217	–0.10905
H	3.27773	1.94375	1.38333
C	1.20051	3.25909	0.07225
H	1.24484	3.47329	1.14171
H	1.74981	4.04979	–0.44382
H	0.15989	3.31145	–0.25607

[$PtCl_2(C_4t\text{-}Bu_4)$] (17')

(file: PtCl2C4tBu4.out / PtCl2C4tBu4_PCM.out)

E(RB+HF−LYP)	–1823.875408 a.u.
Sum of electronic and zero-point energies	–1823.357097 a.u.
Sum of electronic and thermal Gibbs free energies (298.15 K)	–1823.414787 a.u.
ΔG_{solv}(PCM, 298.15 K)	5.8 kcal/mol

	x	y	z
Pt	–0.00001	–0.00005	–1.03810
C	–0.74455	–0.75388	0.84182
C	–0.78669	0.70442	0.84231
Cl	–1.67066	0.02244	–2.69789
Cl	1.67054	–0.02263	–2.69799
C	–1.84682	1.80470	1.04584
C	0.78673	–0.70430	0.84236
C	0.74460	0.75397	0.84175
C	–1.61188	2.43470	2.44558
H	–0.62641	2.87288	2.57428
H	–2.35037	3.22329	2.61095
H	–1.74698	1.68435	3.22999
C	–1.80961	2.85430	–0.09558
H	–2.42315	3.71281	0.19301
H	–0.82183	3.21802	–0.34439
H	–2.23214	2.42033	–1.00270
C	–3.30918	1.32259	1.05746
H	–3.52097	0.62697	1.86836
H	–3.94157	2.20028	1.21484
H	–3.59569	0.88278	0.10553
C	1.84683	–1.80461	1.04595
C	1.61189	–2.43460	2.44570
H	0.62651	–2.87300	2.57434
H	2.35054	–3.22302	2.61115
H	1.74678	–1.68420	3.23010
C	3.30919	–1.32255	1.05753
H	3.59563	–0.88261	0.10564
H	3.52106	–0.62704	1.86851
H	3.94160	–2.20026	1.21472
C	–1.79556	–1.86374	1.08719
C	1.79564	1.86384	1.08700
C	1.80958	–2.85426	–0.09543
H	2.42290	–3.71289	0.19326
H	0.82174	–3.21775	–0.34438
H	2.23230	–2.42041	–1.00251
C	–1.31898	–3.28422	0.70949

H	–0.41104	–3.60379	1.20812
H	–2.10611	–3.98414	0.99864
H	–1.18590	–3.37685	–0.36987
C	–2.12039	–1.85004	2.60511
H	–2.88390	–2.60355	2.81632
H	–1.24474	–2.08060	3.21522
H	–2.50683	–0.88247	2.92845
C	–3.10966	–1.69225	0.27551
H	–2.91634	–1.35495	–0.74288
H	–3.60210	–2.66508	0.21571
H	–3.81424	–1.01750	0.74464
C	1.31901	3.28430	0.70934
H	0.41109	3.60385	1.20804
H	2.10615	3.98424	0.99843
H	1.18588	3.37698	–0.37001
C	2.12057	1.85026	2.60493
H	2.88421	2.60368	2.81595
H	1.24498	2.08110	3.21504
H	2.50683	0.88268	2.92841
C	3.10967	1.69226	0.27519
H	2.91627	1.35485	–0.74314
H	3.60211	2.66509	0.21529
H	3.81429	1.01757	0.74430

***trans*-[$PtCl_2$(*t*-BuC≡C*t*-Bu)$_2$] (*trans*-19')**

(file: trans_PtCl2t-BuCCtBu2.out / trans_PtCl2t-BuCCtBu2_PCM.out)

E(RB+HF–LYP)	–1823.895933 a.u.
Sum of electronic and zero-point energies	–1823.385922 a.u.
Sum of electronic and thermal Gibbs free energies (298.15 K)	–1823.451268 a.u.
ΔG_{solv}(PCM, 298.15 K)	13.2 kcal/mol

	x	*y*	*z*
C	–2.18708	0.61669	0.02178
C	–2.18696	–0.61712	–0.02195
Pt	0.00000	0.00033	–0.00002
Cl	0.00017	0.00049	–2.34542
Cl	–0.00009	0.00029	2.34542
C	–2.66953	–2.02517	–0.07318
C	2.18692	0.61677	–0.02189
C	2.18692	–0.61704	0.02195
C	–2.42945	–2.62664	–1.47375
H	–1.36879	–2.64475	–1.72409
H	–2.81514	–3.64994	–1.49748

H	–2.93875	–2.04430	–2.24407
C	–1.98622	–2.88852	1.00614
H	–2.42994	–3.88799	1.00256
H	–0.91744	–2.98709	0.81321
H	–2.10630	–2.45165	1.99874
C	–4.19208	–1.96882	0.20929
H	–4.39330	–1.55933	1.20154
H	–4.70998	–1.35799	–0.53318
H	–4.60270	–2.98135	0.16527
C	2.67006	2.02467	–0.07301
C	2.43179	2.62566	–1.47410
H	1.37143	2.64393	–1.72567
H	2.81778	3.64884	–1.49777
H	2.94187	2.04290	–2.24360
C	4.19222	1.96796	0.21136
H	4.60325	2.98032	0.16738
H	4.39208	1.55883	1.20403
H	4.71084	1.35662	–0.53021
C	–2.67025	2.02455	0.07304
C	2.66969	–2.02502	0.07318
C	1.98571	2.88873	1.00508
H	2.42995	3.88797	1.00176
H	0.91726	2.98781	0.81060
H	2.10418	2.45215	1.99800
C	2.43103	–2.62594	1.47423
H	1.37062	–2.64384	1.72568
H	2.81665	–3.64927	1.49796
H	2.94120	–2.04336	2.24380
C	1.98538	–2.88892	–1.00508
H	2.42942	–3.88825	–1.00172
H	0.91688	–2.98780	–0.81079
H	2.10414	–2.45231	–1.99795
C	4.19194	–1.96863	–0.21087
H	4.39208	–1.55954	–1.20350
H	4.71053	–1.35742	0.53081
H	4.60272	–2.98109	–0.16681
C	–4.19266	1.96771	–0.20998
H	–4.39339	1.55819	–1.20232
H	–4.71063	1.35667	0.53227
H	–4.60366	2.98009	–0.16606
C	–1.98684	2.88834	–1.00590
H	–2.43102	3.88761	–1.00243
H	–0.91819	2.98738	–0.81247
H	–2.10626	2.45151	–1.99860
C	–2.43084	2.62593	1.47376
H	–1.37026	2.64441	1.72442
H	–2.81693	3.64906	1.49749

H	–2.94016	2.04329	2.24385

***cis*-[PtCl$_2$(*t*-BuC≡C*t*-Bu)$_2$] (*cis*-19')**

(file: cis_PtCl2t-BuCCtBu2.out / cis_PtCl2t-BuCCtBu2_PCM.out)

E(RB+HF–LYP)	–1823.877559 a.u.
Sum of electronic and zero-point energies	–1823.366365 a.u.
Sum of electronic and thermal Gibbs free energies (298.15 K)	–1823.428696 a.u.
ΔG_{solv}(PCM, 298.15 K)	10.4 kcal/mol

	x	*y*	*z*
C	1.85728	0.19598	0.44045
C	1.32698	–0.83581	0.88852
Pt	0.00505	–0.08579	–0.76609
Cl	1.47868	–1.04095	–2.31074
Cl	–1.41507	0.42895	–2.54541
C	2.98553	1.15674	0.17445
C	3.16473	2.08578	1.39712
C	4.26446	0.29883	0.00048
C	2.79232	2.00554	–1.09754
H	2.31918	2.76434	1.51678
H	3.28172	1.51297	2.32016
H	4.06355	2.69282	1.25793
H	4.14805	–0.39989	–0.82864
H	5.11176	0.95747	–0.21182
H	4.49138	–0.26437	0.90796
H	3.63608	2.69505	–1.18935
H	2.75477	1.37866	–1.98713
H	1.87610	2.59493	–1.06477
C	1.29580	–2.10066	1.68421
C	–1.32946	1.02970	0.66490
C	–1.89063	–0.05395	0.42926
C	0.14250	–2.09165	2.70343
H	–0.82096	–2.02390	2.20327
H	0.16147	–3.01509	3.28894
H	0.22908	–1.24661	3.39067
C	1.17614	–3.31622	0.74104
H	1.19858	–4.23800	1.32956
H	0.24783	–3.29065	0.17051
H	1.99901	–3.33678	0.02481
C	2.63772	–2.18785	2.45111
H	3.48244	–2.23561	1.76204

H	2.77326	–1.32927	3.11329
H	2.64571	–3.09426	3.06317
C	–3.03979	–1.02130	0.36099
C	–3.57752	–1.21777	1.80053
H	–4.45057	–1.87541	1.76735
H	–2.83650	–1.67228	2.45917
H	–3.88859	–0.26720	2.23920
C	–2.65304	–2.38393	–0.24180
H	–3.54211	–3.01847	–0.28787
H	–2.25973	–2.27056	–1.25263
H	–1.90767	–2.89828	0.36654
C	–4.16326	–0.38878	–0.49709
H	–3.82968	–0.22565	–1.52022
H	–5.02480	–1.06319	–0.50642
H	–4.48271	0.56875	–0.08033
C	–1.27744	2.39386	1.27843
C	–0.52615	2.33631	2.62568
H	0.48996	1.96367	2.50059
H	–0.47631	3.33699	3.06507
H	–1.04330	1.67956	3.32938
C	–0.62767	3.41952	0.33313
H	–1.11241	3.41367	–0.64500
H	–0.71741	4.42151	0.76187
H	0.43022	3.20835	0.18688
C	–2.74384	2.82026	1.53666
H	–2.75640	3.80432	2.01426
H	–3.30303	2.88490	0.60140
H	–3.25130	2.11576	2.19924

***trans*-[$PtCl_2$(MeC≡C*t*-Bu)$_2$] (*trans*-20a')**

(file: trans_PtCl2t-BuCCtBu2_I1.out / trans_PtCl2t-BuCCtBu2_I1_PCM.out)

E(RB+HF−LYP)	–1587.955429 a.u.
Sum of electronic and zero-point energies	–1587.613464 a.u.
Sum of electronic and thermal Gibbs free energies (298.15 K)	–1587.671707 a.u.
ΔG_{solv}(PCM, 298.15 K)	11.0 kcal/mol

	x	*y*	*z*
C	2.07667	–1.20457	0.33819
C	2.20343	0.01199	0.17541
Pt	–0.00230	–0.46573	–0.04888
Cl	0.30744	–0.01066	–2.33530
Cl	–0.33467	–0.97168	2.22114
C	2.86684	1.34301	0.05250
C	–2.05340	–1.06743	–0.63731

C	–2.20393	0.05234	–0.13908
C	3.58441	1.42583	–1.31360
H	2.87013	1.33833	–2.13244
H	4.10060	2.38711	–1.39432
H	4.32466	0.62867	–1.41538
C	1.86761	2.50615	0.18955
H	2.41114	3.45443	0.15818
H	1.14729	2.49561	–0.62925
H	1.32622	2.45172	1.13666
C	3.90542	1.41658	1.19913
H	3.41869	1.35658	2.17470
H	4.63337	0.60514	1.12566
H	4.44525	2.36580	1.13737
C	2.29337	–2.62756	0.61356
H	2.00793	–3.24323	–0.24227
H	3.35523	–2.79169	0.82090
H	1.71155	–2.93804	1.48293
C	–2.86109	1.31974	0.28232
C	–2.25432	–2.35697	–1.30360
H	–1.67050	–2.40148	–2.22509
H	–1.95718	–3.18472	–0.65597
H	–3.31412	–2.47155	–1.55091
C	–4.34886	1.17761	–0.12754
H	–4.81836	0.33398	0.38341
H	–4.88729	2.08821	0.14907
H	–4.44933	1.03365	–1.20568
C	–2.76523	1.53571	1.80524
H	–1.72939	1.63407	2.12926
H	–3.30494	2.44964	2.06956
H	–3.20379	0.69953	2.35237
C	–2.23336	2.51516	–0.46460
H	–2.78563	3.42682	–0.22009
H	–1.19268	2.65559	–0.17025
H	–2.26229	2.36699	–1.54584

***trans*-[$PtCl_2$(MeC≡C*t*-Bu)$_2$] (*trans*-20b')**

(file: trans_PtCl2MeCCtBu2_I1.out / trans_PtCl2MeCCtBu2_I1_PCM.out)

E(RB+HF–LYP)	–1587.956546 a.u.
Sum of electronic and zero-point energies	–1587.614424 a.u.
Sum of electronic and thermal Gibbs free energies (298.15 K)	–1587.670893 a.u.
ΔG_{solv}(PCM, 298.15 K)	11.2 kcal/mol

	x	*y*	*z*
C	1.56849	0.38188	1.56509

C	2.16980	–0.02299	0.56493
Pt	–0.00001	0.15587	–0.00009
Cl	0.00019	–2.19569	–0.00094
Cl	–0.00020	2.51111	0.00079
C	3.28954	–0.46659	–0.31558
C	–2.16974	–0.02278	–0.56476
C	–1.56876	0.38279	–1.56485
C	3.67172	–1.92199	0.03466
H	2.83423	–2.59660	–0.14289
H	4.51678	–2.23401	–0.58621
H	3.96591	–2.00733	1.08347
C	2.92315	–0.36421	–1.80884
H	3.79230	–0.63951	–2.41265
H	2.10412	–1.04153	–2.05524
H	2.62853	0.65389	–2.07277
C	4.47867	0.47796	–0.01032
H	4.22897	1.51382	–0.24868
H	4.76520	0.42467	1.04272
H	5.34086	0.18000	–0.61363
C	–3.28933	–0.46699	0.31565
C	–3.67120	–1.92234	–0.03520
H	–2.83353	–2.59682	0.14197
H	–4.51613	–2.23483	0.58560
H	–3.96546	–2.00728	–1.08402
C	–4.47866	0.47743	0.01091
H	–5.34078	0.17900	0.61411
H	–4.22919	1.51324	0.24975
H	–4.76524	0.42460	–1.04214
C	1.21624	0.89730	2.89127
H	0.51679	0.23145	3.40143
H	2.12396	0.97792	3.49686
H	0.76157	1.88570	2.80352
C	–1.21695	0.89939	–2.89068
H	–0.51709	0.23439	–3.40139
H	–2.12477	0.97984	–3.49615
H	–0.76293	1.88803	–2.80223
C	–2.92287	–0.36521	1.80894
H	–3.79194	–0.64093	2.41267
H	–2.10370	–1.04249	2.05498
H	–2.62841	0.65283	2.07328

***cis*-[PtCl$_2$(MeC≡C*t*-Bu)$_2$] (*cis*-20a')**

(file: cis_PtCl2MeCCtBu2_I1.out / cis_PtCl2MeCCtBu2_I1_PCM.out)

E(RB+HF–LYP) –1587.951360 a.u.

Sum of electronic and zero-point energies	–1587.608911 a.u.
Sum of electronic and thermal Gibbs free energies (298.15 K)	–1587.663381 a.u.
ΔG_{solv}(PCM, 298.15 K)	7.0 kcal/mol

	x	*y*	*z*
C	–0.92031	–0.66905	–1.49783
C	–1.56700	–0.85728	–0.45736
Pt	–0.00001	0.66271	–0.00007
Cl	–1.32990	2.31086	–0.97476
Cl	1.32973	2.31124	0.97419
C	–2.68182	–1.36697	0.39281
C	1.56724	–0.85674	0.45756
C	0.92036	–0.66877	1.49797
C	–2.23832	–2.63678	1.15096
H	–1.39470	–2.43831	1.81258
H	–3.06789	–3.01077	1.75757
H	–1.94127	–3.42375	0.45383
C	–3.16962	–0.28584	1.37763
H	–4.03039	–0.66391	1.93609
H	–2.39161	–0.01101	2.09172
H	–3.46580	0.62079	0.84764
C	–3.83481	–1.73041	–0.57551
H	–4.17638	–0.84936	–1.12187
H	–3.52018	–2.48790	–1.29764
H	–4.67692	–2.13274	–0.00516
C	2.68185	–1.36706	–0.39250
C	2.23804	–2.63746	–1.14946
H	1.39416	–2.43947	–1.81090
H	3.06735	–3.01199	–1.75609
H	1.94121	–3.42385	–0.45157
C	3.83517	–1.72964	0.57575
H	4.67707	–2.13246	0.00543
H	4.17691	–0.84810	1.12121
H	3.52081	–2.48651	1.29864
C	–0.57706	–0.61278	–2.92424
H	0.46607	–0.87007	–3.11404
H	–1.21152	–1.31325	–3.47568
H	–0.75559	0.39686	–3.30137
C	0.57742	–0.61150	2.92443
H	–0.46594	–0.86758	3.11460
H	1.21125	–1.31234	3.47612
H	0.75705	0.39818	3.30095
C	3.16932	–0.28673	–1.37834
H	4.02987	–0.66524	–1.93686
H	2.39108	–0.01236	–2.09236
H	3.46577	0.62028	–0.84916

***cis*-[PtCl$_2$(MeC≡C*t*-Bu)$_2$] (*cis*-20b')**

(file: cis_PtCl2MeCCtBu2_I2.out / cis_PtCl2MeCCtBu2_I2_PCM.out)

E(RB+HF–LYP)	–1587.948479 a.u.
Sum of electronic and zero-point energies	–1587.605867 a.u.
Sum of electronic and thermal Gibbs free energies (298.15 K)	–1587.660058 a.u.
ΔG_{solv}(PCM, 298.15 K)	6.7 kcal/mol

	x	y	z
C	–1.78592	–0.19825	1.20783
C	–1.68761	0.74640	0.41078
Pt	–0.06116	–0.72829	–0.04464
Cl	–1.60150	–1.91815	–1.32746
Cl	1.64946	–2.04783	–0.92019
C	–2.13262	1.97878	–0.30200
C	1.20529	–0.00815	1.61407
C	1.61028	0.61141	0.61985
C	–1.29017	3.19397	0.13334
H	–0.24303	3.06532	–0.13866
H	–1.66145	4.09511	–0.36252
H	–1.34693	3.34747	1.21369
C	–2.05341	1.78759	–1.82998
H	–2.43966	2.68158	–2.32759
H	–1.02591	1.62609	–2.15868
H	–2.64022	0.92489	–2.14818
C	–3.60785	2.20693	0.11083
H	–4.23215	1.36427	–0.19237
H	–3.70035	2.33900	1.19181
H	–3.98671	3.10991	–0.37620
C	–2.35894	–1.15325	2.16507
H	–1.63797	–1.47544	2.91776
H	–3.20919	–0.68994	2.67470
H	–2.70825	–2.03862	1.62828
C	2.57176	1.43874	–0.17799
C	1.12369	–0.50598	2.99262
H	0.21106	–0.16802	3.48869
H	1.15236	–1.59767	3.01757
H	1.97788	–0.12665	3.56103
C	2.10870	1.67042	–1.62723
H	1.16421	2.21557	–1.66682
H	2.86093	2.26376	–2.15386
H	1.98476	0.72397	–2.15469

C	3.93336	0.70126	–0.18924
H	4.66577	1.30625	–0.73208
H	4.30239	0.54588	0.82742
H	3.84446	–0.26951	–0.67559
C	2.73882	2.79392	0.55100
H	1.80189	3.35220	0.58945
H	3.09180	2.64862	1.57481
H	3.47719	3.40148	0.02029